

Doctoral Theses at NTNU 2005:9

Nils Chr Hagen

**On the Shear Capacity of
Steel Plate Girders
with Large Web Openings**

NTNU
Norwegian University of
Science and Technology
Doctoral thesis
for the degree of doktor ingeniør
Faculty of Engineering Science and Technology
Department of Structural Engineering



624.072.24 H120

Nils Chr Hagen

On the Shear Capacity of
Steel Plate Girders
with Large Web Openings

Universitetsbiblioteket i Trondheim
Teknisk hovedbibliotek
Trondheim

Trondheim, October 2004

Doctoral thesis for the degree of doktor ingeniør

Norwegian University of Science and Technology
Faculty of Engineering Science and Technology
Department of Structural Engineering

 NTNU

Contents

Abstract	iv
Acknowledgements	v
Notation	vi
1 Introduction	
1.1 Background	1
2.1 Objectives	2
2 Previous studies	
2.1 Introduction	5
2.2 Stocky webs	5
2.3 Slender webs	6
2.4 All webs	11
2.5 Stressed skin	12
3 Review and evaluation of load-carrying theories	
3.1 Introduction	13
3.2 Methods based on allowable stresses	14
3.3 Methods based on strength criteria	19
3.4 Stress concentration and plastification	31
3.5 Simplified shear buckling	40
3.6 Rotated stress field method	44
3.7 Modified Vierendeel method	52
3.8 Moment-shear interaction	57
3.9 Tension field method	62
3.10 Stressed skin method	71
3.11 Checkerboard method	81
3.12 Doubler plate method	83
3.13 Other methods	87
3.14 Conclusion	93
4 Prior experiments	
4.1 Introduction	94
4.2 Details of the experiment set-ups	94
4.3 Summary of test results	100
4.4 Discussion	103
4.5 Conclusion	107

5	Simulations of the prior experiments	
5.1	Introduction	108
5.2	Half-fractional factorial design of simulations	108
5.3	Simulations of girders S1 and S3	110
5.4	Conclusion	117
6	Proposal for a new design procedure	
6.1	Introduction	118
6.2	The functions $\chi_{w,mod}$ and ξ_w	118
6.3	The simulations and the factors c_1 , c_2 and c_3	119
6.4	Design in various limit states	120
6.5	Relative comparisons	121
6.6	Overview of simulations	121
7	Simulations of girders with circular openings	
7.1	Introduction	122
7.2	Single opening without stiffening	124
7.3	Single opening with sleeve	156
7.4	Single opening with doubler plate	159
7.5	Two openings without stiffening	163
7.6	Two openings with sleeves	168
7.7	Conclusion	172
8	Simulations of girders with elongated circular openings	
8.1	Introduction	173
8.2	Opening without stiffening	173
8.3	Opening with sleeve	175
8.4	Conclusion	177
9	Simulations of girders with square openings	
9.1	Introduction	178
9.2	Single opening without stiffening	178
9.3	Single opening with horizontal reinforcement	188
9.4	Single opening with vertical stiffeners	191
9.5	Single opening with horizontal reinforcement and vertical stiffeners	193
9.6	Two openings without stiffening	199
9.7	Two openings with stiffeners and reinforcement	202
9.8	Conclusion	206
10	Simulations of girders with rectangular openings	
10.1	Introduction	207
10.2	Opening without stiffening	207
10.3	Opening with stiffeners and reinforcement	209
10.4	Conclusion	211

11	Development of the new design procedure	
11.1	Introduction	212
11.2	Non-conservative results	212
11.3	The adjustment factor c_2	213
11.4	Contribution to shear capacity from vertical stiffeners	217
11.5	Contribution to shear capacity from horizontal reinforcement	218
11.6	Contribution to shear capacity from vert. stiffeners and horiz. reinforcement	218
11.7	Contribution to shear capacity from sleeves and doubler plates	220
11.8	Design of vertical stiffeners	222
11.9	Openings in lower or upper part of webs	223
11.10	Two openings close together	224
11.11	Cut-off on shear capacities	225
11.12	Miscellaneous	227
11.13	Verification of the proposed guidelines	227
12	Conclusions and suggestions	
12.1	Conclusions	229
12.2	Design guidelines	229
12.3	Calculation of shear capacity by means of FE-models	239
12.4	Suggestions for further study	240
	References	241
	Appendices	
A	Overview of simulations	245
B	Design guidelines applied to the simulated girders	246

Abstract

This report presents an investigation of the shear capacities of steel plate girders with web holes, penetrations, cut-outs or openings. The study is motivated by the need for simple guidelines that can be used in practical design of girders in building and offshore structures. Simplicity of method is highly desirable because the value of any calculation decreases sharply if it is not completed before the design is frozen.

The study comprises a review of existing load-carrying theories, including methods based on allowable stresses, strength criteria, simplified shear buckling, rotated stress fields, tension fields and stressed skin.

260 simulations of girders are performed by means of the non-linear finite element program ABAQUS. Results from experiments of large plate girders are used to calibrate the finite element models, in order to ensure that reliable models are used in the simulations.

The simulations comprise girders with webs of height-thickness ratios from 63 to 333. The openings are circular, elongated circular, square and rectangular, with and without sleeves, doubler plates, vertical stiffeners and horizontal reinforcement. Opening sizes are 25 % and 50 % of the girder heights. Single openings and two openings close together are included.

The shear capacities and transverse web displacements in the various limit states are discussed. A new design procedure is proposed for girders with openings. Here, the calculation of the shear capacity in the ultimate limit state (ULS) is linked to the Eurocode 3 for girders without openings. A simplified moment-shear interaction equation is also proposed. A set of design guidelines is given for design based on the LRFD method.

For more complicated cases, and for design in the accidental limit state (ALS), non-linear FE-models may be required. Recommendations for such models are given, based on the experience from the simulations.

Aknowledgements

I would like to express my deepest gratitude to my supervisor, Professor Per Kristian Larsen, for his motivating support, guidance and patience throughout the work.

Thanks are due to SINTEF for free use of the FEM-program ABAQUS.

Furthermore, thanks to my good colleagues in Stål-Consult A/S, in particular Dag Holen and Kristen Solaas, for advice, helpful discussions and comments to the manuscript. Thanks also to Anne Arnesen for drawing many of the figures.

Special thanks should be given to Kristen Solaas as my partner in Stål-Consult A/S, for his understanding and patience during the years this work has lasted.

Finally, I am very grateful to my dear wife Nuniek and our four children for their kind and confident attitude to the project. The study has partly been performed in addition to my ordinary position, and the work would not have been possible without the encouraging support of my wife. She has always been interested and positive, and her contribution is much appreciated.

Notation

Notations and symbols used in this report are defined in the text when they occur for the first time.

Symbol Explanation

A	area, ratio
A_f	cross section area of flange
A_r	cross section area of reinforcement in each tee
$A_{r,max}$	maximum cross section area of reinforcement
A_{wb}	cross section area of bottom tee web
A_{wt}	cross section area of top tee web
B_t	distance from top compression corner to vertical reaction force
B_b	distance from bottom compression corner to vertical reaction force
D	diameter of opening
D_a	length of opening, horizontal dimension of opening
D_{af}	length of fictitious opening, horizontal dimension of fictitious opening
D_h	height of opening, vertical dimension of opening
D_{hf}	height of fictitious opening, vertical dimension of fictitious opening
$D_{h,r}$	clear vertical distance between horizontal reinforcements
D_x	flexural rigidity parallel to stiffeners
D_y	flexural rigidity perpendicular to stiffeners
E	modulus of elasticity
F_a	additional flange force
F_h	horizontal force transferred to the flanges
$F_{s,A}, F_{s,B}$	flange forces at maximum shear in girder "A" and girder "B", respectively
G	shear modulus
H	height (depth) of beam
H_e	efficiency index
I_b, I_t	second moment of area of bottom tee and top tee, respectively
I_{net}	second moment of area for the total net section at center of opening
I_{po}	polar second moment of area of stiffener about the toe
I_{st}	second moment of area of stiffeners or reinforcement incl. effective plate flange
I_T	St. Venant torsional constant of stiffener alone
I_y	second moment of area of stiffener including effective plate flange
I_z	second moment of area of stiffener about its centroid perpendicular to the plate
L	length
L_b	unbraced length of compression flange
L_s	length of stiffener between transverse stiffening
L_1, \dots, L_n	contributions to the length of a fictitious opening
M	primary bending moment at centerline of opening
M_a	primary moment at position "a"
M_{bh}	secondary moment in bottom tee at high moment end
M_{bl}	secondary moment in bottom tee at low moment end

M_{buckl}	moment capacity of girder based on the effective cross section areas
$M_{buckl,mod}$	moment capacity of girder based on the effective cross section areas, with opening subtracted
$M_{buckl,mod,H}$	moment capacity of girder based on the effective flanges and the effective compression part of web
$M_{buckl,mod,Rd}$	design resistance for moment in girder based on the effective cross section areas, with opening subtracted
M_{el}	elastic moment capacity of the gross section of girder, obtained when buckling is disregarded
$M_{el,mod}$	elastic moment capacity of the gross section of girder, obtained when buckling is disregarded and opening subtracted
M_f	moment capacity of girder when only the effective flanges are considered
$M_{f,mod}$	moment capacity of girder when only the effective flanges are considered, and the areas required for the additional flange forces are subtracted
M_h	primary moment at high moment end of opening
M_l	primary moment at low moment end of opening
M_m	maximum moment capacity for beams at location of an opening
M_n	moment capacity of beams at location of an opening
M_p	plastic moment capacity
M_{pb}	plastic moment capacity of bottom tee
M_{pbh}	plastic moment capacity of bottom tee at high moment end
M_{pbl}	plastic moment capacity of bottom tee at low moment end
M_{pfl}	plastic moment capacity of flange
M_{pl}	plastic moment capacity of girder based on effective flanges and full web
$M_{pl,mod}$	plastic moment capacity of girder based on effective flanges and full web with opening subtracted
$M_{p,n}$	plastic moment capacity of chord at end "n" = 1,2,3,4
M_{pr}	plastic moment capacity of ring or reinforcement
M_{pt}	plastic moment capacity of top tee
M_{pth}	plastic moment capacity of top tee at high moment end
M_{ptl}	plastic moment capacity of top tee at low moment end
M_{th}	secondary moment in top tee at high moment end
M_{tl}	secondary moment in top tee at low moment end
M_V	moment capacity at maximum shear
N	axial force in stiffeners
N_n	axial forces in stiffeners at position "n" in stressed skin design
P	tip load
S	horizontal component of tension stress field
S_a	clear horizontal distance between openings
S_h	clear vertical distance between openings
S_t	first moment of area of top tee
T	maximum shear capacity at the location of an opening
T_s	plastic shear capacity of unperforated girder
V	shear force at centerline of opening
$V_{ALS,e}$	tip equilibrium load that gave a tip displacement of 50 or 38 mm
V_b	shear force in bottom tee

V_c	maximum shear capacity for a web without opening, i.e. in pure shear
$V_{c,mod}$	maximum shear capacity modified for opening, i.e. in pure shear
$V_{c,mod,cut-off}$	cut-off value for the nominal maximum shear capacity modified for opening
$V_{c,mod,cut-off,Rd}$	cut-off value for the design resistance modified for opening
$V_{c,mod,Rd}$	design resistance for pure shear modified for opening
$V_{cr,mod}$	modified critical shear force
V_f	shear force [capacity] of flanges
$V_{max,A}$, $V_{max,B}$	maximum shear force in girder "A" and girder "B", respectively
V_m , V_m'	maximum shear capacity of beams at the location of an opening
V_{max}	maximum shear force
$V_{max,A}$, $V_{max,B}$	maximum shear force in girder "A" and girder "B", respectively
V_{mb} , V_{mb}'	maximum shear capacity of bottom tee
$V_{mechanism}$	shear force carried by tension field
V_{mt} , V_{mt}'	maximum shear capacity of top tee
V_{mV}	shear capacity of classic Vierendeel girder
V_{mV}'	shear capacity of non-classic Vierendeel girder
V_n	shear capacity
V_{nb}	shear capacity of bottom tee
V_{nt}	shear capacity of top tee
V_p	plastic shear capacity of unperforated beam
$V_{p,mod}$	plastic shear capacity based on the minimum section through the opening
V_{pt}	plastic shear capacity of top tee
V_t	shear force in top tee, shear force [capacity] of tension field
$V_{SLS,e}$	tip equilibrium load that gave a web transverse displacement of $b/200$
$V_{u,e}$	measured maximum equilibrium load
$V_{u,en}$	measured maximum load not in equilibrium
V_{ult}	total shear capacity based on Cardiff method
$V_{ult,Lee}$	total shear capacity based on the method by Lee (June 1990)
$V_{ult,Lee}'$	modified total shear capacity based on the method by Lee (June 1990)
$V_{ult,mod}$	total shear capacity based on Cardiff method and modified for opening
$V_{u,model}$	maximum equilibrium shear load for model girders
V_{web}	shear force [capacity] of web
W_{eff}	effective section modulus
$W_{eff,mod}$	effective section modulus modified for opening
W_p	plastic section modulus of beam without opening
a	distance between transverse stiffeners
a_c	distance from vertical centerline of opening
a_h , a_t	length of sub-panels in stressed skin design
a_t	width of tension field
b_c	width of compression field
b_e	restored width of tension field
b_f	width of flange
c	distance defining position of hinge in flange
c_a , c_h	vertical and horizontal center distance between openings, respectively
c_r	distance defining position of hinge in reinforcement

C_{rel}, C_{rel}	ratio between two factors that are compared, ratio that is adjusted
C_1	function, factor
C_2	function, adjustment factor
$C_{2,b}$	adjustment factor for bottom tee
$C_{2,basic}$	adjustment factor for a single opening without stiffening
$C_{2,bf}$	adjustment factor for bottom tee for a fictitious opening
$C_{2,f}$	adjustment factor for a fictitious opening
$C_{2,I}$	adjustment factor for a single opening
$C_{2,II}$	adjustment factor for a fictitious opening
$C_{2,off-set}$	adjustment factor for a single opening without stiffening, located eccentric to the horizontal centerline of web
$C_{2,off-set,circ}$	adjustment factor for a single circular opening without stiffening, located eccentric to the horizontal centerline of web
$C_{2,off-set,f}$	adjustment factor for a fictitious opening without stiffening, located eccentric to the horizontal centerline of web
$C_{2,r}$	adjustment factor for a single opening with horizontal reinforcement
$C_{2,s}$	adjustment factor for a single opening with sleeves or doubler plates
$C_{2,t}$	adjustment factor for top tee
$C_{2,t,f}$	adjustment factor for top tee for a fictitious opening
$C_{2,two}$	adjustment factor for two openings
C_3	function, factor
d	distance between vertical members in a Vierendeel girder
e	eccentricity of opening
f_y	yield stress
$f_{y,red}$	reduced axial stress
h	depth of cross section, height of web
h_m	effective width for normal and bending stress
h_n	shortest length of shear failure lines
h_s	distance from stiffener toe to shear centre
h_{st}	dimension for stiffeners, sleeves, doubler plates or horizontal reinforcement
k_a	reduction factor for webs with doubler plates
k_{model}	secant stiffness of model girders
k_{test}	secant stiffness of test girders
k_τ	shear buckling coefficient
$k_{\tau,mod}$	shear buckling coefficient modified for opening
l	buckling length, anchoring length
l_{min}	minimum anchoring length
l_s	connection length between compression and tension fields and flange
m_o	weight of removed plate material in opening
m_s	weight of vert. stiffeners, sleeves, doubler plates and horizontal reinforcement
p_0	opening parameter
q_{fl}	shear flow from web to flanges above and below opening
$q_{fl,nom}$	nominal shear flow from web to flanges above and below opening
$q_{r,o}$	shear flow from horizontal reinforcement to web above and below opening
$q_{r,a}$	shear flow from horizontal reinforcement to web along the anchoring length

C_{rel}, C_{rel}'	ratio between two factors that are compared, ratio that is adjusted
C_1	function, factor
C_2	function, adjustment factor
$C_{2,b}$	adjustment factor for bottom tee
$C_{2,basic}$	adjustment factor for a single opening without stiffening
$C_{2,bf}$	adjustment factor for bottom tee for a fictitious opening
$C_{2,f}$	adjustment factor for a fictitious opening
$C_{2,l}$	adjustment factor for a single opening
$C_{2,lI}$	adjustment factor for a fictitious opening
$C_{2,off-set}$	adjustment factor for a single opening without stiffening, located eccentric to the horizontal centerline of web
$C_{2,off-set,circ}$	adjustment factor for a single circular opening without stiffening, located eccentric to the horizontal centerline of web
$C_{2,off-set,f}$	adjustment factor for a fictitious opening without stiffening, located eccentric to the horizontal centerline of web
$C_{2,r}$	adjustment factor for a single opening with horizontal reinforcement
$C_{2,s}$	adjustment factor for a single opening with sleeves or doubler plates
$C_{2,t}$	adjustment factor for top tee
$C_{2,tf}$	adjustment factor for top tee for a fictitious opening
$C_{2,two}$	adjustment factor for two openings
C_3	function, factor
d	distance between vertical members in a Vierendeel girder
e	eccentricity of opening
f_y	yield stress
$f_{y,red}$	reduced axial stress
h	depth of cross section, height of web
h_m	effective width for normal and bending stress
h_n	shortest length of shear failure lines
h_s	distance from stiffener toe to shear centre
h_{st}	dimension for stiffeners, sleeves, doubler plates or horizontal reinforcement
k_d	reduction factor for webs with doubler plates
k_{model}	secant stiffness of model girders
k_{test}	secant stiffness of test girders
k_τ	shear buckling coefficient
$k_{\tau,mod}$	shear buckling coefficient modified for opening
l	buckling length, anchoring length
l_{min}	minimum anchoring length
l_s	connection length between compression and tension fields and flange
m_o	weight of removed plate material in opening
m_s	weight of vert. stiffeners, sleeves, doubler plates and horizontal reinforcement
p_0	opening parameter
q_{fl}	shear flow from web to flanges above and below opening
$q_{fl,nom}$	nominal shear flow from web to flanges above and below opening
$q_{r,o}$	shear flow from horizontal reinforcement to web above and below opening
$q_{r,a}$	shear flow from horizontal reinforcement to web along the anchoring length

q_s	shear flow from web to sleeves and doubler plates
r	radius, polar coordinate
r_{red}	reduced radius
s_b, s_{bf}	depth of bottom tee, depth of bottom tee for a fictitious opening
s_t, s_{tf}	depth of top tee, depth of top tee for a fictitious opening
t, t_f	thickness of web, thickness of flange
t_{st}	dimension for stiffeners, sleeves, doubler plates or horizontal reinforcement
w	leg length of weld
z, z_t	distance from centroid of section, distance from centroid of top tee
α	ratio between flange area and web area without opening
α	relative (reduced) slenderness
α_L	factor for the position of the inflexion point for secondary moments
α_c	cut-off factor
$\alpha_{c,s}$	cut-off factor for openings with sleeves or doubler plates
$\alpha_{c,r}$	cut-off factor for openings with horizontal reinforcement
β	factor for the effect of sleeves, doubler plates or horizontal reinforcement
γ_{M0}, γ_{M1}	partial factors
δ	diameter of imaginary central circular opening, tip displacement
ε	yield stress factor
η	coefficient
θ	angle, polar coordinate, inclination of tension field
θ_d	inclination of panel diagonal
θ_m	optimum inclination of tension field
$\bar{\lambda}_w$	relative (reduced) slenderness of web
$\bar{\lambda}_{w,G}$	relative (reduced) global slenderness of web
$\bar{\lambda}_{w,G,im}$	relative (reduced) slenderness of web including the interaction between global and local shear buckling
μ	weight ratio
μ_B	weight ratio for girder "B", i.e. a girder that is compared
μ_t	function of geometry and yield stress for reinforced top tee
ν	Poisson's ratio
$\bar{\nu}_t, \bar{\nu}_t$	aspect ratio of top tee, modified aspect ratio of top tee
ξ_A	normalized flange force ratio in girder "A", i.e. a reference girder
$\xi_{A,elastic}$	normalized flange force ratio in girder "A", based on linear analysis
$\xi_{A,N}$	normalized flange force ratio in girder "A" at position "N"
ξ_B	normalized flange force ratio in girder "B", i.e. a girder that is compared
$\xi_{B,N}$	normalized flange force ratio in girder "B" at position "N"
ξ_w	function, additional flange force factor
σ	bending stress, axial stress, normal stress
σ_{compr}	compressive stress
σ_{cr}	[elastic] critical stress
$\sigma_{cr,T}$	[elastic] critical torsional stress

$\sigma_e, \sigma_{e,red}$	equivalent (von Mises) stress and reduced equivalent stress, respectively
$\sigma_{l,1}, \sigma_{h,1}$	stress at low and high moment end, respectively, due to primary moment
$\sigma_{principal}$	principal stress
$\sigma_r, \sigma_\theta, \tau, \theta$	stresses around a small circular opening
$\sigma_t, \sigma_{tension}$	tensile membrane stress and tension stress, respectively
$\sigma_{tl,2}$	stress in top tee at low moment end due to secondary moment
$\sigma_{th,2}$	stress in top tee at high moment end due to secondary moment
$\sigma_{t,y}$	membrane stress producing yield
σ_1, σ_2	principal stresses
τ	shear stress
τ_{cr}	critical shear stress
$\tau_{cr,G}$	critical global shear stress for thin orthotropic plate
$\tau_{cr,mod}$	modified critical shear stress
τ_k	reduced shear stress
$\tau_{k,G}, \tau_{k,L}$	reduced global shear stress and reduced local shear stress, respectively
τ_s	yield shear stress
τ_t	shear stress in top tee
τ_y	yield shear stress
τ_1, τ_2, τ_3	local shear stress in sub-panel 1, 2 and 3, respectively
ϕ	inclination of tension field
χ_f	factor for the contribution to shear capacity from flanges
χ_w	buckling reduction factor for shear capacity of web
$\chi_{w,mod}$	modified reduction factor for shear capacity in ULS
$\chi_{w,mod,A}$	modified reduction factor for girder "A", i.e. a reference girder
$\chi_{w,mod,ALS}$	modified reduction factor in ALS
$\chi_{w,mod,B}$	modified reduction factor for girder "B", i.e. a girder that is compared
$\chi_{w,mod,basic}$	modified basic reduction factor
$\chi_{w,mod,G}$	modified reduction factor based on the proposed design guidelines
$\chi_{w,mod,R}$	modified reduction factor based on rotated stress field theory
$\chi_{w,mod,red}$	modified reduction factor from girder simulations, reduced for model inaccuracy
$\chi_{w,mod,SLS}$	modified reduction factor in SLS
$\chi_{w,mod,V}$	modified reduction factor from Vierendeel theory
ψ	inclination of compression field

Chapter 1

Introduction

1.1 Background

Plate girders are common structural elements in the deck structures of Norwegian offshore platforms. These platforms are producing large quantities of oil and gas and the space available for process equipment is very limited. Often drilling operations are performed simultaneously, requiring also processing of drilling mud and various chemicals. It is inevitable that process pipes, electrical and instrumental cables and ventilation ducts have to be routed through the girder webs. Manholes for access are also required. The height of the girders is usually restricted due to demand for free space below, and the amount of steel used should be kept to a minimum in order to save weight.

The setting of the problem may be illustrated by a structural drawing from the Drilling module on the Snorre B platform. See Fig 1.1. This drawing shows 1/8 of the total "secondary main" plate girder webs in the double bottom of the drilling module. Here, the double bottom consists of a bottom deck plate and a cellar deck plate that are connected by 1500 mm high webs, or bulkheads, at a spacing of 3125 mm.

The secondary main structure also includes a main deck located eight meter above the cellar deck. The drilling module comprises about 50 % of the Snorre B topside structure, the rest includes the Utility module with 25 % and the Process module with 25 %. Total number of openings in the drilling module is about 866 smaller openings for pipe, cables and ducts and 121 larger openings for access or ventilation. Many of the smaller openings are in deck plates, but the total number of web openings in Snorre B are estimated to 300 smaller openings and 200 larger openings of the manhole type.

Processing of oil, gas and mud are by far the most important activities on an offshore platform. Restrictions on size and location of web openings imposed from a structural point of view, are hardly accepted if they interfere with a smooth lay-out of the process equipment. Hence the openings may come in areas with both high normal stress from bending moment and high shear stress. Further they may be located anywhere between the top and bottom flange of a girder. Two openings may well be located close to each other. Many pipes must have a certain inclination, which means that all openings are located at different heights if these pipes penetrate several girders. The highest position of an opening may be very close to the top flange of the girder. In such cases weld-in stiffening around the opening, i.e. a sleeve, will not be feasible due to poor access for welding or sand blasting.

Design calculations for the web openings on Snorre B Drilling module were based on normal and shear stresses in the web without the openings, and the stress modifications due to the openings were based on Vierendeel action above, below and between the openings. In the double bottom the girder flange area was calculated from the effective width of the deck plates. On the compression side this lead to relatively small flanges. Hence, the webs also had to carry normal stresses in order to get sufficient moment capacity. In the main deck the girders had ordinary flanges.

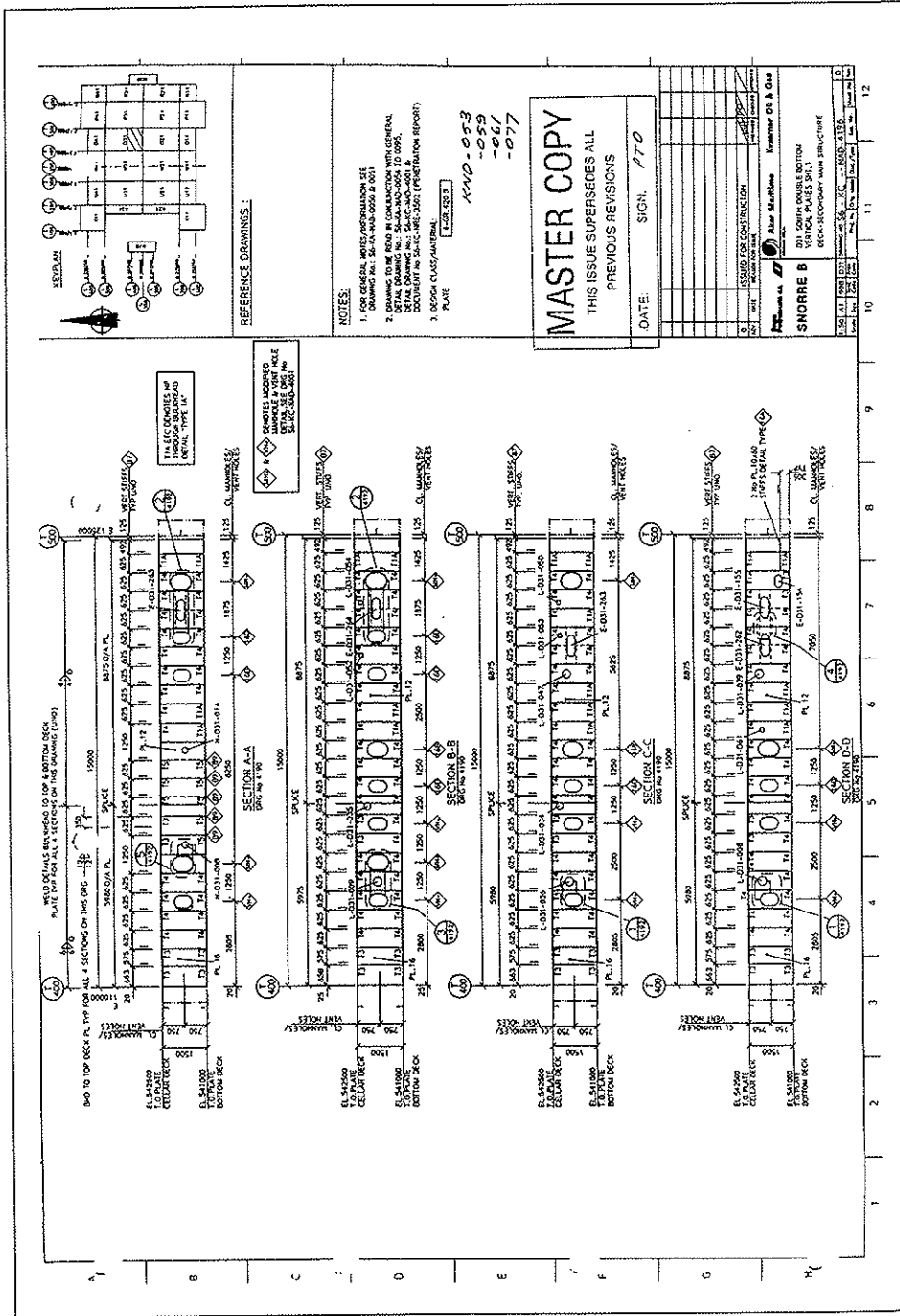


Fig. 1.1 Part of Snorre B topside double bottom

Design calculations were in principle performed for all web openings, excluding only a few that were obviously OK by inspection. A spreadsheet was established to facilitate the calculations, but the amount of calculation work was still high, representing several hundred man-hours.

It is assumed that the design calculations, as described, are conservative. For ultimate and accidental limit state they are probably very conservative as non-linear actions such as tension fields and plastic mechanisms were not considered. On the other hand, the effect of such actions may only be fully utilized in the accidental limit state, as there are restrictions to girder deflections imposed by processing requirements.

A conservative approach to design calculations means that a girder may have got thicker webs, more stiffeners, web inserts and sleeves than it really required. This in turn leads to more weight, more fabrication costs and less processing and storage capacity for the oil and gas platform. The importance of more theoretical knowledge applied to practical problems and solutions seems clear.

In this investigation the term "opening" is used in the meaning of a web penetration, cut-out or hole. The term is consistent with the use in ENV 1993 Annex N (1998).

1.2 Objectives

The present investigation has three primary objectives:

- To obtain efficient and reliable numerical models in order to perform numerical simulations.
- To establish criteria for determination of the shear force capacity in the ultimate limit state and in the accidental limit state.
- To perform numerical simulations using the non-linear finite element program ABAQUS and establish a set of guidelines and a simple formula that will cover a wide range of web openings with a minimum of calculations.

Simplicity of method is highly desirable because the value of any calculation decreases sharply if it is not completed before the design is frozen. Maybe 80 % of all web openings are of a relatively small size, or they are located in positions where the shear capacity is far from fully utilized. It would be more convenient to check girders with such openings based on design guidelines in combination with a simple formula, than on comprehensive calculations.

The main design effort can then be concentrated upon the more complicated configurations. Presumably there will be so many variations of these, that a general design formula to cover them all, will be very hard to find. In such cases a dedicated FE-model should be the best solution. In order to make this non-linear FE-model most efficient, the results from the simulations should be helpful and give more insight in the important parameters and mechanisms.

The main tasks of the present investigation are:

1. To study existing rules and load-carrying theories
2. To make non-linear FE-models using the finite element program ABAQUS. Results from experiments of large plate girders at Norwegian Institute of Technology (NTH) will be used to calibrate the FE-models. FE-models of some test girders have already been developed by Bergsholm (1999), who also compared the numerical simulation results with the test results. Further investigations will be done to study the effect of element size and meshing.
3. To establish criteria for determination of shear capacities. Traditionally, extensive plastification is not tolerated in ultimate limit state design of offshore structures, whereas it is fully accepted in accidental limit state design.
4. To carry out numerical simulations of FE-models with various configurations of web openings. Factors that should be varied are:
 - number of openings
 - web slenderness ratio
 - girder flanges
 - size of openings
 - height position of openings
 - distance between openings
 - sleeves and doubler plates
 - vertical stiffeners
 - horizontal reinforcement
 - bending moment in girder

Configurations similar to Snorre B may be found amongst a few of the simulations, but in general the simulations are not linked to a specific offshore project.

5. To establish a set of design guidelines and simple equations that will cover a large amount of openings with a minimum of calculations.
6. In view of the experience gained from the experiments, to discuss mechanisms and effects that are important in the analysis of complicated configurations involving two or more openings close together.

Chapter 2

Previous studies

2.1 Introduction

In the present chapter a brief survey of previous studies is given, while more detailed descriptions of the most important load-carrying theories are presented in Chapter 3. The survey is divided into two groups; stocky webs and slender webs. Such grouping has been the traditional approach and is connected to shear buckling of webs without openings. To obtain a simplified design approach for webs with openings it would be desirable to merge the two groups. A first step in this direction is done in Section 2.4, where theories suitable for all webs are listed. In Section 2.5 a short description of the stressed skin method is presented. This method may be useful in the further development of methods for webs with openings.

2.2 Stocky webs

Webs without openings are stocky if yield shear stress can develop in the full web height. Hence no shear buckling takes place. This is the case for webs with low height-to-thickness ratio h/t , as in rolled beams and in welded girder with webs in class 1, 2 or 3. For webs of steel with yield stress $f_y = 420 \text{ N/mm}^2$, simple support of all edges and no transverse stiffeners, the limiting ratio is $h/t = 65$. Lower yield stress increases the limit to about 80. Webs in class 4 are also stocky, if transverse stiffeners prevent shear buckling. An example is the Snorre B girders shown in Fig 1.1.

The definition is not altered if openings are present. However, both global shear buckling and local buckling are assumed to take place in stocky webs with openings, before yield shear stress is developed.

For h/t ratios up to 80 and without transverse stiffeners, several analytical methods for calculation of the shear capacity of webs with openings have been developed.

The earliest methods are based on allowable stresses and elastic theory. Bower et al. (1971) published a report on the work and recommendations of a sub-committee of the Structural Division of the ASCE. The work by Bower and also by Redwood (1973) were the basis for a recommendation made by Constrado (1977), which has been used in Norwegian offshore industry. The recommendation considers un-stiffened circular and rectangular openings with diameter or height up to $0,50h$. Some cases of multiple openings are also covered.

In the 1960s methods based on strength criteria and plastic theory came more into use. Bower et al. (1971) considers also such methods. The research continued in the 1970s and 1980s. Surveys made by Redwood (1983) and Darwin and Donahey (1988) review design procedures and contain worked examples and an extensive bibliography for both unreinforced and reinforced circular and rectangular openings. Among the benefits of this research was the realization that a single design approach can be used for both unreinforced and reinforced openings. If reinforcement is needed, horizontal bars above

and below the opening are fully effective. Vertical bars or bars around the opening periphery are neither needed nor cost effective. The approach is included in a guide to design steel and composite beams with web openings, published by the American Institute of Steel Construction: AISC (1990) covers circular and rectangular openings with diameter or height up to $0,70h$, with or without reinforcement. Multiple openings are also covered. In Europe, ENV 1993 Annex N (1998) has provisions for webs with openings up to $0,75h$. Single and multiple, circular and rectangular openings are covered. Rules for girders in ships are given in DnV (1993).

Buckling may occur in stocky webs for un-stiffened openings in the upper h/t ranges. It may be difficult to say if this buckling is of global or local nature. Uenoya and Redwood (1977) studied elasto-plastic buckling of square plates for a wide variety of un-stiffened circular opening sizes and h/t ratios. The study showed that for openings smaller than $0,30h$ the shear capacity is reduced with the factor $(1-D/h)$, where D is the diameter of the opening. This corresponds to the reduction, which follows from the minimum shear area above and below the opening. Hence such openings need no stiffening. For the larger openings the reduction is more than $(1-D/h)$, due to yielding or local buckling from Vierendeel action. Stiffening around the opening might then compensate for the extra reduction. Uenoya and Redwood (1978) studied elasto-plastic buckling of webs with un-stiffened rectangular and circular openings. Heights of the openings were about $0,30h$ for rectangular openings, and diameters were $0,50h$ and $0,60h$ for circular openings. Both in-plane bending and shear were considered. One of the results was that for h/t ratios below 50, the opening shapes and sizes considered do not lead to buckling prior to the development of full plastic strength. In the previous design guides local buckling are prevented by requirements to height-thickness ratios of outstand elements around the opening. AISC (1990) appears to be more liberal than ENV 1993 Annex N (1998). DnV (1993) has no specific requirements to buckling, but states that “[openings] in girders will generally be accepted provided the shear stress level is acceptable and the buckling strength is sufficient”. A similar requirement is included in DnV (2004).

Stocky webs in class 4, i.e. with transverse stiffeners close together, have been studied by Lee, Kamtekar and Little (1989). 52 tests of perforated webs subjected to in-plane bending and shear are described. All but two of the webs had an aspect ratio a/h of 0,7 and each web had a centrally placed opening. The h/t ratios varied between 90 and 180, and this means that some webs were stocky by way of the transverse stiffeners and other were slender. The openings had unreinforced edges and were of either circular or elongated circular shape. The effect of varying the shear/moment ratio in the panel on its strength was studied. Stresses in one test panel were calculated from strain measurements at loads up to collapse. It was found that the experimental results for the stockiest plates could be reasonably predicted using an existing approach based on simple plastic theory.

2.3 Slender webs

Webs without openings in general

Slender webs are defined as all webs that are not stocky. The shear capacities depend on the web yield stress and modulus of elasticity, the h/t ratio, and the aspect ratio a/h as well as the boundary conditions of the web edges.

Unlike columns, which actually are on the verge of collapse as their buckling stage is approached, the slender panels of a plate girder web, bounded by all sides by the girder flanges and transverse stiffeners, are capable of carrying loads far in excess of their critical shear load. Upon reaching the critical load, very slight lateral displacement will have developed in the web. However, they are of no structural significance, because other mechanisms are still present to assist in resisting further loading. When transverse stiffeners are properly spaced and strong enough to act as compression struts, membrane stresses, due to shear forces greater than those associated with the critical buckling load, form diagonal tension fields. The resulting combination in effect provides a truss action, which, without producing yield stress in the steel, furnishes the capacity to resist applied shear forces unaccounted for by the linear buckling theory.

A definition of terms may be useful:

- [Elastic] critical load = load in a component at which the component becomes unstable when using small deflection elastic theory of a perfect structure. In this linearised model a bifurcation takes place when the critical load is reached.
- Buckling capacity = load capacity of a component when post-critical actions are accounted for. Basically, the buckling capacity is limited by the material yield stress and acceptable displacements of the component.

By this definition, terms as “initial buckling load” and “post-buckling capacity” should be avoided.

The existence of post-critical shear capacities in webs without openings has been known since about 1880. Rode (1916) discussed a partial tension field and proposed a field width of 50%. A pure tension field theory proposed by Wagner (1929) is only suitable for structures where extremely thin plates are attached to very rigid boundary elements. This is the case for instance in aircraft structures or for an inner panel in a plate with rigid cross-beams and stiffeners. Further development of diagonal tension methods for aircraft structures is described by Kuhn, Peterson and Levin (1952).

For civil engineering purpose, the major break-through for analytical methods based on tension field action was achieved by Basler and Thürlimann. The methods are described in Basler and Thürlimann (Aug. 1961), Basler (Oct. 1961a) and Basler (Oct. 1961b). Since then several researchers have developed alternative and refined methods which have been corroborated in extensive test programs. The difference between these methods are mainly due to various assumptions of how the tension field is attached to the edges of the web, and about the bending stiffness of the flanges. In the model by Basler and Thürlimann the flanges are assumed to have small bending stiffness and hence the tension field is attached only to the transverse stiffeners. The Cardiff method, described by Porter, Rockey and Evans (1975), utilizes the moment capacity of the flanges and assumes the tension field to be attached both to the flanges and transverse stiffeners. In 1981 Cescotto et al. made numerical simulations of plate girders by means of a non-linear finite element program in order to evaluate several tension field models. The conclusion referred by Dubas and Gehri (1986) was that the Cardiff method gave the best estimates of shear capacity compared to experimental results. NS-ENV 1993-1-1 (1993) uses the Cardiff method or, alternatively, a simple post-critical method. However, in the further development of Eurocode 3, the Cardiff method has been deleted as it gives inaccurate results for certain aspect ratios.

In stead of using the tension field method explicitly, the post-critical capacity can be utilized implicitly through the term “simple post-critical strength”. This method allows

higher values of the global shear buckling stress than the critical stress values. The amount of post-critical shear capacity is mostly based on empirical results. There are also variations between different codes. Alternatively, some codes allow for post-critical action by using the critical shear stress and applying lower safety factors in design checking for such cases.

The simple post-critical shear capacity of webs need not be based on empirical results only, but can be developed from the so-called rotated stress field method, which is due to Höglund (1971) and Höglund (1973). Rod systems are used to model the stress pattern and to calculate the shear capacity. Originally, this method was developed for girders with web stiffeners at the supports only, a structure for which other tension field methods are very conservative. In 1972 there was only two tests available for ratios $h/t > 210$ and no intermediate stiffeners. In Höglund (1973) the allowable shear strengths were reduced for the large slenderness ratios because of the low number of tests. Since then a number of tests have been made, showing that this reduction is not needed. Höglund (1997) reports on shear buckling capacity of steel and aluminum girders and states that the rotated stress field method, with some modifications, was found to give the best agreement with 273 tests on steel plate girders as well as 93 tests on aluminum alloy plate girders in shear. The method is simple to use and is applicable to un-stiffened, transversally and longitudinally stiffened flat plate webs and also to trapezoidally corrugated webs.

Critical shear stresses

Uenoya and Redwood (1977) studied critical shear coefficients for simply supported and clamped plates with circular openings of various sizes. For the range of practical interest, they proposed a formula for any rectangular panel with a central opening. Narayanan and Der Avanessian (1984b) studied critical shear stresses of simply supported plates as well as clamped plates, and suggested approximate design formulae for the practical cases where the openings were not greater than $0,50h$. Openings were circular, rectangular, central, eccentrically, unstiffened or reinforced. Critical shear stresses for reinforced openings were treated by Narayanan and Der Avanessian (1983b).

In the lower h/t ranges of slender webs, failure/collapse will take place as elasto-plastic shear buckling. Uenoya and Redwood (1978) studied elasto-plastic shear buckling of square plates with un-stiffened circular openings.

Simple post-critical method.

No literature describing the use of simple post-critical methods for webs with openings has been found.

Rotated stress field method

Höglund also has developed his rotated stress field method to cover un-stiffened webs with openings. In Höglund (1970) tests are described for welded girders with h/t ratios from 200 to 300. Circular and rectangular openings without local stiffening are included. The girders had pure shear and combinations of moments and shear. Two design methods are described: The first method is based directly on the rod system that is a main idea of the

rotational stiffness method. The second method is a modified version of the Vierendeel method, in order to cover cases with large openings and cases with shear and moment. A brief description of openings with reinforcements is also given. Further, a set of provisions is given for design of openings in pre-fabricated girders from a fabricator of welded girders.

Tension field methods

When an opening is present in a web designed according to tension field theory, the tension field may be reduced, relocated to another position or otherwise disturbed. Smaller openings may not have any influence on the shear capacity.

AISC (1978) uses an indirect form of the Basler method for webs without openings. When this tension field method is used, openings should not be "large". If openings are large, only the critical shear capacity shall be utilized. The thickness of the particular field must be increased if required, or more transverse stiffeners provided. Large opening is here taken to mean a circular opening with diameter more than $0,15h$.

Based on the Cardiff method, Narayanan (1983a) describes theoretical methods of computing the shear capacity of webs containing circular or rectangular openings. The reinforcement required to restore the strength lost by the introduction of the openings is discussed. The ultimate capacity is computed as the sum of four contributions; 1) the critical load, 2) the load carried by the membrane tension, 3) the load carried by the flange and 4) the load carried by the reinforcement, if any. The results of some 70 ultimate load tests on girders containing various forms of openings are summarized. The h/t ratios were 250 and 360 with aspect ratios of 1,0 and 1,5. Maximum opening diameter was $0,90h$. The strength predictions obtained by the theory proposed are shown to be sufficiently accurate in comparison with the values observed in test girders.

Subsequent papers by Narayanan and Der Avanessian elaborate on certain aspects of the proposed methods, but basically the methods are as already described in Narayanan (1983a). In Narayanan and Der Avanessian (1983b) a revised critical shear coefficient for webs with rectangular openings is proposed, and in Narayanan and Der Avanessian (June 1983) another one is proposed.

Narayanan and Der Avanessian (March 1984) extend the method to an un-reinforced circular opening located right in the corner of a web panel, but away from the tension field. Basically the method is the same as in Narayanan (1983a). A small opening in the corner is found to have only minor effect on the total shear capacity. Here, an opening is small if the diameter is less than $0,30h$. Its main effect is to reduce the critical shear stress. A reduction in the critical shear strength slightly increases the strength of the tension field. Hence the total effect is minor and the paper proposes a simplified expression for the shear buckling capacity proportional to the ratio $(1-D/h)$ compared to the web without openings. This is also conservatively applicable when the opening is central. Large openings modify the behavior compared to a web without opening and cause the tension band to form in an eccentric position. In this case the tension band is anchored at one end mainly to a flange plus a short end of stiffener and at the other end mainly to a stiffener plus a short length of flange.

In Narayanan and Der Avanessian (1984b) the authors elaborate on the background for the various reduced critical shear coefficients they have used in their earlier papers. One reason that the formulae proposed in the other papers vary, is because different approximations are better for small openings than for large openings. Narayanan and Der

Avanessian (June 1984) report on further tests of reinforced circular openings and reinforced rectangular openings. Narayanan and Der Avanessian (April 1985) is a shortened version of earlier papers, with detailed refinement of some of the expressions. It concentrates on small rectangular openings, both un-reinforced and reinforced.

Narayanan and Darwish (1985) extend the method described in Narayanan and Der Avanessian (March 1984) to cover openings that are neither central nor in the compression corners of the web panel. Cases of small or large openings are considered. Tests with square and circular openings at various points in square panels are compared with the theory. A simple design method is also justified, in which linear interpolation is used between central and corner positions. For the corner position 90 % of the capacity without opening is adopted, but this is only applicable to small openings.

Key points of the method are also included in ECCS Publication 44 by Dubas and Gehri (ed.) (1986). Here, another expression for the shear buckling capacity of webs with rectangular openings is proposed.

In *Constructional Steel Design – An International Guide*, Maquoi (1992) proposes to use the simplified method by Narayanan and Darwish (1985) for eccentric openings in panels for aspect ratios from 0,8 to 1,25, which he assumes to have been the investigated range. However, in the paper by Narayanan and Darwish the panels all had the aspect ratio of 1,0. It also introduces a limit of validity for non-central openings in the form of a figure showing a permissible region. This region leaves a clearance of $0,35x$ from the compression flange and from the stiffener where the tension band meets the tension flange and a clearance of $0,10x$ from the tension flange and the other stiffener, where x is the lesser panel dimension. It is assumed that this is taken from an earlier German recommendation and not from the paper by Narayanan and Darwish. Quite contrary, Narayanan and Darwish (1985) indicated that an opening right in the corner away from the tension band gives the smallest reduction in the shear buckling capacity of the panel, without any distinction between tension and compression flanges.

For webs with openings and where tension field action is utilized, ENV 1993 Annex N (1998) has provisions for girders with web openings up to $0,75h$. Aspect ratio must be between 1,0 and 3,0. Circular and rectangular openings are covered. CEN (1995) is a background note for the recommendations in ENV 1993 Annex N (1998). However, as the rules for webs without openings that were based on the Cardiff-method, now is deleted from Eurocode 3, it may be expected that the provisions will also be deleted from ENV 1993 Annex N (1998).

Other methods

Narayanan and Rockey (1981) describe a theory for computing the shear capacity of webs with circular openings and present a design method. The h/t ratios tested were 250 and 360 and aspect ratios 1,0 and 1,5. Maximum opening diameter was $0,80h$. The shear capacity was found to vary linearly with the factor $(1-D/h)$. The concept or model of the opening as interrupting the tension field does not appear in this paper, neither does its effect on the critical shear capacity.

The checkerboard method and the doubler plate method are described by Buckland, Bartlett and Watts (1988).

An experimental study by Lee, Kamtekar and Little (1989) comprises webs with ratios $h/t = 90$ and $h/t = 180$ and aspect ratios 0,7. The former belongs to the stocky web category. The openings were circular or elongated and had un-reinforced edges. The approach based on simple plastic theory methods, which was successfully used for stocky webs, could not be applied to the more slender panels. The method based on the tension field approach, proposed by Narayanan and Der Avanessian, was unable to predict the failure loads of the panels.

An alternative to tension field methods is presented in Lee (Feb. 1990). The girders considered had transversely stiffened webs with aspect ratios between 0,7 and 1,5. Height-thickness ratios were about 120, 180, 300 and 370. Openings were centrally located and of circular, rectangular and elongated shapes. The ultimate shear capacity is determined using a theoretical model developed on the basis of stress fields and load-carrying mechanisms observed experimentally from test results, numerically from finite element calculations and simplified to allow for variations in web and opening size. The predictions obtained from the theory are compared with experimental and numerical results available, and it is found that the theory provides reasonably accurate estimates.

Experiments

A comprehensive experiment program was performed at The Norwegian Institute of Technology (NTH) in the years 1978-85 in order to map the parameters that influence the shear capacity of slender plate girders with large web openings. The most important parameters in this program were the size and location of the web opening and the design of various types of stiffening. The experiments are further described in Chapter 4.

2.4 All webs

Some of the methods referred in Section 2.3 are applicable for all webs:

- Rotated stress field method
- Modified Vierendeel method
- Checkerboard method
- Doubler plate method

2.5 Stressed skin

The notation “stressed skin” has its origin from metal sheeting on buildings used as diaphragms to avoid use of bracings. The stressed skin method must not be intermingled with tension field methods. In Norwegian offshore industry it is common practice to use the stressed skin method for design of living quarters and other topside modules.

In stressed skin design the following basic assumptions are made:

- The plate panels of walls and decks are assumed to resist shear stresses only. This means that all normal stresses from membrane actions, including tension stresses, are ignored in the panels.
- Normal stresses are carried by defined axial elements. In living quarters these elements are columns, deck girders and panel edges such as wall to floor connections etc. In the heavier module structures these elements are columns, deck girders and wall trusses.
- Shear forces may be assumed to be redistributed to obtain equal shear flow over the total height or length of a panel.

The stressed skin method is described by Solland and Frank (1988). A typical panel may consist of 6 mm plane steel plate of $h = 3200$ mm with several transverse stiffeners on one side having center to center distances $a = 625$ mm. This gives $h/t = 104$ and $a/h = 0,20$ for each sub-panel. The length of the total panel is usually longer than the height.

Although an efficient stressed skin design requires consideration of ultimate strength and allowance for post-critical behavior of the plate panels, it is not common to utilize pure tension field methods in the design of such panels. But the possible development of tension fields is a main reason to believe that the stressed skin method leads to a safe design.

Discussion of the stressed skin design method as such, is not the scope of the present investigation. However the basic assumptions show much similarity with a beam or plate girder, if the web is assumed to carry shear force only and the flanges are assumed to carry moments. For panels designed by the stressed skin method, Solland and Frank (1988) describe a method of design of local reinforcement around square and rectangular openings. Such design will be of interest in the present investigation and the method is therefore described in more detail in Section 3.10.

Chapter 3

Review and evaluation of load-carrying theories

3.1 Introduction

This chapter describes the most important load-carrying theories for beam and girder webs with openings. The term “beam” is used for I-shaped sections where it is presumed that no buckling of web and flanges occur. The term “girders” is used for all other I-sections.

The starting point is the state-of-the-art methods for beams. Section 3.2 and 3.3 describe two principles; design based on allowable stresses and design based on strength criteria. The opportunity is taken to explain the basic terms and concepts connected to webs with openings. Buckling is not described as such, but requirements to ensure that buckling does not occur, are given. For rectangular openings the design based on strength criteria can be considered as well established. Only minor developments should be expected in the future. For circular openings the current approach is to use a substitute rectangular opening.

For girders, where global and local buckling can occur, the existing load-carrying theories and design methods are described in a sequence that “advance the solution” by continuation. The idea is to start with the simplest methods involving only a few factors and add more methods and factors in small steps. The main objectives are; 1) a simple solution should not be overlooked and 2) good solutions should not be hidden in a morass of possible solutions involving a lot of factors. Hence Section 3.4 describes general stress concentration around circular and rectangular openings, assuming no buckling. Both elastic and plastic theories are covered. Section 3.5 describes simplified shear buckling based on post-critical behavior. This concept is developed for webs without openings. Similar concepts for webs with openings are scarcely found in the literature, but a possible extension to webs with openings is discussed. The rotated stress field method can be considered as an important step in that direction. This method includes plastic theory and is described in Section 3.6. For large rectangular openings a modified Vierendeel method may give better results than the rotated stress field method. The modified Vierendeel method is described in Section 3.7. Moment-shear interaction for both the rotated stress field method and the modified Vierendeel method is presented in Section 3.8. Tension field methods are included in Section 3.9. These methods presume web buckling beyond the critical stage and utilize plastic theory.

The stressed skin method is described in Section 3.10. This method utilizes simplified post-critical strength and plastic theory. It can be used for very thin webs. However it does not allow buckling beyond the simplified post-critical stage and a system of stiffeners around an opening is compulsory. A closely related method is the checkerboard method in Section 3.11.

By using doubler plates, the full shear capacity of a web can be restored. The doubler plate method is included in Section 3.12.

Section 3.13 covers the method proposed by Lee (June 1990).

A conclusion of all theories is included in Section 3.14.

To ensure a clear distinction between existing theories and my contribution to them, each section starts with the theories as described in the literature. My contribution is the discussions at the end of each section and the conclusion in Section 3.14.

3.2 Methods based on allowable stresses

3.2.1 General

The principle is: When global shear and moment are given in the center of an opening, shear and bending stresses in the sections at each end of the opening are calculated based on elastic theory. The design is accepted if the shear stresses, the bending stresses or combinations of those, all are below or equal to some allowable stress values.

Methods of analysis may conveniently be described in three categories; 1) analytical or numerical solutions of differential equations of the theory of elasticity, 2) finite element analyses and 3) approximate methods based on assumptions permitting various parts of the beams to be dealt with by elementary beam theory. Methods of the first and second category are referred in Redwood (1983). Analytical methods will always remain to be of interest, both from a historical point of view and because fundamental issues usually come to knowledge. Methods based on early use of finite element analyses are perhaps more doubtful. The performance of elements has improved and the numbers of elements that can be used in an FE-model have increased considerably since those analyses were made.

For the use in the present thesis, only the third category will be explained in some detail. The description may appear comprehensive for a method that ought to be replaced by other methods. But it should provide a good background to the subsequent descriptions. It also corresponds to the design approach that is used for many other and larger structures in Norwegian offshore industry.

3.2.2 Approximate analysis

When the term “allowable stress” is used, the loads are usually un-factored and all safety factors appear as reduction in the allowable stresses. But, the principles of the allowable stress methods are not altered if the term “design stress” is used. Safety factors are then split between factors that increase the loads and factors that reduce the design stress. Hence the method also corresponds to elastic design in the ultimate limit state.

The forces at an opening are depicted in Fig. 3.2.1 a) and b). Fig. a) shows the opening, and D_a and D_h are the length and the height of the opening, respectively. The global shear and moment acting at the vertical centerline through the opening are denoted V and M . The global moment is also called the primary moment. Fig. b) shows a more detailed picture. The part above the opening is denoted the top tee. It is subjected to shear V_t and secondary moments M_{tl} and M_{th} . The part below the opening is denoted the bottom tee. It is subjected to shear V_b and secondary bending moments M_{bl} and M_{bh} . The acting forces on the tees in the center of the opening are shown as filled arrows. The reaction forces at the tee ends are shown as open arrows. The subscripts t and b stand for top and bottom, and the subscripts l and h point to the low and high moment end of the opening. The terms “low moment end” and “high moment end” are related to the size of the primary moment at these positions. The term “tee” is used also for a reinforced section.

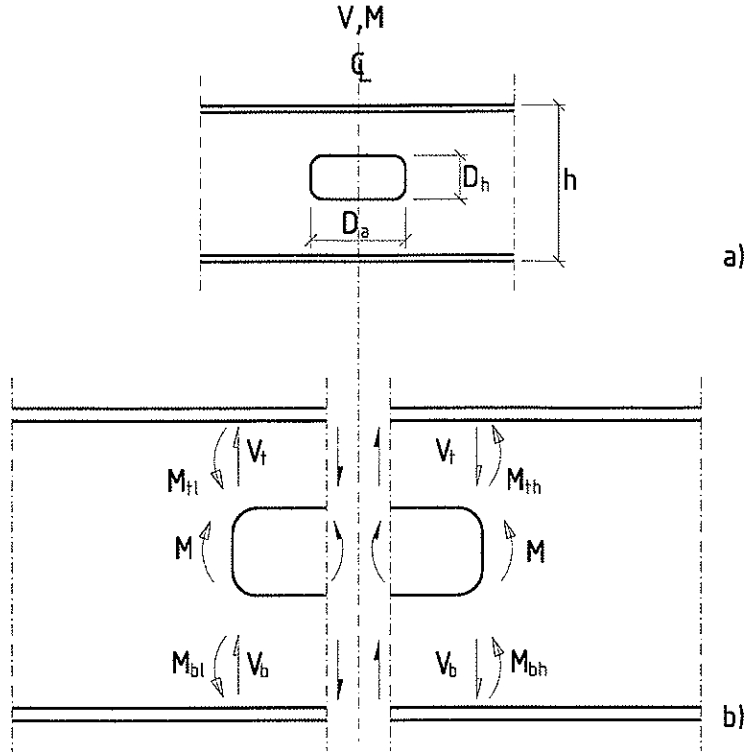


Fig. 3.2.1 Forces at web opening

Based on equilibrium

$$V = V_t + V_b \tag{3.2.1}$$

$$V_t = \frac{M_t + M_{th}}{D_a} \tag{3.2.2}$$

$$V_b = \frac{M_{bl} + M_{bh}}{D_a} \tag{3.2.3}$$

$$M_l = M - M_t - M_{bl} = M - \frac{VD_a}{2} \tag{3.2.4}$$

$$M_h = M + M_{th} + M_{bh} = M + \frac{VD_a}{2} \tag{3.2.5}$$

M_l and M_h are equal to the primary moments at the low and high moment end of the opening, respectively. Failure modes are shown in Fig. 3.2.2. The behavior depends on the ratio of primary moment-to-shear. For high primary moment-to-shear ratios the failure is approaching the pure bending mode. See Fig. 3.2.2. a). For medium and low moment-to-shear ratios the shear and secondary bending moments increase, causing increasing differential, or Vierendeel, deflection to occur through the opening. See Fig. 3.2.2. b).

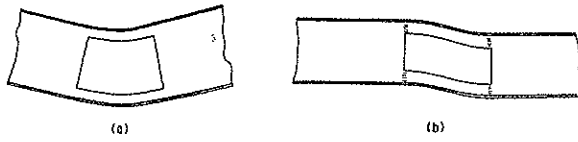


Fig. 3.2.2 Failure modes at web openings [from AISC (1990) Fig.5.2]

The bending stresses due to primary moments in each end are given by

$$\sigma_{l,1}(z) = \sigma_{h,1}(z) = -\frac{M}{I_{net}} z \quad (3.2.6)$$

where index "1" points to "primary". I_{net} is the second moment of area for the total net section at center of opening, that is including horizontal reinforcement, if any, and excluding the opening. z is the distance from the centroid of the net section, with positive direction upwards.

For the distribution of shear and secondary moments, the structure is static indeterminate. It is made static determinate by the following approximations; 1) the top and bottom shear are distributed according to local stiffness of the top and bottom tees and 2) the secondary moments are equal at each end of the top and bottom tees, respectively. The latter approximation implies that inflexion points are located in the middle of the top and bottom tees. This is often called the Vierendeel approach because of the analogy with calculation of Vierendeel girders.

The approximations result in the following equations

$$\frac{V_t}{V_b} = \frac{\frac{D_a^2}{12I_t} + \frac{3,1}{A_{wt}}}{\frac{D_a^2}{12I_b} + \frac{3,1}{A_{wb}}} \approx \frac{A_{wt}}{A_{wb}} \quad (3.2.7)$$

$$M_{tt} = M_{th} = \frac{V_t D_a}{2} \quad (3.2.8)$$

$$M_{bt} = M_{bh} = \frac{V_b D_a}{2} \quad (3.2.9)$$

I_t and I_b are the second moment of areas of the top and bottom tee. A_{wt} and A_{wb} are the web areas of the top and bottom tees.

The stresses in the top tee are

$$\tau_t(z_t) = \frac{V_t S_t}{I_t} \quad (3.2.10)$$

$$\sigma_{t,2}(z_t) = \frac{M_{tt}}{I_t} z_t \quad (3.2.11)$$

$$\sigma_{th,2}(z_t) = -\frac{M_{th}}{I_t} z_t \quad (3.2.12)$$

Index "2" points to "secondary". z_t is the distance from the centroid of the top tee, with positive direction upwards. S_t is the first moment of area for the top tee. The stresses for the bottom tee are similar.

Moment-shear interaction is handled by adding the bending stresses from the primary and secondary moments. Fig. 3.2.3 represents a typical result. Often the highest bending stresses at the opening edge occur in the low moment end, while the highest stresses in the flanges occur in the high moment end.

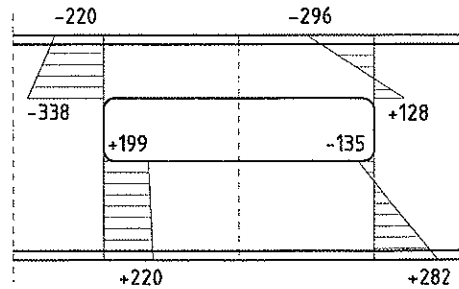


Fig. 3.2.3 Resulting bending stresses in both ends of a web opening.

Bending and shear stresses are combined by the von Mises criterion to check yield. The allowable stresses are usually given by some national or international code.

Local buckling must be checked. Post-critical capacities cannot be utilized, because this alters the section properties and disturb the assumption that the secondary moments are equal in low and high moment end. Hence, the flanges and reinforcement must comply with class 3 criteria for normal stresses. For un-stiffened parts of the web above and below openings, buckling check can be simplified by limits to the width-to-thickness ratio. Bower et al. (1971) recommends a limit of 16 for such parts.

At last, lateral buckling of the compression flange, vertical buckling of the tee in compression and transverse buckling of the reinforcement should be checked.

The deflections in Fig. 3.2.2 are exaggerated. Methods for calculating real deflections of beams with openings are proposed in the literature, but such calculations are usually not required when design is based on allowable stresses. Exceptions can be beams with very long openings and low primary moment-to-shear ratios.

Corner radii should be the greater of $2t$ and 16 mm to avoid excessive stress concentrations.

Concentrated loads above or below the opening should be avoided.

Circular openings are more difficult to analyze because the varying depth of the tees complicates the behavior under both moment and shear. Some methods commonly used to analyze stresses in haunched member connections can be used in conjunction with the assumption of inflexion points at the mid-length of the opening under pure shear. However, Bower et al. (1971) states that there is adequate information to use the described method for circular openings too, provided the circular opening is replaced by a rectangular opening whose height and length are $0,9D$ and $0,45D$, where D is the diameter of the circular opening.

Variations of the method are mainly connected to the following issues:

- Shear stress is taken as average shear stress in stead of the pure elastic stress given by Eqs. (3.2.10). This anticipates some plastic behavior.
- Simplification of the equations such that the effect of the opening can be given directly in terms of, for example, the height and length of opening and web and flange areas.
- To calculate the effect of the opening in terms of a reduced maximum allowable stress and to compare this stress with the stress in the beam that is computed on the basis of the gross section of the beam. Often such approaches are connected to the use of certain national codes.

3.2.3 Discussion

If openings are rectangular, the method explained follows strict elementary beam theory. Except for distribution of shear to the top and bottom tee and the Vierendeel approach, the calculation of stresses follows the path that is used in most linear finite element programs. The stress check is similar to the code check that is performed for the design of offshore structures by using SESAM, one of the most common finite element programs in Norway.

An alternative to the method is to make an FE-model of the opening including a part of the beam to each side. If a rectangular opening is modeled with a fine mesh and linear elements, the results are usually quite similar to results calculated by the described method. Such comparisons have given the method a good reputation amongst design engineers. In addition the method is easy to follow by hand calculations or to implement in a spreadsheet.

However the features described for an FE-analysis are not necessarily a proof of the quality of the method. Two main reasons are advanced against it:

- 1) The calculated stresses are inaccurate. The method can locate the positions where high stresses occur, but it does not give those stresses with high precision. Stress concentrations in the corners are not included. Round corners reduce the stress concentrations, but they do not remove them. To calculate the stress concentrations with some confidence, for example to be used in fatigue analyses, the method must be replaced by analytical methods. Alternatively, finite element analyses can be used, but very fine meshing is required in the areas of high stresses.
- 2) The method does not show the full strength of a ductile structure. Yielding in a very small area is the limiting factor when fatigue and buckling are excluded. The results are usually conservative. In real structures yielding can take place in large areas before the maximum strength is reached. To calculate the maximum strength more accurately, plastic theory must be used. Alternatively, non-linear finite element analysis can be used.

For circular openings and for the approximated variations of the method, the accuracy of the results may be even more doubtful.

The buckling checks are basically the same as those required for the method based on strength criteria. The discussion of these issues is included in Section 3.3.3.

3.3 Methods based on strength criteria

3.3.1 General

The principle is: When global shear and moment are given in the center of an opening, these are compared with shear and moment capacities by means of interaction equations. The capacities are based on plastic theory. The design is accepted if the interaction equations give a value below or equal to some design values.

Design methods based on strength criteria have been developed because the design methods based on allowable stresses, or elastic response, do not give an accurate prediction of strength or margin of safety. Using strength criteria, the design of web openings has historically consisted of the construction of moment-shear interaction diagrams of the type illustrated by the dotted line in Fig. 3.3.1.

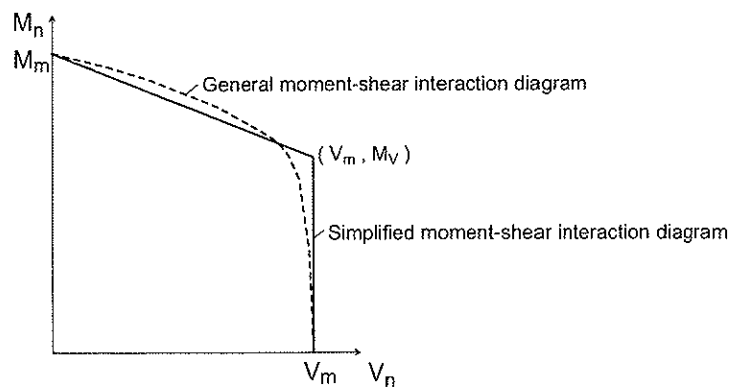


Fig. 3.3.1 Moment-shear interaction diagrams

The shear capacity is influenced by the acting secondary moment and the primary moments in non-linear ways even when buckling is excluded. For a certain web opening in a certain beam, an accurate interaction diagram must therefore be constructed point by point. Basically, the diagram is valid only for that opening and beam and cannot be used for other openings.

For design it is preferable to generate the interaction diagrams more simply. This has been done by calculating the maximum moment capacity and the maximum shear capacity and connecting these points with a curve or series of straight line segments. Various proposals have been made and some of these require a third point that represents the maximum moment that can be carried at maximum shear. See the solid line in Fig. 3.3.1. Virtually all methods agree on the maximum moment capacity M_m . This represents the bending strength at an opening subjected to zero shear. The methods differ in how they calculate the maximum shear capacity V_m and what curve shape is used to complete the interaction diagram. The maximum shear capacity has been calculated for specific cases, such as concentric un-reinforced openings, eccentric un-reinforced openings and eccentric reinforced openings. The result has been a series of special interaction equations.

AISC(1990) uses a method that is further simplified. A single approach can generate a family of equations, which may be used to calculate the shear capacity of openings with and without reinforcement. The basic procedure is explained below.

3.3.2 AISC method

General

The forces acting at a web opening are similar to those shown in Fig. 3.2.1 assuming now that the shear V and moment M are factored forces. As Eqs. (3.2.1) to (3.2.5) are based on equilibrium, they are still valid for the present method.

Failure modes are similar to those shown in Fig. 3.2.2.

Moment-shear interaction

Primary bending and shear occur simultaneously at most locations within beams. At a web opening, the two forces interact to produce lower strength than are obtained under pure bending or pure shear alone. Fortunately, at web openings in beams, the interaction between primary bending and shear is weak. Neither the primary bending strength nor the shear strength drop off rapidly when openings are subjected to combined bending and shear. Utilizing this effect, the present method assumes the following:

- M_m and V_m can be calculated separately, assuming no interaction.
- The interaction between the nominal primary bending and shear capacities M_n and V_n is governed by

$$\left(\frac{M_n}{M_m}\right)^3 + \left(\frac{V_n}{V_m}\right)^3 = 1 \quad (3.3.1)$$

Eq. (3.3.1) is represented by the super-elliptical curve in Fig. 3.3.2.

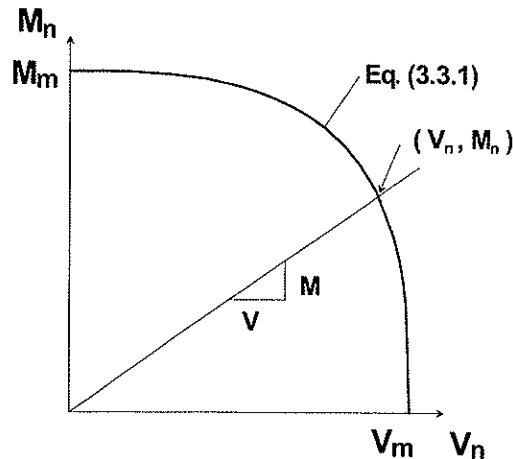


Fig. 3.3.2 Design interaction curve

Maximum capacity for primary moment

See Figs. 3.3.3 and 3.3.4. W_p is the plastic section modulus of beam without opening. $e = |e|$ is the eccentricity of opening. A_r is the cross section area of the reinforcement in each tee.

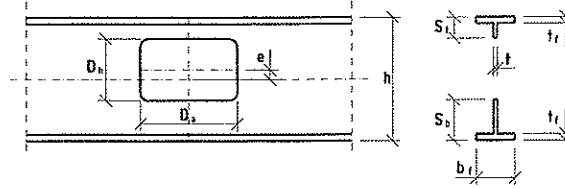


Fig. 3.3.3 Beam with un-reinforced opening

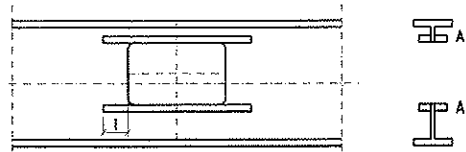


Fig. 3.3.4 Beam with reinforced opening

For beams with un-reinforced openings, the primary moment capacity in pure bending is

$$M_m = f_y \left[W_p - D_h t \left(\frac{D_h}{4} + e \right) \right] \quad (3.3.2)$$

For reinforced openings, Eq. (3.3.2) is modified, depending on $te < A_r$ or $te > A_r$.

Maximum capacity for shear and secondary moment

V_m is calculated for the pure shear condition, assuming that $M_m = 0$. This means that there are no axial forces in the top and bottom tees. Eqs. (3.2.1) to (3.2.3) give

$$V_m = V_{mt} + V_{mb} \quad (3.3.3)$$

$$V_{mt} = \frac{M_{ptl} + M_{pth}}{D_a} = \frac{2M_{pt}(V_{mt})}{D_a} \quad (3.3.4)$$

$$V_{mb} = \frac{M_{pbl} + M_{pbh}}{D_a} = \frac{2M_{pb}(V_{mb})}{D_a} \quad (3.3.5)$$

M_{pt} and M_{pb} are the plastic capacities for secondary moments. Subscripts t and b point to top and bottom tee and h and l point to high and low moment end of opening. The Vierendeel approach is used, assuming that the moment capacities are equal in each end of the top and bottom tees.

Unfortunately, there is interaction between the shear and the axial stresses from the secondary moments: The available axial stresses $f_{y,red}$ in the tee webs, contributing to the plastic moment capacity, are reduced by the von Mises criterion

$$f_{y,red} = \sqrt{f_y^2 - 3\tau^2} \quad (3.3.6)$$

where the shear stresses τ are functions of V_{mt} and V_{mb} . From this it follows that the plastic neutral axes of the tees are functions of the shear, and hence also influence the contributions from the beam flange and the reinforcement. The overall result is that Eqs. (3.3.4) and (3.3.5) are third order equations. These equations must be solved by iteration, since a closed-form solution cannot be obtained.

Approximated closed-form solutions

For practical design, however, closed-form solutions are desirable. Approximated solutions require one or more additional assumptions, which may include; 1) a simplified version of the von Mises yield criterion, 2) limiting plastic neutral axis locations in the tees to specified locations and 3) ignoring local equilibrium within the tees. The form of solutions for V_{mt} and V_{mb} depends on the particular assumptions selected. AISC (1990) uses all three assumptions. A brief description of the AISC approach is as follows:

- The von Mises criterion is simplified using a linear approximation

$$f_{y,red} = f_y \sqrt{2} - \tau \sqrt{3} \quad (3.3.7)$$

The value $\sqrt{2}$ is selected to provide the best fit with data. A maximum shear cutoff is also applied. For low shear, the reduced axial stress may be greatly overestimated.

- The flange stresses are not used to calculate the secondary moment capacities. The plastic neutral axis usually lies in the flange and the flange thickness is small relative to the depth of the tee. Thus, the contribution of the flanges to the secondary moment capacity is small.
- A major simplification is made in the distribution of stresses. See Fig. 3.3.5. The shear and axial stresses are assumed to be uniform through the tee web depth, ignoring local equilibrium.

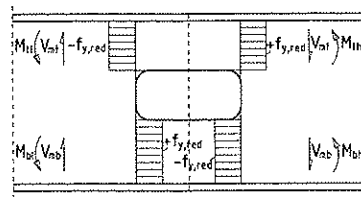


Fig. 3.3.5 Simplified axial stress distribution for opening at maximum shear

The top tee is used to develop an equation for the maximum shear capacity of a tee without reinforcement in general form. Equilibrium for moments taken about the top of the flange at the low moment end of the opening gives

$$\frac{V_{mt} D_a}{2} = f_{y,red} \frac{s_t^2}{2} \quad (3.3.8)$$

where s_t is the depth of the top tee.

Using Eq. (3.3.7), and inserting $\tau = \frac{V_{mt}}{s_t t}$, $V_{pt} = \frac{f_y}{\sqrt{3}} s_t t$ and $v_t = \frac{D_a}{s_t}$ in Eq. (3.3.8) result in the following linear equation for the maximum shear capacity:

$$V_{mt} = \left[\frac{\sqrt{6}}{v_t + \sqrt{3}} \right] V_{pt} \leq V_{pt} \quad (3.3.9)$$

For reinforced openings, Eq. (3.3.9) is modified to:

$$V_{mt} = \left[\frac{\sqrt{6} + \bar{\mu}_t}{\bar{v}_t + \sqrt{3}} \right] V_{pt} \leq V_{pt} \quad (3.3.10)$$

where $\bar{\mu}_t$ and \bar{v}_t are functions of geometry and yield stress. $\bar{\mu}_t$ includes the positive contribution of the reinforcement to the secondary moment capacity and \bar{v}_t approximates the negative effect from movement of the plastic neutral axis.

The shear capacity of the bottom tee is given by suitable substitutions in Eqs. (3.3.8) to (3.3.10).

Design checking

The factored forces M and V at the center of the opening are checked using the design interaction curve in Fig. 3.3.2 by plotting the point $(V/V_m, M/M_m)$. If the point lies inside the curve, the design is accepted. This is the same as the following requirement:

$$\left(\frac{M}{M_m} \right)^3 + \left(\frac{V}{V_m} \right)^3 \leq 1 \quad (3.3.11)$$

Buckling

Plastic section properties are presumed. AISC (1990) gives explicit guidelines for various buckling modes:

- Web buckling. There are limits on the opening parameter p_o , the web height-to-thickness ratio, the opening length-to-height ratio, the shear capacity, the height of the opening and on tee depths and aspect ratios:

$$p_o \approx \frac{D_a}{D_h} + \frac{6D_h}{h} \leq 5,6 \quad (3.3.12)$$

$$\frac{h}{t} \leq 67 \quad (3.3.13)$$

$$\frac{D_a}{D_h} \leq 2,2 \quad \text{and} \quad V_{m,max} = 0,45V_p \quad \text{when} \quad \frac{h}{t} \leq 67 \quad (3.3.14)$$

$$\frac{D_a}{D_h} \leq 3,0 \quad \text{and} \quad V_{m,max} = 0,67V_p \quad \text{when} \quad \frac{h}{t} \leq 54 \quad (3.3.15)$$

$$\frac{D_h}{h} \leq 0,70 \quad (3.3.16)$$

$$\frac{s_t}{h} \geq 0,15 \quad \text{and} \quad \frac{s_b}{h} \geq 0,15 \quad (3.3.17)$$

$$\frac{D_a}{s_t} \leq 12 \quad \text{and} \quad \frac{D_a}{s_b} \leq 12 \quad (3.3.18)$$

The depth of beam has been replaced by h for simplification in this presentation and the yield stress $f_y = 420 \text{ N/mm}^2$ has been assumed in Eqs. (3.3.13) to (3.3.15). The limit on p_o also serves to ensure that the linearisation of the von Mises stress provides conservative predictions for the beam shear strength, even if web buckling is not a factor. $V_p = \frac{f_y}{\sqrt{3}}ht$ is the plastic shear capacity of the web without opening. The

minimum depths of tees are based on the need to transfer some load over the opening and lack of test data for shallower tees. The limit on the aspect ratio of the tees is based on lack of test data for beams with greater aspect ratios.

- Local buckling of compression zone in tee webs when reinforcement is used. No guidelines given.
- Local buckling of compression flange.

$$\frac{b_f}{2t_f} \leq 8,4 \quad (3.3.19)$$

where b_f and t_f are the breadth and thickness of the flange.

- Lateral buckling of compression flange. In beams with un-reinforced openings or reinforced openings with the reinforcement placed on both sides of the web, the torsional constant of the beam should be multiplied by

$$\left[1 - \left(\frac{D_a}{L_b} \right) \frac{D_h t - 2A_r}{t(H + 2b_f)} \right]^2 \leq 1 \quad (3.3.20)$$

where L_b is unbraced length of compression flange and H is the depth of beam. $A_r = 0$ for beams with reinforcement on only one side of the web. Beams reinforced on one side of the web should not be used for long laterally unsupported spans. For shorter spans, the lateral bracing closest to the opening should be designed for an additional load equal to 2 % of the force in the compression flange.

- Vertical buckling of tee in compression without reinforcement should be investigated as an axially loaded column, but is not required when the aspect ratio of the tee web is less or equal to 4.
- Vertical buckling check of tee in compression with reinforcement is only required for large openings in regions of high primary moment.
- Local buckling of reinforcement. Similar to the compression flange.
- Transverse buckling of reinforcement. No guidelines given.

Deflection

Methods for calculating the deflection of a beam caused by openings are given. The material is more utilized in plastic theory and deflections are generally larger than in the method based on allowable stresses. In most cases, however, the influence of a single opening is small.

Other considerations

- Corner radii should be the greater of $2t$ and 16 mm to avoid excessive stress concentrations.
- Concentrated loads above or below the opening are not allowed.
- Circular openings without reinforcement may be designed using the expressions for rectangular openings, if the following substitutions are made:

$$D_h = D \quad \text{for bending} \quad (3.3.21)$$

$$D_h = 0,9D \quad \text{for shear} \quad (3.3.22)$$

$$D_a = 0,45D \quad \text{for bending and shear} \quad (3.3.23)$$

- Circular openings with reinforcement may be designed using the expressions for rectangular openings, if the following substitutions are made:

$$D_h = D \quad \text{for bending and shear} \quad (3.3.24)$$

$$D_a = 0,45D \quad \text{for bending and shear} \quad (3.3.25)$$

- Reinforcement. A limit is placed on the size of the reinforcement that can be included in the equations, based on the yield shear strength of the web:

$$A_{r,max} \leq \frac{D_a t}{2\sqrt{3}} \quad (3.3.26)$$

which also limits the maximum shear capacity that can be obtained at the opening.

- Reinforcement should preferably be placed on both sides of web, but can be on one side only, if the following requirements are met:

$$A_r \leq \frac{A_f}{3} \quad (3.3.27)$$

$$\frac{D_a}{D_b} \leq 2,5 \quad (3.3.28)$$

$$\frac{s_l}{t} \leq 18 \quad \text{and} \quad \frac{s_b}{t} \leq 18 \quad (3.3.29)$$

$$\frac{M}{VH} \leq 20 \quad (3.3.30)$$

where A_f is the flange area and $f_y = 420 \text{ N/mm}^2$ is assumed for Eq. (3.3.29). The criteria are designed to limit reductions in strength caused by out of plane displacements from by eccentric loading of the reinforcement. Eq. (3.3.30) limits the use of unsymmetrical reinforcement if the primary moment is high. In such cases the out of plane displacements of the web can be severe. For shear, the lateral displacement mode caused by the unsymmetrical reinforcement changes, and this allows a greater capacity to be developed.

- Reinforcement must be sufficiently anchored to develop the full yield strength of the bars, since this is presumed for the design method. This requires an anchoring length

$$l_{min} = \frac{A_r \sqrt{3}}{2t} \quad (3.3.31)$$

If the anchoring length is at least 50 % of the opening length, a single fillet weld can be used in the opening part of the reinforcement and double fillets in the anchoring parts.

- Spacing of openings. To avoid interaction between openings, the following requirements should be followed for rectangular openings:

$$S_a \geq h \quad \text{and} \quad S_a \geq D_a \left(\frac{\frac{V}{V_p}}{1 - \frac{V}{V_p}} \right) \quad (3.3.32)$$

where S_a is the clear space between openings. The criteria are meant to ensure that a plastic mechanism involving interaction between openings will not develop, instability

of the web posts between openings will not occur, and web posts between openings will not yield in shear.

For circular openings

$$S_a \geq 1,5D \quad \text{and} \quad S_a \geq D \left(\frac{V}{\frac{V}{V_p}} \right) \quad (3.3.33)$$

3.3.3 Discussion

Approximated interaction diagram

Inn AISC(1990) the interaction between primary moment and shear is represented by a simplified interaction diagram, given by Eq. (3.3.1). An alternative may be to use the basic plastic theory directly, including axial forces in the top and bottom tee from the primary moment. In the present thesis this has been done by means of a spreadsheet. The purpose is to see if this procedure is a practical thing to do and if the result is in accordance with Eq. (3.3.1). A brief description is as follows:

Eqs (3.2.1) to (3.2.3) give

$$V_n = V_{nt} + V_{nb} \quad (3.3.34)$$

$$V_{nt} = \frac{2M_{pt}(V_{nt}, M_n)}{D_a} \quad (3.3.35)$$

$$V_{nb} = \frac{2M_{pb}(V_{nb}, M_n)}{D_a} \quad (3.3.36)$$

which are similar to Eqs. (3.3.3) to (3.3.5), but now V_n is a function of V_{nt} , V_{nb} and M_n .

Two approaches are possible; 1) to find the shear capacity V_n when the primary moment is given and 2) to find the primary moment capacity M_n when the shear is given. Both approaches should give the same interaction diagram. A solution is to start with the first approach and continue with the second approach.

The approaches are of course the same as finding the interaction diagram point by point. An example is made for an HE1000A with a square opening with sides equal to $0,50h$. It is fairly easy to find the shear capacity when $M = 0$ by using a spreadsheet. Also to find the primary moment capacity when $V = 0$ is easy. It is more tedious to find the primary moment capacity when $V > 0$. The diagram is shown in Fig. 3.3.6.

Fig. 3.3.6 also shows the interaction diagram given by Eq. (3.3.1) for comparison with the approach described above. Here, M_m and V_m is calculated from Eqs. (3.3.2) and (3.3.9). Even though the value for V_m in itself is slightly conservative, the curve given by AISC, somewhat surprisingly seems to be non-conservative for the smaller shears.

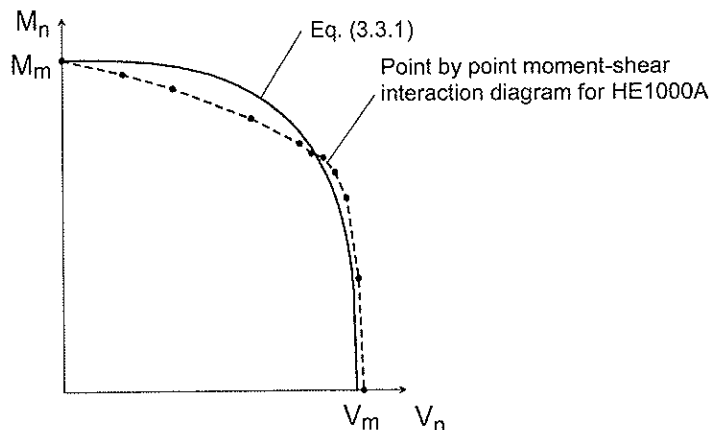


Fig. 3.3.6 Interaction diagram for HE1000A with a square opening with sides $0,50h$

It is however felt that in general the moment-shear interaction approach proposed by AISC is better to use in practical design. The concept that moment and shear capacities are calculated separately, followed by design check based on combination of the topical interaction ratios, is a preferred method to keep the overview of the design intact. Spread sheet solutions are useful, but cannot completely compensate for this purpose.

An interaction curve to be used for design purpose must include also precautions against factors not included in the theoretical models. Eq. (3.3.1) has been proven by many practical tests. At this point in the present thesis, the findings of the calculated example should be regarded as an indication that the use of another, more conservative, curve should be further investigated.

Reduced yield stress based on the von Mises criterion and linearisation.

Being an approximation in itself, the von Mises criterion could be replaced by the Tresca criterion, which is frequently used in plastic theory. The Tresca criterion assumes that yield occur when the maximum shear stress reaches a critical value, which in this case for plane stress would be $0,5f_y$.

The von Mises criterion is used in almost all design rules. It is also simple to apply in computations. Another benefit is that for un-reinforced tees, the reduced yield stress criterion automatically leads to normal stresses in the outmost fibers that are far less than the yield stress. Hence class 1 is not required for the tee webs, actually some kind of class 4 is sufficient.

However, considering the von Mises criterion as such as a good solution, the linearisation of the same criterion should not be accepted. The approximation in Eq. (3.3.7) is rather coarse and can lead the solution astray. Actually some restrictions have had to be put on the opening sizes to limit bad results of this approximation. Another result is, for example, if the maximum reinforcement of Eq. (3.3.26) is used: Then the yield shear strength of the tee web is expected to be obtained. But Eq. (3.3.10) does not give $V_{mt} = 1,0V_{pt}$. Today, when spreadsheets are available, linearisation is perhaps less important than before, and the von Mises criterion should preferably be used as is.

Constant shear stress

The real shear stress is approximated as a constant shear stress over the height of the tee webs. Especially for un-reinforced tees, this is far from the real stress distribution. Also this solution is not a pure lower bound solution, because the requirement for equilibrium is not fulfilled on fiber level.

Another approach could be to assume a “reservation” for the shear force in a section of the web near or around the plastic axis of symmetry, such that this part do not contribute to the secondary moment capacity. The rest contributes with full yield stress. For openings without reinforcement this is difficult, because the plastic axis of symmetry usually lays in the flange. For reinforced sections this approach is applicable and is consistent with a frequent simplification that the flanges and the reinforcement take the moments and the web takes the shear.

However, two arguments point at keeping the assumption as is. Firstly, for a lower bound solution it usually sufficient to satisfy the yield and equilibrium requirements in the average sense. Actually this is a basic assumption behind much elastic and plastic theory. Secondly, together with von Mises yield criterion, it leads to smaller normal stresses in the outmost fibers. This probably limits the local buckling in the corners. See further below.

Thin flanges

It is presumed that flange thickness is so small that it has minor influence on the calculation of shear capacities. When spreadsheets are used, the approximation is perhaps less important, but should still be allowed. The error made is usually small and in many cases the overview of particular solutions and equations is considerably improved.

Web buckling

The AISC (1990) restriction on the web h/t ratio is mainly connected to the contribution from the web to the primary moment capacity. No restriction is placed on the global shear buckling capacity of the web without opening and it is assumed that the requirement for primary moment capacity will cover global shear buckling as well. In NS-ENV 1993-1-1 (1993) the h/t ratio for beams without openings are limited to about 52 for steel with $f_y = 420 \text{ N/mm}^2$, if buckling is not considered.

For beams with openings, AISC (1990) states that the combined restrictions of web h/t ratio, the opening shape, location and sizes, together with a reduction in shear capacity, will avoid both global web buckling and local transverse buckling of the tee webs. No restriction is placed on the width-to-thickness ratio of the outstand tee webs for un-reinforced openings. The result is that rather high width-to-thickness ratios are allowed. One explanation could be that small openings give smaller secondary bending stresses acting in tee webs with high width-to-thickness ratios, while large openings give higher secondary bending stresses acting in tee webs with low width-to-thickness ratios.

The liberal width-to-thickness ratios can be illustrated by the following example, see Fig. 3.3.8. Assuming $h/t = 67$ for the web, an allowable opening of $0,77h \times 0,35h$ is placed entirely in the lower half of the web. The width-to-thickness ratio of the upper tee is 34, corresponding to class 4 for axial stress. The maximum secondary bending stress in the tee

in the example is calculated to $0,66f_y$, far more than the design buckling stress of an outstand element with width-to-thickness ratio 34. The reason could be that the consideration of the tee web as outstand element is not relevant, because the bending stress is rapidly reduced outside the end of the tee and towards the midpoint of the tee.

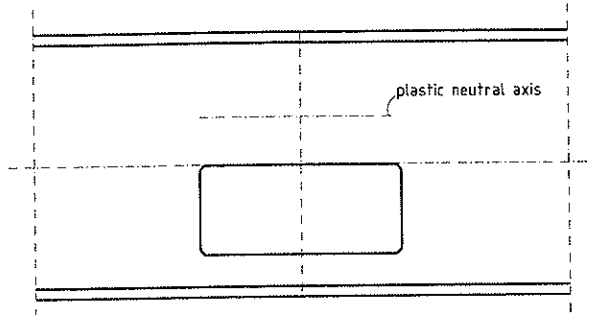


Fig. 3.3.7 Opening in lower half of web

For small openings, Eqs. (3.3.14) and (3.3.15) give a severe reduction in shear capacity. Even a very small opening gives minimum 33 % reduction compared to the web without opening. It should be questioned if this limit is necessary. An improved formulation, giving no reduction when the opening size goes to zero, is probably better.

Local buckling of the compression zone in the web above or below the opening when reinforcement is used is normally not governing for beams, because: Class 1 for axial stresses requires a width-to-thickness ratio of 25 for steel with $f_y = 420 \text{ N/mm}^2$. The requirement to avoid global buckling for bending is a height-thickness ratio of maximum 67 for the web without opening. It is therefore only for very eccentric openings that the web above or below a reinforced opening will not qualify for class 1.

Transverse buckling of reinforcement

Apparently, AISC (1990) has no requirement to check transverse buckling of reinforcement. Presumably this is covered by the restrictions on opening sizes and the requirement to use reinforcement on both sides of web, if primary moments are of some size. The issue is also sparsely described in the literature.

Circular openings

The use of substitution rectangular openings in design of webs with circular openings can be questioned for the following reasons:

- There is relatively sparse evidence behind the method. Almost all literature points to Redwood (1969) as the origin. Later, Redwood and Shrivastawa proposed the criterion that is adopted in AISC (1990).
- The substitution may be a reasonable approach for un-stiffened openings, as it actually includes some of the increased width of the tee web where the secondary moments due

to shear are checked. However, if reinforcement is required, the method will hardly give an optimum solution as it gives only horizontal reinforcement above and below the opening. As previously explained, the main purpose of the reinforcement is to carry the secondary moments. The optimum solution should be reinforcement bars that are tangential to the circular opening and have certain angles relative to the horizontal centerline of the opening. A generalization of such reinforcement is the sleeve, i.e. a circular reinforcement bar that is placed symmetrically on the inside of the opening.

Circular openings with reinforcements have been investigated by Levy, McPerson and Smith (1948), but only based on allowable stresses and experiments. FE-models were of course not in use. The conclusion was that sleeves are the optimum solution from a weight point of view. In recent years, Buckland, Bartlett and Watts (1988) have investigated circular openings with doubler plates, based on allowable stresses and FEM-analyses.

Hence it seems that one of the most common opening designs in offshore structures, namely the circular opening with sleeves, need more investigations based on strength criteria. Many approximations have been made to arrive at design recommendations for rectangular openings. The accuracy of the results may be questioned even for rectangular openings and are not improved by further approximations for circular openings. Maybe a better solution would be to develop a separate set of recommendations for circular openings. One example show this: For rectangular openings the horizontal reinforcement must be load-carrying in order to increase the shear capacity, as otherwise the shear and secondary moment are acting on a section equal to the minimum section where the shear is acting alone. A buckling stiffener will never be sufficient if the goal is to arrive at maximum shear capacity. This is different for a circular opening. Here the shear and secondary moment act in a larger section than the minimum section where the shear is acting alone. No reinforcement at all, or only a buckling ring stiffener on one side, can perhaps be a relevant solution. If this is true it may have favorable consequences both from an economic and weight point of view.

3.4 Stress concentration and plastification

3.4.1 General

To study the local buckling phenomenon around the periphery of circular openings, and at corners of rectangular openings, it is useful to start with stress concentration based on elastic theory. This is also valuable in order to estimate the necessary extent of the plastified zones that have to be developed when design is based on strength criteria.

Adopting the usual split between primary moment capacity and shear capacity, the most important issue is the stress concentration for pure shear. The contribution from the web to the primary moment capacity of a girder is usually small, and hence the stress concentration from primary moment is not investigated here.

3.4.2 Analytical solutions

Elastic stress in an infinitely large plate

For pure shear in an infinitely large plate without buckling, the shear stress τ can be transformed into the two principal stresses $\sigma_{tension} = \sigma_1$ and $\sigma_{compr} = \sigma_2$. See Fig 3.4.1.

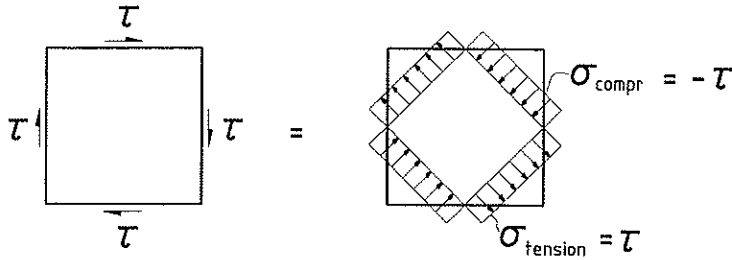


Fig. 3.4.1 Pure shear stress transformed into two principal stresses

It can be shown that

$$\sigma_{tension} = \tau \quad (3.4.1)$$

$$\sigma_{compr} = -\tau \quad (3.4.2)$$

Elastic stress around small circular openings

If a small circular opening is introduced, stresses around the opening are given by

$$\sigma_r = \tau \left(1 + \frac{3D^4}{16r^4} - \frac{D^2}{r^2} \right) \cos 2\theta \quad (3.4.3)$$

$$\sigma_\theta = -\tau \left(1 + \frac{3D^4}{16r^4} \right) \cos 2\theta \quad (3.4.4)$$

$$\tau_{r,\theta} = -\tau \left(1 - \frac{3D^4}{16r^4} + \frac{1D^2}{2r^2} \right) \sin 2\theta \quad (3.4.5)$$

where r and θ are polar coordinates. θ is the angle between the radius vector and the direction of the principal tensile stress in the plate without the opening. σ_r is the normal stress in the r -direction and σ_θ is the normal stress perpendicular to the r -direction. $\tau_{r,\theta}$ is the shear stress in the same directions. The solution can be found in Timoshenko and Gere (1963) and is derived from the uniaxial analytical solution obtained by Kirsch in 1898, based on a stress function.

The stresses are symmetric relative to the center of the opening. At 45° from the horizontal section through the opening, the σ_θ stress reach a peak value of $\pm 4\tau$ at the boundary of the opening, but rapidly approaches the principal stress when the distance r

increases. In these sections the $\tau_{,\theta}$ stress is zero. In the horizontal and vertical sections through the opening, the σ_{θ} stress is zero. Here, the $\tau_{,\theta}$ stress is also zero, but rapidly approaches a maximum value of $1,33\tau$ when the distance r increases. From the maximum value, the $\tau_{,\theta}$ stress slowly approaches τ for increasing r .

Elastic stress around circular openings in a web of finite width

The effect of the opening is of localized character. This justifies the application of Eqs. (3.4.3) to (3.4.5), derived for an infinitely large plate, to a web of finite width. Timoshenko and Gere (1963) state that for a plate width not less than $4D$, the error in σ_{θ} does not exceed 6 %.

Elastic stress around small square openings

If a small square opening is introduced in an infinitely large plate, stresses will be concentrated at the corners. The analytical problem is more complicated than around a circular opening. Solutions similar to Eq. (3.4.3) to (3.4.5) are not available. Analytical solutions of the *boundary* stress of square openings with rounded corners in plates under uni-axial tension parallel to the sides have been derived by, among others, Greenspan (1944). By combining the solution for tension in one direction with the similar solution for compression in the direction normal to the first one, it is possible to find a solution for square openings orientated as case "A" in Fig. 3.4.2.

However, orientation "B" in Fig. 3.4.2 is more common in practice. For this orientation and uni-axial tension, Kikukawa (1953) has developed iterative methods to calculate the extreme fiber stress at the boundary of the opening. Complex stress functions and conformal mapping are used to find the stress acting in an arbitrary point along the boundary of rhombic openings including the square. By combining the solution for tension in one direction with the similar solution for compression in the direction normal to the first one, it should be possible to find a solution for shear acting on square openings when the corners are orientated as case "B". The calculations are laborious and the author does not know if such solution has been presented in the literature.

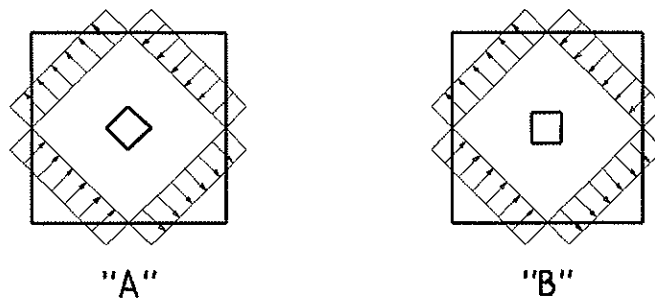


Fig. 3.4.2. Orientation of square openings

Elastic stress around square openings in a web of finite width

No analytical solutions are known for case "B" in Fig. 3.4.2.

Plastification around circular and square openings

No analytical solutions have been studied.

3.4.3 Discussion

General

In order to study the stress distributions more in detail, finite element analyses were carried out for circular openings and for square openings of configuration "B". Both linear elastic and elasto-plastic analyses were performed for square plates with openings having diameter and side dimensions 10 % and 75 % of the plate dimensions. Corner radii were 1/16 of the opening dimension.

Elastic stress around small openings

Figures 3.4.3 and 3.4.4 show the square plates with circular and square openings, where the opening dimensions are 10 % of the plate sides. The applied loads are shear stresses equal to $0,90\tau$ along all plate sides, i.e. the maximum possible loads expected to be carried if full plastification occurs in the minimum sections through the openings. However, neither plastification nor buckling are assumed in these models, where the purpose is to show the von Mises elastic stress concentrations. Areas where the stresses exceed $f_y = 420 \text{ N/mm}^2$ are shown in color. The color spectra are approximately the same for both figures and a direct comparison between circular and square openings is possible.

For the circular opening, the stresses exceed the yield stress by a relative small amount in the minimum sections through the openings. High stress concentrations occur at the edge of the opening at 45° with the horizontal sections, but the areas where the stresses exceed the yield stress are very small. Here, the von Mises stresses consist almost only of σ_θ - stress.

For the square opening, the stresses also exceed the yield stress with a relative low amount in the minimum sections through the openings, but the areas are larger. High stress concentrations occur at the corners of the opening. The peak values are very high, but the areas where the stresses exceed the yield stress are smaller than for the circular opening.

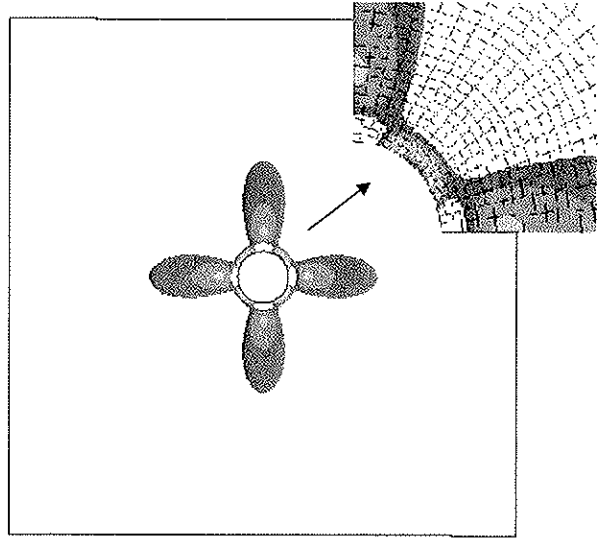
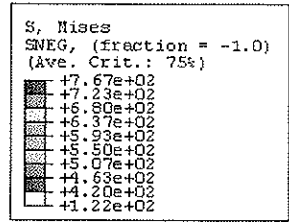


Fig. 3.4.3 Elastic stress around a small circular opening

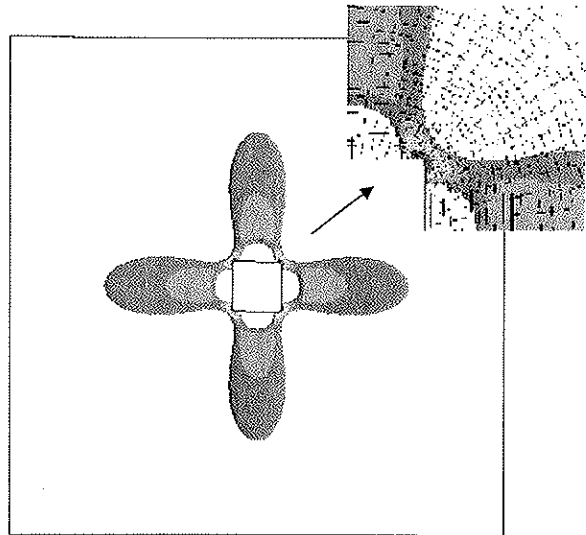
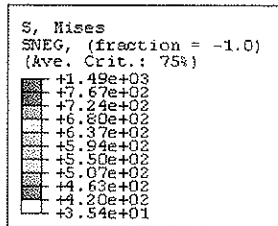


Fig. 3.4.4 Elastic stress around a small square opening

Plastification around small openings

Figures 3.4.5 and 3.4.6 show plastification of the previous plates with approximately the same load as before, but now assuming an elasto-plastic material. The purpose of the analysis is to show the amount of plastification at the edge of opening at 45° with the horizontal sections for the circular opening, and at the corners for the square opening.

The models can take 100 % and 98,8 % , respectively, of the loads applied on the elastic models, even though large displacements are then present. Hence, the figures show the situations when 98 % of the maximum loads are applied, i.e. when the displacements are still relatively small. Areas where plastification occurs are shown in light-grey color. Otherwise the colors show stresses below the yield stress. The color spectra are approximately the same for both figures and a direct comparison between circular and square openings is possible.

For the circular opening, the areas of plastification are relatively small in the minimum sections through the opening. They do not extend to the edge of the opening, and they are separated from the plastified areas at the edge of the opening, which are located at 45° with the horizontal. These areas are also small and they do not extend outside a square with side dimensions $1,2D$.

For the square opening, the areas of plastification are larger. In the horizontal and vertical sections near the corners, the plastification extends to the plate edges, reflecting that the plate is near collapse. However, for only 1 % smaller load, the plastification areas in the minimum sections through the opening are separated from small plastified areas at the corners.

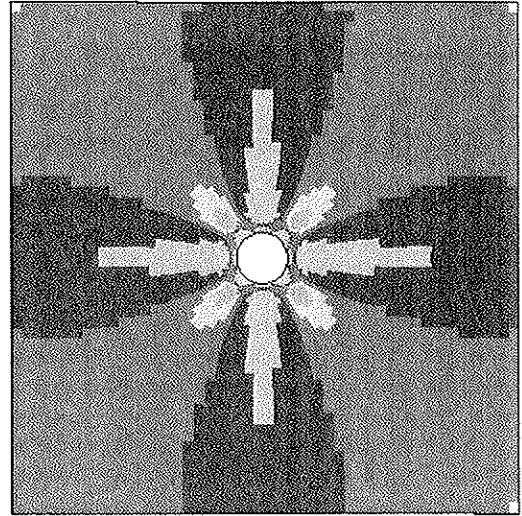
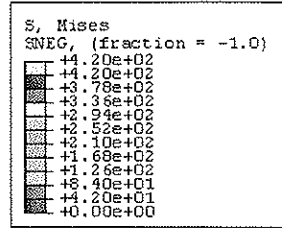


Fig. 3.4.5 Plastification around a small circular opening

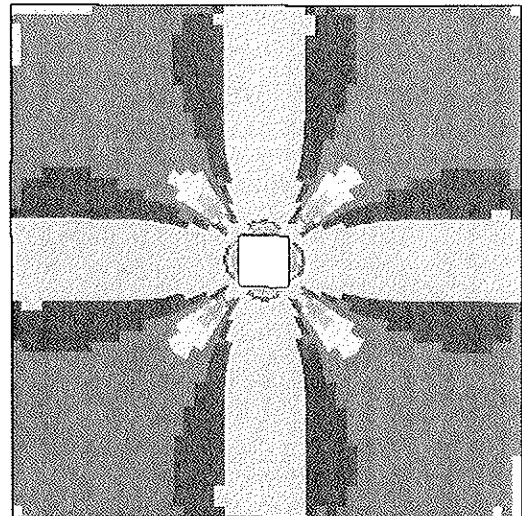
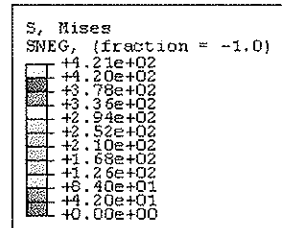


Fig. 3.4.6 Plastification around a small square opening

Plastification around large openings

Figures 3.4.7 and 3.4.8 show square plates with circular and square openings, where the diameter and sides are 75 % of the plate sides. The materials are elasto-plastic. Buckling is suppressed. The purpose is to show the amount of plastification at the edge of opening at 45° with the horizontal sections for the circular opening, and at the corners for the square opening.

The loads are uniform shear stresses along all plate sides. The maximum shear expected to be carried in the minimum sections through the openings corresponds to $0,25\tau_y$, applied at the plate sides. Taking this load as 100 %, the collapse load is 91 % for the plate with circular opening and 35 % for the plate with square opening. However, the displacements are large. Hence the figures show the situations when 86 % and 25 % of the $0,25\tau_y$ are applied, i.e. when the displacements are still relatively small. Areas where plastification occurs are shown in light-grey color. Otherwise the colors show stresses below the yield stress. The color spectra are approximately the same for both figures.

For the circular opening, the areas of plastification are relatively small in the minimum sections through the opening. They do not extend to the edge of the opening, and they are separated from the plastified areas at the edge of the opening, which are located at 45° with the horizontal. These areas are larger, but do not extend outside a square with side dimensions $1,2D$.

For the square opening, the areas of plastification are much smaller, which of course reflects that the total load is less than 1/3 of the plate with circular opening. Plastification occurs only in small areas near the edge at the corners.

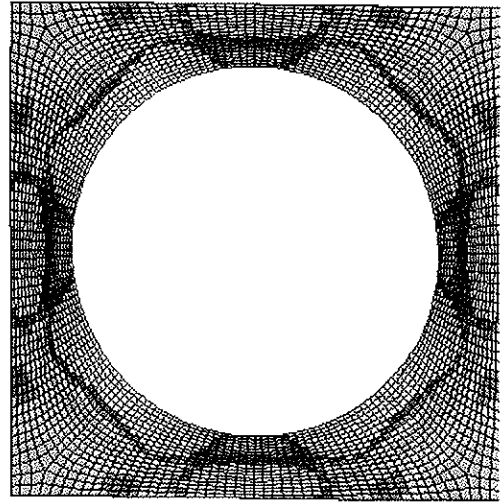
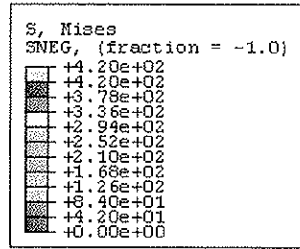


Fig. 3.4.7 Plastification around a large circular opening

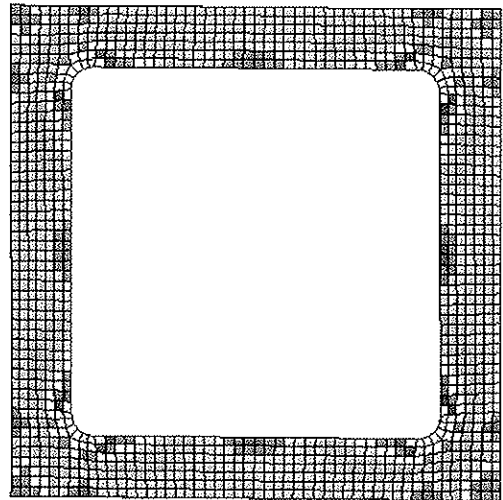
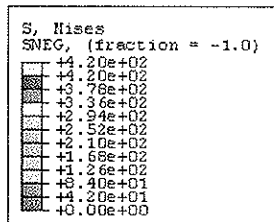


Fig. 3.4.8 Plastification around a large square opening

3.5 Simplified shear buckling

3.5.1 General

Shear buckling for webs is first presented in line with the latest proposal to the Eurocode for girders without openings, i.e. prEN 1993-1-5: 20xx. 2003 Eurocode 3: *Design of steel structures – Part 1-5: Plated structural elements*. Stage 34 draft. In the present investigation this document is referred to as EC3 or EC3 Part 1-5. Similar concepts for web with openings are not found in the literature, but a possible extension of the method to webs with openings is discussed in Section 3.5.3.

3.5.2 Shear capacity for webs without openings

The shear capacity of a web loaded in shear is given by

$$V_c = \chi_w \frac{f_y}{\sqrt{3}} ht \quad (3.5.1)$$

where χ_w is a reduction factor that accounts for plastification, varying yield stress, initial imperfections and post-critical behavior of the web. χ_w is based on experimental results and is a function of the relative slenderness

$$\bar{\lambda}_v = \sqrt{\frac{\tau_y}{\tau_{cr}}} \quad (3.5.2)$$

Here, τ_{cr} is the critical shear stress given by

$$\tau_{cr} = k_\tau \left[\frac{\pi^2 E}{12(1-\nu^2)} \right] \left(\frac{t}{h} \right)^2 \quad (3.5.3)$$

E is the modulus of elasticity and ν is the Poisson's ratio. The shear buckling coefficient k_τ is a function of boundary conditions and the web aspect ratio. For the case with four simply supported edges and $a/h \geq 1$,

$$k_\tau = 5,34 + \frac{4,00}{(a/h)^2} \quad (3.5.4)$$

The factor χ_w depends also on the stiffness of the end posts of the web. Table 3.5.1 shows the values as given in EC3 Part 1-5 when η is taken as 1,00. If presented as a diagram, the function χ_w is called a buckling curve.

Table 3.5.1 The buckling reduction function χ_w

	χ_w for rigid end post	χ_w for non-rigid end post
$\bar{\lambda}_w < 0,83$	1,00	1,00
$0,83 \leq \bar{\lambda}_w < 1,08$	$0,83 / \bar{\lambda}_w$	$0,83 / \bar{\lambda}_w$
$\bar{\lambda}_w \geq 1,08$	$1,37 / (0,7 + \bar{\lambda}_w)$	$0,83 / \bar{\lambda}_w$

3.5.3 Discussion

General

Critical shear loads/stresses are difficult to verify experimentally. A true bifurcation seldom if ever occurs, and instead non-linear material behavior, initial imperfections, boundary conditions and post-critical strength dominate the result. Basically, the critical shear stress is an auxiliary figure, which is used to define the reduced slenderness $\bar{\lambda}_w$. It is only in combination with the curves for χ_w , based on experiments, that the resulting shear capacity is reliable.

From Eq.(3.5.1) it can be seen that

$$V_c = \chi_w \frac{f_y}{\sqrt{3}} ht = \tau_k ht \quad (3.5.5)$$

$$\chi_w = \frac{\tau_k}{\tau_y} \quad (3.5.6)$$

where τ_k is the reduced shear stress, as often presented in older codes and in the literature.

No buckling

For some purpose, for instance where fatigue is a problem, the design requirement can be that no buckling must occur. It is possible to use curves where the post-critical action is excluded. In NS-ENV 1993-1-1 (1993) a such curve was given as follows:

$$\text{when } \bar{\lambda}_w \leq 0,8 \quad \rightarrow \tau_k = \tau_y \quad (3.5.7)$$

$$\text{when } 0,8 < \bar{\lambda}_w < 1,25 \quad \rightarrow \tau_k = [1 - 0,8(\bar{\lambda}_w - 0,8)]\tau_y \quad (3.5.8)$$

$$\text{when } \bar{\lambda}_w \geq 1,25 \quad \rightarrow \tau_k = \frac{1}{\bar{\lambda}_w^2} \tau_y = \tau_{cr} \quad (3.5.9)$$

For slender plates, this curve assumes that τ_k is neither reduced nor increased from the critical stress.

Buckling of webs with openings

Use of the simple shear buckling method, as described in the previous section, also for webs with openings is an interesting idea. A possible procedure could be:

- A modified critical stress, i.e. determined by a modified shear buckling coefficient $k_{\tau, \text{mod}}$, is calculated by means of parametric equations, based on FEM-analyses.
- $\bar{\lambda}_w$ is calculated according to Eq. (3.5.2)
- The reduction function χ_w for webs without openings is used to find the shear capacity by means of Eq. (3.5.1).

Some negative aspects of this procedure may be as follows:

The modified critical shear stress would be

$$\tau_{cr, \text{mod}} = k_{\tau, \text{mod}} \left[\frac{\pi^2 E}{12(1-\nu^2)} \right] \left(\frac{t}{h} \right)^2 \quad (3.5.10)$$

where $k_{\tau, \text{mod}}$ is the only parameter available to include the influence of the opening. Shear and secondary moments as well as global and local critical loads must be reflected in this coefficient. Hence it must be expected that many sub-parameters are required in $k_{\tau, \text{mod}}$.

In the literature some proposals for $k_{\tau, \text{mod}}$ are found, for example from Narayanan (1983a), based on a linear reduction with the size of the opening:

$$k_{\tau, \text{mod}} = \left(1 - \frac{D}{h}\right) k_{\tau} \quad (3.5.11)$$

However, this coefficient is used only when the modified shear stress is used to give the *modified critical shear force* for a web with opening

$$V_{cr, \text{mod}} = \tau_{cr, \text{mod}} ht = \tau_{cr} \left(1 - \frac{D}{h}\right) ht = \tau_{cr} (h - D)t \quad (3.5.12)$$

The modified critical shear stress is applied over the full web height, or alternatively the full critical shear stress is applied over the minimum section at the opening. The term modified critical shear load is only used in the tension field methods, where the modified critical shear stress is applied over the full web height. The critical shear load is only a small part of the total shear capacity for tension field methods. The influence of the opening size is also covered by means of the other contributions to the total shear capacity.

A problem occurs if the modified critical shear stress is to be used in the simplified shear buckling method. Here, the modified critical shear stress has to go through the relative slenderness and the function χ_w , in order to give the shear buckling strength. If there is only *one* function χ_w , the effect of the minimum section at the opening will not be covered for most plates, unless there is a non-linear modification to the critical stress. An example shows this: A plate without opening with relative slenderness 0,59 has $\chi_w = 1$

according to Table 3.5.1. If this plate gets an opening with diameter $D = 0,50h$ and $k_{\tau, \text{mod}}$ according to Eq. (3.5.11) is used, the modified slenderness increases to 0,83 . Table 3.5.1 still gives $\chi_w = 1$. Clearly this will be wrong, as the reduction in shear strength for this stocky plate is at least 50 %, corresponding to the reduction of the minimum section. For slender plates the difference may be less, but it should be obvious that the function for $k_{\tau, \text{mod}}$ have to be rather comprehensive. In principle, there will be one function for each D/h ratio.

Alternatively, Eq. (3.5.1) could be modified to include *directly* the minimum section through the opening:

$$V_{c, \text{mod}} = \chi_w \frac{f_y}{\sqrt{3}} (h - D)t \quad (3.5.13)$$

However, the effect of secondary bending and local buckling would still require a nonlinear $k_{\tau, \text{mod}}$ for each D/h ratio.

Modified functions χ_w

This is probably a better solution. All effects of openings are to be included in modified functions of χ_w , now called $\chi_{w, \text{mod}}$. For circular openings, there will be one curve for each D/h ratio. Square openings will have similar curves. For rectangular openings the curves must reflect both the ratios of the length and height of the opening to the height of the web. Eq. (3.5.1) is modified to

$$V_{c, \text{mod}} = \chi_{w, \text{mod}} \frac{f_y}{\sqrt{3}} ht \quad (3.5.14)$$

Eqs. (3.5.2) to (3.5.4) are not modified. The effect of the opening shall not be included in the shear buckling coefficient and the term $k_{\tau, \text{mod}}$ is not required. k_{τ} shall reflect the boundary conditions and aspect ratio of the web. But, as the edges are normally assumed simply supported, k_{τ} is finally including only the aspect ratio of the web.

The functions $\chi_{w, \text{mod}}$ may be found analytically, by experiments or by FEM-analyses. Actually, the methods of Sections 3.6 and 3.7 are to a large extent analytical solutions of Eq. (3.5.14), but for one particular k_{τ} only.

3.6 Rotated stress field method

3.6.1 General

The rotated stress field method for webs without openings is based on Höglund (1972). Originally it was developed for girders with web stiffeners at the ends only, a structure for which other tension field methods are very conservative. In Höglund (1997) the influences of transversal and longitudinal webs stiffeners, rigid flanges and bending moment are studied. The method is primarily aimed at shear capacities, but combinations of primary moment and shear can be handled by interaction equations. It is valid for all web slenderness ratios, but the rotation of the stress field disappears for low slenderness ratios. The method results in a buckling curve similar to the curve in Table 3.5.1 and hence it can be seen as an analytical variant of the proposal in EC3 Part 1-5.

In the following section the rotated stress field method is presented for webs with openings. Apparently that was also the first use of the method, as webs with circular and rectangular openings are described in Höglund (1970).

3.6.2 Circular openings

General

The following presentation is based on Höglund (1970). Transverse stiffeners are provided at the ends only, and flange bending capacities are disregarded. In the present section the method is explained for shear acting alone. The cases of primary moments acting alone and the moment-shear interaction are described in Section 3.8.

Behavior

For small shear forces the stress distribution around the opening is nearly symmetric relative to the center of the opening. The compression stresses and the tension stresses are of equal magnitude. The largest stresses occur at the edge of the opening at inclinations located 45° from the horizontal section through the opening. The web, having some initial displacements before the force is applied, gets only small additional transverse displacements. With increasing force the average compression stresses at the 45° -inclinations reach a maximum before they decrease. The tension stresses, acting at the 45° -inclinations perpendicular to the former, increase more than the increase in the shear force. At the same time a change in stress distribution takes place around the opening. The maximum tension stress moves towards the vertical section through the center of opening. This occur both on the upper and lower side of the girder. A small change of the maximum compression stresses towards the vertical section can also be seen. The redistribution of stresses follow from buckling of the web due to the compression stresses.

Theory

When the shear force is just below its ultimate value, the web has out-of-plane displacements and the stresses have reached yield in some areas. This complicated state is described by means of the model shown in Fig. 3.6.1.

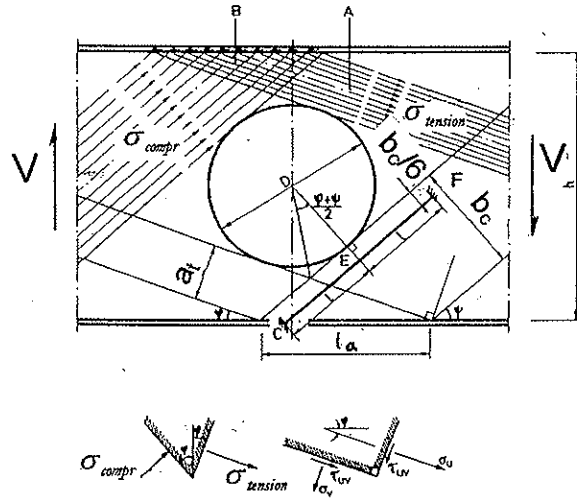


Fig. 3.6.1 Calculation model for girder with circular opening and shear [Höglund (1970) Fig. 2.18]

The shear is carried by two tension fields of width a_t and two compression fields of width b_c . The stress in the tension fields is $\sigma_{tension}$ and the stress in the compression fields is σ_{compr} . Positive signs for $\sigma_{tension}$ and σ_{compr} are to be applied in all equations. The inclinations of the tension and compression fields are described by angles ϕ and ψ , respectively. Hence six variables must be determined. To achieve this, the variables a_t , b_c , $\sigma_{tension}$ and σ_{compr} are expressed in terms of h , t , D , f_y , ϕ and ψ . The last two variables, ϕ and ψ , are found by one equilibrium equation and the maximization of the shear capacity. A detailed description is as follows:

Geometrical considerations give

$$a_t = \frac{1}{2} \frac{\frac{1}{h \cos \phi} - \frac{D}{h} \left(1 + \tan \frac{\phi + \psi}{2} \right)}{1 - \tan \phi \cot(\phi + \psi)} \quad (3.6.1)$$

$$b_c = a_t \frac{\sin \psi}{\sin \phi} \quad (3.6.2)$$

The stress $\sigma_{tension}$ is determined from two alternative yield criteria:

- 1) Yield in area A.

$$\sigma_{tension} = f_y \quad (3.6.3)$$

- 2) Yield in area B is based on the von Mises criteria applied to stresses in directions having angles ϕ and $\pi/2 - \phi$ to the horizontal

$$\sigma_e = \sqrt{\sigma_{tension}^2 + \sigma_{tension} \sigma_{compr} (1,5 \cos 2(\phi + \psi) + 0,5) + \sigma_{compr}^2} \quad (3.6.4)$$

In Fig. 3.6.3 there is a small triangle above the opening that has no stress. It is assumed that some redistribution of stress can take place here and hence the equivalent stress is reduced in proportion to the height of triangle and the remaining part of the web above the opening. Hence, the final requirement for yield in area B is

$$\sigma_{e,red} = \sigma_e \frac{a_t \sin \psi}{\sin(\phi + \psi)} \frac{2}{h - D} \leq f_y \quad (3.6.5)$$

The stress σ_{compr} is calculated as the elastic critical stress for a plate strip with unit width, thickness t and a buckling length l .

$$\sigma_{compr} = \sigma_{cr} = \frac{\pi^2 E}{12(1 - \nu^2)} \frac{t^2}{l^2} \quad (3.6.6)$$

The strip is assumed to be located $b_c/6$ from the edge of the opening, and parallel with the direction of the compression stress. The length l is one half of the line CEF in Fig. 3.6.1, where the midpoint E is determined by a perpendicular from the center of opening. The strip is assumed to have a fixed support at C and to be symmetric around E. Hence, the buckling length is

$$l = \frac{D}{2} \tan\left(\frac{\phi + \psi}{2}\right) + \frac{a}{\sin(\phi + \psi)} - \frac{a \cos \psi}{6 \sin \phi} \quad (3.6.7)$$

The flanges are assumed to have no bending stiffness in the web plane and hence cannot take vertical stresses from the web. Equilibrium in vertical direction for the stresses between web and flange gives

$$\sigma_{tension} a_t t \sin \phi = \sigma_{compr} b_c t \sin \psi \quad (3.6.8)$$

The ratio between the angles is

$$A = \frac{\phi}{\psi} \quad (3.6.9)$$

The shear capacity is

$$V_m = 2\sigma_{tension} a_t t \sin \phi \quad (3.6.10)$$

Eqs. (3.6.1) and (3.6.9) are inserted in Eq. (3.6.10) and V_m is derived with respect to ϕ . The result is set equal to zero. This gives

$$\begin{aligned} & (\cot \phi + \cot(1+A)\phi) \frac{D}{h} \left(\sin \phi + \cos \phi \tan \frac{1+A}{2} \phi + \sin \phi (1 + \tan^2 \frac{1+A}{2} \phi) \right) \frac{1+A}{2} \\ & - \left(1 - \frac{D}{h} (\cos \phi + \sin \phi \tan \frac{1+A}{2} \phi) \right) \left(\frac{1}{\sin^2 \phi} - \frac{1+A}{\sin^2(1+A)\phi} \right) = 0 \end{aligned} \quad (3.6.11)$$

For a certain D/h and h/t ratio, a value is chosen for A , whereby ϕ can be found from Eq. (3.6.11). Then Eq. (3.6.1) gives a_t , Eq. (3.6.7) gives l and Eq. (3.6.6) gives σ_{compr} . Further, Eqs. (3.6.2) and (3.6.8) give $\sigma_{tension}$, but Eqs. (3.6.3) to (3.6.5) put limits to $\sigma_{tension}$. For the valid $\sigma_{tension}$, the shear capacity is calculated from Eq. (3.6.10). The procedure must be repeated for new values of A until a *maximum* shear capacity V_m is reached.

Results

Yield criteria B implies yielding in the minimum section, and is governing for small openings with small h/t ratios. Yield criteria A corresponds to a sort of Vierendeel action, and is governing for small openings and large h/t ratios, and for large openings and all h/t ratios. Large openings is here taken as $D > 0,70h$.

General diagrams give the shear capacities as ratios V_m/V_p , based on ratios of D/h and h/t . Here, V_p is the yield shear capacity of the web, assuming no opening and no buckling. One diagram covers all webs having a certain yield stress. The design for various values of D , h and t is then very simple. Fig. 3.6.2 shows a diagram for $f_y = 260 \text{ N/mm}^2$. The diagram is taken from Höglund (1970) and shows $T/T_s = V_m/V_p$. Further, the diagram includes an alternative ordinate axis α , which represents the relative slenderness axis..

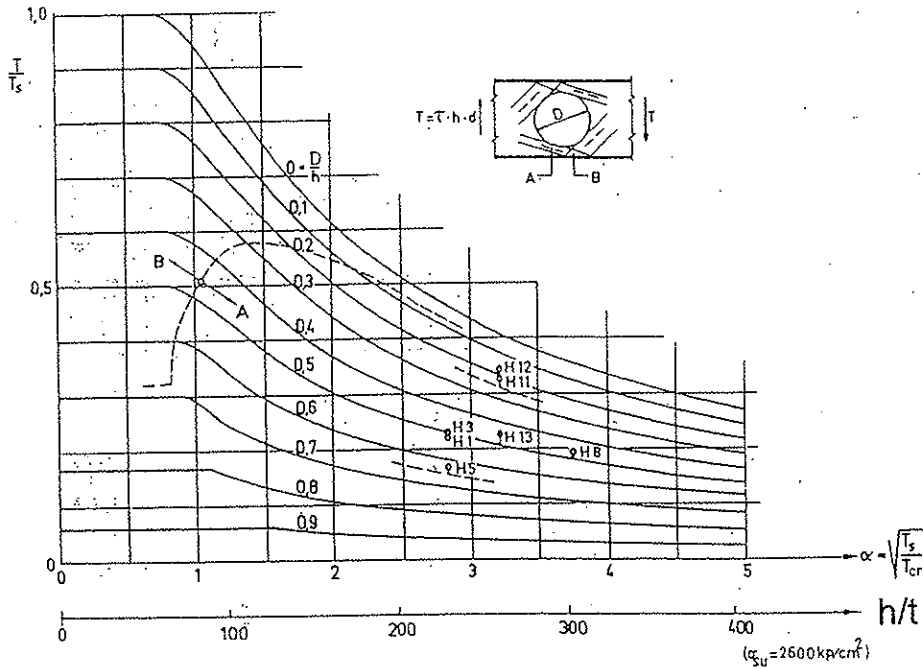


Fig. 3.6.2 Calculated ratios of $T/T_s = V_m/V_p$ as functions of D/h and h/t ratios. Circular openings and $f_y = 260 \text{ N/mm}^2$. [Höglund (1970) Fig. 2.19]

Fig. 3.6.3 shows a general view of the rotated stress field method for various opening sizes and values of relative slenderness. The density of the lines is proportional to the stresses: High density implies high stress. The figure is taken from Höglund (1970), where τ_c corresponds to τ_y and α is similar to $\bar{\lambda}_w$.

The figure also shows three aspects of the normal forces in flanges. These are

- Additional compression force
- Concentration of the transfer of forces at opening
- Location of the inflection point.

The stress patterns in flanges are shown as thin and bold inclined lines above and below the girders. Thin lines show stress patterns when the webs have pure shear stress without openings and buckling. Bold lines show the theoretical stress patterns for the same shear stress when the webs have openings and/or can buckle.

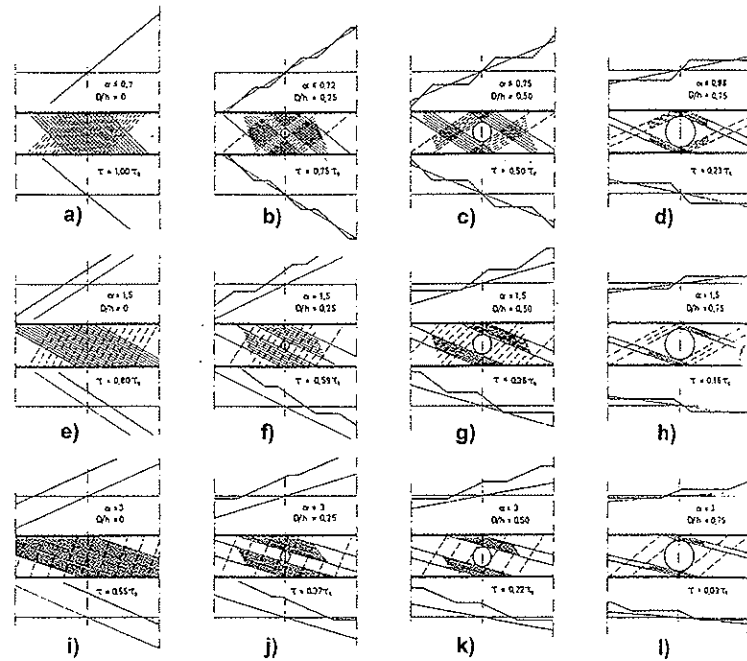


Fig. 3.6.3 Compression and tension fields, as well as stresses in the flanges, compared with stresses for a plane web without opening at the same shear force. [re-arranged from Höglund (1970) Fig. 2.20]

3.6.3 Rectangular openings

General

The following presentation is based on Höglund (1970).

Behavior

The behavior for rectangular openings is similar that to for circular openings. Transverse displacements are concentrated to the two corners of the opening where the web is in compression, here called the “compression corners”. In the two other corners plastic hinges are formed. The inflexion points for the secondary moments are not located in the centerline through the opening, but are moved towards the compression corners.

Theory

The calculation model is shown in Fig. 3.6.4. The inflexion points are given by the intersections between the centerlines of flanges and the centerlines of compression and tension fields.

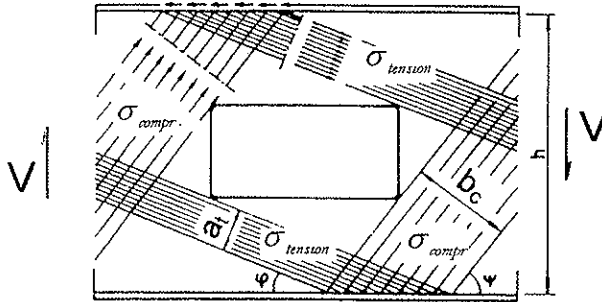


Fig. 3.6.4 Calculation model for girder with rectangular opening and shear. [Höglund (1970) Fig. 3.11]

The same equations and calculation procedure are used as for a circular opening, with a few exceptions:

- The width of tension fields, Eq.(3.6.1) is replaced by

$$a_t = \frac{h - D_o}{2} \cos \phi - D_o \sin \phi + \frac{h - D_o}{2} \frac{\sin \phi}{\tan \psi} \quad (3.6.12)$$

- For yield in area B, Eq. (3.6.4) is replaced by

$$\sigma_{e,red} = \sigma_c \frac{1}{1 + \frac{D_o \sin \phi}{a_t}} \quad (3.6.13)$$

- For the buckling length, Eq. (3.6.7) is replaced by

$$l = \left(\frac{h - D_o}{2} - \frac{a_t \cos \psi}{6} \right) \frac{1}{\sin \psi} \quad (3.6.14)$$

- Eq. (3.6.11) is replaced by

$$\cos 2\phi - \left(\frac{2D_o}{h - D_o} - \frac{1}{\tan A\phi} \right) \sin 2\phi - \frac{\sin^2 \phi}{\sin^2 A\phi} = 0 \quad (3.6.15)$$

Results

General diagrams similar to Fig. 3.6.2 give the shear capacities as ratios V_m/V_p , based on ratios of D_a/h , D_h/h and h/t . One diagram covers all webs having a certain D_a/D_h ratio and a certain yield stress. However, various ratios of D_a/D_h require separate diagrams. Diagrams for square and rectangular openings and $f_y = 260 \text{ N/mm}^2$ can be found in Höglund (1970).

3.6.4 Discussion

Simplified shear buckling by means of functions $\chi_{w, \text{mod}}$

In Fig. 3.6.2 the ratio $T/T_s = V_m/V_p$ is by definition equal to $\chi_{w, \text{mod}}$ and α is identical to $\bar{\lambda}_w$. Apparently the diagram then shows the solution that was proposed in the last part of Section 3.5.3: The shear capacity is given by Eq. (3.5.14), all effects of openings are included in $\chi_{w, \text{mod}}$ by means of separate curves for each D/h ratio, and the shear buckling coefficient k_τ includes only the aspect ratio of the web.

A closer study of Höglund (1970) shows that the diagram is valid only for $k_\tau = 5,34$, i.e. for a web with aspect ratio $a/h > 5$. Transverse stiffeners are assumed only at the ends of girders. If transverse stiffeners are applied along a girder, it is not necessarily possible to use higher values of k_τ and expect that the diagram gives correct shear capacities. However, this is not an objection to the method, it is more an indication that the solution is not influenced by k_τ . Fig. 3.6.1 and Eq. (3.6.6) show that the solution depends on local, column type buckling at the edges of opening and has no connection with global buckling covered by k_τ . Transverse stiffeners must be very close to the opening to give an increased shear capacity, i.e. they have to be within the area covered by the buckling length l . And even then an increased k_τ cannot be expected to give correct values of the shear capacity.

A preliminary conclusion is that the shear capacity of webs with openings can be given by Eq. (3.5.14), where $\chi_{w, \text{mod}}$ is given for each D/h ratio as function of the relative slenderness, provided $k_\tau = 5,34$. Here, the material yield stress is included both directly through Eq. (3.5.14) and indirectly through the relative slenderness.

In Höglund (1970) the calculations of $\chi_{w, \text{mod}}$ are based on $f_y = 260 \text{ N/mm}^2$. But, in the diagram in Fig. 3.6.2, values of $\chi_{w, \text{mod}}$ are alternatively given as a function of the relative slenderness. However, the paper does not prove that other values of yield stress can be handled by this measure.

The compression stress of Eq. (3.6.6) is not influenced by the yield stress, but the tension stress given by Eqs. (3.6.3) to (3.6.5) is influenced. The combined effect is the result of a maximum value governed by Eq. (3.6.11). It can hardly be expected that the effect is reflected 100 % correctly in Eq. (3.5.14) and the relative slenderness ratio. It might be that the approximation is acceptable. Alternatively, the functions $\chi_{w, \text{mod}}$ may be given as curve sets, with one set for each yield stress. As the relative slenderness then will cover only the modulus of elasticity and the h/t ratio, the best solution will probably be to give $\chi_{w, \text{mod}}$ as functions of the h/t ratios only.

Local buckling

For slender webs, the shear capacity calculated by the rotated stress field method is limited by local, column type buckling. The success of the method depends on the correctness of the assumption of the buckling lengths, from which Eq. (3.6.6) is established. By varying this parameter, the shear capacities can be adapted to experimental results. Höglund (1970) states that the chosen length, location and boundary conditions are the best choice, based on available results.

The local, column type buckling is based on elastic critical stress only. Local elasto-plastic buckling, if any, is not included. Hence, the results might be somewhat non-conservative. This can be adjusted by modifying σ_{comp} in Eq. (3.6.6) before further calculations.

3.7 Modified Vierendeel method

3.7.1 General

Besides the rotated stress field method, Höglund (1970) also presents a modified Vierendeel method, suitable for larger rectangular openings. According to Höglund, the rotated stress field method gives larger shear capacity for small openings and slender webs than the modified Vierendeel method. For a square opening with side lengths $0,50h$ both methods give approximately same result. For larger openings the modified Vierendeel method gives larger shear capacity and probably is the best method.

3.7.2 Rectangular openings

General

The following presentation is based on Höglund (1970). He describes the method with primary moment and shear acting together. However, in order to be consistent with the description in Section 3.6.3, the primary moment is assumed to be zero in the following presentation.

Theory

The calculation model is shown in Fig. 3.7.1

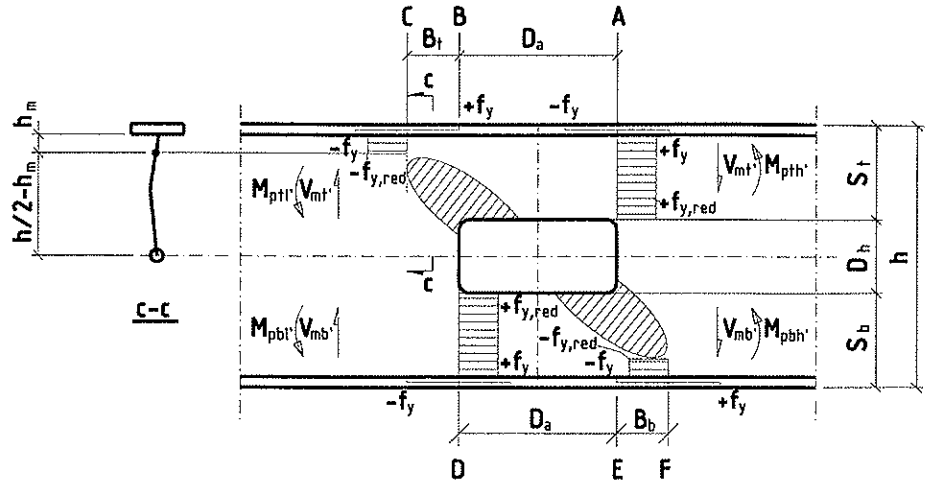


Fig. 3.7.1 Calculation model of modified Vierendeel method for girder with rectangular opening and shear.

The total shear capacity is denoted V_m' , where the subscript ' is included to show the similarity with V_m of Section 3.3.

$$V_m' = V_{mt'} + V_{mb'} \quad (3.7.1)$$

$$V_{mt'} = \frac{M_{ptt'} + M_{pth'}}{B_t + D_a} \quad (3.7.2)$$

$$V_{mb'} = \frac{M_{pbt'} + M_{pbh'}}{B_b + D_a} \quad (3.7.3)$$

$M_{ptt'}$, $M_{pth'}$, $M_{pbt'}$ and $M_{pbh'}$ are the moment capacities of the tees at C, A, D and F, respectively. Again the subscript ' is included to show the similarity with the secondary moment capacities of Section 3.3. However, here the locations at C and F are not at the tee ends, as they are in Section 3.3. B_t and B_b are explained below.

The hatched areas in the two compression corners are assumed to be non-effective for normal and bending stress, but effective for shear. The effective width for normal and bending stress is assumed to be

$$h_m = 15t \leq s_t \quad (3.7.4)$$

The plastic moment capacities of the top tee at C and A are

$$M_{ptt'} = f_{y,red} \frac{h_m^2}{2} \quad (3.7.5)$$

$$M_{pth'} = f_{y,red} \frac{s_t^2}{2} \quad (3.7.6)$$

The requirement is similar for the bottom tee. These approximations assume that the plastic neutral axes are located in the flanges. $f_{y,red}$ is the normal stress that contributes to the plastic moment capacity of the tee webs, when the yield stress is reduced for shear stress by the von Mises criteria. See Eq. (3.3.6). The shear stress in the top tee is

$$\tau_t = \frac{V_{m'}'}{s_t t} \quad (3.7.7)$$

and similar for the bottom tee.

The vertical reaction force in the two compression corners cannot act at the edge of the opening, as normal for beams, but is assumed to act at distances B_t from the top corner and B_b from the bottom corner. These distances depend on the local buckling capacity of the web. The dimensions $2B_t$ and $2B_b$ must be sufficiently large to distribute the reaction force without local, column type buckling. The elastic critical stress of a plate strip with unit width is given by Eq. (3.6.6), and the buckling length, as depicted in Section c-c of Fig. 3.7.1, is assumed to be

$$l = 0,9 \left(\frac{h}{2} - h_m \right) \quad (3.7.8)$$

This gives

$$B_t = \frac{V_{m'}'}{2t\sigma_{cr}} = \frac{V_{m'}'}{2t \frac{\pi^2 E}{12(1-\nu^2)} \frac{l^2}{t^2}} = 0,37 \frac{V_{m'}'}{Et^3} (h - 2h_m)^2 \quad (3.7.9)$$

Results

Eqs (3.7.1) to (3.7.3) are functions of the shear force (capacity) both in the nominator and the denominator, and hence can only be solved by iterations. Unfortunately h_m is given as a function of t only, instead of h/t , and it is strictly not possible to calculate generalized diagrams of the shear capacity as functions of D_a/h , D_h/h and h/t similar to Fig. 3.6.2. Höglund (1970) has actually presented such diagrams, but the value for h_m is not clear.

3.7.1 Discussion

General

Figs. 3.7.2 and 3.7.3 may illustrate the difference between the common Vierendeel approach and the modified method.

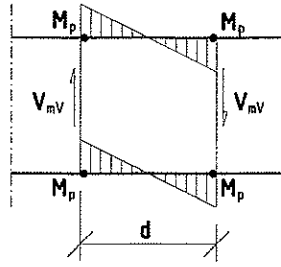


Fig. 3.7.2 Classic Vierendeel girder

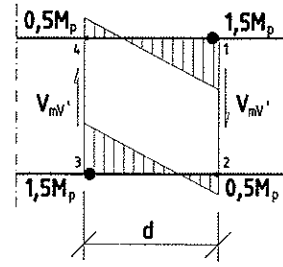


Fig. 3.7.3 Modified Vierendeel method

In the classic Vierendeel girder the upper and lower chord have approximately same stiffness. It is also presumed that the chord stiffness and plastic moment capacity M_p are equal in each end of the chords. Secondary moment diagrams are shown in the figure and the shear capacity is

$$V_{mv} = \frac{4M_p}{d} \quad (3.7.10)$$

An exact solution according to plastic theory requires that the conditions of equilibrium, presence of a mechanism and yielding are all satisfied. This is the case for all Vierendeel girders if

$$V_{mv} = \frac{\sum_1^4 M_{p,n}}{d} \quad (3.7.11)$$

$M_{p,n}$ is the plastic moment capacities at the ends $n = 1, 2, 3$ and 4 . The four values are not necessarily equal, but two of them have to comply with class 1 criteria and the two remaining with class 2. If the plastic moment capacities for instance are as shown in Fig. 3.7.3, the shear capacity of the girder is

$$V_{mv'} = \frac{1,5M_p + 0,5M_p + 1,5M_p + 0,5M_p}{d} = \frac{4M_p}{d} \quad (3.7.12)$$

and hence the same as for the classic girder. Fig. 3.7.3 shows that the inflexion points have moved, but this has no influence on the shear capacity, as long as there is extra moment capacity at two of the chord ends.

In a girder with opening there is of course no extra capacity in the two tension corners unless reinforcement is provided. Hence, for girders with un-reinforced openings there must be a certain reduction in the shear capacity due to buckling. However, even in that case a great amount of the shear capacity is intact even if local buckling occurs in the compression corners.

The modified Vierendeel analogy may violate plastic theory in a strict sense, because the vertical members in the model may also buckle. Even though this buckling is not

completely of the column type, it must lead to increased values of the length d in Fig. 3.7.3, followed by reduced shear capacity according to Eqs. (3.7.12). Hence, the shear capacity of the girder reaches a maximum value, and this value is reduced upon further loading of the girder.

No local buckling

For slender webs, the shear capacity calculated by the modified Vierendeel method is primarily determined by local, column type buckling of the web near the vertical sides of the opening. The success of the method depends on the assumption of the buckling length, from which Eqs. (3.7.8) is established. By varying this length, the shear capacities can be adapted to experimental results. For rectangular openings in the rotated stress field method the buckling length decreases with increasing height of the opening and for the modified Vierendeel method it is independent of the size of the opening.

The value of B_t should be expected to go towards zero for h/t ratios below 60 to be consistent with previous practice for stocky plates.

The choice of $15t$ as the effective width of the tee section in compression seems reasonable when compared to the allowable tee webs of Section 3.3: The modified Vierendeel method is to be used only for openings with heights equal to or more than $0,50h$. The remaining tee web of a beam/girder with $h/t = 60$ is just $15t$, when the opening height is $0,50h$.

The local, column type buckling is based on elastic critical stress only. Local elasto-plastic buckling, if any, is not included. Hence the results might be somewhat non-conservative. This can be adjusted by modifying σ_{compr} in Eq. (3.6.6) before further calculations.

Deflections

Local, column type buckling shall not occur. This means that webs with openings, designed according to the rotated stress method or the modified Vierendeel method, have only small transverse displacements when the shear capacity is reached. Some parts of the tension areas are plastified, but not more in slender webs than in stocky webs. Hence the global deflection of a girder with openings, designed according to the said methods, is expected to be comparable with the deflection of a beam with openings, designed according to the method based on strength criteria.

3.8 Moment-shear interaction in girders

3.8.1 General

The following presentation is based on Höglund (1970). Similar to Section 3.3 the design approach is based on interaction diagrams, and the maximum moment and shear capacities must be calculated. However, Höglund uses three curves to describe the interaction, compared to the single curve in Section 3.3.3. The interaction is developed for the rotated stress method and the modified Vierendeel method. Hence the pure shear capacities are already described in Section 3.6 and 3.7, and the presentation below comprises the pure moment capacity and the interaction curves.

3.8.2 Circular openings

Maximum capacity for primary moment

When a primary moment is acting alone, the moment capacities are:

- 1) Plastic moment capacity based on effective flanges and full web, but with the opening subtracted. No restrictions to the web height-to-thickness ratio apply, as buckling of the web for bending moment is limited by Eq. (3.8.2).

$$M_{pl,mod} = M_m \quad (3.8.1)$$

where M_m is given by Eq. (3.3.2)

- 2) Moment capacity when only the effective flanges and the effective parts of the web are considered

$$M_{buckl,mod,H} \approx f_y (A_f + h_m t) (h - y_{upper} - y_{lower}) \quad (3.8.2)$$

where h_m is the effective width of the compression part. y_{upper} and y_{lower} are the distances from the centroids of the compression and tension parts of the web in the vertical section through the center of opening to the centroids of flanges. Hence, the *area* of the tension part of the web is taken equal to the compression part, but for y_{lower} the real tension part is considered. For simplification the distance between the centroid of flanges is taken as h .

$$h_m = 30t \left(1 - \frac{D}{h} \right) < \frac{h}{2} \quad (3.8.3)$$

Additional forces in flanges caused by shear

Compared to the uniform transfer of shear for webs without openings, web openings concentrate the transfer of forces to the flanges. The horizontal force transferred to the flanges above and below the opening is

$$F_h = \sigma_{tension} a_f t \cos \phi + \sigma_{comp} b_f t \cos \psi \quad (3.8.4)$$

where the variables are defined in Section 3.6.2. The force is typically transferred along the triangle B in Fig. 3.6.1, where the tension and compression fields meet. In principle this is the same as explained in Section 3.3 for stocky webs, where the flanges contribute to the secondary moment capacity and increased shear stress is acting above and below openings.

The additional flange forces cause a reduction in the primary moment capacity. When the full shear capacity is utilized, the primary moment capacity is taken as

$$M_{f,mod} = M_f \left(1 - \frac{F_a}{f_y A} \right) \approx f_y A_f h \left(1 - \frac{F_a}{f_y A} \right) \quad (3.8.5)$$

F_a is the additional flange force and A is the area of the girder section without opening.

$$F_a = \frac{S}{2} \quad \text{when } l_a \leq D \quad (3.8.6)$$

$$F_a = \frac{S D}{2 l_a} \quad \text{when } l_a > D \quad (3.8.7)$$

S is the horizontal component of the tension stress field and l_a is the connection length between the compression and tension stress fields and the flange. See Fig. 3.6.1.

$$S = \sigma_{tension} a_f t \cos \phi \quad (3.8.8)$$

Moment-shear interaction

For members with both shear and primary moment acting together, the modes of stress redistribution is different for beams and girders, but the result may be quite similar. For beams the bending moment can be redistributed to the flanges when the web yields. In girders the moment redistribution takes place by buckling of the web. Small transverse displacements of the web from the original plane result in the transfer of bending moment from the web to the flanges. This does not reduce the shear capacity of the web, because the shear is mostly carried by tension stress in the tension fields.

The following interaction equations are proposed:

$$\frac{V}{V_m} \leq 1 \quad \text{when } M < M_{f,mod} \quad (3.8.9)$$

$$\frac{V}{V_m} + \left(\frac{M - M_{f,mod}}{M_{pl,mod} - M_{f,mod}} \right)^2 \leq 1 \quad \text{when } M \geq M_{f,mod} \quad (3.8.10)$$

$$\frac{M}{M_{buckl,mod.H}} \leq 1 \quad (3.8.11)$$

A typical interaction diagram is depicted in Fig. 3.8.1.

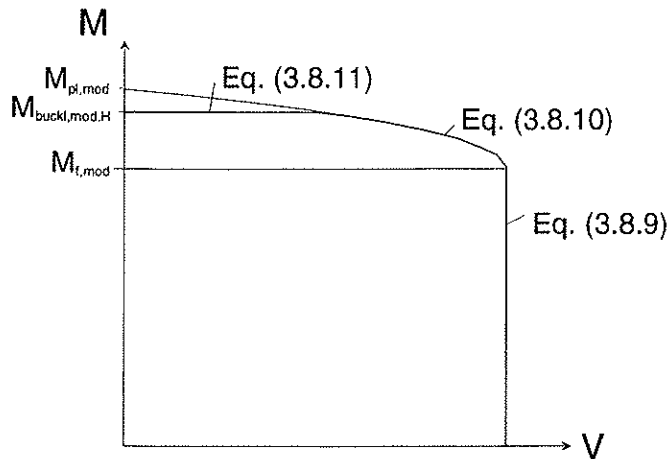


Fig. 3.8.1 Interaction diagram based on rotated stress field theory

3.8.3 Rectangular openings

Maximum capacity for primary moment

When a primary moment is acting alone, Eqs. (3.8.1) to (3.8.3) can be used with $D = D_h$, provided some requirements against buckling of the tee above the opening are fulfilled. The buckling modes are shown in Fig. 3.8.2. If the buckling capacities are reduced compared to the capacities based on yield stress, the primary moment capacities according to Eqs. (3.8.1), (3.8.2) or (3.8.5) are reduced in proportion to these reductions.



Fig. 3.8.2 Possible buckling modes for the tee section in compression. [Figure from Höglund (1970)]

- a) Lateral buckling of tee in the flange plane. The risk for this buckling mode is somewhat increased for girders with openings compared to girders without openings, because of increased stresses in the flanges. The compression flange should be laterally braced not far from the opening.
- b) Torsional buckling of flange. For girders with thin webs without openings, the connection between flange and web provides only a small contribution to the torsional buckling capacity of the flange. The contribution is further reduced if the web has an opening. It is reasonable to assume hinged connection between flange and web when torsional buckling of the flange is checked.
- c) Buckling of tee vertically upwards. The thin web can only take small compression stresses near the free edge due to lateral buckling of the edge. See Fig. 3.8.3. The hatched region is assumed not to transmit stress because of buckling, and the stiffness for bending of the tee upwards is reduced. The tee is assumed fixed at both ends and hence the buckling length is $l = 0,5D_a$. The tee web is in tension at both ends and the effective width of the tee web is assumed to be $h_m = 18t$ for a simplified, constant section over the full length. Based on this the tee can be checked as a column with axial load. Secondary moments are disregarded.
- d) Buckling of tee vertically downwards. The horizontal stresses are concentrated at the corners of the opening and the web will probably first buckle there. When the web buckles in the corners the resultant of the compression forces moves upwards. The tee section is thereby compressed eccentrically and will bend downwards. See Fig. 3.8.4. Hatched regions are assumed not to transmit stress because of buckling. The tee is hinged in both ends and the buckling length assumed to be $l = (D_a + D_b)$. The tee web compression is reduced at the midpoint and the effective width of the tee web is assumed to be s_f for a simplified, constant section over the full length. Based on this, the tee can be checked as a column with axial load. Secondary moments are disregarded. Simplified considerations show that buckling downwards can be disregarded if $s_f > 36t$.

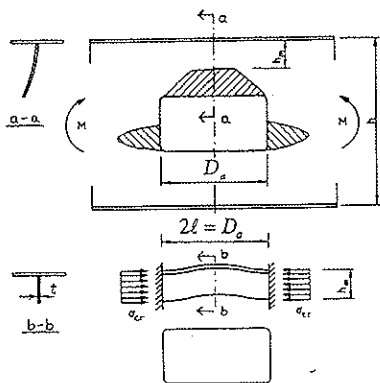


Fig. 3.8.3 Buckling of tee vertically upwards
[Figure from Höglund (1970)]

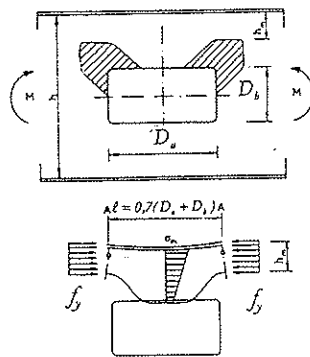


Fig. 3.8.4 Buckling of tee vertically downwards
[Figure from Höglund (1970)]

Additional forces in flanges caused by shear

The normal forces in the flanges follow similar patterns as described for circular openings. For the rotated stress field method, Eq. (3.8.1) is valid. For the modified Vierendeel method, no equation is given in Höglund (1970).

Moment-shear interaction

For shear and primary moments acting together, it is assumed that Eqs. (3.8.9) to (3.8.11) can be used. However, Höglund (1970) does not state this explicitly, but points to the fact that his interaction diagrams for rectangular openings using the modified Vierendeel method resemble his interaction diagrams for circular openings.

3.8.4 Discussion

The presence of additional forces in flanges makes the use of the rotated stress field method complicated in practice. The generalized diagram in Fig. 3.6.2 cannot be used directly, because some information about stress, width and angle of the topical tension stress field must also be at hand, in order to calculate the additional flange force to be used in Eq. (3.8.5). A simpler solution would be to include all interaction effects in one single equation similar to Eq. (3.3.1).

A brief study of Fig. 3.6.3 may point against the use of Eq. (3.3.1): In this figure the sub-figures a, b, c and d are actually showing a beam with no web buckling and Eq. (3.3.1) is valid. Additional flange forces due to secondary moments can be seen and these are covered by Eq. (3.3.1). Sub-figures e), f), g), and h show a girder with moderate web slenderness. Here the additional flange forces are caused both by rigid end-post action and secondary moments. Apparently, the forces are larger than for a beam, at least for the small to medium size openings. Sub-figures i), j), k) and l) show a girder with high web slenderness. Here, the additional flange forces are even more pronounced.

The importance of the additional flange forces should be considered relative to the total flange force capacity. For rolled beams the ratio of flange area to web area is high to moderate. Hence the influence of the additional flange forces is low and Eq. (3.3.1) is valid. For girders, at least in the offshore industry, the ratio of flange area to web area is moderate to low, and the influence of additional flange forces is relatively higher.

Square and rectangular openings with the long side parallel to the flanges induce higher additional flange forces compared to circular openings.

Based on the considerations above, it is concluded that the additional flange forces should be considered for girders with openings. Such forces may also be included for beams, but are expected to have little influence.

3.9 Tension field method

3.9.1 General

The use of a tension field method to calculate the shear capacity of webs with openings is described by Narayanan (1983a). However, it may be more convenient to explain the method by starting from its basis, which is the Cardiff method and no opening.

3.9.2 Without opening

General solution

The Cardiff method is presented in Porter, Rockey and Evans (1975). The following presentation is based on this paper, but some rearrangements of the equations are made to fit in with the subsequent presentation in Section 3.6.3 and 3.6.4 for openings.

The loading of a web can be divided into three stages:

- 1) Critical shear. With a perfectly flat plate there is a uniform shear stress throughout the web prior to buckling. A principal tensile stress of magnitude τ is acting at 45° to the flange and a principal compressive stress of the same magnitude is acting at 135° . This stress system exists until the shear stress τ equals the critical shear stress τ_{cr} .
- 2) Post-critical behavior. Once the critical shear stress is reached, the web cannot sustain any increase in compressive stress and it buckles. This causes a change in the load-carrying system, and any additional load has to be supported by a tensile membrane stress σ_t . Under the action of this membrane stress, the flanges clearly bend inwards and the extent of the tensile membrane stress field is greatly influenced by the rigidity of the flanges.
- 3) Determination of the ultimate shear load. On further loading, the tensile membrane stress, plus the critical shear stress, produce yielding in the web. Failure occurs when hinges are formed in the flanges, which together with the yield zone form a plastic mechanism and the web fails.

The critical shear stress τ_{cr} is given by Eq. (3.5.3). The membrane stress producing yield is defined as $\sigma_{t,y}$, see Fig. 3.9.1a. Since there is a uniform shear stress within the web, $\sigma_{t,y}$ is of constant value throughout the yielded region WXYZ. Plastic yielding could extend beyond boundaries WXYZ, but it is a *minimum* requirement that the complete region WXYZ must yield for a mechanism to develop. It is not necessary to know the nature of the distribution of the stress field outside this region.

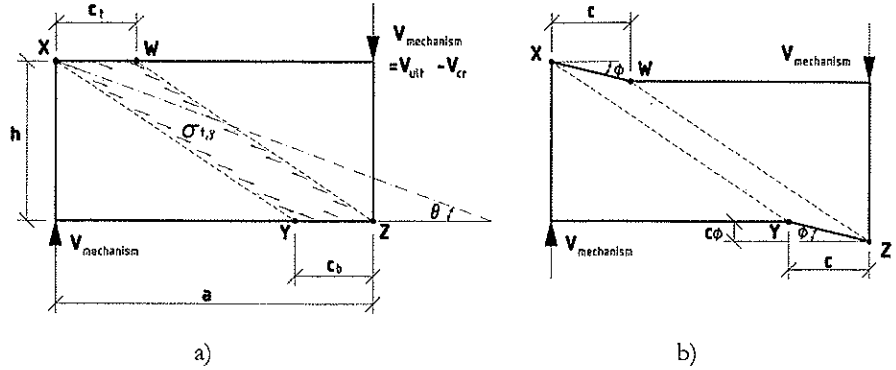


Fig. 3.9.1 Collapse mode for pure shear, showing forces developed in the post-critical stages

The failure load can be determined from a consideration of the mechanism developed in stage 3, see Fig. 3.9.1 b). It is important to recognize that the stresses shown in Fig. 3.9.1 a) are the membrane stresses developed after the plate buckles. Thus, there will be an inclined membrane field of uniform magnitude acting throughout the region WXYZ. It is therefore possible to consider the region WXYZ as cut out from the web, and its action upon the flanges and the adjacent web material replaced by the inclined membrane stresses as shown in Fig. 3.9.1 a). Based on virtual work the load carried by the tension field is

$$V_{mechanism} = \sigma_{t,y} h t \left[\cot \theta - \frac{a}{h} \right] \sin^2 \theta + \frac{4M_{pf}}{c} + \sigma_{t,y} c t \sin^2 \theta \quad (3.9.1)$$

θ is the inclination of the tension field and M_{pf} is the full plastic moment of the flange.

The internal plastic hinge in the flange will occur at the point of maximum flange bending moment, where the shear is zero. Hence the position of the hinge may be obtained by considering the equilibrium of the beam section WX.

$$c = \frac{2}{\sin \theta} \sqrt{\frac{M_{pf}}{\sigma_{t,y}}} \quad \text{valid for } 0 \leq c \leq a \quad (3.9.2)$$

In principle there may be one value c_t for the top flange and another value c_b for the bottom flange. Fig. 3.9.1 b) shows a case where the two values are equal. Combining Eq. (3.9.1) and (3.9.2), the final expression for $V_{mechanism}$ is obtained:

$$V_{mechanism} = \sigma_{t,y} h t \sin^2 \theta \left(\cot \theta - \frac{a}{h} \right) + 2c t \sigma_{t,y} \sin^2 \theta \quad (3.9.3)$$

The total capacity is

$$V_{ult} = \tau_{cr} h t + \sigma_{t,y} h t \sin^2 \theta \left(\cot \theta - \frac{a}{h} \right) + 2c t \sigma_{t,y} \sin^2 \theta \quad (3.9.4)$$

where the first term is the contribution from the critical shear load. The second term is the contribution of the true Basler solution, when the flanges are considered incapable of carrying any transverse loading. The third term is the contribution of the flanges. The second and third term is illustrated by Fig. 3.9.2. It should be noted that the tension field is not the same as the region WXYZ in Fig. 3.9.1a.

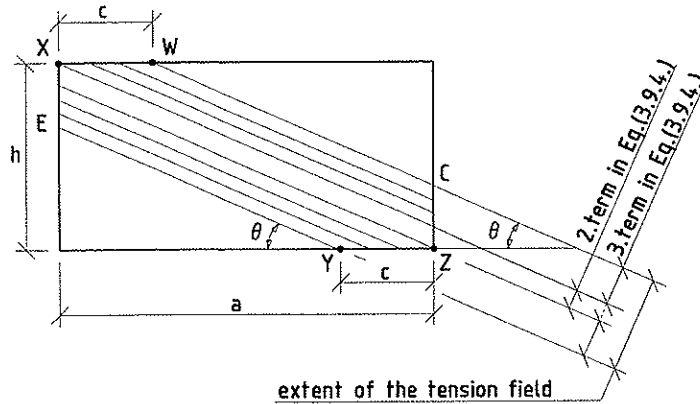


Fig. 3.9.3 Tension field of the Cardiff-method

The critical shear stress is acting also within the tension field. The membrane stress $\sigma_{i,y}$ is therefore calculated from the von Mises criterion:

$$\sigma_{i,y} = -1,5\tau_{cr} \sin 2\theta + \sqrt{f_y^2 + \tau_{cr}^2 [(1,5 \sin 2\theta)^2 - 3]} \quad (3.9.5)$$

For a given girder, the critical shear stress is fixed, and the only variable on the right hand side of Eq. (3.9.3) is θ . Eq. (3.9.3) has been obtained as an upper bound (mechanism) solution. A corresponding lower bound (equilibrium) solution is possible and is identical to the mechanism solution. Hence the optimum angle of θ will produce a maximum value for V_{ult} . This angle, θ_m , will normally lie in the region between $0,5\theta_d$ and 45° , where θ_d is the inclination of the panel diagonal.

Particular solutions

The Cardiff solution given as Eq. (3.9.4) is a continuous solution and embraces many of the classical solutions as particular cases:

- a) When $\tau_{cr} = \tau_y = f_y / \sqrt{3}$. This is the case when the web yields before it buckles. The web is unable to develop a tension field and there is no lateral loading on the flanges.

$$V_{ult} = \tau_y h t + \frac{4M_{pf}}{a} \quad (3.9.6)$$

b) When M_{pf} is large. Rigid flanges give a fully developed tension field across the web.

$$V_{ult} = \tau_{cr}ht + 0,5\sigma_{t,y}ht + \frac{4M_{pf}}{a} \quad (3.9.7)$$

c) When M_{pf} is large and the web is very thin.

$$V_{ult} = 0,5f_yht + \frac{4M_{pf}}{a} \quad (3.9.8)$$

The first term is the Wagner tension field solution for an infinitely thin web having non-deflecting boundary members. This occurs for $M_{pf} > 8a^2f_y$.

d) When $M_{pf} = 0$. Thin flanges give the true Basler solution:

$$V_{ult} = \tau_{cr}ht + \sigma_{t,y}ht \sin^2 \theta \left(\cot \theta - \frac{a}{h} \right) \quad (3.9.9)$$

e) When the aspect ratio a/h increases.

$$V_{ult} = \tau_{cr}ht \quad (3.9.10)$$

f) When the aspect ratio a/h decreases. This is the same as increasing τ_{cr} , which is explained in point a) above. No tension field will develop.

3.9.3 Circular openings

Centrally located openings without reinforcement

Narayanan (1983a) deducts the ultimate shear capacity of webs with one circular opening in a similar way as explained in Section 3.9.2. He proposes the following equation:

$$V_{ult,mod} = \tau_{cr,mod}ht + \sigma_{t,y}ht \sin^2 \theta \left(\cot \theta - \frac{a}{h} \right) + 2ct\sigma_{t,y} \sin^2 \theta - \sigma_{t,y}Dt \sin \theta \quad (3.9.11)$$

This is similar to Eq. (3.9.4), but with a fourth term subtracted, corresponding to the lost shear capacity from the membrane stress acting in the section of the opening. See Fig. 3.9.3. In addition, $\tau_{cr,mod}$ is given by Eq. (3.5.10). Indirectly this value is included also in the second and third term.

A restriction is imposed to the size of openings: An opening must be contained within the part of the tension field that is anchored to the web, i.e. the true Basler solution:

$$D_{max} = h \left(\cot \theta - \frac{a}{h} \right) \sin \theta \quad (3.9.12)$$

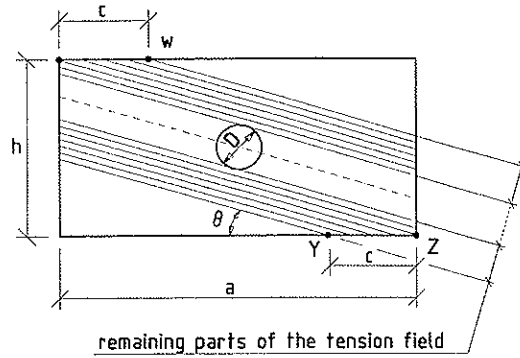


Fig. 3.9.3 Tension field for web with centrally located circular opening

Centrally located openings with reinforcement

If the remaining shear capacity is too small, the web may be reinforced around the opening. In Narayanan (1983a) the idea is to restore some of the width of the tension field by means of a circular reinforcing ring within the opening, see Fig. 3.9.4. The width is restored inwards, i.e. a reinforcement will not alter the total width of the tension field. The following equation is proposed:

$$V_{ult,mod} = \tau_{cr,mod}ht + \sigma_{t,y}ht \sin^2 \theta \left(\cot \theta - \frac{a}{h} \right) + 2ct\sigma_{t,y} \sin^2 \theta - \sigma_{t,y}(D - b_e)t \sin \theta \quad (3.9.13)$$

Eq. (3.9.13) corresponds to Eq. (3.9.11), but the fourth term is reduced with b_e , i.e. the restored width of the tension field. When M_{pr} is the plastic moment capacity of the ring,

$$b_e = 4 \cdot \sqrt{\frac{M_{pr}}{\sigma_{t,y}t}} \quad (3.9.14)$$

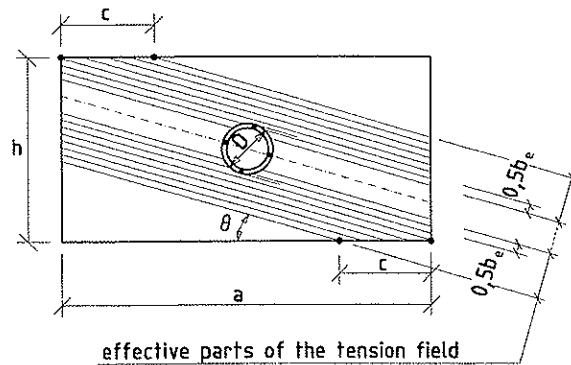


Fig. 3.9.4 Tension field for web with centrally located circular opening with reinforcement

Eccentrically located openings

The tension field in an un-perforated web is developed predominantly along a diagonal. When an opening is located in the centerline of the field, it does not matter where it is located along the diagonal. But if the opening is located eccentrically to the diagonal, the shear capacity may increase or decrease, depending on the location and size of the opening.

A favorable case is a small opening entirely outside the tension field, see Fig. 3.9.5. In Narayanan (1983a) the shear capacity is then given by Eq. (3.9.14) without the fourth term. A small reduction is included only through $\tau_{cr,mod}$. Some investigations indicate that the critical shear stress increases, but Narayanan recommends to disregard this effect.

The case is worse when an opening is located as shown in Fig. 3.9.6, i.e. when some part of a rather large opening is inside the tension field. Narayanan (1983a) deals with this problem and presents an equation for the shear strength of webs with such openings. However, the problem is very rare in practice and hence it is not further presented here.

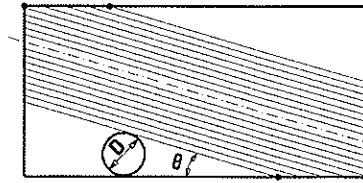


Fig. 3.9.5 Eccentrically located opening outside a tension field

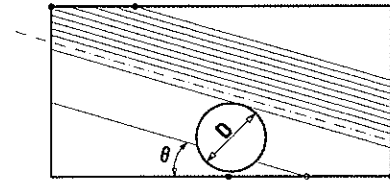


Fig. 3.9.6 Eccentrically located opening partly inside a tension field

3.9.4 Rectangular openings

Centrally located openings without reinforcement

Following the same principles as explained above for circular openings, Narayanan (1983a) has studied webs with rectangular openings. The equation for the shear capacity reads

$$V_{ult,mod} = \tau_{cr,mod}ht + \sigma_{t,y}ht \sin^2 \theta \left(\cot \theta - \frac{a}{h} \right) + 2ct\sigma_{t,y} \sin^2 \theta - \sigma_{t,y}\delta \sin \theta \quad (3.9.15)$$

where the length δ is equivalent to the diameter of an imaginary central circular opening.

$$\delta = \sqrt{D_a^2 + D_b^2} \sin \left(\text{Arc tan} \frac{D_b}{D_a} + \theta \right) \quad (3.9.16)$$

A limit to the size of the openings reads

$$D_{h,max} = h \left(1 - \frac{a + D_a}{h} \tan \theta \right) \quad (3.9.17)$$

This limit is more restrictive than for the circular opening, but Narayanan states that openings having larger heights than $D_{h,max}$ are unlikely to be met in practice.

Centrally located openings with reinforcement

In Narayanan (1983a) the idea is to restore some of the width of the tension field by means of flat bars above and below the opening, as depicted in Fig 3.9.7. The width is restored inwards, i.e. a reinforcement will not alter the total width of the tension field. The following equation is proposed:

$$V_{ult,mod} = \tau_{cr,mod}ht + \sigma_{t,y}ht \sin^2 \theta \left(\cot \theta - \frac{a}{h} \right) + 2ct\sigma_{t,y} \sin^2 \theta - \sigma_{t,y}(\delta - 2c_r \sin \theta)t \sin \theta \quad (3.9.18)$$

Eq. (3.9.18) is similar to Eq. (3.9.5), but the fourth term is reduced with $2c_r \sin \theta$, i.e. the restored width of the tension field.

$$2c_r \sin \theta = 4 \cdot \sqrt{\frac{M_{pr}}{\sigma_{t,y}t}} \quad (3.9.19)$$

M_{pr} is the plastic moment capacity of the reinforcement.

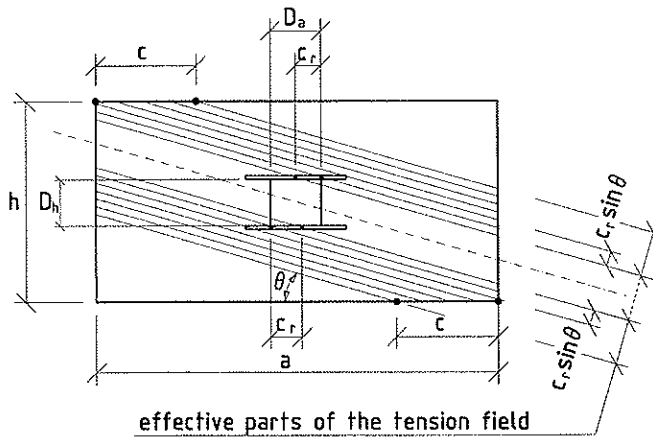


Fig. 3.9.7 Tension field for web with centrally located rectangular opening with reinforcement

Eccentrically located openings

Rectangular openings are studied in Narayanan and Darwish (1985). The effect of the opening is similar to that of circular openings. However, the problem is considered very rare in practice and hence not further presented here.

3.9.5 Discussion

General

The tension field theory for webs without openings is old and well known. It is however not frequently used in Norwegian offshore structures. One reason may be that the method is thought to give permanent displacements in the Serviceability Limit State (SLS). This is especially the case if the shear capacity is based on contribution from the flanges. If only the true Basier solution is utilized, the difference between SLS and ULS is less and the buckling occurs perhaps mostly in the elastic range.

For webs with openings the tension field method has probably never been used in Norwegian offshore industry.

Critical shear stress

It is common practice to calculate the critical shear strength as explained in Section 3.5.2 and 3.5.3. No regard is given to the fact that the tension field actually alters the static system of the web. Selberg (1973) studied this issue. For webs without openings, even small tension stresses in one or both directions will considerably increase the critical shear stress. For webs without openings, the shear capacity is found for a system completely different from the plane web without opening. This is the case both before and after local buckling at the edges of opening.

However, the critical shear stress can also be seen merely as an adjustment factor, that is not coupled to a specific physical phenomenon. By means of the critical shear stress, the shear capacities of the tension field method are closer to experimental results. Also, the critical shear stress gives a continuous transition of the tension field method for slender plates without openings to the particular solution for stocky plates. Here, the maximum critical stress is limited to the yield shear stress.

The role of the critical shear stress is more doubtful for webs with openings. Besides the lack of physical meaning, the transition from slender plates to stocky plates cannot be handled by a modified critical shear stress as given in Eqs. (3.5.10) and (3.5.11). Regardless of opening D/h ratio, the modified critical shear stress will reach the limit of the yield shear stress for decreasing web slenderness. Here, Eq. (3.9.11) for circular openings give the same shear capacity as Eq. (3.9.4) for webs without openings.

The best use of the tension field method for webs with openings are probably for very slender webs. Here, the contribution to the shear capacity from the critical shear stress is small. Hence, the question of correct critical shear stress may be of minor importance.

Small aspect ratios

In NS-ENV 1993-1-1 (1993) the minimum aspect ratio of 1,0 is recommended. This is justified by an increasing τ_{cr} for lower ratios and the assumption that a tension field will not develop. However, it was for aspect ratios down to 0,5 that Wagner (1928) developed his pure tension field theory and it was only then that the flanges could give sufficient strength. Actually, there is no theoretical lower limit for the aspect ratio as τ_{cr} also depends on the h/t ratio.

Flanges and the primary moment-shear interaction

When the flanges are used to increase the width of the tension field, the capacity of the flanges to take normal forces is reduced. Hence, some of the primary moment capacity of the girder is lost. Both girders with or without openings are influenced by this effect. In principle it is not difficult to handle this. A procedure is given in NS-ENV 1993-1-1 (1993) for webs without openings. For webs with openings the procedure might be extended to cover also the additional forces caused by shear, as explained in Section 3.8.4. However, in practice this effect is a major obstacle, as there is no longer a weak interaction between shear strength and primary moment capacity. By using only the true Basler solution for the shear capacity and the flanges only for the primary moment capacity, there is no moment-shear interaction for girders without openings. NS-ENV 1993-1-1 (1993) allows this simplification.

Width of the tension band at openings and at anchorage

The shear capacity in Eq. (3.9.11) is based on a tension field that is simply reduced with the width of the opening. The outer width of the tension field is not altered. This seems conservative for the following reasons:

- In Fig. 3.9.4 the tension field is split into two parts. The white areas outside the two parts have small stresses; theoretically these areas only carry the τ_{cr} stress. In a section through the opening normal to the centerline of the tension fields, it can be seen that the white areas extend into this section. It is likely to believe that these areas will be stressed to yield, and make the tension fields wider at the opening.
- To achieve wider tension fields at the opening, it should not be required that the tension bands are wider in their full lengths. A small modification of the direction of each tension band might be counteracted by some compression in the inactive areas between the tension fields, even after local column type buckling of these areas.
- A reduced width of the area between the two parts of the tension field is not unlikely at the anchorage. Compared to the tension field without opening, the total force to be anchored is reduced. The reduction might be considered to take place from the outside of the tension band and inwards, leaving the part that is anchored to the web and omitting the part that is anchored to the flanges. If so, the true Basler solution would be sufficient at the anchorage, at least for the larger openings.

The idea is illustrated in Fig. 3.9.8.

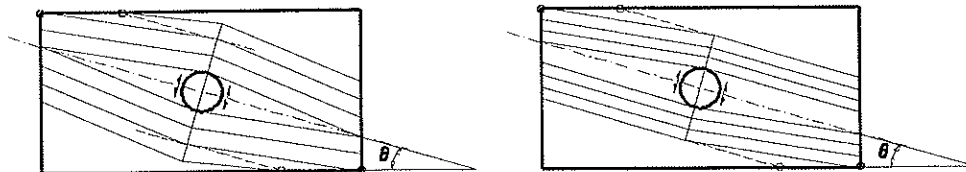


Fig. 3.9.8 Alternative configurations of tension fields at openings.

Small openings allowed in AISC rules

AISC (1978) allows girder webs without openings to be designed by the true Basler solution. It also allows smaller openings, up to $D = 0,15h$, to be located within tension fields without reduction in shear capacity. This is consistent with the ideas of the previous section: A small extension of the tension fields compensates for the opening, while nothing happens at the anchorage, since the tension is as before.

Reinforcing rings

The theory for reinforcement around openings utilizes the bending stiffness of the rings. The result is quite heavy rings. A better solution may be to apply doubler plates, as depicted in Section 3.12. The theory remains the same, but the bending capacity of the reinforcement is improved.

3.10 Stressed skin method

3.10.1 General

A brief description of the stressed skin method and its application for design of living quarters is given in Section 2.5. Most design recommendations and theories of structural effects for openings in beam and girder webs are not applicable for stressed skin design. For stressed skin the capacity of panels with major openings is governed by buckling of stiffeners, while for openings in beams the yield capacity around the opening is governing. It is therefore developed special formulas for stressed skin structures.

In the context of this thesis, the question may be reversed, i.e. perhaps the stressed skin method can be used to design girder webs with openings?

The stressed skin method is in use today also for design of reinforced openings in beam webs. The method is preferred for its simplicity, and because the buckling strengths of reinforcement and stiffeners are addressed in an orderly way. The problem of transverse buckling of reinforcement is, for example, only briefly described in the method based on strength criteria referred in Section 3.3.

A special variant of the stressed skin method is the Checkerboard method, which is presented in Section 3.11.

The following presentation is based on Solland and Frank (1988).

3.10.2 Without openings

General

A typical plate panel is shown in Fig. 3.10.1. The basic assumptions for the stressed skin method are presented in Section 2.5. The requirements to a shear panel necessary to fulfil these assumptions are summarized as follows:

- Stiffeners should provide the shear panel with satisfactory global shear strength and postcritical capacity.
- Local plate panels between stiffeners should have satisfactory shear strength and postcritical capacity.
- Stiffeners should have capacity against local and torsional buckling in excess of their global buckling strength.
- Shear panels should resist all transverse loads acting in combination with in-plane shear.

Buckling of the whole panel including stiffeners is denoted global shear buckling, as opposed to buckling of the portion of the plane plating between stiffeners, which are denoted local shear buckling.

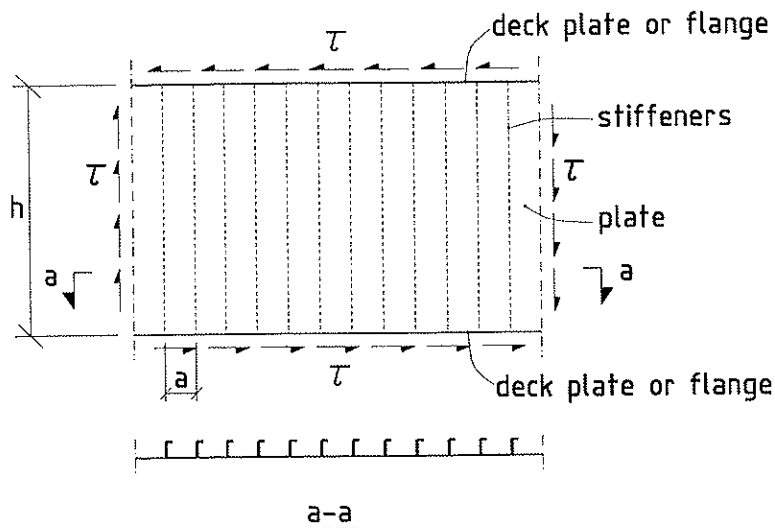


Fig. 3.10.1 Typical plate panel

The stressed skin theory also allows the use of corrugated plate panels. The corrugations replace the stiffeners and provide the required global shear strength, while the local shear strength requirements apply to the plate panels between the fold lines of the corrugations. In the following discussion only flat plate with stiffeners is considered.

Global shear buckling

The critical shear stress for a thin orthotropic plate is given by

$$\tau_{cr,G} = 36 \frac{D_x^{0,25} D_y^{0,75}}{h^2 t} \quad (3.10.1)$$

where h is the height and t is the thickness of the panel. D_x and D_y are the flexural rigidities per unit length parallel and perpendicular to the stiffeners.

$$D_x = \frac{Et^3}{12(1-\nu^2)} \quad (3.10.2)$$

$$D_y = \frac{EI_y}{a} \quad (3.10.3)$$

where I_y is the second moment of area of the stiffener, including an effective plate flange, and a is the distance between stiffeners.

The global reduced shear stress $\bar{\tau}_{k,G}$ is a function of the reduced slenderness

$$\bar{\lambda}_{w,G} = \sqrt{\frac{\tau_y}{\tau_{cr,G}}} \quad (3.10.4)$$

and curves similar to Eqs. (3.5.7) to (3.5.9).

Local shear buckling

The local reduced shear stress $\bar{\tau}_{k,L}$ is calculated as explained in Section 3.5.1 and 3.5.2, assuming local panels of size a times h and simply supported edges. The amount of local post-critical shear strength that can be utilized, depends on the code that are used in the design. However, as the global shear buckling interacts with the local shear buckling in a way that is not yet fully understood, care should be shown when taking advantage of the post-critical capacity.

Interaction between global and local shear buckling

The possible interaction between global and local shear buckling is accounted for by using a cross section for I_y in Eq. (3.10.3), based on the effective plate width of $30t$.

Stiffeners

The reliability of the stressed skin method rests on global post-critical strength, even if such strength is not explicitly utilized. Also, in an actual structure, there will probably be some

normal stresses in the shear panel, even if the state of stress is idealized by shear stress only. To ensure that normal stresses do not force the stiffeners into early collapse and hence damage the required stiffness for global shear buckling, some requirements are required to avoid web and flange buckling as well as torsional buckling. See below for panels with openings.

Transverse loads

For panels in offshore structures such loads are commonly wind and deck loads. Bending stresses due to these loads are included in separate capacity checks of both plate and stiffeners. For girder webs this is less important.

3.10.3 With openings

General

The method is primarily aimed at rectangular openings. The approach for analyzing a panel with an opening is similar to the analysis of a panel without opening and hence the same requirements apply. In addition it is assumed that the effect of the opening on the total shear panel is limited to the area of the calculation model.

Calculation model

The calculation or analysis model is shown in Fig. 3.10.2. A plate panel of thickness t is subjected to global shear stresses τ acting along the outer boundaries of the model. At the top and bottom boundaries there will often be axial elements in form of decks or flanges. At the vertical boundaries there may be stiffeners. However, there is no requirement to the boundaries apart from the assumption that the plate panel is simply supported along the top and bottom boundary. In Fig. 3.10.2 the opening is approximately square and is shown somewhere in the middle of the panel, but the calculation model allows the opening to be of any rectangular shape and to be located anywhere inside the panel, including in the corners.

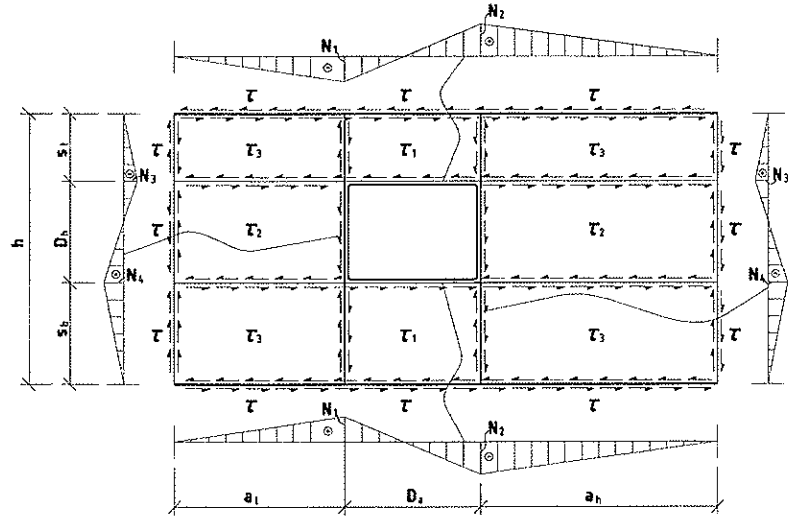


Fig. 3.10.2 Calculation model for a panel with an opening.

An extra stiffener system is located around the opening and divides the plate into sub-panels. Local shear stresses in the sub-panels are obtained by the following equations:

$$\tau_1 = \frac{\tau h}{s_i + s_b} \tag{3.10.5}$$

$$\tau_2 = \frac{\tau(a_i + D_o + a_h)}{a_i + a_h} \tag{3.10.6}$$

$$\tau_3 = \frac{\tau h - \tau_2 D_h}{s_i + s_b} \tag{3.10.7}$$

The local shear stresses introduce axial forces in the stiffeners around the opening. The axial forces vary along the length of the stiffeners as shown in Fig. 3.10.2. Maximum absolute values of the axial forces are

$$N_1 = |(\tau_2 - \tau_3)a_i t| \tag{3.10.8}$$

$$N_2 = |(\tau_2 - \tau_3)a_h t| \tag{3.10.9}$$

$$N_3 = |(\tau_1 - \tau_3)s_i t| \tag{3.10.10}$$

$$N_4 = |(\tau_1 - \tau_3)s_b t| \tag{3.10.11}$$

Stiffeners

If stiffeners are placed on one side of the plate only, they are subjected to varying eccentricity moments. For calculation purposes, these moments can be considered equal to

the axial force multiplied by the distance from the plate centerline to the centroid of the stiffener section including an effective plate width of $30t$.

The stiffeners must be checked for flexural buckling due to the axial forces and the eccentricity moments. Special care should be taken in determining the buckling lengths of the stiffeners due to the varying axial force, changing from compression to tension, and the fact that the stiffeners are not laterally supported at the points where the axial forces are changing signs. The whole stiffener length should be used as basis when calculating the buckling length and not only the part subject to compression. A simplification is to use a buckling length of each stiffener equal to the extension of the opening in the direction of the stiffener. Once the buckling lengths are found, the stiffeners are checked as ordinary beam-columns.

To avoid web and flange buckling in stiffeners, they must fulfil certain requirements to width-to-thickness ratios. Compared to section classes, the requirements are between Class 2 and 3 for axial stress.

To avoid torsional buckling of stiffeners, the following requirement should be satisfied

$$\sigma_{cr,T} = \frac{GI_T}{I_{po}} + \frac{\pi^2 E h_s^2 I_z}{I_{po} L_s^2} > 2,5 f_y \quad (3.10.12)$$

where I_T is the St.Venant torsional constant of the stiffener, I_{po} is the polar second moment of area of the stiffener about the toe and I_z is the second moment of area of the stiffener about its centroid perpendicular to the plate. h_s is the distance from the shear center of the stiffener to its toe and L_s is the length of stiffener between transverse supports.

Local shear buckling

Each sub-panel is checked for local shear buckling similar to panels without openings.

3.10.4 Discussion

Interaction between global and local shear buckling

The calculation of shear buckling capacities for plates with stiffeners can be done in various ways. A more conservative approach than stated in Solland and Frank (1988), is to use Eqs. (3.10.1) to (3.10.3), but to replace the yield shear stress by $\tau_{k,L}$ when the reduced slenderness for global buckling is calculated. Hence

$$\bar{\lambda}_{wG,int} = \sqrt{\frac{\tau_{k,L}}{\tau_{cr,G}}} \quad (3.10.13)$$

is used in stead of Eq. (3.10.4).

Recently, the shear capacity of plates with stiffeners in Norwegian offshore structures is often based on more general methods, that is available in common spreadsheets for plate buckling. Such methods intend to handle bi-axial stresses, shear and transverse loads in one batch, and presumably some simplifications have been necessary to achieve this. Also, some post-buckling capacity may have been anticipated. As the main purpose is to cover bi-axial stress and transverse loads, it may therefore be questioned whether these methods always give reasonable and safe solutions for pure shear.

Requirement to stiffeners

A simplification is to use class 1 for horizontal stiffeners and class 2 for vertical stiffeners, the classes refers to axial stress.

Calculation model in general

The stressed skin method for plates with openings is simple and very useful for hand calculations and spreadsheets. The forces are calculated from a general concept, which is connected neither to certain codes nor to buckling.

The calculation model is twice static indeterminate. This is handled by assuming 1) same shear stress above and below the opening and 2) same shear stress on each side of the opening. These assumptions result in equal shear stress in all four corner panels. The absolute values of the axial forces in the horizontal stiffeners are equal, but with opposite sign in the top and bottom stiffener. The values of the axial forces in the vertical stiffeners are also equal, but with opposite sign in the left and right stiffener. The inflexion points are located on vertical and horizontal lines, not necessarily going through the center of the opening.

Similar to girder webs, the secondary moments may be considered held by the axial forces in horizontal stiffeners and flanges. In general, the secondary moments will be of different magnitude in all four corners of the opening, a result quite different from the usual Vierendeel approach. The Vierendeel distribution of secondary moments appears only as a particular solution, i.e. when the model is double symmetrical.

Forces at the boundaries of the calculation model

The global shear stresses τ act along the boundaries of the calculation model, but this does not imply that there is continuous transition between the outer and inner shear stresses. Axial members are required to distribute and level out the shear stresses. In stiffened shear panels, the horizontal axial members usually consist of decks or flanges, and the vertical axial members consist of two of the vertical stiffeners. If stressed skin theory is used for girder webs, horizontal members at the boundaries are provided by the girder flanges. However, vertical members at the boundaries may not always be at hand, as it would often be un-economical to provide four vertical stiffeners for each opening. In that case parts of the web plate have to serve as vertical members and limited axial capacity is expected, especially for members in compression.

Maximum absolute values of the axial forces in the upper and lower flanges in sections through the opening are

$$N_5 = \left| \frac{M}{h} + \tau(0.5D_a + a_h)t - \tau_3 a_h t \right| = \left| \frac{M}{h} + \frac{\tau D_a t}{2} + (\tau - \tau_3) a_h t \right| \quad (3.10.14)$$

$$N_6 = \left| \frac{M}{h} - \tau(0.5D_a + a_t)t + \tau_3 a_t t \right| = \left| \frac{M}{h} - \frac{\tau D_a t}{2} - (\tau - \tau_3) a_t t \right| \quad (3.10.15)$$

M is the primary moment in the vertical centerline of the opening. The values are the same in each flange, but have opposite sign in the top and bottom flange. The second term in each equation represents the normal increase that will be in any girder flange due to shear in web. The last term in each equation comprises the real increase in flange forces caused by the opening these additional flange forces have inflexion points located on the same vertical line as the inflexion points of the horizontal stiffeners.

The maximum absolute values of the axial forces in the outer vertical members are

$$N_7 = |(\tau_3 - \tau) s_t t| \quad (3.10.16)$$

$$N_8 = |(\tau_3 - \tau) s_b t| \quad (3.10.17)$$

These values are the same in each member, but have opposite sign in the left and right member. The inflexion points are located on the same horizontal line as the inflexion points for the inner vertical stiffeners.

Primary moment-shear interaction

The interaction is given by Eqs. (3.10.14), (3.10.15) and the following requirement

$$N_5 \leq A_f f_y \quad (3.10.18)$$

$$N_6 \leq A_f f_y \quad (3.10.19)$$

where A_f is the smallest flange area of the top and bottom flanges. Unfortunately the interaction must be calculated from case to case. In general, it is not possible to establish simple interaction equations like Eq. (3.3.1).

A typical interaction diagram

However, it may be interesting to establish a diagram for a typical girder with a rectangular opening designed by the stressed skin method:

A girder with an opening of length D_a and height D_h is reinforced by horizontal reinforcement such that full yield shear stress can be developed above and below the opening. Assuming no buckling, the shear capacity is

$$V_m = \tau_y(h - D_h)t = \frac{f_y}{\sqrt{3}}(h - D_h)t \quad (3.10.20)$$

If a shear force V is acting, the shear stress above and below the opening is

$$\tau_1 = \frac{V}{(h - D_h)t} = \frac{V}{V_m} \frac{f_y}{\sqrt{3}} \quad (3.10.21)$$

Assuming a single symmetric calculation model, the maximum flange force is given by Eq.(3.10.14) as

$$N_s = \frac{M}{h} + \tau_1 \frac{D_a t}{2} = \frac{M}{h} + \frac{V}{V_m} \frac{f_y}{\sqrt{3}} \frac{D_a t}{2} \quad (3.10.22)$$

In this case, single symmetric means that the model is symmetric relative to the vertical centerline through the opening. Eq. (3.10.18) gives

$$\frac{M}{h} + \frac{V}{V_m} \frac{f_y}{\sqrt{3}} \frac{D_a t}{2} \leq A_f f_y \quad (3.10.23)$$

Primary moment capacity of the girder without opening, counting only the flanges, is

$$M_f = A_f f_y h \quad (3.10.24)$$

The flange area can be expressed as a ratio α of the web area without opening

$$A_f = \alpha h t \quad (3.10.25)$$

which leads to the interaction equations

$$\frac{V}{V_m} \leq 1 \quad (3.10.26)$$

$$\frac{M}{M_f} + \frac{1}{2\sqrt{3}} \frac{D_a}{\alpha h} \frac{V}{V_m} \leq 1 \quad (3.10.27)$$

The shape of the interaction diagram is independent of the height of the opening, but depends on the ratios D_a/h and α . Assume, for example, that the opening has a length $D_a = 0,50h$ and the ratio

$$\alpha = \frac{A_f}{ht} = \frac{2000}{1000 * 3} = \frac{2}{3} \quad (3.10.28)$$

Eq. (3.10.27) then reads

$$\frac{M}{M_f} + 0,22 \frac{V}{V_m} \leq 1 \quad (3.10.29)$$

The interaction is shown in Fig. 3.10.3. It appears to be relatively strong for this particular girder with rather small flanges. If the opening is twice as long, or if the secondary moment in the top tee is distributed to one side only, the factor 0,22 in Eq. (3.10.29) must be replaced by 0,44. The dotted line in Fig. 3.10.3 shows this effect.

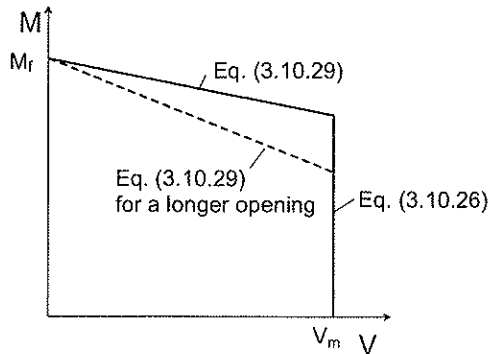


Fig. 3.10.3 Interaction diagram for a typical girder with rectangular openings designed by the stressed skin method

Eccentrically located openings

Eccentrically located openings can also be handled by the stressed skin method. The shear stresses are not altered if an opening is moved, for example, from the center towards the lower half of a web. The forces and buckling lengths of the horizontal stiffeners are not altered, either, but the forces and buckling lengths of the vertical stiffeners increase. This observation may be a reason to assume the following:

- If the vertical stiffeners, or the vertical part of the web without stiffeners, have sufficient strength, the location of the opening has no influence on the shear strength.
- If the vertical stiffeners, or the vertical part of the web without stiffeners, are weak, a re-location of the opening off the web horizontal centerline reduces the shear strength.

Lower bound solutions

As the plates can buckle from shear and the stiffeners from axial compression, the stressed skin method rarely gives lower bound solutions in the strict sense. However, if the smallest value of the critical shear stress or the reduced shear stress of each sub-panel can be considered as a sort of "guaranteed yield stress", the sub-panels do not violate the lower bound condition. Further, it is possible to choose two of the corner plate shear stresses such that all stiffeners are in tension. Then the stressed skin method provides a lower bound solution.

If a particular set of corner plate shear stresses is assumed, the axial forces in stiffeners and flanges must be calculated from case to case. Eqs. (3.10.5) to (3.10.11) and (3.10.14) to (3.10.17) are not valid. In general the forces increase and there are not necessarily any inflexion points.

3.11 Checkerboard method

3.11.1 General

In the stressed skin method, the static indeterminate calculation model with eight panels can alternatively be solved by assuming that two corner panels have zero shear stress. These assumptions replace the common assumptions of equal shear stress in the panels above and below the opening and of equal shear stress in the panels on each side of the opening. The corner panels with zero shear can be placed on one side of the opening, above or below the opening or diagonally on each side of the opening. All configurations appear as a sort of checkerboard pattern. This is the basis for the checkerboard method described in Buckland, Bartlett and Watts (1988). However, they use only two panels over the height of the girders. The following presentation is based on this paper.

3.11.2 Multiple openings

Fig. 3.11.1 shows a part of a large web in an offshore structure with several openings. The shaded areas are reserved for openings and assumed to have zero shear stress.

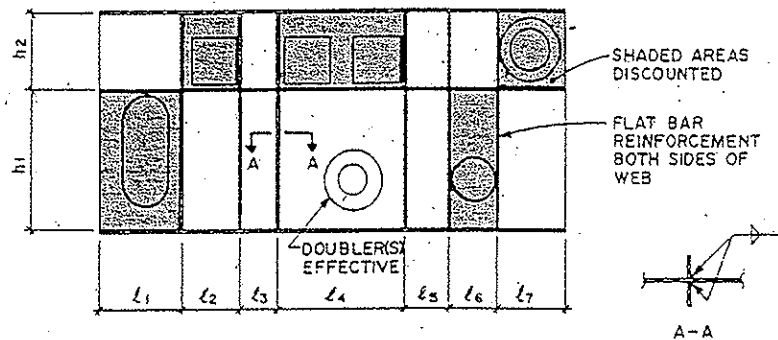


Fig. 3.11.1 Checkerboard solution for web panel with large openings
[Buckland et al. (1988) Fig. 20 b]

The checkerboard method is based on plastic analysis and the basic assumption is that the steel is sufficiently ductile such that only equilibrium need be considered and strain compatibility is ignored. Thus all web panels are assumed to have uniform shear and the global moments are assumed carried by the top and bottom flanges only.

A set of design equations for the shear forces in panels and axial forces in the vertical stiffeners is established. The checkerboard can be divided into sub-models for calculation.

Buckling is not considered, but vertical reinforcement/stiffeners made of flatbars on both side of the web are proposed.

In order to plastify the webs the reinforcement and their welds must not fail prematurely. They were therefore designed to carry forces 10 to 20 % greater than the calculated values.

3.11.3 Discussion

Buckland, Bartlett and Watts (1988) do not mention the term “stressed skin”, and do not calculate the shear stresses as such. However, the checkerboard method seems to be a variant of the stressed skin method. Hence the discussions in Section 3.10.4 apply.

A true checkerboard pattern is difficult to apply if there is only two panels over the height of a girder. A system with three panels plus one opening is static determinate and cannot have the corner panel without shear stress, unless the horizontal reinforcement is anchored in an adjacent structure. Similarly, a system with five panels plus one opening is one time static indeterminate, and can have only one corner panel without shear stress. Actually, true checkerboard patterns occur only as particular solutions. Configurations with alternating panels with zero stress must usually rely on additional panels at each end to obtain equilibrium. It can be difficult to divide the calculation model into sub-models. An analysis of the full girder including the extra panels may be required. However, the analysis is still fairly simple. Figs. 3.11.2 a) and b) show incomplete and completed calculation models.

With only two panels over the height of a web, the axial forces in vertical members may be large. Also, when a continuous horizontal reinforcement is used, the forces in this may be solely in tension or compression. In Fig. 3.11.2 b) the force is tension, but in general this depends on the checkerboard pattern and the direction of the shear force in web.

The checkerboard method establishes a theoretically static determinate system in large parts of the structure. If the inactive shear panels are really missing, the structure is static determinate in practice also. There are small possibilities for redistribution of forces, especially for the vertical members.

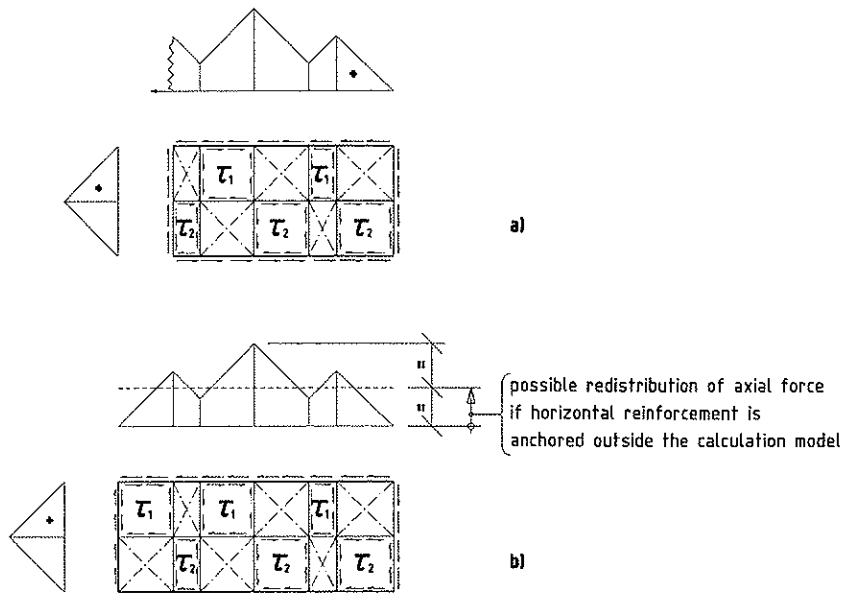


Fig. 3.11.2 Checkerboard models. a) Incomplete model and b) Completed model

3.12 Doubler plate method

3.12.1 General

The methods described in previous sections have not aimed at recovering the full shear capacity of the web without opening. The upper limit is the shear capacity of the minimum section above and below the opening. By using doubler plates the possibility exists to increase the shear capacity up to the full shear capacity of the web without opening. Fig. 3.12.1 shows this principle for a circular opening. Two alternatives are shown, one with a doubler plate on one side only and the other with doubler plates on both sides. The latter solution is frequently termed "tripler plates".

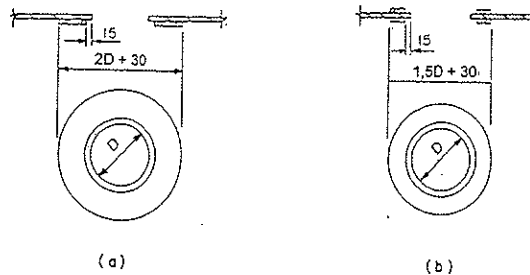


Fig. 3.12.1 Doubler plates on one or both sides of web [Buckland et al. (1988) Fig. 5]

The use of doubler plates in girder webs is described in Buckland, Bartlett and Watts (1988). Circular and rectangular openings in webs of deck girders in an offshore structure are covered. Elastic and plastic theory is considered, of which only the findings based on plastic theory is referred below.

3.12.2 Circular openings

Doubler plate geometry

The basic idea is as follows: If an opening can be reinforced, by doubler or otherwise, so that the remainder of the web can attain yield before the reinforced opening fails, a major simplification ensues: the stress field outside the reinforcement is uniform, namely at yield. In other words, the web stresses outside the reinforcement are not affected by the presence of the opening or its reinforcement. This means that one opening is unaffected by the presence of a second opening, provided their reinforcements do not overlap. Similarly, a reinforced opening may be close to the edge of a plate without this affecting the web.

The analysis is based on earlier work by Weiss, Prager and Hodge (1952), who derived the required thickness of reinforcement plates that will not fail before the web is fully yielded. Buckland et al. develop the theory somewhat further and present the required doubler plate thickness as a function of the web thickness, the diameter of the opening and the diameter of the doubler plate.

If the diameter of the doubler plate is twice the diameter of the opening, the thickness of one doubler plate has to be $1,79t$ according to Buckland et al. This is approximately the same as $1,73t$ proposed by Weiss et al.

The total thickness, including the web, amounts to $2,79t \approx 3$. It is proposed to use two doubler plates of thickness t , one on each side of the web. This solution is shown in Fig. 3.12.2. The main reason for using two plates is that the required volume of fillet welds around the plates for two plates amounts to only 50 % of the volume required for one plate alone.

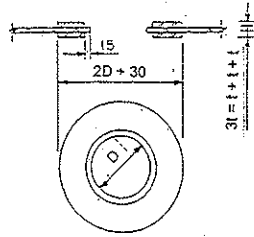


Fig. 3.12.2 Doubler plate solution restoring the full shear strength of web

Shear capacities

The aim is to present a simple design procedure. Hence the shear capacity of a web with opening is taken as

$$V_m = k_d V_p \quad (3.12.1)$$

V_p is the plastic shear capacity of the web without opening and k_d is a reduction factor; $k_d = 0,33$ without doubler plates, $k_d = 0,67$ for one doubler plate, and $k_d = 1$ for two doubler plates. The reduction is assumed to take place over the full height of the web, independently of the size of the opening.

Eq. (3.12.1) is clearly conservative for small openings, as one diminutive opening without doubler plates reduces the capacity to only 33 % of the full capacity. Hence a modification is proposed for opening diameters smaller than $0,25h$. It is assumed that the effect of the reduction does not work outside a diameter of $4D$. The shear capacity for smaller openings is

$$V_m = \left(1 - \frac{4(1-k_d)D}{h} \right) V_p \quad (3.12.2)$$

For example, an opening of $0,20D$ without doubler plates gives a shear capacity that is 46 % of full shear capacity.

Moment-shear interaction

No primary moment-shear interaction is considered.

Welds

The doubler plates are usually fillet welded along both its inside and outside perimeters. To be consistent with the method of analysis, all force transfer must occur at the outside perimeter. The weld around the inside perimeter is only a seal weld. The part of the force transferred to each plate must be directly proportional to the ratio of the thicknesses. Hence, in the case of one standard doubler plate of thickness equal to the web, one half of the applied force must be transferred to the doubler plate.

Both shear, compressive or tensile stresses in the web impart shear into the weld. The stresses in the web are summed vectorially to $\sigma_{principal}$ and the weld sized by the maximum value found round the perimeter. The capacity of the weld is taken as the yield shear stress on the throat of the weld.

$$\sigma_{principal} t \frac{2t}{3t} \leq \tau_y \frac{w}{\sqrt{2}} \quad (3.12.3)$$

where w is the leg length of the weld. This gives

$$\sigma_{principal} \leq \tau_y \frac{3\sqrt{2}}{4} \frac{w}{t} = 1,06\tau_y \frac{w}{t} \quad (3.12.4)$$

Buckling

According to Buckland et al the stability of web openings reinforced by doubler plates is not a problem. No evidence of buckling was found for the case of a reinforced plate in shear, but a Japanese investigation of the case of uni-axial compression showed a marked increase in buckling capacity.

In the case of un-reinforced openings, it is referred to Höglund's investigations. Buckland et al state that buckling capacity is reduced, but, as they use only 1/3 of the full capacity, it is unlikely that buckling will be the governing criterion in practical design.

3.12.3 Rectangular openings

For rectangular openings Buckland et al propose doubler plates to be designed as frames that carry the shear force of the opening with no help from the surrounding parts of the web. The frames are designed by plastic theory and the secondary moments have to be carried without stiffeners.

3.12.4 Discussion

In design of tanks and pressure vessels with openings, a rule of thumb for doubler plates is to maintain the cross section through the opening. Both solutions in Fig. 3.12.1 recover the cross section if the thickness of each doubler plate is the same as the main plate. But it turns out that this is not sufficient to restore the shear strength of a web with opening to the full shear strength of the web without opening. The rather heavy thickness required may in the first hand be astonishing. However, after a second thought, it may be explained as follows:

Consider a shear force approximately equal to the shear capacity of the minimum section above and below the opening. One component of the force couple from the secondary moments can be taken by compression/tension not far in from the edge of the opening. The other component of the force couple can be taken somewhere else in the web, because this part of the web is not in yield from shear. Now, assume that one doubler plate of twice the diameter of the opening, and of the same thickness as the web, is introduced. This plate will restore the section above and below the opening to the full web section. Consider that the shear is increased to the full shear force of the web. The shear stress is at yield both in the minimum section and in the rest of the web. One component of the force couple from the secondary moment can be taken by compression/tension in the doubler plate. But the other component cannot be taken outside the doubler plate, as the rest of the web already is in yield. Hence *all* the extra secondary moments have to be taken in the doubler plate. The thickness of the doubler plate has to be more than the thickness of the web.

Considering this explanation, the thickness required to restore the full shear capacity should be accepted. However a reduction of the shear capacity to 1/3 of the full capacity if no doubler plate is used, seems very conservative.

Full restored shear capacity, i.e. by means of two doubler plates, gives a weight increase of five times the weight of the material removed from the opening.

Primary moment-shear interaction is expected to occur for the part of shear, which is not taken by the doubler plates. When doubler plates are used and $D < 0,50h$, no *more* interaction due to the opening should be expected. The doubler plates are themselves supporting the extra shear and the flanges are not influenced.

The largest possible leg length of a fillet weld between web and a doubler plate is $w = t$. Eq. (3.12.4) gives

$$w \geq \frac{\sigma_{\text{principal}}}{1,06\tau_y} t \quad (3.12.5)$$

For a web in pure yield shear stress, the principal stress is equal to the yield shear stress. Hence, to carry the full shear capacity of the web, the fillet welds of the doubler plates must be almost as big as the largest possible weld.

For rectangular openings, double plates are usually thicker and less efficient than for circular openings. This is a consequence of the relatively larger secondary moments of rectangular openings than for circular openings. Doubler plates may still be a good solution for small rectangular openings. However, for rectangular openings of some size, doubler plates are rarely efficient compared to replacement of the web with a thicker plate in the minimum section and to use vertical stiffeners and horizontal reinforcement.

3.13 Other methods

3.13.1 General

An alternative method to the tension field methods is presented in Lee (Feb. 1990), based on a numerical study in Lee (June 1990). The following presentation is based on these papers.

3.13.2 Circular and elongated openings

Numerical study

The numerical study comprises 22 transversely stiffened webs. ABAQUS with the four-node quadrilateral shell element S4R is used for the simulations. The material was assumed to be elastic-perfectly plastic. An initial imperfection in agreement with the buckling mode due to shear is specified in the compression quadrants of the openings. Typical computed stress fields for $D/h = 0,50$ and $h/t = 180$ are shown in Fig. 3.13.1. The solid line shows the direction of tension field according to Narayanan (1983a).

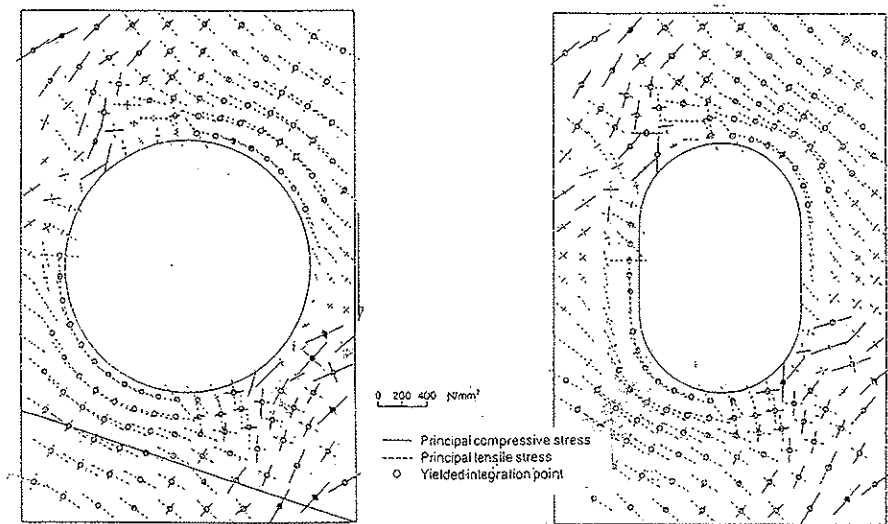


Fig. 3.13.1 Typical stress fields obtained from finite element analyses. [Lee (June 1990) Figs.5a and b]

Typical load-deflection curves are shown in Fig. 3.13.2. The curve for transverse deflections at the edge of the circular opening in Fig. 3.13.1 is plotted for a point along the tension diagonal, i.e. for a point that has compression tangentially to the opening edge.

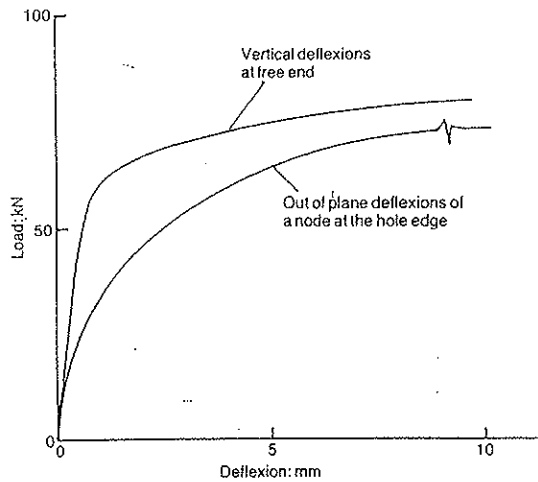


Fig. 3.13.2 Typical load-deflection curves [Lee (June 1990) Fig. 4]

The stress fields obtained at collapse generally display the following features:

- Yielding in the web is independent of the web buckling stress
- High compressive stresses occur along the tension diagonal of the web, even in very slender webs and webs with very large openings.
- Two regions of pure tension, the “tension bands”, occur in the web at yield, one above the opening and the other below it. The tension bands do not extend fully to the flange-web junctions and they carry most of the shear in the web.
- Evidence of beam action, i.e. a two-directional stress system, exists immediately above and below the opening near the flange-web junction, indicating that locally the transverse forces on the flanges are likely to be small.

The results also provide evidence that the stress fields are more affected by the size of the opening than by the exact opening shape, and that the flexural strength of flanges has no significant influence on stress fields. A flange with no flexural strength can still develop post-critical strength in the web.

Theory

A web with a medium size circular opening is considered, see Fig. 3.13.3. The two yielded tension bands, ABCD and EFGH, are each inclined at angle θ to the flanges. A and E are located on the same vertical section and so are B and F. Hence the positions A and B, and also E and F, are symmetrical about the centerline of the panel. C and H are at the mid-depth of the panel, and both BC and EH are tangents to the circular opening, allowing the maximum widths of the tension bands to be obtained.

At the flange-web junctions along AB and EF, it is assumed that the principal stresses are of equal magnitudes, but of opposite sign, and are inclined at $\pm 45^\circ$ to the flanges, resulting in no transverse forces on the flanges. Away from the boundaries AB and EF, and

within the tension bands, the stresses have the value of the yield stress in tension. At the corners of the web, high tensile and compressive stresses are present. Outside the tension bands and away from the corners, the web has buckled and is assumed to make no contribution in resisting the external shear.

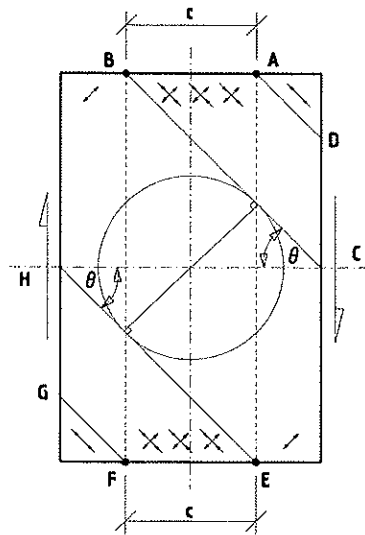


Fig.3.13.3 Simplified stress assumed

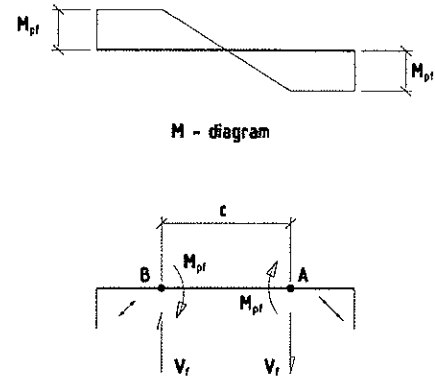


Fig. 3.13.4 Equilibrium of the top flange in the theoretical model

The geometry of the model is such that the overall depth of the tension bands is constant over the panel length. The flanges are assumed to remain elastic between AB and EF, and have yielded elsewhere so as to satisfy the yield condition to the left of A and to the right of B, since between AB and EF there are no transverse forces on the flange. This also implies that the shear in the flanges is constant between AB and EF, i.e. the total shear force on any vertical section is also constant. Thus the hinge positions are at A, B, E and F. Considering equilibrium of the top flange shown in Fig. 3.13.4, one obtains

$$V_f = \frac{2M_{pf}}{c} \tag{3.13.1}$$

M_{pf} is the plastic moment capacity of the flange and c is the distance between hinges A and B. The shear forces V_f at A and B are supported by the high tensile and compressive forces in the corners of the web.

Consider now Fig. 3.13.3 and the vertical section through AE. Here, according to Lee, the only internal force from the web resisting the external shear, is that from the top tension band. It has the magnitude

$$V_t = f_y c t \sin \theta \tag{3.13.2}$$

The vertical component of this force is

$$V_{web} = f_y ct \sin^2 \theta \quad (3.13.3)$$

The contributions from top and bottom flanges are $2V_f$. Hence the total shear capacity is

$$V_{ult.Lee} = f_y ct \sin^2 \theta + \frac{4M_{pf}}{c} \quad (3.13.4)$$

The moment capacity of the flanges is reduced for axial forces in the flanges from primary moment, and according to Lee, this can be used to construct interaction diagrams.

Tension band patterns

The distance c and the angle θ in Fig. 3.13.3 depend only on the aspect ratio of the web and of the opening size. Certain geometrical rules are established:

- For small openings the point B is in the upper left corner. A tangent to the opening is drawn from B to a point C on the opposite side of the web. For the smallest openings, the point C is below the horizontal centerline through the opening.
- For increasing opening diameters, point B is still in the upper left corner, but point C moves up to the horizontal centerline through the opening.
- For further increased diameters, point C is on the horizontal centerline through the opening and on the side of the web. The tangent is now drawn from point C to point B, which moves from the corner towards the vertical centerline of the opening.
- For larger diameters, point B stops at the vertical line from the left side of the opening. The tangent is now drawn from the fixed point B to the point C, which is allowed to move above the horizontal centerline through the opening.

Equations can be established, but are not referred here. A few examples of patterns are shown in Fig. 3.13.5. As the patterns are independent of the bending capacity of flanges, it is not possible to maximize the ultimate strength.

For elongated openings, the constructions of tension band patterns are similar to those of the circular openings.

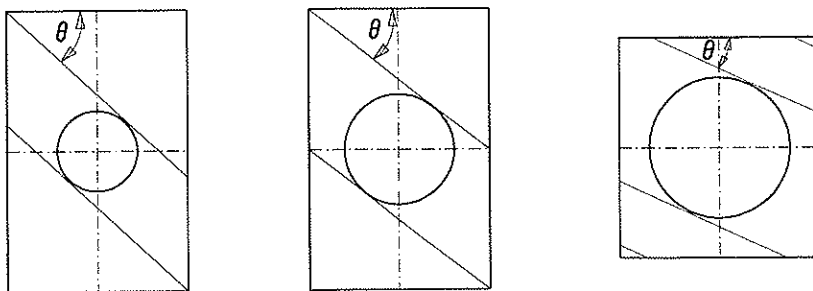


Fig. 3.13.5 Various tension bands for circular openings

3.13.3 Rectangular openings

Lee proposes to use the theory established for circular openings also for rectangular openings. The requirement that the borders of the tension bands must be tangents to the opening is relaxed to go through the corners of the openings.

3.13.4 Discussion

Numerical study

The numerical analyses presented by Lee (June 1990) are interesting especially because the principal stresses around many openings are visualized both with size and directions. The stresses are presented for the middle layer of the elements and hence represent mainly membrane stresses. Briefly stated the stress pictures show the following:

- Inflexion points are located towards the compression quadrants
- Tension bands can easily be seen
- High compression stresses are also acting, in some cases the stresses are reaching the yield stress and occur as “compression bands”.

The simulations indicate that buckling is a global phenomenon. Very small aspect ratios increase the shear capacity. When the aspect ratios are increased, the shear capacities decrease to a certain level, and remain constant for further increased aspect ratios. The buckling seems to be plate type buckling: The transverse deflection shown in Fig. 3.13.2 is progressive for increasing load, but has no limit point.

The theory presented by Lee (Feb. 1990)

In the first place the theory appears simple and useful for practical design. Calculated capacities are noted to give reasonably accurate estimates of shear capacities of webs with openings. Unfortunately the theory contains some severe errors that in the end makes the good results appear as mere coincidences. The objections are as follows:

- The shear capacity given by Eq. (3.13.4) has two terms; the first term shows the contribution from the web and the second term the contribution from the flanges. The shear capacity from the web originates from the tension band in the web section AE of Fig. 3.13.3. According to Lee, this is the only force in the web at this section. But Lee has omitted a reaction force from the other tension band that ends at E. Where can this force be? It is impossible that the force can go through the flanges to the end of the web, because the flanges cannot take more shear than already given by the second term of Eq. (3.13.4). In addition, Lee himself has pointed at large compression stresses in the end of the tension bands at the flange-web junction, and he has stated that no forces are transferred to the flanges along the distance c . The answer is therefore that a sort of “compression band” also exist in the section AE. Due to symmetry, the reaction force to the lower tension band must be equal to the tension force in the upper tension band. Hence Eq. (3.13.4) should be modified to

$$V_{ult, Lee} = 2f_y ct \sin^2 \theta + \frac{4M_{pf}}{c} \quad (3.13.5)$$

- However, the shear capacity given by Eq. (3.13.5) is most likely overestimated, because the angle θ is too big. The geometric conditions given by Lee, always place the distance c symmetrically above the opening. The numerical simulations often show that the inflexion area is moved towards the compression quadrant.
- No yield criteria are established for the ends of the tension bands at the flange-web junction. Theoretically, yield tension stress cannot exist together with yield compression stress in the same point. However, a larger area than given by the boundaries of the tension bands alone may explain this.
- The primary moment-shear interaction is only influenced by the last term in Eq. (3.13.4). If this term is omitted, there is no interaction in the theory proposed by Lee. Certainly the tension and compression bands have counterparts in the flanges.

3.14 Conclusion

3.14.1 General

The review and evaluation of load-carrying methods have shown that many factors are involved on the determination of the shear capacities, and it is not quite clear how the results are related to the different limit states. The rotated stress field method and the modified Vierendeel method can handle openings in all webs, but not openings with reinforcements. The tension field methods cover all openings in slender webs, but the transverse web displacements may be large. The stressed skin and checkerboard methods cover all rectangular openings with reinforcement, but not circular openings. Some amendments to the existing methods might be possible, but an important conclusion should be that the shear capacities cannot be given neither by means of one universal method nor one equation.

However, it should be possible to give useful and generalized shear capacities based on diagrams and guidelines. Diagrams similar to Fig. 3.6.2 may be the basis, and some secondary factors, that are less important to the result, may be eliminated. The diagrams can be based on theoretical methods, experiments, or numerical simulations. A brief outline of a proposed design procedure is given in Chapter 6.

3.14.2 Shear capacities in the various limit states

None of the reviewed methods give shear capacities in the Fatigue Limit State - FLS. Sufficiently accurate elastic stresses around openings in webs can only be found by FEM-analyses, and the problem will not be further investigated in the present thesis.

The Serviceability Limit State - SLS is a state that is frequently encountered in the life span of a structure, and in this limit no accumulation of plastic strains or fatigue damage should take place due to stress redistribution. For all webs second order effects will amplify the initial transverse web displacements, and in the strict sense it is impossible to avoid some redistribution of stresses. But, the plastic strains and transverse web displacements can be curbed by means of restrictions to the shear stress level, for instance by using only the critical shear stress in the design. None of the reviewed methods give the shear capacities in SLS. The allowable stress method and the doubler plate method may in practice be such methods, but the results are not very accurate.

However, if the limitations to plastic strain or fatigue are disregarded, the remaining SLS requirement is the transverse web displacements. In the allowable stress method, the method based on strength criteria, the rotated stress field method, the stressed skin method and the doubler plate method it is stated that buckling shall not occur. Even though some buckling is *inevitable*, these methods utilize only a limited part of the post-buckling capacity, and the transverse web displacements are expected to be relatively small.

In the Ultimate Limit State - ULS the aim is to find the maximum shear capacity. Only the method based on strength criteria and the Cardiff tension field method are such methods in the strict sense. However, the rotated stress field method, the modified Vierendeel method, the stressed skin method, the checkerboard method and the doubler plate method may in practice be ULS-methods.

In the Accidental Limit State - ALS the aim is to find the shear capacity for large vertical deflections of a beam or girder. None of the methods are ALS-methods.

Chapter 4

Prior experiments

4.1 Introduction

In 1978 rather sparse information of the performance of slender plate girders with openings was available. Therefore Division of Steel Structures at Norwegian Institute of Technology (NTH) started an experiment program in order to map the parameters that influence the shear capacity of slender plate girders with large web openings. During six years up to 1985 a total of 15 plate girders were tested. The web slendernesses were chosen to ensure that web buckling should be a governing factor. The most important parameters were the size and location of the web opening and the design of various types of stiffening.

The experiment program was carried out by Kjell Sollid. The first eight experiments are described in an unpublished, preliminary report by Sollid (1983). The remaining seven experiments are described in a later unpublished report by Sollid (1985). In addition several students have participated in the experiments and wrote their M. Sc. reports based on some particular girders. No summary or conclusion from the complete experiments has been published.

Today, more information and design models are of course available also for slender plate girders. However much of this is based on rather small scale models. A main feature of the experiments at NTH is the size of the plate girders: With web height up to 1,0 m, these are almost in a scale 1:1 of girders in practical use. Hence the experiment girders can be assumed to have realistic weld stresses and fabrication tolerances.

For the purpose of this investigation, the details of the experiment set-ups are explained in Section 4.2 with a summary of the results in Section 4.3. These sections are based on Sollid (1983) and Sollid (1985). The author's contribution is the discussion in Section 4.4 and the conclusion in Section 4.5.

4.2 Details of the experiment set-ups

4.2.1 General

All experiments were performed on welded plate girders that acted statically as short cantilevered girders fixed in all degrees of freedom at one end and loaded with a point load in the other end. Fig. 4.2.1 shows the test arrangement in principle.

All girders were loaded in load increments until their maximum loads were reached. After this, displacement control was used in order to determine the remaining load carrying capacities and the governing collapse mechanisms. The load/displacements results and strain measurements were recorded.

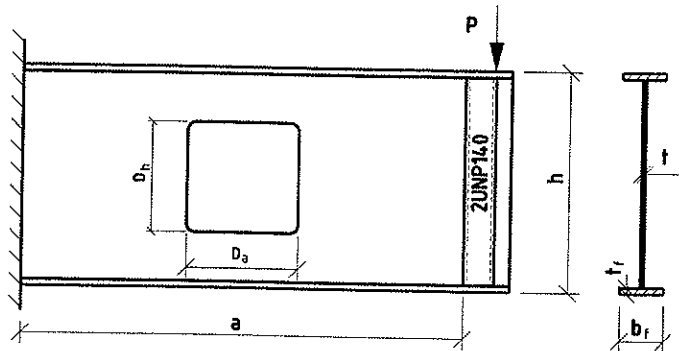


Fig. 4.2.1 Test arrangement in principle

4.2.2 Girders

The experiments were performed as two groups:

The first group consisted of eight girders, which were numbered S1 to S8. All girders had length 2,0 m, web height 1,0 m and web thickness 3 mm. Hence, the web slenderness ratio $h/t = 333$ and the aspect ratio $a/h = 2,0$ were the same for all girders in the group. All flanges were 200 x 10 mm.

The second group consisted of seven girders, which were numbered S9 to S15. All girders had length 1,5 m, web height 0,75 m and web thickness 3 mm. The web slenderness ratio $h/t = 250$ and aspect ratio $a/h = 2,0$ were again the same for all girders in the group. All flanges were 200 x 10 mm.

Overviews of the girders, openings and their locations are given in Tables 4.2.1 and 4.2.2. The first girder in each group had no opening and is used as a reference girder.

For all girders, the vertical load was transferred by two UNP 140 stiffeners that were welded to the web and flanges. These vertical stiffeners were given large bending stiffness in order to ensure that the tension field diagonal could be sufficiently anchored. At the other end a 50 x 250 mm end plate with 24 predrilled holes $\varnothing 25$ was welded to web and flanges.

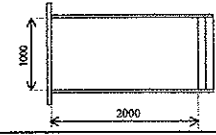
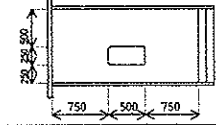
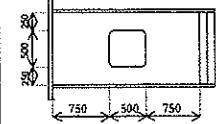
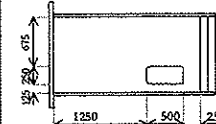
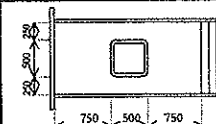
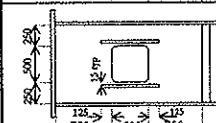
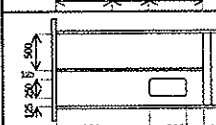
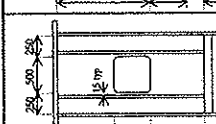
The web plates were made of hot rolled plates in material St 37-2 DIN 17100 with nominal $f_y = 235 \text{ N/mm}^2$ and the flanges from hot rolled flat bars in ship quality grade DnV A with nominal $f_y = 255 \text{ N/mm}^2$. Stiffeners were made of hot rolled plates or sections in St 37-2. No material data is provided for the 50 mm end plates.

In order to document the real yield and tensile strengths, tension specimens were taken from both the web and flange plates. The strength values for each girder web were based on six specimens, while both flanges together had strength values based on three specimens. The tensile specimens were tested according to DIN 50125/17100 by means of an Instron testing machine. Mean values for the yield stress are included in Table 4.4.1.

Specimens were also taken from the material that was used for stiffeners around the openings. Mean value for the yield stress was 290 N/mm^2 .

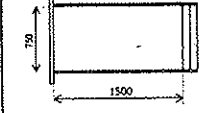
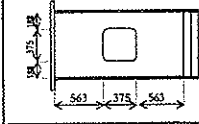
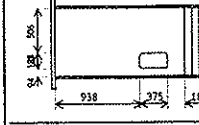
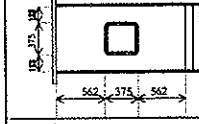
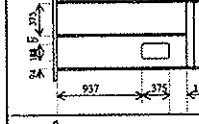
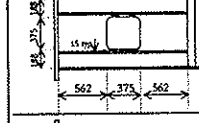
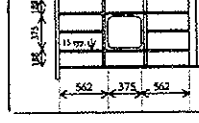
The plate and stiffener dimensions were measured.

Table 4.2.1 Test girders S1 to S8

Figures	
	S1
	S2
	S3
	S4
	S5
	S6
	S7
	S8

All webs nominal 3 x 2000 x 1000 mm
 All flanges nominal 200 x 10 mm
 All slenderness ratios $h/t = 333$
 All aspect ratios $a/h = 2,0$

Table 4.2.2 Test girders S9 to S15

Figures	
	S9
	S10
	S11
	S12
	S13
	S14
	S15

All webs nominal 3 x 1500 x 750 mm
 All flanges nominal 10 x 200 mm
 All slenderness ratios $h/t = 250$
 All aspect ratios $a/h = 2,0$

In order to reduce the initial displacements of the webs, each web plate was cut to correct size in one piece in a shearing machine. Also each flange was cut in one piece from a flat bar that already had the correct width as rolled. A longitudinal shallow groove was machined in each flange and the web plate was placed in these grooves before it was welded to the flanges. Weld sizes were not recorded. All openings were made by flame cutting with minimum heat supply in order to limit deformations from residual stresses. Corner radii were always $r = 10t = 30$ mm. In spite of the precautions, initial deformations of the web were measured prior to testing. For the two girders S1 and S9 without openings, maximum initial displacements of 12 and 1,6 mm respectively were reported. For the other girders the maximum displacements varied between 13 mm for S6 and 1,2 mm for S14.

4.2.3 Test rig

The test rig is shown in Fig. 4.2.2. It consisted of a large steel restraining structure that was bolted to steel rails in the strong floor of the test laboratories, and a hydraulic loading system. Each test girder was bolted to the restraining structure by means of 20 M22 8.8 bolts. The bolts were pre-tensioned, but the procedure used is not documented.

In spite of the large stiffness of the reaction structure, some deflection of the rig occurred during testing. However, these deflections were measured and subsequently accounted for in the data reductions.

The load was applied by means of a hydraulic jack of type Amsler having 400 kN capacity. The jack was suspended from a portal frame that was bolted to the strong floor. Each end of the jack had spherical hinges. By means of a load cell and a displacement meter, both load and displacement control were possible.

In order to prevent lateral buckling, all girders were equipped with two special guides at the loaded end. The guides allowed vertical displacement only, without taking up any vertical loads. At the same time the guides supported any lateral load coming from, for instance, skew positioning of the hydraulic jack or non-symmetric configuration of the test girders, when these were loaded to collapse.

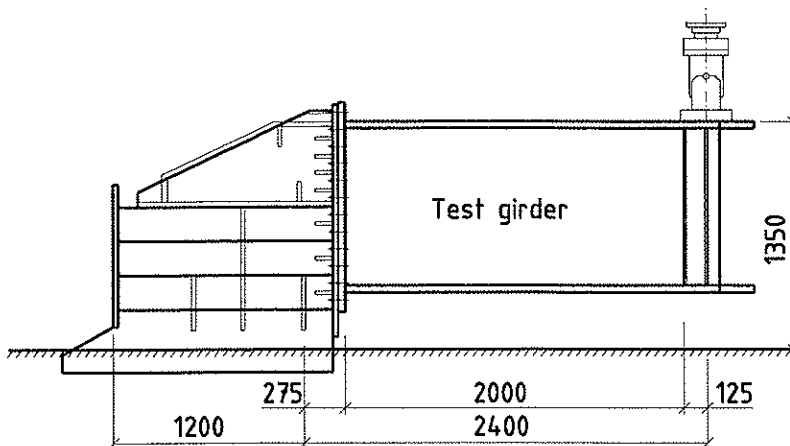


Fig. 4.2.2 Test rig

4.2.4 Instrumentation

The instrumentation was divided in the following four measurement groups:

- 1) Load/vertical displacement of the hydraulic jack: An XY-plotter gave a continuous plot of the load/displacement diagram for the jack. The diagram was used to monitor the behavior of the test girders, for instance to alter the load steps when the load of a test girder approached its maximal level. The accuracy of measurement was $\pm 1\%$.
- 2) Vertical displacement of bottom flange: Six mechanical meters were used to record the vertical displacement of the test girders, and the measured values were recorded manually. A typical arrangement is shown in Fig. 4.2.3. Meter no. 1 measured vertical displacement of the stiffener in the loaded end, and meters nos. 2 and 3 measured the vertical displacement of the bottom flange at the opening. Meters nos. 4, 5 and 6 measured the displacements of the restraining block. The accuracy of measurements was $\pm 0,01$ mm.

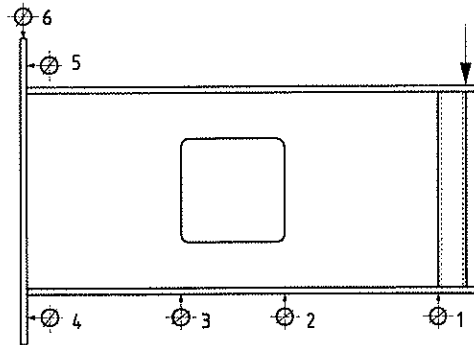


Fig. 4.2.3 Mechanical displacement meters

- 3) Transverse displacement of the web: An aluminum beam equipped with mechanical meters was used to measure transverse displacements of the webs. Seven meters with center distance 125 mm were used for Girders S1 to S8, and five meters with center distance 125 mm were used for Girders S9 to S15. Fig. 4.2.4 shows the measuring bridge in principle. In each end the bridge had prongs that were placed against the web plates, and two spring-loaded magnets held the bridge in position while the values were recorded. For each load step the measurements were taken at three to five positions along the girder. Hence, for Girder S1 measurements were taken in a grid consisting of seven points over the web height and four positions along the girder length, i.e. a (7 by 4) grid. For the other girders the grid varied from (7 by 5) for Girder S2 to (5 by 3) for Girder S13. The values were recorded manually. Before and after the tests the bridge was calibrated against a perfectly plane plate. The accuracy of each meter was 0,01 mm, but, as the bridge was moved and re-applied in various positions, the total accuracy is less.

The use of the measuring bridge was restricted by the range of the meters, which was ± 12 mm. Larger displacements could only be observed qualitatively.

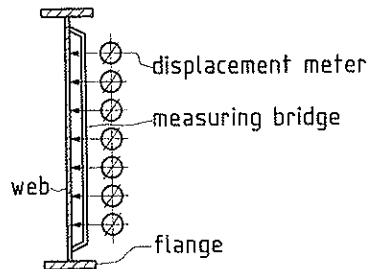


Fig. 4.2.4 Measuring bridge in principle.

- 4) Strain in girder flanges and web: Strain gauges were glued on one side of the web and on the upper surface of the upper flange and on the lower surface of the lower flange. The objective of the strain gauge measurements was to calculate the stresses in the girders in order to compare with the various tension field theories. Both uniaxial and rosette type gauges were used, with gauge lengths were 3 mm and 2 mm, respectively. A "Solartron 3530 Orion Data Logging System" was used to record the measurements.

The reasons for using strain gauges on one side only were: 1) One side had to be free in order to allow the measurements of the transverse displacements of the webs, 2) It was chosen to have strain gauges in as many positions as possible in order to get a better picture of the stress variations around openings and stiffeners, and 3) It was planned to make measurements by photogrammetry of the large displacements, whereby pictures undisturbed by strain gauges would be needed.

4.2.5 Photogrammetry

A ruled net was painted in black on a white background on one side of the web, in order to make measurements of transverse displacements by photogrammetry. Such measurements were for various reasons not performed. However, by these nets, the large displacements are clearly visible on photographs.

4.2.6 Testing procedure

After installation of the test girder and the hook-up of the instrumentation, the girder was given an initial load cycle up to about 20 % of the expected ultimate load. This was done in order to overcome initial friction and possible eccentricities in the loading and restraining system.

The test itself was initially carried out under load control, and the load was applied in increments of about 20 kN. After each increment the actuator was locked in position, i.e. the displacement was kept constant for some minutes. During this period a relaxation took place until an equilibrium situation was obtained at a load 2 to 4 % lower than the initially applied load. As soon as the proportionality point between load and displacement was exceeded, the test was switched to displacement control. Here, displacement increments of 5 to 10 mm were used to record the entire response curve. The test was normally terminated when the vertical displacement of the actuator reached 40 to 50 mm.

4.3 Summary of test results

A brief summary of Sollid's (1985) test results is given in Table 4.3.1. Column 4 shows the measured maximum equilibrium load, $V_{u,e}$, and Column 5 shows the measured maximum load not in equilibrium, $V_{u,en}$. Column 6 gives the calculated shear capacity based on yield in the minimum section through the opening, as

$$V_{p,mod} = \frac{f_y}{\sqrt{3}}(h - D_h)t \quad (4.3.1)$$

where D_h is the height of the opening. The yield stress f_y is based on the measured values, and nominal values of the web dimensions are used. Column 7 gives the ratio between the values in columns 5 and 6. Further, in Column 8, the measured “% relaxation” is shown. The term relaxation is difficult to interpret from Sollid's reports, but from Minsaas (1983) it is assumed to be the strain value that is measured when the girder had reached its maximum equilibrium load.

Table 4.3.1 Test results

1	2	3	4	5	6	7	8
Girder	Opening [mm]	Stiffeners	$V_{u,e}$ [kN]	$V_{u,en}$ [kN]	$V_{p,mod}$ [kN]	$V_{u,en}/V_{p,mod}$ [kN]	Relax. [%]
S1	None	No	218	226	566	0,40	3,5
S2	500 x 250	No	153	159	431	0,37	4
S3	500 x 500	No	93,1	96,3	286	0,34	3,2
S4	500 x 250	No	136	143	429	0,33	4
S5	500 x 500	Yes	130	134	290	0,46	2,8
S6	500 x 500	Yes	130	136	287	0,47	4
S7	500 x 250	Yes	170	173	394	0,44	..
S8	500 x 500	Yes	203	209	249	0,84	2,9
S9	None	No	165	167	349	0,48	..
S10	375 x 375	No	69,2	74,1	171	0,43	6,5
S11	375 x 188	No	105	111	251	0,44	5,4
S12	375 x 375	Yes	112	115	181	0,64	3
S13	375 x 188	Yes	153	159	277	0,57	3,7
S14	375 x 375	Yes	164	170	183	0,93	3,7
S15	375 x 375	Yes	199	207	207	1,00	3,6

Fig. 4.3.1 gives the response curves, i.e. tip load P versus tip displacement δ for girders S1 to S8. The loads are taken as the equilibrium loads, and the displacements are adjusted for the flexibility of the test rig. The similar response curves for girders S9 to S15 are given in Fig. 4.5.2.

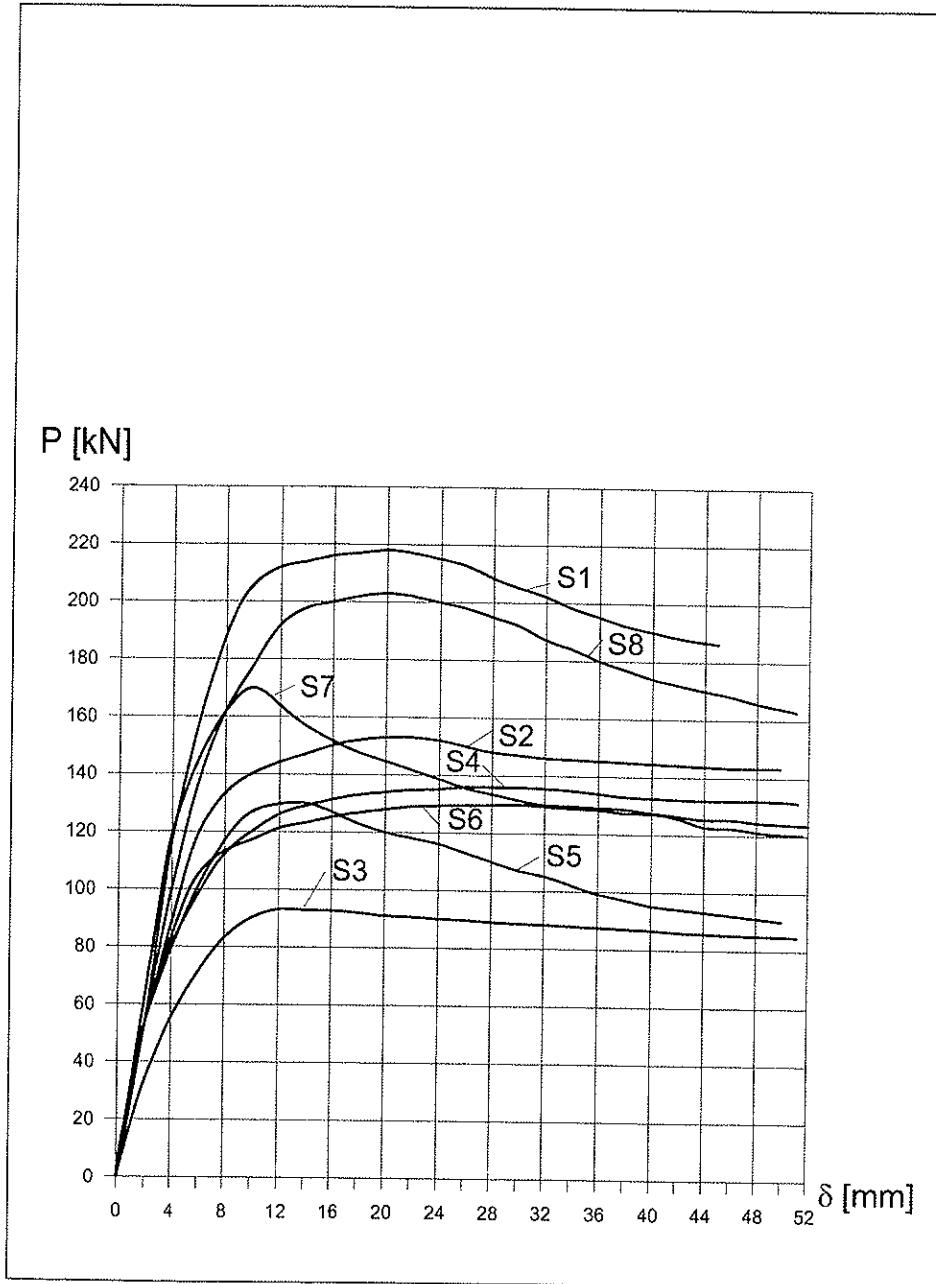


Fig. 4.3.1 Response curves for girders S1 to S8 [revised from Sollid (1983)]

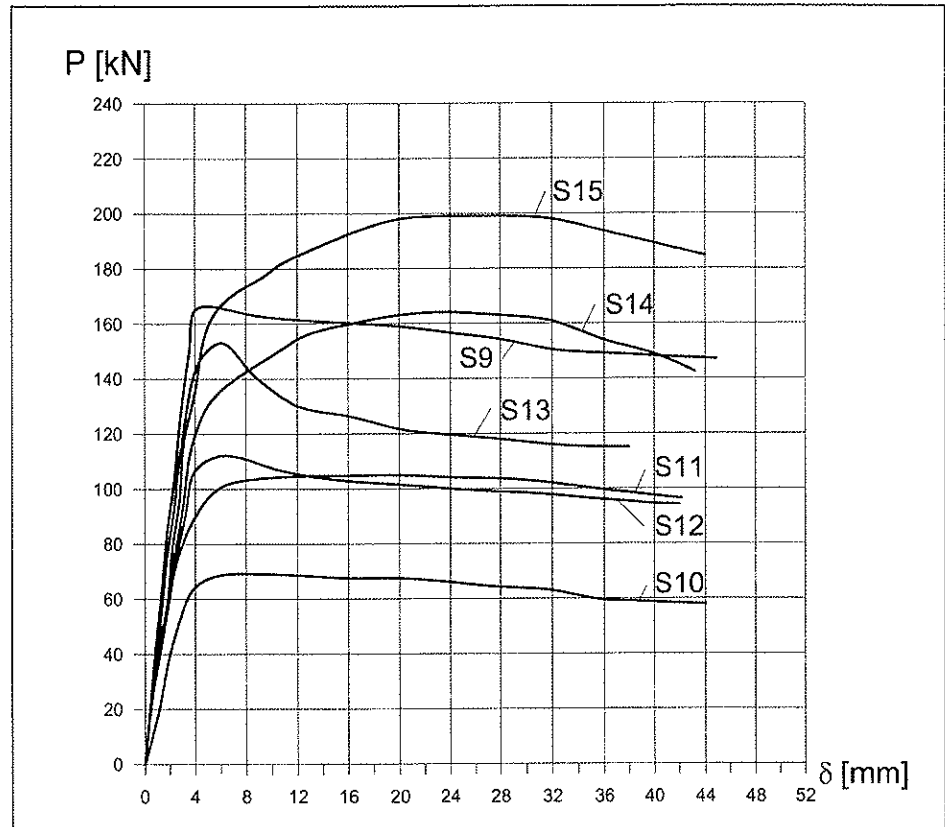


Fig. 4.3.2 Response curves for girders S9 to S15 [revised from Sollid (1985)]

As seen from Fig. 4.3.1, girders S1 to S8 all display a ductile behavior well into the inelastic range. For practical reasons the tests were terminated for a tip displacement of about 50 mm, and at this stage the transverse displacements of the webs reached about 100 mm. The tension field was well established, which accounts for the high shear capacity beyond the ultimate load. For girders S2, S3 and S4, which had openings but no stiffeners, only a few percent reduction in the shear capacity was observed at 50 mm vertical displacement. Girder S7, which was equipped with a horizontal stiffener at mid height, was the only one that displayed a buckling tendency as indicated by the drop in load carrying capacity. However, even this girder retained more than 75 % of its shear capacity at 50 mm vertical displacement.

Sollid states that the transverse web displacements were considerable even before the maximum shear capacities were attained. Such displacements will probably not be accepted in a Serviceability Limit State condition. However, if such girders are part of a static indeterminate structure, that have a possibility for redistribution of forces, the girders will contribute to a structure with large rest shear capacity after the maximum shear capacity has been attained. Consequently, the structure will show a larger safety margin against total and sudden failure/collapse.

4.4 Discussion

4.4.1 General

Sollid did not make any conclusion for girders S9 to S15. However, the conclusion would probably have been quite similar to what is written in Section 4.3. As seen from Fig. 4.3.2 Girder S13 shows behavior similar to S7, which is expected as they have the same type of stiffening. Also girders S5 and S12, both with “sleeves” in the openings, show tendencies to buckling. S14 and S15 are remarkable as these girders, with 50 % opening and comprehensive stiffening, have shear force capacities that are bigger than for the similar Girder S9 without opening and stiffening.

Weld sizes are not recorded, but are assumed to have been continuous fillet welds with 3 to 3,5 mm throat thickness. This is the minimum size that is applicable in practice, but still rather large, relative to the 3 mm webs. The welding may have caused some of the initial transverse displacement of the web. The maximum allowable built-in web displacement according to the fabrication standard Norsok Standard M-101 (1997) is 0,75 % of the web height, which means 7,5 mm for girders S1 to S8 and 5,6 mm for girders S9 to S15. Five girders, S1, S3, S6, S7 and S10, did not comply with the Norsok requirement.

The value of the strain measurements can be questioned. As the strain gauges were placed on one side only, it is not possible to separate membrane strains from bending strains. The bending strains in the webs were caused by transverse displacements of the web plates, which turned out to be of significant magnitude in most part of the tests. The membrane stresses calculated from the strains hence become more inaccurate as the transverse displacements increase. For this reason the strain measurements will not be used in the present investigation.

Only one test was made for each type of specimen. It is therefore impossible to estimate the statistical variation in the test results due to for instance building tolerances, material properties, load application or instrumentation errors. However, the tests should give a qualitative impression of the efficiency of the various stiffener systems and serve as a basis for comparison with numerical simulations.

4.4.2 ULS shear capacities

In Table 4.4.1 the shear capacities are presented similar to the proposal in Section 6.2, i.e.

$$V_{u,e} = \chi_{w,mod} \frac{f_y}{\sqrt{3}} ht \quad (4.4.1)$$

where $V_{u,e}$ is the maximum equilibrium load. Column 5 shows the measured web transverse displacement when $V_{u,e}$ was reached. The web yield stress is based on the measured values, and nominal values of the web dimensions are used. In order to see the effect of the various stiffener systems, the girders are presented in decreasing order of the reduction

factor $\chi_{w,mod}$. The symbol .. means that no value is available, mostly because the transverse displacements were too large to be measured.

Girder S15 obtained the best result, but also S14 and S8 had efficient stiffener systems. For the girders with the largest openings, S8 was considerably better than S6, however the stiffeners were also much larger. The capacities of S6 and S5 were almost equal; a remarkable result considering the usual requirement for stiffeners to be anchored, as in Girder S6. However, in ALS Girder S6 kept most of its capacity, while for Girder S5 the capacity dropped almost to the value of the unstiffened Girder S3. For the smaller openings without stiffeners, there was a relative small difference between Girders S2 and S4.

Table 4.4.1 ULS shear capacities

1	2	3	4	5	6	7
Girder	Opening [mm]	Stiffeners	f_y [N/mm ²]	Maximum displacement [mm]	$V_{u,e}$ [kN]	$\chi_{w,mod}$
S8	500 x 500	Yes	288	..	203	0,41
S1	None	No	327	..	218	0,38
S7	500 x 250	Yes	303	13	170	0,32
S2	500 x 250	No	332	..	153	0,27
S4	500 x 250	No	330	..	136	0,24
S6	500 x 500	Yes	331	..	130	0,23
S5	500 x 500	Yes	335	..	130	0,22
S3	500 x 500	No	330	..	93	0,16
S15	375 x 375	Yes	319	<1,0	199	0,48
S9	None	No	269	..	165	0,47
S14	375 x 375	Yes	281	11	164	0,45
S13	375 x 188	Yes	285	6,5	153	0,41
S11	375 x 188	No	258	..	105	0,31
S12	375 x 375	Yes	279	12	112	0,31
S10	375 x 375	No	264	..	69	0,20

4.4.3 SLS and transverse displacement of webs

The experiments gave a large number of measured transverse displacements for given load levels. Pronounced increases in the transverse displacements for loads near the critical load were only observed for girders S1 and S3, in both cases for loads higher than the critical values. Evidence of column type buckling at the edge of openings were not observed, the transverse displacements showed a progressive, but even, increase similar to the curve in Fig. 3.13.2.

As previously explained, shear capacities in SLS can in the strict sense hardly be based on a limit on the transverse displacements. However, it would be of interest to see how large the shear was, when a certain transverse displacement was reached. Table 4.4.2 shows

the shear force corresponding to a transverse displacement of $h/200$, based on displacements from the loads only and disregarding the initial displacements.

The presentation is similar to that of the ULS shear capacities in the previous section, i.e.

$$V_{SLS,e} = \chi_{w,mod,SLS} \frac{f_y}{\sqrt{3}} ht \quad (4.4.2)$$

where $V_{SLS,e}$ is the tip equilibrium load corresponding to a web displacement of $h/200$ from the loads. No transverse displacement values are known for Girders S5 and S8. Column 8 shows the ratio between $V_{SLS,e}$ and the maximum equilibrium load, $V_{u,e}$. In order to see the effect of the various stiffener systems, the girders in each group are presented in decreasing order of $\chi_{w,mod,SLS}$.

Girder S15 obtained approximately the maximum possible shear force; i.e. yield shear stress in the minimum section through the opening. The maximum transverse displacement was less than 1 mm. However, this girder had an extensive amount of stiffening, not normally encountered for girders. Not unexpected, Table 4.4.2 shows that high shear capacities with small transverse displacements can only be achieved with stiffeners. But Girder S6 showed that horizontal stiffeners above and below the opening only, are hardly sufficient. For the smaller openings without stiffeners, the shear force for Girder S4 is considerably lower than for Girder S2. In the latter case the tension field has hardly developed yet, but even then an opening within the tension field seems to have a negative effect. At last, it can be seen that regarding limited transverse displacements, webs with openings have not necessarily reduced capacity compared to girders without openings; i.e. Girder S9 showed poor performance.

Table 4.4.2 Shear forces for maximum web transverse displacements equal to $h/200$

1	2	3	4	5	6	7	8
Girder	Opening [mm]	Stiffeners	f_y [N/mm ²]	$h/200$ [mm]	$V_{SLS,e}$ [kN]	$\chi_{w,mod,SLS}$	$V_{SLS,e}/V_{u,e}$
S7	500 x 250	Yes	303	5,0	80	0,15	0,47
S6	500 x 500	Yes	331	5,0	45	0,08	0,35
S1	None	No	327	5,0	<40	<0,07	<0,18
S2	500 x 250	No	332	5,0	37	0,06	0,24
S3	500 x 500	No	330	5,0	24	0,04	0,26
S4	500 x 250	No	330	5,0	15	0,03	0,11
S15	375 x 375	Yes	319	3,8	199	0,48	1,00
S13	375 x 188	Yes	285	3,8	125	0,34	0,82
S14	375 x 375	Yes	281	3,8	117	0,32	0,71
S12	375 x 375	Yes	279	3,8	85	0,23	0,76
S10	375 x 375	No	264	3,8	31	0,09	0,45
S11	375 x 188	No	258	3,8	31	0,09	0,30
S9	None	No	269	3,8	14	0,04	0,08

4.4.4 ALS

Displacements are usually not a limiting factor in ALS. However, for the purpose of comparison between girders with various opening and stiffeners systems, it would be of interest to see how large the shear force was when a certain tip displacement was reached. Table 4.4.3 presents the shear forces when the tip displacement is limited to 50 mm for the first group, and 38 mm for the second group. This corresponds to displacements of $L/80$, where L is twice the length of the cantilever girders. For S1 the measurements was discontinued at 44 mm.

The presentation is similar to the presentations for ULS and SLS, i.e.

$$V_{ALS,e} = \chi_{w,mod,ALS} \frac{f_y}{\sqrt{3}} ht \quad (4.4.3)$$

where $V_{ALS,e}$ is the tip equilibrium load that corresponds to the given tip displacement. Column 8 shows the ratio between $V_{ALS,e}$ and the maximum equilibrium load. The girders in each group are presented in decreasing order of $\chi_{w,mod,ALS}$.

Girder S15 obtained the best result, but also S14 and S8 had efficient stiffener systems. S6 was considerably better than S5. For the girders with the sleeve stiffeners, S5 and S12, the results are not conclusive: Girder S5 was not much better than S3 without stiffeners, but S12 was much better than S10 without stiffeners. For the smaller openings without stiffeners, there was a relative small difference between S2 and S4.

Table 4.4.3 Shear forces based on maximum tip displacements

1	2	3	4	5	6	7	8
Girder	Opening [mm]	Stiffeners	f_y [N/mm ²]	Tip displ [mm]	$V_{ALS,e}$ [kN]	$\chi_{w,mod,ALS}$	$V_{ALS,e}/V_{u,e}$
S1	None	No	327	44	187	0,33	0,86
S8	500 x 500	Yes	288	50	164	0,33	0,81
S2	500 x 250	No	332	50	144	0,25	0,94
S7	500 x 250	Yes	303	50	124	0,24	0,73
S4	500 x 250	No	330	50	132	0,23	0,97
S6	500 x 500	Yes	331	50	120	0,21	0,92
S5	500 x 500	Yes	335	50	91	0,16	0,70
S3	500 x 500	No	330	50	86	0,15	0,92
S15	375 x 375	Yes	319	38	191	0,46	0,96
S9	None	No	269	38	149	0,42	0,90
S14	375 x 375	Yes	281	38	151	0,41	0,92
S13	375 x 188	Yes	285	38	115	0,31	0,75
S11	375 x 188	No	258	38	99	0,29	0,94
S12	375 x 375	Yes	279	38	95	0,26	0,85
S10	375 x 375	No	264	38	59	0,17	0,85

4.5 Conclusion

The prior experiments showed that

- The girders displayed a ductile behavior well into the inelastic range
- Most girders kept the high shear capacity beyond the ultimate load.
- Tension fields were well established.
- Transverse web displacements for girders with un-stiffened openings showed a progressively, but even, increase up to high values when the maximum shear capacity was reached.
- If limits are placed on transverse web displacements, the shear capacities of girders with un-stiffened openings may be rather low, but not necessarily lower than for similar girders without openings.

Chapter 5

Simulations of the prior experiments

5.1 Introduction

In order to obtain efficient and reliable FE-models, the test results for girders S1 and S3 are used to calibrate the FE-models. The effects of element size, element type, material properties, imperfection shape and imperfection size are studied by means of numerical simulations and half-fractional factorial designs at two levels. The half-fractional factorial design is explained in Section 5.2, the simulations in Section 5.3 and a conclusion is given in Section 5.4.

5.2 Half-fractional factorial design of simulations

5.2.1 General

For each girder five factors (or variables) are investigated, each factor having two levels (or variations). In a general factorial design this leads to $2 \times 2 \times 2 \times 2 \times 2 = 2^5 = 32$ combinations for each girder. However, by assuming that higher order interactions are negligible, it is possible to find the main effects and two-factor interactions by performing only half the number of combinations, i.e. 16 runs for each girder. The combinations are selected and analyzed according to a certain procedure called half-fractional design. The procedure below is based on Box, Hunter and Hunter (1978).

5.2.2 Design matrix

The factors and the levels are:

- 1) Element size: 20 x 20 mm or 40 x 40 mm
- 2) Element type: S4R5 or S4R
- 3) Material: Elasto-perfectly plastic or elasto-plastic with strain hardening
- 4) Imperfection shape: 1. or 2. eigenmode
- 5) Imperfection amplitude: 1,0 or 7,5 mm

A more detailed explanation is given in Section 5.3.

The design matrix for the FE-models is shown in Table 5.2.1. FE-models are generated only for the runs that are marked with an asterisk. These runs are chosen from the criteria that the product of the individual elements in columns 1, 2, 3 and 4 shall have the same sign as the elements of Column 5. The result is a 2^{5-1} – design with resolution five. A such design does not confound the main effects and the two-factor interactions with each other, but does confound the two-factor interactions with three-factor interactions, and so on.

The design is used for both girders S1 and S3, i.e. 16 simulations for each girder.

Table 5.2.1 Design matrix for FE-models of girders S1 and S3

Factor	-	+
1 = element size	20x20 mm	40x40 mm
2 = element type	S4R5	S4R
3 = material	perfectly plastic	strain hardening
4 = imperfection shape	1. eigenmode	2. eigenmode
5 = imperfection amplitude	1,0 mm	7,5 mm

Run	1	2	3	4	5	1234	12345
1	-	-	-	-	-	+	-
*2	+	-	-	-	-	-	+
*3	-	+	-	-	-	-	+
4	+	+	-	-	-	+	-
*5	-	-	+	-	-	-	+
6	+	-	+	-	-	+	-
7	-	+	+	-	-	+	-
*8	+	+	+	-	-	-	+
*9	-	-	-	+	-	-	+
10	+	-	-	+	-	+	-
11	-	+	-	+	-	+	-
*12	+	+	-	+	-	-	+
13	-	-	+	+	-	+	-
*14	+	-	+	+	-	-	+
*15	-	+	+	+	-	-	+
16	+	+	+	+	-	+	-
*17	-	-	-	-	+	+	+
18	+	-	-	-	+	-	-
19	-	+	-	-	+	-	-
*20	+	+	-	-	+	+	+
21	-	-	+	-	+	-	-
*22	+	-	+	-	+	+	+
*23	-	+	+	-	+	+	+
24	+	+	+	-	+	-	-
24	-	-	-	+	+	-	-
*26	+	-	-	+	+	+	+
*27	-	+	-	+	+	+	+
28	+	+	-	+	+	-	-
*29	-	-	+	+	+	+	+
30	+	-	+	+	+	-	-
31	-	+	+	+	+	-	-
*32	+	+	+	+	+	+	+

5.3 Simulations of girders S1 and S3

5.3.1 FE-models

The model of Girder S3 is shown in Fig. 5.3.1 with the mesh of 20 x 20 mm elements. The model of Girder S1 is similar. As mentioned, meshes of 40 x 40 mm elements are also used. Web and flanges are modeled with thickness based on the measured values from the test girders.

The elements are of type S4R or S4R5. Type S4R is a 4-node doubly curved thin shell element, having six degrees of freedom per node, reduced integration with hourglass control and finite membrane strains. The element type S4R5 is similar to S4R, but has only five degrees of freedom per node.

The elasto-perfectly plastic material is modeled with a curve based on modulus of elasticity $E = 210\,000\text{ N/mm}^2$ up to the yield stress, a horizontal curve to 25 % strain, and is reduced to 1 N/mm^2 at 25 % strain and above. The elasto-plastic material with strain hardening has a similar curve, but from the yield stress the curve is horizontal to 2 % strain, increasing linearly to the ultimate tensile stress at 20 % strain, is horizontal to 25 % strain, and is reduced to 1 N/mm^2 at 26 % strain and above. Yield and ultimate tensile stress are based on the measured values from the test girders.

The imperfection shapes are based on eigenmodes created by ABAQUS. For girder S1 the shape of the 1. mode is two “buckles” across the compression diagonal. The shape of the 2. mode is two buckles across the tension diagonal. For girder S3 the shape of the 1. mode is a local buckle at the lower compression corner of the opening. The shape of the 2. mode is a local buckle in the upper tension corner of the opening.

The imperfections are modeled with amplitudes 1,0 mm, alternatively 7,5 mm. The latter amplitude conforms to the maximum built-in displacement allowed by Norsok N-101 (1997). As known, the test girders did not comply with this requirement, but it was expected that an amplitude based on the general Norsok requirement would be sufficient for the non-linear analyses to work properly.

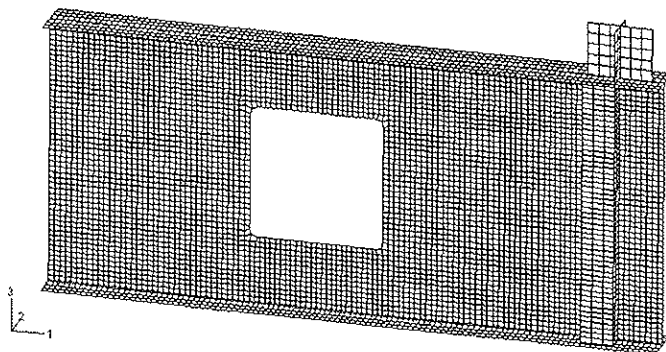


Fig. 5.3.1 FE-model of Girder S3

In the right end the UNP 140 profiles are extended with some plates in a cross shaped section above the top flanges, that simulate the jack. In the other end the models are fixed in all degrees of freedom.

The loads are applied under displacement control, by means of an increasing displacement up to 50 mm of the upper center point in the cross shaped section, i.e. the tip point. Hence the applied shear loads appear as the values of the reaction forces in this point.

ABAQUS Standard, version 5.8 is used for the simulations.

5.3.2 Results for shear capacities

The simulations give response curves of the reaction force versus tip displacement. The ultimate shear capacities $V_{u,model}$ for the 16 models of Girder S1 are shown in Table 5.3.1. The results are presented in increasing order of the shear capacities. The last column shows the ratios of the ultimate shear capacities of the models and the measured result of the test Girder S1, i.e. $V_{u,e} = 218$ kN.

Table 5.3.1 Models of Girder S1 and ultimate shear capacities

Run	Model	Factors					$V_{u,model}$ [kN]	$V_{u,model}/V_{u,e}$
		1	2	3	4	5		
29	S1205H27	-	-	+	+	+	213,3	0,98
27	S1206P27	-	+	-	+	+	213,6	0,98
3	S1206P11	-	+	-	-	-	215,1	0,99
5	S1205H11	-	-	+	-	-	215,5	0,99
17	S1205P17	-	-	-	-	+	215,8	0,99
23	S1206H17	-	+	+	-	+	216,2	0,99
32	S1406H27	+	+	+	+	+	219,9	1,01
2	S1405P11	+	-	-	-	-	220,4	1,01
8	S1406H11	+	+	+	-	-	220,9	1,01
26	S1405P27	+	-	-	+	+	221,1	1,01
22	S1405H17	+	-	+	-	+	222,2	1,02
20	S1406P17	+	+	-	-	+	223,0	1,02
9	S1205P21	-	-	-	+	-	303,7	1,39
12	S1406P21	+	+	-	+	-	315,7	1,45
15	S1206H21	-	+	+	+	-	318,0	1,46
14	S1405H21	+	-	+	+	-	350,0	1,61

The ultimate shear capacities $V_{u,model}$ for the 16 models of Girder S3 are shown in Table 5.3.2, presented in increasing order of the shear capacities. The last column shows the ratios of the ultimate shear capacities of the models and the measured result of the test Girder S3, i.e. $V_{u,e} = 93,1$ kN. All shear capacities from the models are above this value.

Table 5.3.2 Models of Girder S3 and ultimate shear capacities

Run	Model	Factors					$V_{u,model}$ [kN]	$V_{u,model}/V_{u,e}$
		1	2	3	4	5		
23	S3206H17	-	+	+	-	+	97,1	1,04
3	S3206P11	-	+	-	-	-	97,1	1,04
17	S3205P17	-	-	-	-	+	97,6	1,05
5	S3205H11	-	-	+	-	-	97,8	1,05
27	S3206P27	-	+	-	+	+	98,0	1,05
20	S3406P17	+	+	-	-	+	100,6	1,08
8	S3406H11	+	+	+	-	-	100,8	1,08
22	S3405H17	+	-	+	-	+	101,3	1,09
32	S3406H27	+	+	+	+	+	101,4	1,09
2	S3405P11	+	-	-	-	-	101,5	1,09
26	S3405P27	+	-	-	+	+	102,1	1,10
29	S3205H27	-	-	+	+	+	102,8	1,10
15	S3206H21	-	+	+	+	-	144,3	1,55
9	S3205P21	-	-	-	+	-	145,1	1,56
12	S3406P21	+	+	-	+	-	151,7	1,63
14	S3405H21	+	-	+	+	-	189,0	2,03

Table 5.3.3 shows the estimates of the main and two-factor effects, based on the half-fractional factorial design. Large main effects of factors 4 and 5 can be seen and there is also a large two-factor effect of the same factors. This means that both the shape and size of the imperfections are important. The 1. eigenmode and the 7,5 mm amplitude give much better agreement with the tests than the alternatives. However, Tables 5.3.1 and 5.3.2 indicate that it is sufficient that either the 1. eigenmode or the 7,5 mm amplitude is used.

The other effects are relatively smaller, but the estimates indicate that 20 x 20 mm elements, element type S4R, and elasto-perfectly plastic material should be preferred. The estimates also show that these factors are relatively more important for Girder S3 compared to Girder S1.

Table 5.3.3 Estimated factorial effects on ultimate shear capacities from FE-models of girders S1 and S3

Girder	Average [kN]	Main effects		Two-factor effects	
			[kN]		[kN]
S1	244,0	1 =	10,3	12 =	-6,1
		2 =	-2,5	13 =	2,3
		3 =	5,9	14 =	4,3
		4 =	50,8	15 =	-3,4
		5 =	-51,8	23 =	-4,0
				24 =	-2,8
				25 =	2,5
				34 =	5,8
				35 =	-6,4
				45 =	-53,1
S3	114,3	1 =	8,6	12 =	-4,1
		2 =	-5,8	13 =	4,1
		3 =	5,1	14 =	4,9
		4 =	30,1	15 =	-6,3
		5 =	-28,3	23 =	-6,0
				24 =	-5,1
				25 =	4,1
				34 =	5,0
				35 =	-4,0
				45 =	-28,2

5.3.3 Results for girder stiffness

Table 5.3.4 shows a comparison of girder stiffnesses of models and test girders. The secant stiffness k_{model} are based on tip displacements for 2/3 of the ultimate shear capacities. The results are presented in increasing order of stiffnesses for each group of models. The last column shows the ratios of the stiffnesses of the models and the measured stiffness of the test girders, i.e. $k_{test} = 28,1$ kN/mm for Girder S1 and $k_{test} = 13,2$ kN/mm for Girder S3. The stiffnesses of the models are all higher than these values.

Estimates from half-fractional factorial design show large main effects of eigenmodes and imperfection amplitude, and also a large two-factor effect of the same factors. Table 5.3.4 indicates that the imperfection amplitude is most important, and that the models had smaller amplitudes compared to the test girders. Factors 1, 2 and 3 had little effect.

Table 5.3.4 Model girder stiffnesses for 2/3 of the ultimate shear capacities

Group	Run	Model	Factors					k_{model} [kN/mm]	k_{model}/k_{test}
			1	2	3	4	5		
S1	29	S1205H27	-	-	+	+	+	32,39	1,15
	27	S1206P27	-	+	-	+	+	32,41	1,15
	26	S1405P27	+	-	-	+	+	32,60	1,16
	32	S1406H27	+	+	+	+	+	32,65	1,16
	23	S1206H17	-	+	+	-	+	33,66	1,20
	17	S1205P17	-	-	-	-	+	33,69	1,20
	22	S1405H17	+	-	+	-	+	33,90	1,21
	20	S1406P17	+	+	-	-	+	34,02	1,21
	3	S1206P11	-	+	-	-	-	36,84	1,31
	5	S1205H11	-	-	+	-	-	36,80	1,31
	2	S1405P11	+	-	-	-	-	36,92	1,31
	8	S1406H11	+	+	+	-	-	36,95	1,31
	15	S1206H21	-	+	+	+	-	46,81	1,67
	9	S1205P21	-	-	-	+	-	47,64	1,70
	12	S1406P21	+	+	-	+	-	47,80	1,70
14	S1405H21	+	-	+	+	-	51,62	1,84	
S3	26	S3405P27	+	-	-	+	+	17,04	1,29
	32	S3406H27	+	+	+	+	+	17,14	1,30
	27	S3206P27	-	+	-	+	+	17,25	1,31
	17	S3205P17	-	-	-	-	+	17,37	1,32
	22	S3405H17	+	-	+	-	+	17,37	1,32
	23	S3206H17	-	+	+	-	+	17,39	1,32
	20	S3406P17	+	+	-	-	+	17,41	1,32
	2	S3405P11	+	-	-	-	-	17,97	1,36
	8	S3406H11	+	+	+	-	-	18,06	1,37
	5	S3205H11	-	-	+	-	-	18,10	1,37
	3	S3206P11	-	+	-	-	-	18,19	1,38
	29	S3205H27	-	-	+	+	+	18,57	1,41
	9	S3205P21	-	-	-	+	-	28,14	2,13
	15	S3206H21	-	+	+	+	-	30,58	2,32
	14	S3405H21	+	-	+	+	-	32,74	2,48
12	S3406P21	+	+	-	+	-	33,31	2,52	

5.3.4 Wall clock time to make solutions

Table 5.3.5 shows a comparison of wall clock times for the models of Girder S3. Wall clock time is the time the computer needs to produce a complete response curve. The results are presented in increasing order of time. The absolute number of seconds depends on the computer itself, but the relative wall clock times are expected to be a measure of the effectiveness of the models. Hence the last column shows the ratios of the times from the models and the model with the fastest solution. Three models did not give complete response curves.

Not unexpected, the most important factors are the element size and type. The models with 40 x 40 mm elements and five degrees of freedom give the fastest solutions. The fastest model is S3405P11. This model is more than five times faster than the model that gives the best result for the shear capacity, i.e. S3206H17. It is interesting to see from Table 5.3.2 that the fastest model gives only 5 % higher shear capacities than the best model.

Table 5.3.5 Solution time for models of Girder S3

Run	File	Factors					Wall clock time [s]	Ratio
		1	2	3	4	5		
2	S3405P11	+	-	-	-	-	2484	1,00
22	S3405H17	+	-	+	-	+	2494	1,00
26	S3405P27	+	-	-	+	+	2955	1,19
20	S3406P17	+	+	-	-	+	3242	1,31
8	S3406H11	+	+	+	-	-	3347	1,35
32	S3406H27	+	+	+	+	+	3845	1,55
17	S3205P17	-	-	-	-	+	9403	3,79
5	S3205H11	-	-	+	-	-	9832	3,96
29	S3205H27	-	-	+	+	+	12368	4,98
23	S3206H17	-	+	+	-	+	13158	5,30
27	S3206P27	-	+	-	+	+	13801	5,56
3	S3206P11	-	+	-	-	-	14206	5,72
15	S3206H21	-	+	+	+	-	20655	8,32
14	S3405H21	+	-	+	+	-
12	S3406P21	+	+	-	+	-
9	S3205P21	-	-	-	+	-

5.3.5 Improved modeling technique

The previous models were established as ordinary input-files in ABAQUS Standard version 5.8. In order to utilize the inter-active modeling capabilities of ABAQUS, a new model E3206H17 is made by means of ABAQUS CAE version 6.3.1. This model is similar to model S3206H17 for Girder S3, except that the element sizes gradually increase away from the opening. Hence the minimum element size is about 20 x 20 mm and the maximum size about 40 x 40 mm. The purpose is: 1) To check that the new ABAQUS version worked properly, and 2) to get faster solutions without loosing too much precision. The result is as follows:

- The model can be made in CAE, but in order to include prescribed imperfections by means of buckling eigenmodes and amplitudes, the solution has to be run in ABAQUS Standard version 6.3.1.
- The ultimate shear capacity of model E3206H17 is 99,9 kN or about 1,07 times the measured result for Girder S3. The model gives about 3 % higher shear capacity compared to the best model, i.e. S3206H17.
- The model girder stiffness for 2/3 of the ultimate shear capacity is 17,32 kN/mm or about 1,31 times the measured stiffness for Girder S3, or about the same stiffness as model S3206H17.
- The wall clock time for solution is 3495 s , compared to 4435 s for S3206H17 on the same computer. Hence model E3206H17 is about 20 % faster.
- Compared to the measured values of Girder S3, model E3206H17 gives about the same shear capacity in SLS, based on $h/200$ maximum web displacements from the loads. For ALS, the model gives 2 % higher shear capacity, based on 50 mm maximum tip displacements.

5.3.6 Transverse web displacements

The transverse web displacements of model E3206H17 at maximum shear is shown in Fig. 5.3.2. Colors show displacements in 5 mm steps and the maximum displacement is about 45 mm. Initial displacements are included in the model, but are not included in the values of Fig. 5.3.2.

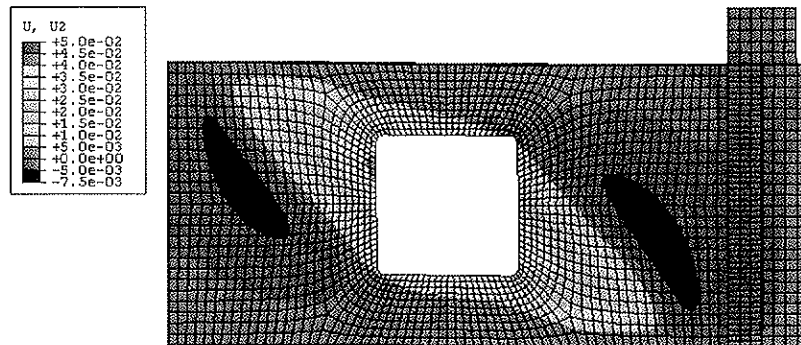


Fig. 5.3.2 Model E3206H17, transverse web displacements at maximum tip load

5.3.7 Stresses

Von Mises stresses of model E3206H17 at maximum shear is shown in Fig. 5.3.3. The values are based on the stresses in the surface of web. Stresses above $f_y = 330 \text{ N/mm}^2$ are shown in light grey, while the other colors show stresses in steps of 10 % of f_y . The areas of plastification are relatively small.

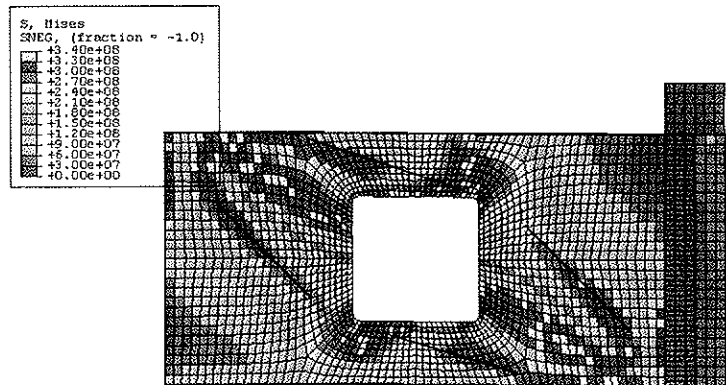


Fig. 5.3.3 Von Mises stress in Model E3206H17 at maximum tip load

5.4 Conclusion

The simulations show that

- Good estimates of shear capacities can be achieved by means of simple ABAQUS models. Imperfections must be applied; the 1. eigenmode and amplitudes based on 0,75 % of the web height are sufficient. The computed results for the best models should be regarded to be from 0 to 10 % on the non-conservative side.
- The girder stiffness based on 2/3 of the ultimate shear capacity may be overestimated by 15 to 32 % by the best models.
- Figs. 5.3.2 and 5.3.3 depict displacements and stresses for the same applied load. If the areas of large buckles are disregarded, a pattern of tension fields may be seen, as marked by inclined lines in Fig. 5.3.3. The lines above and below the opening intersect with the flanges relatively far from the corners of the web. Some authors explain this with bending capacity of the flanges. However, at the actual step time, the flange bending is still relatively small. Hence the reason is probably more related to compression fields in the corners of the web.
- The webs of the test girders must be considered as having fixed supports in the vertical sides; in the right end by way of the two U-sections and in the left end by the 50 mm end plate. This phenomenon does not influence the comparison of test results versus the simulated results, because the models have included the U-profiles and have fixed left ends of the web. However, for the following simulations, the models should include an extra web panel in each end, in order to ensure that the stiffness in the web corners is not overestimated.

Chapter 6

Proposal for a new design procedure

6.1 Introduction

When designing girders with web openings it is tempting to use the same design procedure as given in the latest proposal to the EC3, Part 1-5 for girders without openings. As discussed in Section 3.5.3, all effects on the shear capacity from web openings may be included in one function $\chi_{w,mod}$. In addition a function ξ_w may be needed to account for the additional flange forces caused by the openings, as discussed in Section 3.8.2. The resulting shear and primary moment capacities are used in interaction equations, derived from the moment-shear interaction equations for girders without openings. Alternatively, the AISC (1990) moment-shear interaction equation for beams with openings may be a solution.

It should be emphasized that this is not a new load-carrying model, it is a system of organizing experimental data, theoretical methods and numerical simulations. The results can be used directly for design purposes, and various effects and theories can be compared. The presentation of the shear capacity is similar to that of the rotated stress field method and the modified Vierendeel method. The results of these methods can be included directly in the design procedure. However, for openings not covered by these methods, numerical simulations may be sufficient to establish the functions $\chi_{w,mod}$ and ξ_w without the need for supporting load-carrying theories.

Values of $\chi_{w,mod}$ and ξ_w may be given in diagrams, tables and equations. The proposed procedure is also suitable for implementation in spreadsheets.

6.2 The functions $\chi_{w,mod}$ and ξ_w

The shear capacity is given as

$$V_{c,mod} = \chi_{w,mod} \frac{f_y}{\sqrt{3}} ht \quad (6.2.1)$$

The additional flange force is given as

$$F_a = \xi_w V \quad (6.2.2)$$

In principle, two diagrams are needed for each opening configuration; one for the shear capacity and one for the additional flange force caused by the opening. The term "opening configuration" means the opening shape with or without reinforcement. Hence, one configuration comprises circular openings, another configuration is circular openings with sleeves, a third configuration is square openings with horizontal reinforcement, etc.

Each diagram may include curves for several D/h ratios. However, the total number of diagrams would soon be more confusing than informative. To limit the number of

diagrams, it is necessary to split the functions $\chi_{w,mod}$ and ξ_w into sub-functions, depending on primary, secondary and tertiary factors. Hence

$$\chi_{w,mod} = c_1 c_2 c_3 \quad (6.2.3)$$

where c_n denotes the sub-functions. A similar equation is valid for ξ_w .

The primary factors are

- h/t ratios
- D/h ratios
- f_y
- $\sqrt{\frac{f_y}{E}}$
- Transverse web stiffeners independent of opening

The secondary factors are

- Opening shape
- Reinforcement
- Vertical position of openings
- Multiple openings
- Distance between openings

The tertiary factors are

- Girder flange area, bending and torsional stiffness.

6.3 The simulations and the factors c_1 , c_2 and c_3

The objective is to determine the functions (or factors) c_1 , c_2 and c_3 , and the simulations presented are mainly planned for this purpose. An attempt to use half-fractional factorial design for the simulations was left in favor of a design based on “advance the solution” by continuation. A brief outline of the simulations is as follows.

- 1) The simulations are performed in four girder groups, based on opening shapes. The shapes are circular, elongated circular, square and rectangular.
- 2) Areas of girder flanges are chosen as a certain ratio of the web areas. Bending and torsional stiffness of girder flanges are set to very low values. This is conservative and the effect on the shear capacity is minor. Hence, the factor c_3 is set to

$$c_3 = 1 \quad (6.3.1)$$

for all simulations. The extra shear capacity provided by the flanges will rarely be used in practice and a major reduction in the number of diagrams is achieved.

3) One set of secondary factors is chosen as basis:

- Circular shape
- No reinforcement
- Vertical position of the center of openings in the horizontal centerline of webs.
- One opening

For this set the factor c_2 is defined as $c_2 = 1$.

4) The primary factors comprise three h/t ratios, two D/h or D_h/h ratios, two yield stress values, two $\sqrt{f_y/E}$ ratios and four configurations of transverse web stiffeners.

5) The factors c_1 are defined as

$$c_1 = \chi_{w,\text{mod},\text{basic}} = \chi_{w,\text{mod}} \text{ when } c_2 = 1 \text{ and } c_3 = 1 \quad (6.3.2)$$

where $\chi_{w,\text{mod}}$ is the result when simulations are performed with the basic set of secondary factors. It should be noted that there are many values for $\chi_{w,\text{mod},\text{basic}}$, because there are several variations of the primary factors. The simulations are described in Section 7.2 and the values for $\chi_{w,\text{mod},\text{basic}}$ from the simulations are listed in Table 7.2.3.

6) The adjustment factors c_2 are found from simulations of model pairs of girders with same primary factors, but with alternative sets of secondary factors. The factors are defined as

$$c_2 = \frac{\chi_{w,\text{mod}}}{\chi_{w,\text{mod},\text{basic}}} \quad (6.3.3)$$

where $\chi_{w,\text{mod},\text{basic}}$ and $\chi_{w,\text{mod}}$ are the reduction factors, when the simulations are performed with the basic and the alternative set of secondary factors, respectively. Each girder pair gives a value c_2 , and by combining two or more values it is possible to establish c_2 as functions of secondary factors.

6.4 Design in various limit states

A development of the proposed method is presented in Chapter 11, and design guidelines are given in Section 12.2. The method considers ULS only. However, the results of the simulations regarding SLS and ALS are also considered to some extent. Consecutive discussions are included in Chapter 7 to 10.

6.5 Relative comparisons

The simulations also give opportunities to show directly the loss or gain in shear capacity for alternatives of the secondary factors. For example, it is possible to see the effect of horizontal reinforcement on one or both sides of web, when all other factors are constant. Such comparisons are performed consecutively through the report and are presented in the tables of Chapters 7 to 10 as

$$c_{rel} = \frac{\chi_{w,mod,B}}{\chi_{w,mod,A}} \quad (6.5.1)$$

Subscript B denotes the girder that is compared, and subscript A denotes the girder that it is compared to. A vast number of comparisons is possible. The chosen comparisons are based on the author's experience from practice. Detailed explanation is given in the respective tables or sections.

6.6 Overview of simulations

An overview of all simulations is given in Appendix A.

Chapter 7

Simulations of girders with circular openings

7.1 Introduction

The basic FE-model represents a girder 1,0 x 4,0 m without opening. The web is modeled with 40 x 40 mm S4R elements and the flanges with 40 mm beam elements of type B31. Shell element thickness and beam element section properties are to be varied. All four edges of the web are simply supported. The flanges are laterally supported along the whole girder.

At the left end of the model all translations are fixed. At the other end the model is free, but a special lever arm with large stiffness EI is modeled in order to achieve a static system that is fixed for global moment, but free for vertical and longitudinal displacement. The static system is shown in Fig. 7.1.1. The tip of the lever arm is located in the center of the girder, i.e. where also the centers of openings are to be placed. The load is applied in the form of a vertical displacement up to 100 mm of the tip of the lever arm. This creates a pure state of shear with no moment in the vertical centerline through the opening.

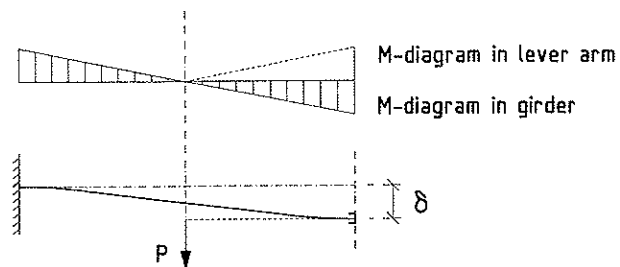


Fig. 7.1.1 Static system of simulations

The material is modeled as steel with $f_y = 420 \text{ N/mm}^2$ and almost elasto-perfectly plastic. A small strain hardening of 10 N/mm^2 is included in order to monitor the maximum strain in an easy way by means of the maximum stress. Above 30 % strain the material is modeled as perfectly-plastic.

Variations of the basic FE-model consist of one or two circular openings with $D = 0,25h$ and $D = 0,50h$, as well as models with sleeves, transverse stiffeners and doubler plates. Smaller elements, approximately $20 \times 20 \text{ mm}$, are applied around the openings. Fig. 7.1.2 shows the model with one circular opening $D = 0,50h$.

Results from the simulations are:

- Response curves for shear force versus tip displacement
- Maximum shear forces
- Response curves for transverse web displacement versus tip displacement
- Transverse web displacement plots at maximum shear
- Stress plots at maximum shear
- Flange forces in vertical sections in the opening at maximum shear

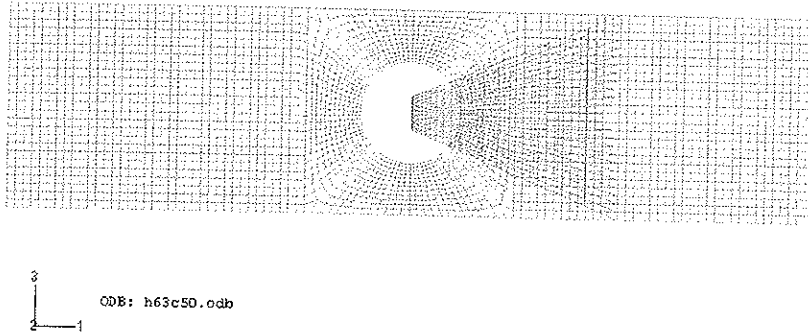


Fig. 7.1.2 FE-model of girder with circular opening, including lever arm

Compared to the models in Chapter 5, the basic FE-model without opening shows most similarity to Model S1406P17. This model gave a shear capacity 2 % above the tests result for Girder S1. The girders with circular openings have no corresponding model in Chapter 5. The variations of the basic FE-model with square openings described in Chapter 9 may be compared to Model E3206H17 in Chapter 5. This model gave a shear capacity 7 % above the test results for Girder S3. Hence, there is reason to believe that the shear capacities presented in Chapters 7 to 10 are slightly on the non-conservative side. No effort is made to modify the results from the simulations to account for inaccuracy. However, possible non-conservative results are considered in the development of the design guidelines based on the simulations, see Chapter 11.

Running two simulations without buckling and three simulations with buckling further check the performance of the model without opening. The simulations without buckling are run to see if the model can simulate full plastic shear. The girders had very small bending stiffness of flanges in order to minimize the contribution to shear capacity from the flanges. However, the axial stiffness of flanges are varied. Girder E63FS has a ratio of $A_f/A_w = 6$ and achieves a reduction factor $\chi_{w,mod} = 1,00$. Girder E63 has a ratio of $A_f/A_w = 2$ and achieves $\chi_{w,mod} = 0,97$. Both girders have sufficient flange area to take the moment in the ends of the girders by flanges only. However, the models can only obtain full shear capacity for girders with very large flanges. This is due to the interaction effect of moment and shear in the web near the ends of the model. For models with openings, this phenomenon is less important, because the shear never reaches the full shear capacity at the ends.

The simulations with buckling are run to compare the performance of the models with the proposal to EC3, i.e. the curve given in Table 3.5.1 for girders with rigid end posts. Girders I63, I125 and I250 have web thickness 16, 8 and 4 mm, giving ratios $h/t = 63, 125$ and 250, respectively. The girders have very small bending stiffness of flanges and a ratio of $A_f/A_w = 2$. According to EC3, the shear capacities are not reduced by moment-shear interaction in this case. Imperfections are applied as 2. eigenmode with amplitude 7,5 mm. Preliminary runs with 1. eigenmode gave unreliable, i.e. high shear capacities. The results are plotted in Fig. 7.1.3, which also shows the buckling curve given in Table 3.5.1, calculated for $k_r = 5,59$. The results are good for $h/t = 125$ and 250. For $h/t = 63$ the simulated shear capacity is somewhat lower than given by the EC3 proposal.

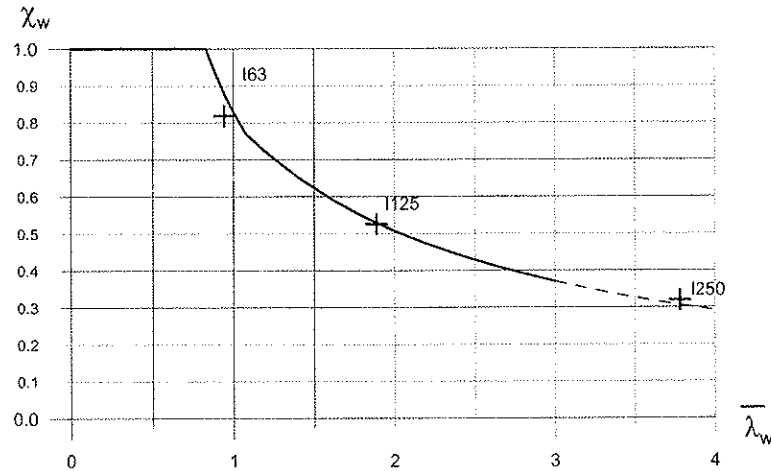


Fig. 7.1.3 Simulated shear buckling capacities for girders without openings compared to EC3

7.2 Single opening without stiffening

7.2.1 Comparison with the rotated stress field method

Nine simulations are performed in order to study the rotated stress field method. Three girders have no openings, three girders have openings with $D = 0,25h$ and three girders have openings with $D = 0,50h$. The h/t ratios are 63, 125 and 250. In order to compare directly to the diagram of Fig. 3.6.2, the material is modeled with $f_y = 260 \text{ N/mm}^2$, but otherwise the girders are as explained in Section 7.1. In general the girder names are in the format Hxx or HxxCyy, where xx refers to the h/t ratio and yy refers to the D/h ratio in %. Hence a girder with $h/t = 125$ and no opening is called H125, while a girder with $h/t = 250$ and opening diameter $0,50h$ is called H250C50.

The results for $\chi_{w,mod}$ are given in Table 7.2.1 together with values from rotated stress field theory taken from Fig. 3.6.2. Column 7 shows the ratio of simulated values to the values from the rotated stress field method. In Fig. 7.2.1 the simulated results are plotted together with the relevant curves from the rotated stress field method.

The simulated values are generally lower than the values from the rotated stress field method, but the difference is small for the girders with openings. The rotated stress field method should be regarded as very good for small openings in stocky plates and for small and large openings in very slender plates. For large openings in stocky plates and small and large openings in medium slender plates the rotated stress field theory seems to be somewhat non-conservative. This may be due to the use of the critical buckling stress in Eq. (3.6.6) with no correction for elasto-plastic buckling.

The simulated values are obtained for a 4 m long girder, while the values from the rotated stress field method relate to an infinitely long girder. The influence of this is small, and probably not relevant at all for the girders with openings. For the girders without

openings the influence is conservative in favor of the simulations, as all simulated values are lower than the values from the rotated stress field method.

For the girders without openings, the simulated values are considerably lower than the values given by the rotated stress field method. However, the importance of this is minor, as such cases may be covered by the proposal to EC3. The proposed curve for girders with rigid end supports is included as a dotted line in Fig. 7.2.1. In the same way as shown in Section 7.1, the simulations agree quite well for medium and slender plates. For stocky plates, the simulated results are again lower than the proposal to EC3.

Table 7.2.1 Comparison between simulations and rotated stress field theory

1	2	3	4	5	6	7
Run	Girder	h/t	D/h	Simulated $\chi_{w,mod}$	Rotated stress field theory $\chi_{w,mod,R}$	$\chi_{w,mod}/\chi_{w,mod,R}$
13	H63	63	-	0,89	0,99	0,90
14	H125	125	-	0,62	0,75	0,83
15	H250	250	-	0,37	0,43	0,86
16	H63C25	63	0,25	0,75	0,75	1,00
17	H125C25	125	0,25	0,54	0,57	0,95
18	H250C25	250	0,25	0,33	0,33	1,00
19	H63C50	63	0,50	0,48	0,50	0,96
20	H125C50	125	0,50	0,35	0,38	0,92
21	H250C50	250	0,50	0,22	0,22	1,00

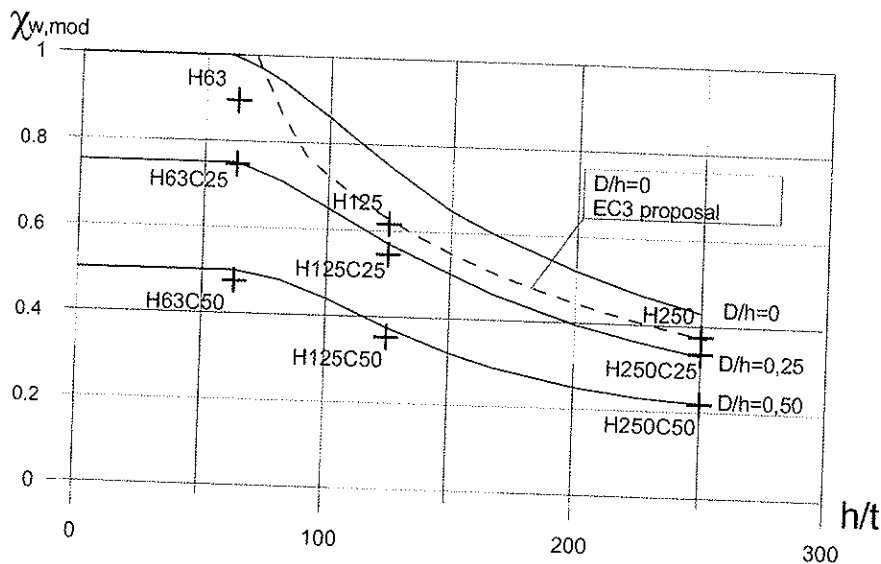


Fig. 7.2.1 Simulated results compared to curves from rotated stress field theory and EC3 proposal

7.2.2 Transverse displacements and stresses in webs

Plots of the transverse web displacement at maximum shear are shown in Figs. 7.2.2 to 7.2.4 for the medium slender webs of girders H125, H125C25 and H125C50. Light grey color shows positive displacements larger than 5 mm and black color negative displacements larger than 5 mm. Positive displacements are away from the viewer. The maximum transverse displacements at maximum shear are 20 mm, 23 mm and 24 mm for H125, H125C25 and H125C50, respectively. This indicates that the openings have a relatively small influence on the transverse displacements at maximum shear.

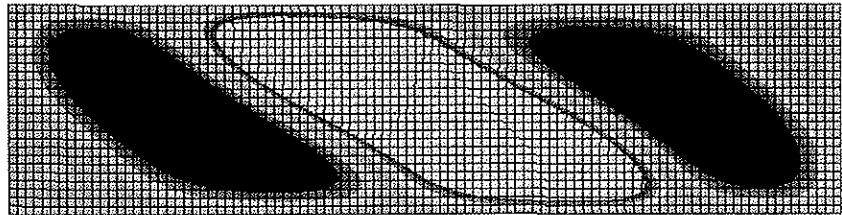


Fig. 7.2.2 Transverse web displacement at maximum shear in Girder H125

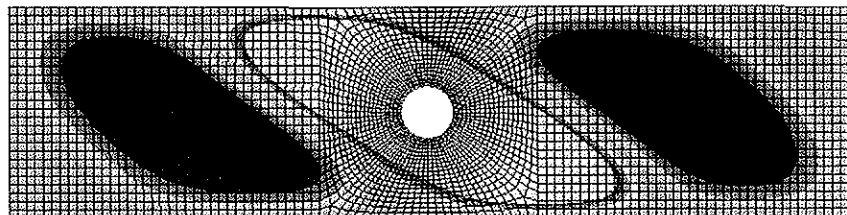


Fig. 7.2.3 Transverse web displacement at maximum shear in Girder H125C25

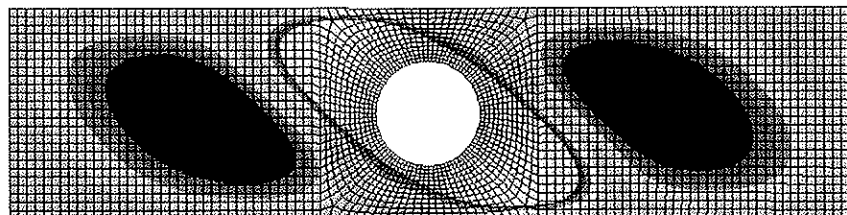


Fig. 7.2.4 Transverse web displacement at maximum shear in Girder H125C50

Plots of von Mises stress at maximum shear are shown in Figs. 7.2.5 to 7.2.7 for the same girders. The plots show the quilted (non-averaged) stress on the negative surface of web elements, i.e. the surface away from the viewer. The negative surface is most strained in a buckle with positive displacement. The legend is the same for the three figures. Areas of plastification are shown in light grey color.

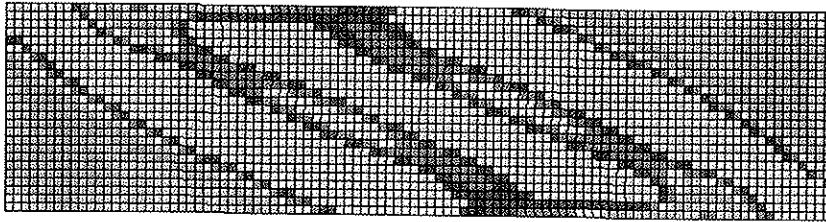
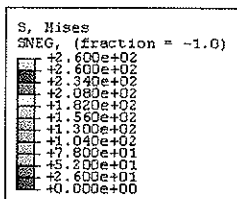


Fig. 7.2.5 Von Mises stress at maximum shear in Girder H125

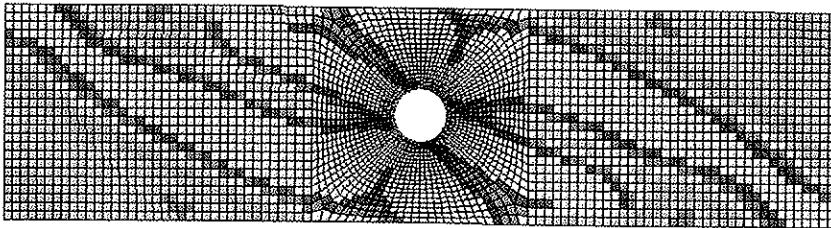


Fig. 7.2.6 Von Mises stress at maximum shear in Girder H125C25

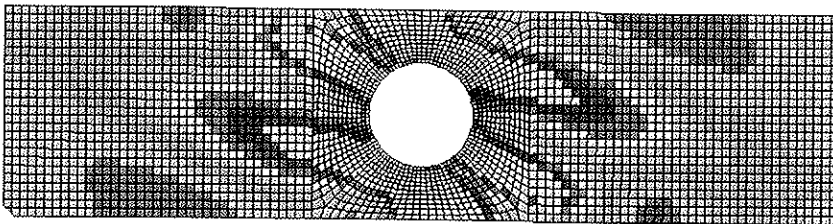


Fig. 7.2.7 Von Mises stress at maximum shear in Girder H125C50

It might be interesting to also consider the stresses in the middle and positive surfaces of elements. Figs. 7.2.8 and 7.2.9 show these stresses for Girder H125C50. The legend is the same as in Fig. 7.2.5. Unfortunately, ABAQUS is unable to show the stress in the middle surface of the left region around the opening, but the stress is supposed to be point-symmetric to the stress in the right region around the opening.

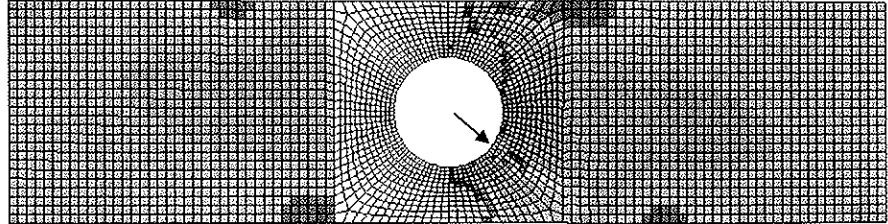


Fig. 7.2.8 Von Mises stress at maximum shear in the middle surface of Girder H125C50

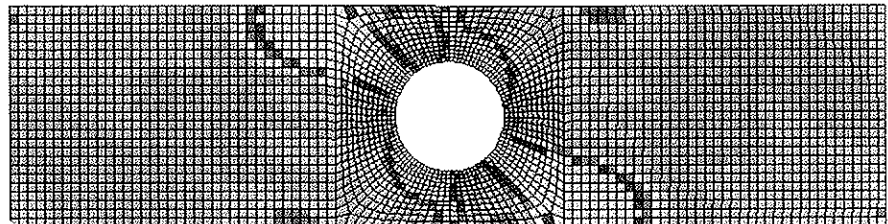


Fig. 7.2.9 Von Mises stress at maximum shear in the positive surface of Girder H125C50

The areas of plastification at maximum shear are larger for Girder H125 than for H125C25 and H125C50, but are small in all girders. Plastic strains do not exceed 1 %.

Girder H125C50 has a ratio $D/t = 63$. Figs. 7.2.7 to 7.2.9 show that the von Mises stresses reach $f_y = 260 \text{ N/mm}^2$ over the whole element thickness at the edge of opening in the middle of the buckle. A closer look at an element in the 45° section to the vertical, marked with an arrow in Fig. 7.2.8, shows that the stresses are mainly due to out-of-plane bending. The average minimum principal stress $\sigma_2 = -162 \text{ N/mm}^2$, based on $\sigma_2 = +67$, $\sigma_2 = -270$ and $\sigma_2 = -284 \text{ N/mm}^2$, respectively, at the integration points on the negative, the middle and the positive surfaces.

7.2.3 Buckling

The response curve for shear force versus tip displacement for Girder H125C50 is shown in Fig. 7.2.10. Time 1,00 = 100 mm tip displacement. The response curves for the other eight girders, including those without openings, have similar shape. The curves display a buckling tendency as indicated by the drop in load-carrying capacity.

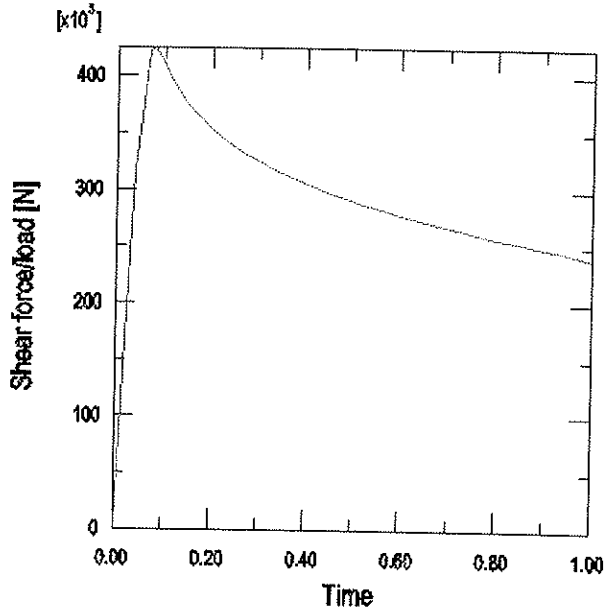


Fig.7.2.10 Response curve for Girder H125C50

The transverse web displacement at maximum shear, i.e. *before* a possible buckling takes place, is depicted in Fig. 7.2.4. In order to study the buckling phenomenon in more detail, the response curve for the transverse displacement of edge node 377 is shown in Fig. 7.2.11. This node is situated near the 45° section to the vertical and is marked with an arrow in Fig. 7.2.8.

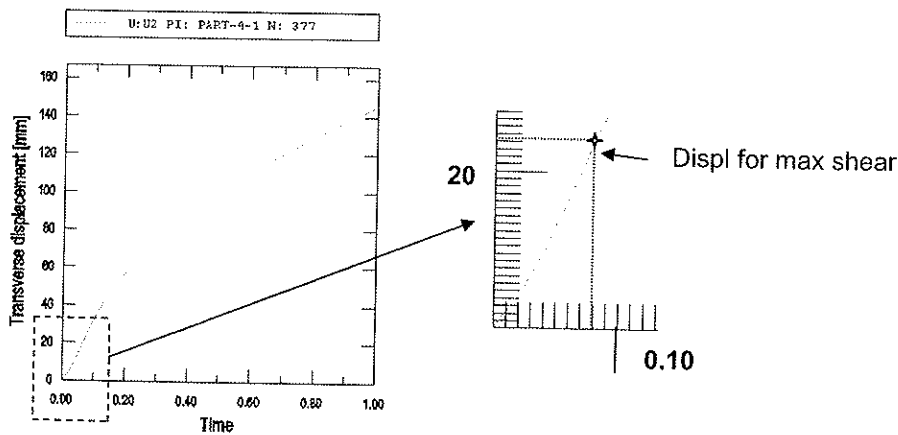


Fig.7.2.11 Response curve for transverse displacement of edge node 377 in Girder H125C50

As shown, there is a slight nonlinear tendency for the first two increments, but there is no evidence of local, column type buckling when maximum shear is reached. Fig. 7.2.12 shows the buckle around the opening at this load level. The colors show positive transverse displacements in 5 steps up to the maximum displacement of 24,3 mm. Negative buckles are omitted in order to simplify the figure. Fig. 7.2.13 shows the buckle at 9,6 mm vertical tip displacement, i.e. after some decrease in shear capacity. The colors show transverse displacements as described above. Additional light-grey color shows the area where the transverse displacements have exceeded the previous maximum value of 24,3 mm. Local buckling modes superimposed on the global buckling mode are not seen. The global buckling mode has increased somewhat, but the surface at the edge is still smooth with no sign of abrupt changes.

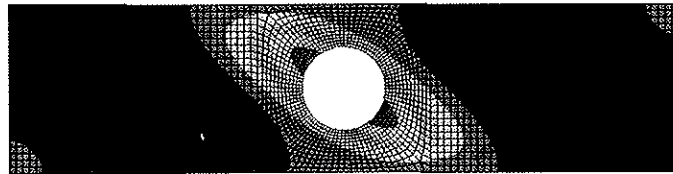
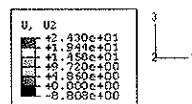


Fig.7.2.12 Buckle around opening in Girder H125C50 at step time 0,0775

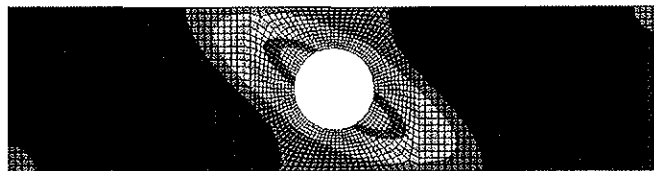
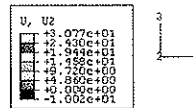


Fig. 7.2.13 Buckle around opening in Girder H125C50 at step time 0,0962

The exact definition of global or local buckling may not be particularly important. However, from the previous figures it should be clear that the force resultants of the compression stress fields have to be relocated away from the opening as the amplitude of the buckle increases. The reduction in shear capacity from the maximum value follows. The length of the buckle around the opening increases more slowly. Two adjacent buckles are located in the black areas of Figs. 7.2.12 and 7.2.13, and can also be seen in Fig. 7.2.4. These buckles disappear with increasing tip displacement, i.e. when the shear decreases. Hence, more space is gradually provided for the buckle around the opening. Finally the buckle has the form and extent as shown in Fig. 7.2.14. The color code is the same as in Fig. 7.2.13.

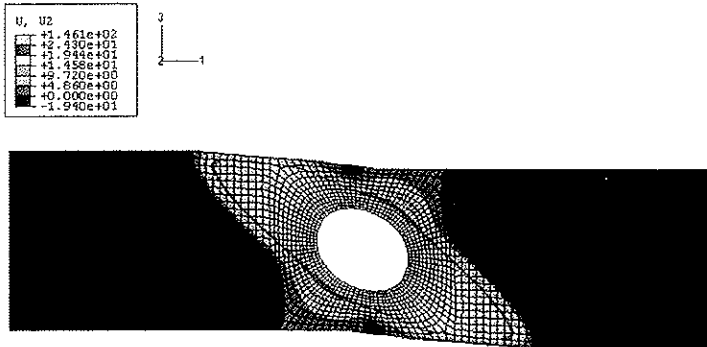


Fig. 7.2.14 Buckle around opening in Girder H125C50 at step time 1,0000

7.2.4 Influence of the yield stress f_y

In order to study the influence of varying the yield stress alone, the simulations of the six girders with openings of Section 7.2.1 are repeated, but now with $f_y = 420 \text{ N/mm}^2$. The results for $\chi_{w,mod}$ are given in Table 7.2.2. These results and the results from Table 7.2.1 are plotted in Fig. 7.2.15 as a function of the relative slenderness. The relative slenderness is based on $k_r = 5,59$ for all simulations.

Fig. 7.2.15 also shows the EC3 proposal for webs without openings, together with scaled curves for 75 % and 50 % of the proposal. It can be seen that the results from the simulations of webs with openings $D/h = 0,25$ are above the 75 % curve except for the lowest slenderness. Similarly, the results from the webs with $D/h = 0,50$ are above the 50 % curve except for the lowest relative slenderness. This interesting observation is investigated further in next section.

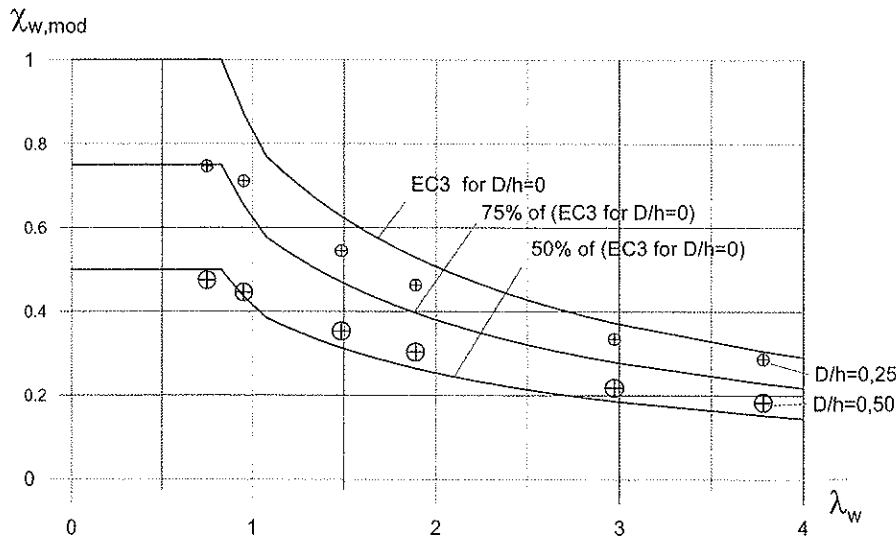
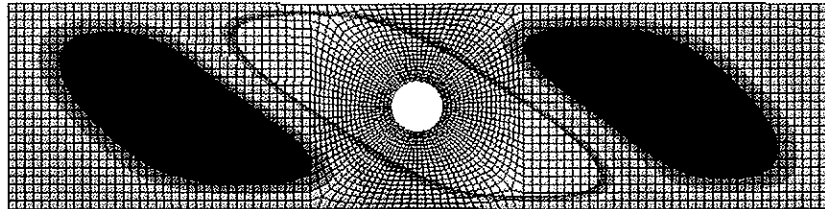
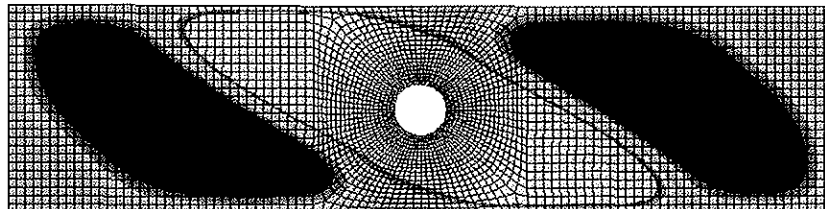


Fig 7.2.15 $\chi_{w,mod}$ for relative slenderness when $k_r = 5,59$

Table 7.2.2 $\chi_{w,mod}$ for girders with $f_y = 420 \text{ N/mm}^2$

1	2	3	4	5
Run	Girder	h/t	D/h	Simulated $\chi_{w,mod}$
25	I63C25	63	0,25	0,71
26	I125C25	125	0,25	0,46
27	I250C25	250	0,25	0,29
28	I63C50	63	0,50	0,45
29	I125C50	125	0,50	0,30
30	I250C50	250	0,50	0,18

Figs. 7.2.16 and 7.2.17 depict the influence of the yield stress on the form of the buckles for the medium slender webs of H125C25 and I125C25. Transverse web displacements at maximum shear are shown. Light grey color shows positive displacements larger than 5 mm and black color negative displacements larger than 5 mm. Even though the yield stress is increased by 62 % from H125C25 to I125C25, maximum shear capacity is increased by 37 %, maximum transverse displacement by 78 % and maximum length of the buckle by 12 %. The widths and inclinations of the buckles are almost the same. The relative slenderness increases from 1,49 for H125C25 to 1,89 for I125C25. According to EC3 the shear capacity increases 36 % for corresponding girders without openings. This leads to the conclusion that the shear capacity in girders with openings is governed by a combination of yield stress and buckling, and the relative slenderness and buckling reduction factor for girders without openings may be relevant parameters for determination of shear capacities for girders with openings.

Fig. 7.2.16 Buckles at maximum shear in Girder H125C25 ($f_y = 260 \text{ N/mm}^2$)Fig. 7.2.17 Buckles at maximum shear in Girder I125C25 ($f_y = 420 \text{ N/mm}^2$)

7.2.5 Additional flange forces

In order to study additional flange forces in girders with openings, normalized flange force ratios are plotted in Fig. 7.2.18. Girder I125 without opening is chosen as a reference girder, i.e. the girder that the other girders are compared to. The flange force at maximum shear in I125 is denoted $F_{s,A}$, and the maximum shear in I125 is denoted $V_{max,A}$. Hence, subscript "A" points at the reference girder. The normalized flange force ratio for Girder I125 is

$$\xi_A = \frac{F_{s,A}}{V_{max,A}} \quad (7.2.1)$$

The girders that are compared are I125C25 and I125C50. These girders have the same slenderness as I125, but with circular openings $D/h = 0,25$ and $D/h = 0,50$, respectively. The flange force at maximum shear in these girders is denoted $F_{s,B}$, and the maximum shear is denoted $V_{max,B}$. The subscript "B" points at the girders that are compared. The normalized flange force ratios for girders I125C25 and I125C50 are taken as

$$\xi_B = \frac{F_{s,B}}{V_{max,B}} \quad (7.2.2)$$

The values of ξ_A and ξ_B vary along the girders, and the particular values at distances $D/2$ from the vertical centerline are denoted $\xi_{A,C25}$, $\xi_{A,C50}$, $\xi_{B,C25}$ and $\xi_{B,C50}$. The subscripts "C25" and "C50" refer to the positions given by the vertical tangents for the openings with $D/h = 0,25$ and $D/h = 0,50$, respectively. See Fig. 7.2.18.

For Girder I125 a flange force ratio $\xi_{A,elastic}$ may be determined based on geometrical and material linear analysis, i.e. with buckling disregarded. Fig. 7.2.18 shows that the curves ξ_A and $\xi_{A,elastic}$ are almost parallel, which confirms the theory shown in Fig. 3.6.3 e). The tension band gives a constant additional flange force.

The ξ_B curves show that the openings give further additional flange forces, which in normalized values are most pronounced for the largest opening. However, in absolute values the largest additional flange forces occur for the smallest opening, thus confirming the curves shown in Fig. 3.6.3 f) and g).

The factor ξ_w represents the part of the additional flange force that is due to the opening, and is determined as

$$\xi_w = \xi_{B,C25} - \xi_{A,C25} \quad \text{for } D/h = 0,25 \quad (7.2.3)$$

$$\xi_w = \xi_{B,C50} - \xi_{A,C50} \quad \text{for } D/h = 0,50 \quad (7.2.4)$$

ξ_w is depicted in Fig. 7.2.18 as the vertical distance between the dots on the curves.

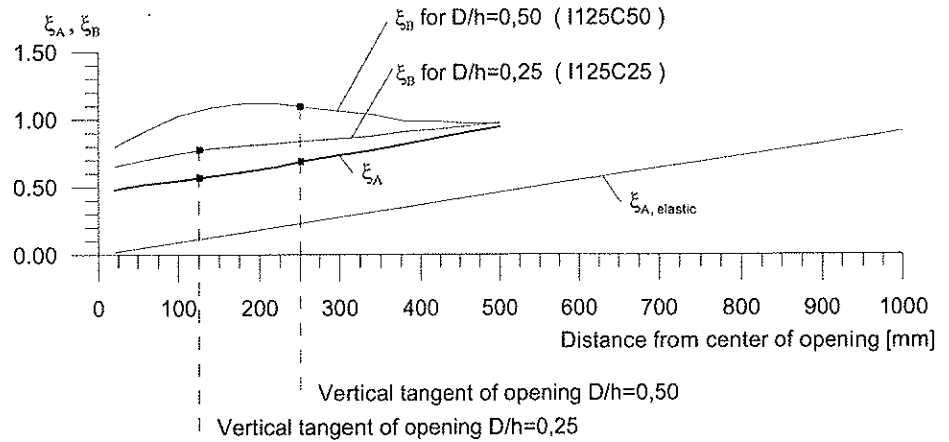


Fig. 7.2.18 Normalized flange forces of girders I125, I125C25 and I125C50 plotted along top flange

7.2.6 Influence of transverse stiffeners

On $\chi_{w,mod}$

The influence of transverse web stiffeners on the reduction factor $\chi_{w,mod}$ are studied by means of 36 simulations. 27 girders with stiffener locations giving aspect ratios 2, 1 and 0,5 are analyzed. Nine of the previous girders without stiffeners are also included for comparison; these girders have an aspect ratio of 4. This means that three h/t ratios, three D/h ratios and four a/h ratios are considered.

The results are shown in Table 7.2.3. Columns 3 and 4 give the web and opening dimensions. Column 6 gives the stiffener dimensions on the form $FL_{yy} \times zz$, with yy being the width and zz the thickness. All stiffeners comply with the EC3 stiffness requirements for girders without openings. The stiffness criteria are fulfilled with a margin of 0 to 88 %, and all stiffeners have $h_{st}/t_{st} = 8$. However, in four of the girders with slender webs the stiffeners buckled prior to the web buckling. These cases are marked with an asterix in Table 7.2.3. The imperfections used in the analyses are based on the eigenmodes that give the largest buckle at the opening. The imperfection amplitudes are taken as 7,5 mm for all girders, except for those with aspect ratio 0,5, where the amplitude of 4,05 mm is used.

Table 7.2.3 $\chi_{w,mod}$ for various values of h/t , D/h , a/h and stiffeners dimensions

1	2	3	4	5	6	7	8
Run	Girder	h/t	D/h	a/h	Stiffeners	$\chi_{w,mod}$	$\bar{\lambda}_w$
22	I63	63	0	4	-	0,82	0,95
31	I63T2	63	0	2	FL100x12,5	0,86	0,89
40	I63T1	63	0	1	FL100x12,5	0,93	0,74
49	I63T0	63	0	0,5	FL100x12,5	0,98	0,45
23	I125	125	0	4	-	0,53	1,89
32	I125T2	125	0	2	FL63x8	0,58	1,78
41	I125T1	125	0	1	FL80x10	0,77	1,46
50	I125T0	125	0	0,5	FL100x12,5	0,90	0,89
24	I250	250	0	4	-	0,32	3,78
112	I250T2c	250	0	2	FL40x5 *	0,45	3,55
42	I250T1	250	0	1	FL50x6 *	0,48	2,92
51	I250T0	250	0	0,5	FL63x8	0,79	1,78
25	I63C25	63	0,25	4	-	0,71	0,95
34	I63C25T2	63	0,25	2	FL100x12,5	0,72	0,89
43	I63C25T1	63	0,25	1	FL100x12,5	0,74	0,74
52	I63C25T0	63	0,25	0,5	FL100x12,5	0,77	0,45
26	I125C25	125	0,25	4	-	0,46	1,89
35	I125C25T2	125	0,25	2	FL63x8	0,50	1,78
44	I125C25T1	125	0,25	1	FL80x10	0,63	1,46
53	I125C25T0	125	0,25	0,5	FL100x12,5	0,71	0,89
27	I250C25	250	0,25	4	-	0,29	3,78
113	I250C25T2c	250	0,25	2	FL40x5 *	0,35	3,55
45	I250C25T1	250	0,25	1	FL50x6 *	0,46	2,92
54	I250C25T0	250	0,25	0,5	FL63x8	0,55	1,78
28	I63C50	63	0,50	4	-	0,45	0,95
37	I63C50T2	63	0,50	2	FL100x12,5	0,45	0,89
46	I63C50T1	63	0,50	1	FL100x12,5	0,46	0,74
55	I63C50T0	63	0,50	0,5	FL100x12,5	0,48	0,45
29	I125C50	125	0,50	4	-	0,30	1,89
38	I125C50T2	125	0,50	2	FL63x8	0,32	1,78
47	I125C50T1	125	0,50	1	FL80x10	0,36	1,46
56	I125C50T0	125	0,50	0,5	FL100x12,5	0,43	0,89
30	I250C50	250	0,50	4	-	0,18	3,78
114	I250C50T2c	250	0,50	2	FL40x5	0,21	3,55
48	I250C50T1	250	0,50	1	FL50x6	0,29	2,92
57	I250C50T0	250	0,50	0,5	FL63x8	0,36	1,78

The values of $\chi_{w,mod}$ for the 24 girders with openings in Table 7.2.3 are plotted against the h/t ratios, see Fig. 7.2.19. For each D/h ratio there is one curve for each aspect ratio. The aspect ratios are denoted T4, T2, T1 and T0, the numbers relating to the actual ratio. T0 refers to aspect ratio 0,5.

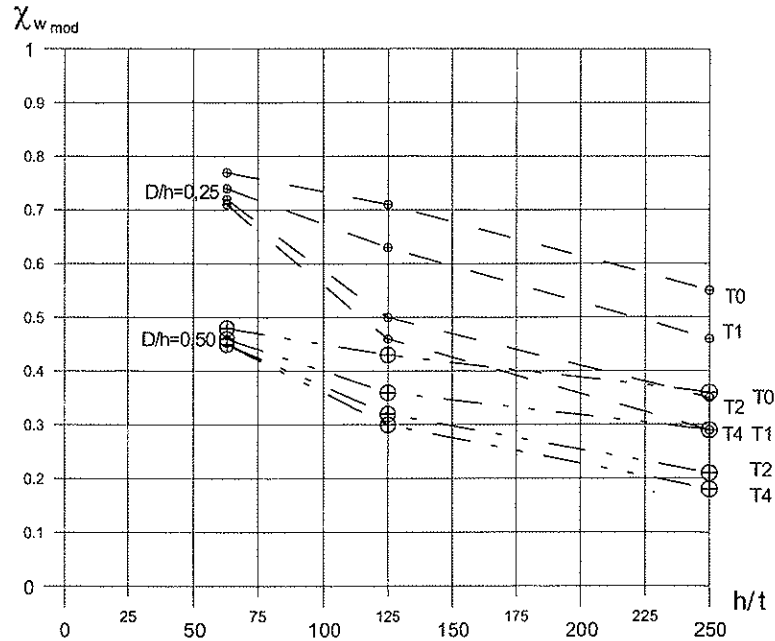


Fig 7.2.19 $\chi_{w,mod}$ for $f_y = 420 \text{ N/mm}^2$ and various aspect ratios.

Fig. 7.2.20 depicts the reduction factor χ_w for girders with transverse stiffeners in the same way as in Fig. 7.2.15 for the girders without stiffeners. Values of χ_w and $\chi_{w,mod}$ are plotted against the relative slenderness. The following legend is used in the figure; the cross represents simulations with $D/h = 0$ and the small and large circles refer to simulations with $D/h = 0,25$ and $D/h = 0,50$, respectively. The relative slenderness is based on the values $k_\tau = 5,59$ for aspect ratio 4, $k_\tau = 6,59$ for aspect ratio 2, $k_\tau = 9,34$ for aspect ratio 1 and $k_\tau = 25,36$ for aspect ratio 0,5. Fig. 7.2.20 also shows the EC3 proposal for webs without openings, together with scaled curves for 75 % and 50 % of the proposal.

The results from the simulations of girders with $D/h = 0,25$ lie above the 75 % curve except for the lowest relative slenderness. Similarly, the results from the girders with $D/h = 0,50$ are above the 50 % curve except for the lowest relative slenderness.

For the girders without openings there are more variation in the results. Not unexpected, some of the slender webs with transverse stiffeners show shear capacities far above the EC proposal. The main explanation is tension field action, and there is no intention in EC3 to fully include this effect. Another reason may be non-conservative imperfection modes. The girders without openings were analyzed with a large buckle in the location where the opening was to be placed in the other girders. In the adjacent plate

panels the buckles where smaller. All possible combinations of eigenmodes giving buckles in opposite directions in adjacent plate panels are not investigated.

The imperfection modes used for webs with openings are assumed to be conservative. The largest imperfection amplitude occurs in the part of the plate containing the opening. Adjacent parts will probably not buckle, as the shear capacity here is higher.

An overview of the stiffener configurations and their influence on buckle shapes is shown in Fig. 7.2.21.

$\chi_{w,mod}$

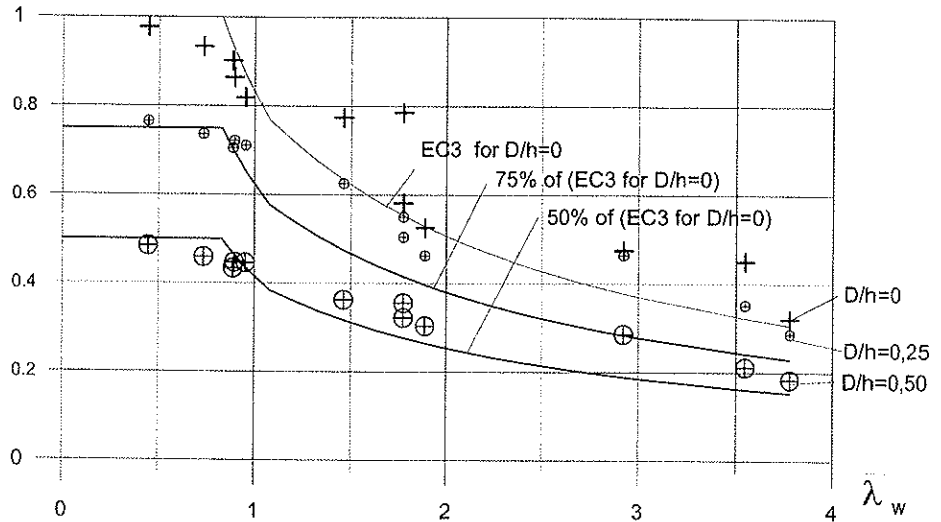


Fig. 7.2.20 $\chi_{w,mod}$ for relative slenderness when $f_y = 420 \text{ N/mm}^2$

The diagram in Fig. 7.2.19 gives, to some extent, a picture of the influence of transverse stiffeners on the shear capacity. However, the scaled curves in Figs. 7.2.15 and 7.2.20 represent a much more general description of the effect. Referring to Section 6.3 and Eq. (6.3.2), the scaled buckling curves show the function

$$c_1 = \chi_{w,mod,basic} = \left(1 - \frac{D}{h}\right) \chi_w \quad (7.2.5)$$

χ_w is the function given in Table 3.5.1. This leads to the conclusion, that the shear capacities of girders with openings may be derived from the global buckling of girders without openings. Eq. (7.2.3) shows that the main reduction in shear capacity is chosen to be represented by the factor $(1-D/h)$. This factor constitutes an upper limit for the shear capacity of girders with openings when $\chi_w = 1,0$. Simply speaking it gives the relative remaining shear area of a web with opening.

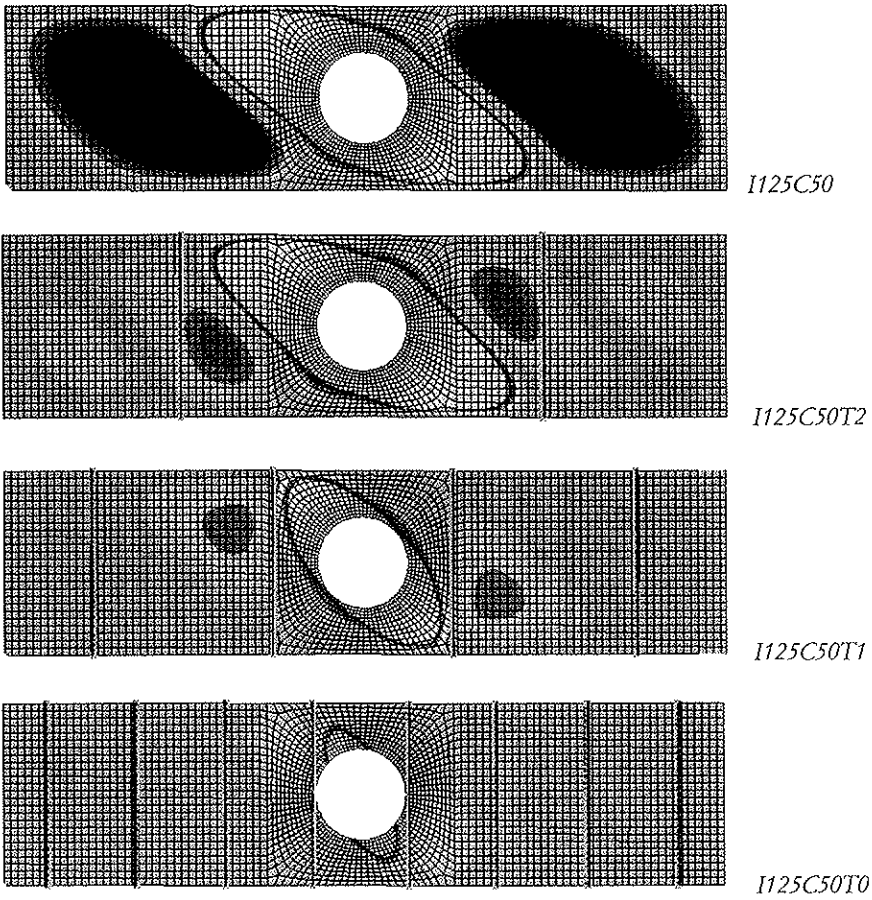


Fig. 7.2.21 Influence of transverse stiffeners on buckles at maximum shear of four girders with various aspect ratios.

Influence of transverse stiffeners on the additional flange forces

The influence of the transverse stiffeners on flange forces is shown in Table 7.2.4 in terms of the ratio ξ_w . Values of ξ_w are calculated for the 24 girders of Table 7.2.3 that have openings. The similar 12 girders in Table 7.2.3 without openings are used as reference girders. The calculations are performed as described in Section 7.2.5.

Table 7.2.4 ξ_w for various values of h/t , D/h and a/h

1	2	3	4	5	6	7	8	9	10
Run	Girder	h/t	D/h	a/h	$\xi_{A,C25}$	$\xi_{A,C50}$	$\xi_{B,C25}$	$\xi_{B,C50}$	ξ_w
22	I63	63	0	4	0,28	0,38	-	-	-
25	I63C25	63	0,25	4	0,28	-	0,34	-	0,06
28	I63C50	63	0,50	4	-	0,38	-	0,63	0,25
31	I63T2	63	0	2	0,22	0,32	-	-	-
34	I63C25T2	63	0,25	2	0,22	-	0,31	-	0,09
37	I63C50T2	63	0,50	2	-	0,32	-	0,62	0,30
40	I63T1	63	0	1	0,21	0,32	-	-	-
43	I63C25T1	63	0,25	1	0,21	-	0,27	-	0,06
46	I63C50T1	63	0,50	1	-	0,32	-	0,59	0,27
49	I63T0	63	0	0,5	0,18	0,28	-	-	-
52	I63C25T0	63	0,25	0,5	0,18	-	0,20	-	0,02
55	I63C50T0	63	0,50	0,5	-	0,28	-	0,48	0,20
23	I125	125	0	4	0,58	0,70	-	-	-
26	I125C25	125	0,25	4	0,58	-	0,79	-	0,21
29	I125C50	125	0,50	4	-	0,70	-	1,09	0,39
32	I125T2	125	0	2	0,56	0,66	-	-	-
35	I125C25T2	125	0,25	2	0,56	-	0,68	-	0,12
38	I125C50T2	125	0,50	2	-	0,66	-	1,02	0,36
41	I125T1	125	0	1	0,35	0,45	-	-	-
44	I125C25T1	125	0,25	1	0,35	-	0,49	-	0,14
47	I125C50T1	125	0,50	1	-	0,45	-	0,94	0,49
50	I125T0	125	0	0,5	0,26	0,35	-	-	-
53	I125C25T0	125	0,25	0,5	0,26	-	0,25	-	-0,01
56	I125C50T0	125	0,50	0,5	-	0,35	-	0,63	0,28
24	I250	250	0	4	1,13	1,23	-	-	-
27	I250C25	250	0,25	4	1,13	-	1,37	-	0,24
30	I250C50	250	0,50	4	-	1,23	-	1,85	0,62
112	I250T2c	250	0	2	1,12	1,21	-	-	-
113	I250C25T2c	250	0,25	2	1,12	-	1,25	-	0,13
114	I250C50T2c	250	0,50	2	-	1,21	-	1,56	0,35
42	I250T1	250	0	1	0,53	0,61	-	-	-
45	I250C25T1	250	0,25	1	0,53	-	0,78	-	0,25
48	I250C50T1	250	0,50	1	-	0,61	-	1,21	0,60
51	I250T0	250	0	0,5	0,42	0,49	-	-	-
54	I250C25T0	250	0,25	0,5	0,42	-	0,46	-	0,04
57	I250C50T0	250	0,50	0,5	-	0,49	-	0,77	0,28

Fig. 7.2.22 presents curves for ξ_w as functions of the h/t ratio for the girders of Table 7.2.4, i.e. for $f_y = 420 \text{ N/mm}^2$. For each D/h ratio, there is one curve for each aspect ratio. The aspect ratios are named T4, T2, T1 and T0, where the numbers are related to the aspect ratio. T0 refers to aspect ratio 0,5.

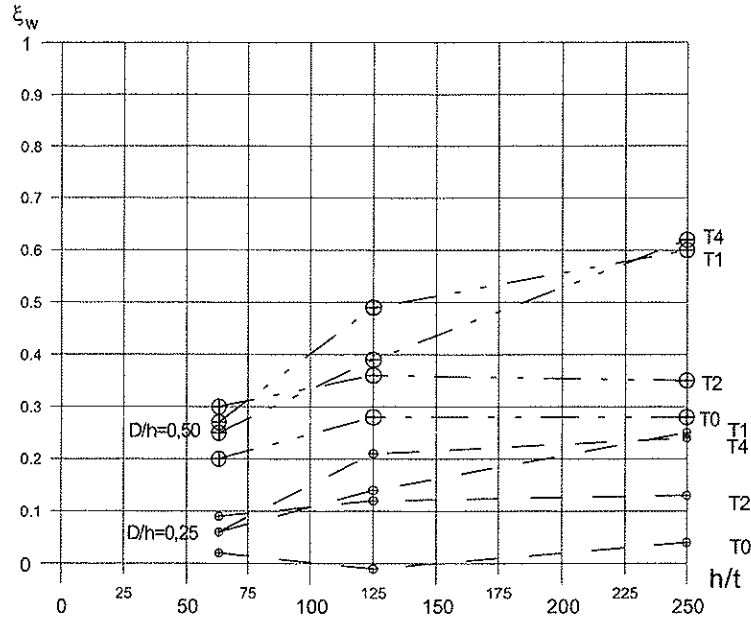


Fig 7.2.22 ξ_w for $f_y = 420 \text{ N/mm}^2$ and various aspect ratios.

Fig. 7.2.22 gives a congested picture of the influence of transverse stiffeners on ξ_w , and it might be of interest to present the values of ξ_w in a similar way as for $\chi_{w,mod}$ in Fig. 7.2.20. This is done in Fig. 7.2.23, where ξ_w is plotted against the relative web slenderness.

The results in Fig. 7.2.23 are rather scattered. It is difficult to see a pattern that is similar both for the small and large openings. The flange forces are certainly not a function of the relative slenderness. Even though, for illustrative reasons, the following curves are included in Fig. 7.2.23

$$\xi_w = 0,9 \frac{D}{h} (\lambda_w)^{-0,33} \quad (7.2.6)$$

for $D/h = 0,25$ and $D/h = 0,50$. Eq. (7.2.6) is clearly conservative for $D/h = 0,25$, which shows that the influence of the opening decreases more than the D/h ratio.

It can be concluded that it is a comprehensive task to derive diagrams or equations for ξ_w . Other measures should be taken to include the effect of flange forces in the proposed design procedure. This is done in Section 7.2.7.

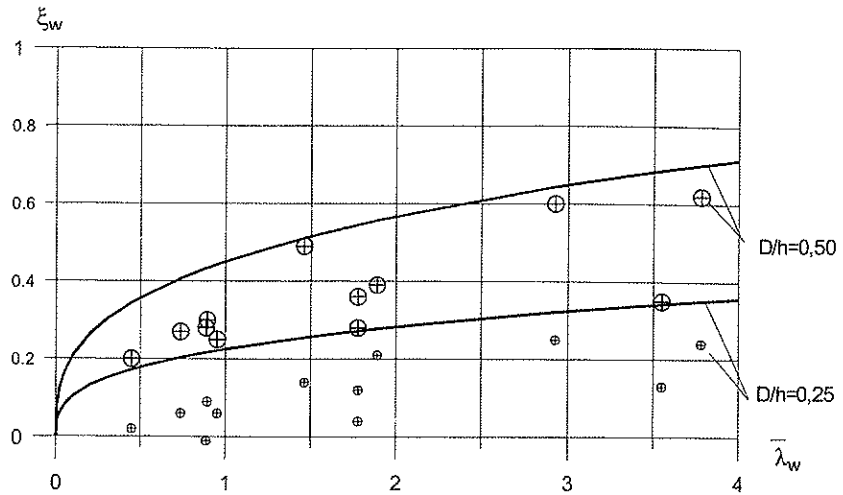


Fig. 7.2.23 ξ_w as a function of relative slenderness ($f_y = 420 \text{ N/mm}^2$)

Influence of transverse stiffeners on girder stiffness

Table 7.2.5 shows the tip vertical displacement δ for maximum shear V_{max} , and the secant stiffness

$$k_{model} = \frac{V_{max}}{\delta} \quad (7.2.7)$$

for the girders. k_{model} is an expression for the average slope of the response curve from zero to max shear. Most of the girders have almost linear response up to maximum shear, as shown in Fig. 7.2.10. Three girders did not show the typical response curve, and these are noted with an asterisk in the table.

The actual values of k_{model} are of minor importance, as they vary with girder sizes. However, by grouping girders with same web thickness and flange sizes, some useful results can be achieved. In Table 7.2.5 three girder groups are formed. The girder without opening and transverse stiffeners is the reference girder in each group. In the table c_{rel} is the ratio of the actual stiffness to the stiffness of the reference girder. Hence, it is possible to see the relative influence of opening size, transverse stiffeners and combinations of these.

Not unexpected, transverse stiffeners increase girder stiffness. For the girders with thinnest webs the increase is up to 300%. The influence of openings with $D/h = 0,25$ is small and in some cases increases the stiffness. For $D/h = 0,50$ the stiffness may be reduced to 67% of the stiffness without the opening. Transverse stiffeners can in many cases compensate for reduced stiffness due to openings.

Table 7.2.5 Tip displacement and girder stiffness

1	2	3	4	5	6	7	8	9
Run	Girder	h/t	D/h	a/h	V_{max} [kN]	δ [mm]	k_{model} [kN/mm]	C_{rel}
22	I63	63	0	4	3176	18	176	1,00
25	I63C25	63	0,25	4	2758	16	172	0,98
28	I63C50	63	0,50	4	1730	12	144	0,82
31	I63T2	63	0	2	3353	17	197	1,12
34	I63C25T2	63	0,25	2	2801	16	175	0,99
37	I63C50T2	63	0,50	2	1736	12	145	0,82
40	I63T1	63	0	1	3631	20	182	1,03
43	I63C25T1	63	0,25	1	2856	18	159	0,90
46	I63C50T1	63	0,50	1	1781	13	137	0,78
49	I63T0	63	0	0,5	3791	*	*	*
52	I63C25T0	63	0,25	0,5	2900	15	193	1,10
55	I63C50T0	63	0,50	0,5	1879	16	117	0,67
23	I125	125	0	4	1019	17	60	1,00
26	I125C25	125	0,25	4	898	16	56	0,94
29	I125C50	125	0,50	4	589	13	45	0,76
32	I125T2	125	0	2	1128	16	71	1,18
35	I125C25T2	125	0,25	2	979	14	70	1,17
38	I125C50T2	125	0,50	2	625	12	52	0,87
41	I125T1	125	0	1	1502	18	83	1,39
44	I125C25T1	125	0,25	1	1214	14	87	1,45
47	I125C50T1	125	0,50	1	704	12	59	0,98
50	I125T0	125	0	0,5	1749	18	97	1,62
53	I125C25T0	125	0,25	0,5	1369	14	98	1,63
56	I125C50T0	125	0,50	0,5	842	12	70	1,17
24	I250	250	0	4	310	22	14	1,00
27	I250C25	250	0,25	4	278	16	17	1,23
30	I250C50	250	0,50	4	178	*	*	*
112	I250T2c	250	0	2	437	22	20	1,41
113	I250C25T2c	250	0,25	2	341	18	19	1,34
114	I250C50T2c	250	0,50	2	205	15	14	0,97
42	I250T1	250	0	1	461	*	*	*
45	I250C25T1	250	0,25	1	450	14	32	2,28
48	I250C50T1	250	0,50	1	277	12	23	1,64
51	I250T0	250	0	0,5	762	18	42	3,00
54	I250C25T0	250	0,25	0,5	534	12	45	3,16
57	I250C50T0	250	0,50	0,5	345	9	38	2,72

Influence of transverse stiffeners on shear capacity in ALS

Table 7.2.6 shows the influence of transverse stiffeners on the shear capacity in ALS. The girders are the same as in Table 7.2.4. The values for $\chi_{w,mod,ALS}$ are based on 100 mm tip displacement. By calculating the ratio between the values of $\chi_{w,mod}$ in ULS and ALS, some useful conclusions can be made. Column 7 shows that all ratios are below one. Hence, the shear capacity of ULS can never be sustained in ALS, neither for webs without openings nor for webs with circular openings. Basically, all response curves have shapes as in Fig. 7.2.10. For I250C50T0 only 34 % of the ULS capacity remained for 100 mm tip displacement.

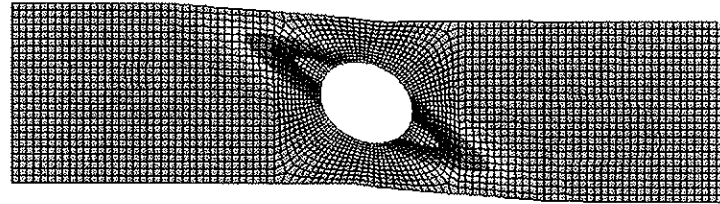
It should be noted that in these girders the flanges have negligible bending stiffness and give no significant contribution to the shear capacity. The test girders S1 and S9 in Chapter 4 showed a less tendency to reduced shear capacity in ALS. See Figs. 4.3.1 and 4.3.2. Presumably this is because the contributions from flanges and strain hardening counteract the effect of large buckles.

In the table c_{rel} shows the influence of the opening relative to the corresponding web and stiffener configuration without opening, by the ratio of the actual shear capacity to the shear capacity of the reference case. Girder I125C50 has $c_{rel} = 0,19/0,36 = 0,53$. It can be seen that the shear capacities for openings $D/h = 0,25$ are more than 71 % of those of the corresponding configuration without opening. For openings $D/h = 0,50$ the capacities are more than 45 % of the corresponding girders without openings. However, the shear capacities are probably further reduced for tip displacements larger than 100 mm.

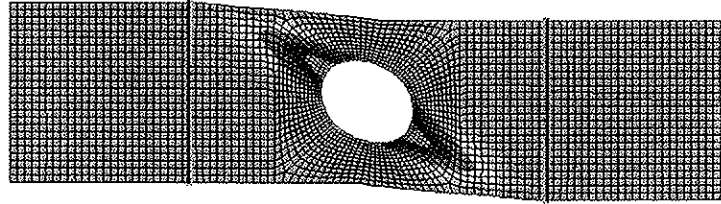
Fig. 7.2.24 shows transverse displacements in ALS of girders I125C50, I125C25T2, I125C50T1 and I125C50T0. Note that the color legend is different from the legend used in Fig. 7.2.17: The colors in Fig. 7.2.24 show displacements in steps of 25 mm, i.e. green shows small displacements, red displacements up to 125 mm and light grey displacements above 125 mm.

Table 7.2.6 $\chi_{w,mod}$ in ALS for various h/t , D/h , a/h ratios and comparison with ULS

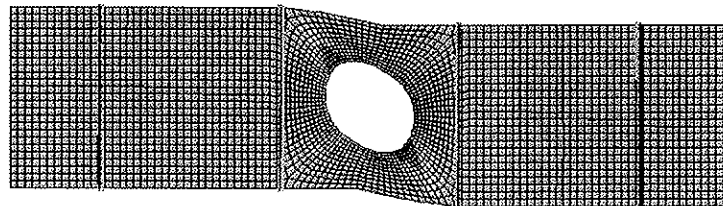
1	2	3	4	5	6	7	8
Run	Girder	h/t	D/h	a/h	ALS $\chi_{w,mod,ALS}$	$\chi_{w,mod,ALS}/\chi_{w,mod}$	C_{rel}
22	I63	63	0	4	0,53	0,64	.
31	I63T2	63	0	2	0,56	0,65	.
40	I63T1	63	0	1	0,69	0,74	.
49	I63T0	63	0	0,5	0,73	0,74	.
23	I125	125	0	4	0,36	0,68	.
32	I125T2	125	0	2	0,34	0,59	.
41	I125T1	125	0	1
50	I125T0	125	0	0,5
24	I250	250	0	4	0,25	0,78	.
112	I250T2c	250	0	2
42	I250T1	250	0	1
51	I250T0	250	0	0,5
25	I63C25	63	0,25	4	0,41	0,58	0,78
34	I63C25T2	63	0,25	2	0,42	0,58	0,75
43	I63C25T1	63	0,25	1	0,49	0,66	0,71
52	I63C25T0	63	0,25	0,5	0,57	0,74	0,78
26	I125C25	125	0,25	4	0,26	0,57	0,72
35	I125C25T2	125	0,25	2	0,30	0,59	0,87
44	I125C25T1	125	0,25	1	0,23	0,37	..
53	I125C25T0	125	0,25	0,5	0,34	0,48	..
27	I250C25	250	0,25	4	0,19	0,66	0,76
113	I250C25T2c	250	0,25	2
45	I250C25T1	250	0,25	1
54	I250C25T0	250	0,25	0,5
28	I63C50	63	0,50	4	0,32	0,71	0,61
37	I63C50T2	63	0,50	2	0,29	0,64	0,52
46	I63C50T1	63	0,50	1	0,31	0,67	0,45
55	I63C50T0	63	0,50	0,5	0,39	0,81	0,53
29	I125C50	125	0,50	4	0,19	0,63	0,53
38	I125C50T2	125	0,50	2	0,19	0,59	0,56
47	I125C50T1	125	0,50	1	0,23	0,64	..
56	I125C50T0	125	0,50	0,5	0,22	0,51	..
30	I250C50	250	0,50	4	0,13	0,73	0,54
114	I250C50T2c	250	0,50	2	0,15	0,71	..
48	I250C50T1	250	0,50	1	0,10	0,34	..
57	I250C50T0	250	0,50	0,5	0,16	0,44	..



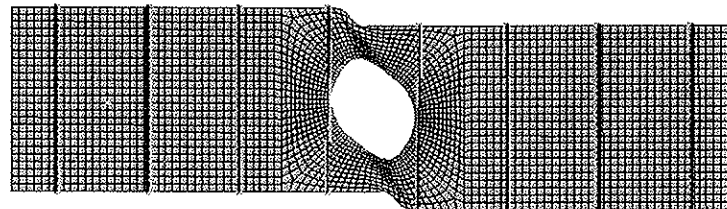
I125C50



I125C50T2



I125C50T1



I125C50T0

Fig. 7.2.24 Influence of transverse stiffeners on displacements in ALS for girders I125C50, I125C25T2, I125C50T1 and I125C50T0

7.2.7 Tension field action

In EC3 some tension field action is included in the curve for χ_w , but not to the full extent as proposed by the theories in Section 3.9. Neither will a design method for web openings that uses the χ_w as basis, include the tension field action of, for instance, the Cardiff method. Fig. 7.2.20 shows that tension field action occurs also for webs with openings. However, the relative contribution to shear capacity from a tension field diminishes with increasing opening size. While some simulations of girders *without* openings give shear capacities far above the EC3 buckling curve, the shear capacities of the similar girders with openings $D/h = 0,50$ are about the EC curve scaled with a factor 0,50. This corresponds to the theory of Narayanan et al, referred in Section 3.9.3, where the diameter of the opening was directly subtracted from the width of the tension field.

For reasons of simplification, and consistency when the opening size goes to zero in the limit, the proposed design rules should not include more tension field action than given in EC3. The theories of Narayanan et al are therefore not further investigated here.

7.2.8 Results below the EC3 curve

For some girders with stocky and medium slender webs without openings the results from the simulations lie below the EC3 curve, see Fig. 7.2.20. Possible explanations for this may be

- Conservative FE-modelling. In the simulations the contribution to shear capacity from flanges has deliberately been excluded. In EC3 the contribution from the flanges may be added to the shear capacity of the web proper by an additional factor χ_f . However, to the extent that experimental data forms the basis for the EC3 curve, the flange contribution cannot be completely eliminated.
- The non-linear analyses themselves. In non-linear analyses with imperfections the shear capacity can never reach the result without imperfections.

Fig. 7.2.20 depicts a similar pattern for the girders with openings, which lie below the scaled curves. However, for these girders the reasons may also be that

- Buckling at openings reduces the shear capacity more than the reduction given by χ_w
- Yield shear stress cannot develop over the full shear area in T-sections

For the reason of consistency when the opening size goes to zero in the limit, it is preferred to let the scaled curves have the same shape as the EC curve. Proposals to cover the low results are discussed in Chapter 11.

7.2.9 Shear and primary moment interaction

In girders with large flanges

The combined effects of shear and primary moment are studied by means of six simulations of one typical girder. The girder is based on the same geometry and initial imperfections as used for Girder I125C50 with shear only. However, the flanges are changed from a general section with very low bending stiffness to a rectangular section FL 500x32 with corresponding bending stiffness. This is done in order to simulate the non-linear material properties of the flanges, which may be important when large primary moments are acting. ABAQUS does not accept non-linear material properties for the general section. The areas of the flanges are not changed. In Model P125C50M0a the load is shear only, applied as previously by tip displacement. The shear capacity is 3 % higher than the shear capacity of Girder I125C50. Hence the influence of the flange bending stiffness is relatively small, and the results from the previous girders are conservative.

For the four models P125C50M35 to P125C50M69 the loads are applied in two steps. In the first step, a chosen value of primary moment is applied as a force couple to the flanges near the right end of the girder, giving compression in the upper flange and tension in the lower flange. The primary moments are constant along the girder and there is no shear force. In the second step, the applied primary moment is kept constant, and shear force is applied by tip displacement. Due to the moment caused by the shear force the resulting moment varies along the girder. However, in a vertical section through the center of the opening the resulting moment is independent of the shear force and is equal to the applied primary moment.

For Model P125C50M70 a primary moment somewhat higher than the expected moment capacity for pure moment was tried. The analysis stopped for a value slightly less, and this value was taken as the maximum moment capacity of the girder. The moment found by this method was about 2 % higher than the calculated $M_{buckl,mod}$, which is defined below. Hence, the simulations give accurate results for primary moments. There was no second step, as this model simulated pure moment.

For most models the response curves showed only a very small descending path after the maximum shear was reached, before the analyses ended due to numerical problems. Apparently, this type of non-linear analyses is demanding. However, the author is convinced that the maximum shear and primary moment values are found with sufficient accuracy.

The results are shown in Table 7.2.7 and plotted in the interaction diagram of Fig. 7.2.25.

Table 7.2.7 Shear and primary moment interaction

1	2	3	4	5
Run	Girder/Model	V_{max} [kN]	M [kNm]	Remarks
160	P125C50M0a	609	0	
162	P125C50M35	580	3575	2 steps
163	P125C50M55	536	5720	2 steps
164	P125C50M65	445	6434	2 steps
165	P125C50M69	133	7006	2 steps
161	P125C50M70	-	7149	

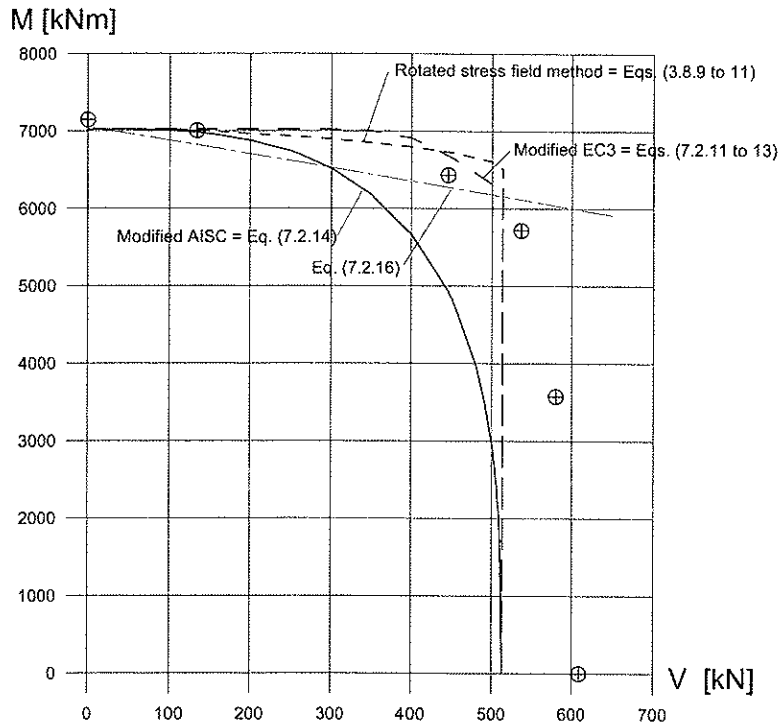


Fig. 7.2.25 Interaction diagram for the girder in Table 7.2.7, i.e. with large flanges

In order to compare the simulated results with those from available theories and design proposals, a straight line and three curves are included in Fig. 7.2.25. The straight line, marked with Eq. (7.2.16), is explained in the next section. The curves are marked with “Rotated stress field method”, “Modified EC3” and “Modified AISC”, and are explained below.

The curve marked “Rotated stress field method” is given by Eqs. (3.8.9 to 11), with additional flange forces based on ξ_w from Table 7.2.4.

The curve marked “Modified EC3” is based on the proposal in EC3 for girders without openings, but the author has made some modifications in order to include openings and additional flange forces as follows:

EC 3 gives the interaction equations for girders without openings as

$$\frac{V}{V_c} \leq 1 \quad (7.2.8)$$

$$\frac{M}{M_{el}} + \left(1 - \frac{M_f}{M_{pl}}\right) \left(2 \frac{V}{V_c} - 1\right)^2 \leq 1 \quad \text{when } V \geq 0,5V_c \quad (7.2.9)$$

$$\frac{M}{f_y W_{eff}} \leq 1 \quad (7.2.10)$$

Here V_c is the shear capacity in pure shear. M_{pl} is the plastic moment capacity, and M_{el} is the elastic moment capacity based on gross section properties, in both cases with buckling disregarded. $f_y W_{eff} = M_{buckl}$ is the moment capacity when only the effective areas are included, i.e. with buckling considered. M_f is the moment capacity when only the effective flanges are considered. For the purpose of this investigation the partial factors and the subscript "Rd" are omitted from the equations as given in EC3.

Assuming that Eqs. (7.2.8) to (7.2.10) may be modified to include webs with openings, the new equations are

$$\frac{V}{V_{c,mod}} \leq 1 \quad (7.2.11)$$

$$\frac{M}{M_{el,mod}} + \left(1 - \frac{M_{f,mod}}{M_{pl}}\right) \left(2 \frac{V}{V_{c,mod}} - 1\right)^2 \leq 1 \quad (7.2.12)$$

$$\frac{M}{M_{buckl,mod}} \leq 1 \quad (7.2.13)$$

$V_{c,mod}$ is the shear capacity according to Eq. (6.2.1). M_{pl} is the plastic moment capacity when opening and buckling are disregarded. $M_{el,mod}$ is the elastic moment capacity of the modified gross section, obtained when the section of the opening is subtracted and buckling disregarded. $M_{buckl,mod}$ is the moment capacity when only the modified effective areas are included, i.e. when buckling is considered and the opening subtracted. $M_{f,mod}$ is the moment capacity when only the effective flanges are considered, and the areas required for the additional flange forces subtracted. The additional flange forces may be based on Eq. (6.2.2) with ξ_w from Eq. (7.2.6).

The capacities for the girder in Table 7.2.7 are calculated, and the curve marked "Modified EC3" in Fig. 7.2.25 is based on the following values:

- $V_{c,mod} = 513$ kN
- $M_{pl} = 7560$ kNm
- $M_{el,mod} = 7210$ kNm
- $M_{buckl,mod} = 7023$ kNm
- $M_{f,mod} = 6720 - 0,39V$, where $\xi_w = 0,39$ from Table 7.2.4.

The curve in Fig. 7.2.25 marked "Modified AISC" is derived from the AISC (1990) design curve for beams, i.e. Eq. (3.3.1), and modified by the author to the form

$$\left(\frac{M}{M_{buckl,mod}}\right)^3 + \left(\frac{V}{V_{c,mod}}\right)^3 = 1 \quad (7.2.14)$$

where $V_{c,mod}$ is the shear capacity according to Eq. (6.2.1) and $M_{buckl,mod}$ is the moment capacity when only the effective areas are included, i.e. when buckling is considered and the opening subtracted.

The capacities for the girder in Table 7.2.7 are calculated, and the curve for Eq. (7.2.14) in Fig. 7.2.25 is based on the following values

- $V_{c,mod} = 513$ kN
- $M_{buckl,mod} = 7023$ kNm

In the interaction diagram in Fig. 7.2.25 the design proposals may be deemed conservative if the plotted results are outside the curves. It can be seen that both the rotated stress field method and Eqs. (7.2.11) to (7.2.13) are non-conservative in the upper right corner of the diagrams, while Eq. (7.2.14) is conservative. The latter curve is also simpler to use in design, as it does not require knowledge about the additional flange forces caused by the opening.

Interaction in girders with small flanges

In the simulations described in the previous section, the area of the flange was twice the area of the web. The additional flange force, caused by the maximum shear force at the opening, is less than 6 % of the axial force capacity of the flange. It should be expected that the influence of the additional flange force is difficult to observe in the simulations. For small flanges the additional flange forces may be more important. Hence, a girder with small flanges is studied by means of six simulations.

The girder is similar to the girder of the previous section, except that the flanges are taken as rectangular sections FL 200x10. Hence, the flange area is only 25 % of the gross web area, and equal to the net web area in the opening. The flange bending stiffness is also reduced. The additional flange force at maximum shear is about 45 % of the axial force capacity of the flange. In the section that forms a vertical tangent to the opening, the plastic neutral axis is located in the web. Such girders are not often seen in practice, but may occur in offshore deck structures, where the flanges consist of thin deck plates.

The results are presented in Table 7.2.8 and in the interaction diagram of Fig. 7.2.26.

Table 7.2.8 Shear and primary moment interaction

1	2	3	4	5
Run	Girder/Model	V_{max} [kN]	M [kNm]	Remarks
170	Q125C50M0a	540	0	
172	Q125C50M6	398	638	2 steps
173	Q125C50M10	185	1020	2 steps
174	Q125C50M11	113	1148	2 steps
175	Q125C50M12	50	1250	2 steps
171	Q125C50M13d	-	1276	

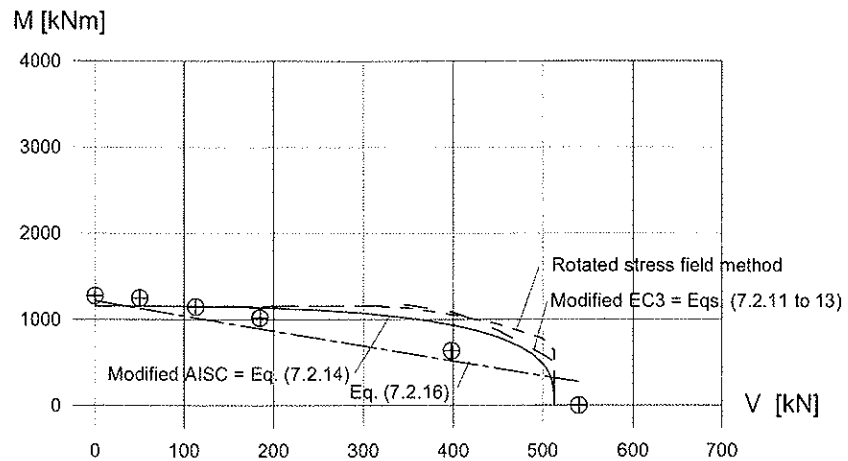


Fig. 7.2.26 Interaction diagram for the girder in Table 7.2.8, i.e. with small flanges

Curves similar to those presented in the previous section are included in Fig. 7.2.26. The curve for Eqs. (7.2.11 to 13) is based on

- $V_{c,mod} = 513$ kN
- $M_{pl} = 1680$ kNm
- $M_{ct,mod} = 7330$ kNm
- $M_{buckl,mod} = 1156$ kNm
- $M_{f,mod} = 840 - 0,39V$, where $\xi_w = 0,39$ from Table 7.2.4.

The curve for Eq. (7.2.14) is determined for

- $V_{c,mod} = 513$ kN
- $M_{buckl,mod} = 1156$ kNm

The scale of the diagram of Fig. 7.2.27 is the same as in Fig. 7.2.26. This is done to visualize the large reduction in maximum moment capacity. The maximum shear capacity is the same in both diagrams.

The interaction curve based on the rotated stress field method and the curve based on Eqs. (7.2.11) to (7.2.13) do not fit well with the plotted results. For three simulations even the curve based on Eq. (7.2.14) appears to be non-conservative. However, a closer look at the simulations reveals that the low shear capacities are not caused by additional flange forces, but by web buckling in sections away from the opening. The explanation is as follows:

In a girder with a web opening the primary moment will have its maximum value at the vertical centerline of the opening only if the shear force is zero, i.e. when the primary moment is constant along the girder. When there is a shear force in the web, the primary moment must increase at locations away from the opening, as it is presupposed that significant loads cannot be applied to the girder above the opening. If the primary moment

in the centerline is M and the shear is V , the primary moment in a section at a distance a_c from the vertical centerline of the opening reads

$$M_a = M + Va_c \quad (7.2.15)$$

In this section, without opening, the design criteria according to Eq. (7.2.10) is

$$\frac{M_a}{M_{buckl}} = \frac{M + Va_c}{M_{buckl}} \leq 1 \quad (7.2.16)$$

where M_{buckl} is the moment capacity of the effective cross sectional areas.

For the girder with *large* flanges, Eq. (7.2.16) is plotted in Fig. 7.2.25 for the values $M_{buckl} = 7056$ kNm and $a_c = 1,75h$. The ratio $M_{buckl}/M_{buckl,mod} = 1,005$. As seen, Eq. (7.2.16) is governing only for a limited range of large primary moments.

For the girder with *small* flanges, Eq. (7.2.16) is plotted in Fig. 7.2.26 for the values $M_{buckl} = 1218$ kNm and $a_c = 1,75h$. The ratio $M_{buckl}/M_{buckl,mod} = 1,054$. Here, Eq. (7.2.16) governs for nearly all primary moments, except for very large or small moments.

Fig. 7.2.27 shows the buckled shape for model Q125C50M11 at maximum shear interacting with a moment equal to 99 % of $M_{buckl,mod}$. The maximum transverse displacement is 16 mm, i.e. $h/63$.

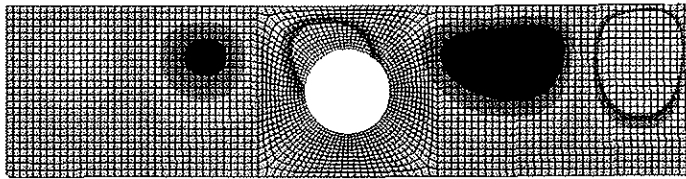


Fig. 7.2.27 Buckles for Model Q125C50M11 at maximum shear and $M = 0,99M_{buckl,mod}$

The phenomenon described by above seems to be overlooked by most authors. It may be argued that Eq. (7.2.16) is somewhat trivial, because design checks of a real girder must include the sections away from the openings, so the smaller shear capacity will be found anyway. Furthermore, the results are strongly dependent on the distance a_c , which again is closely related to the girders studied in the present simulations.

However, in the author's opinion, Eq. (7.2.16) contributes to a major simplification of the design of openings in girders with large primary moments, as it illustrates the governing case. Also the girders considered in the present simulations are quite similar to real girders, where transverse stiffeners are used only at positions where a major change in the shear force takes place. For many girders the ratios $M_{buckl}/M_{buckl,mod}$ are near 1,0 even for large openings, and Eq. (7.2.16) may be governing also for positions of the maximum primary moment closer to the opening. When Eq. (7.2.16) is governing, the effect of the additional flange forces is not important, and sleeves will not increase the shear capacity.

Interaction in girders with small flanges and transverse stiffeners

Eq. (7.2.16) may be useful, but the possibility of cases where the additional flange forces are governing, is perhaps not completely eliminated. To investigate such cases, six simulations are made for a girder with transverse web stiffeners.

The girder is similar to the previous Q-girder with small flanges, but it has transverse stiffeners FL 80x10 on one side of the web at spacing h . Hence, the aspect ratio $a/h = 1$ and in this respect the girder corresponds to Girder I125C50T1 in Table 7.2.3. The initial imperfections from I125C50T1 are used. At maximum shear, the additional flange force is about 41 % of the axial force capacity of the flange.

To ensure that Eq. (7.2.16) is not governing, the primary moment is applied as a force couple to the flanges at the position of the first transverse stiffener to the right side of the opening, indicated by arrows in Fig. 7.2.29. This corresponds to a situation where the maximum resulting primary moment from the applied moment and from the shear is acting at this position. Otherwise, the analyses are performed as described in the previous section.

The results are presented in Table 7.2.9 and in the interaction diagram of Fig. 7.2.29.

Table 7.2.9 Shear and primary moment interaction

1	2	3	4	5
Run	Girder/Model	V_{max} [kN]	M [kNm]	Remarks
180	Q125C50T1M0a	678	0	
182	Q125C50T1M6	642	638	2 steps
183	Q125C50T1M10	496	1020	2 steps
184	Q125C50T1M11	389	1148	2 steps
185	Q125C50T1M12	203	1250	2 steps
181	Q125C50T1M13d	-	1271	

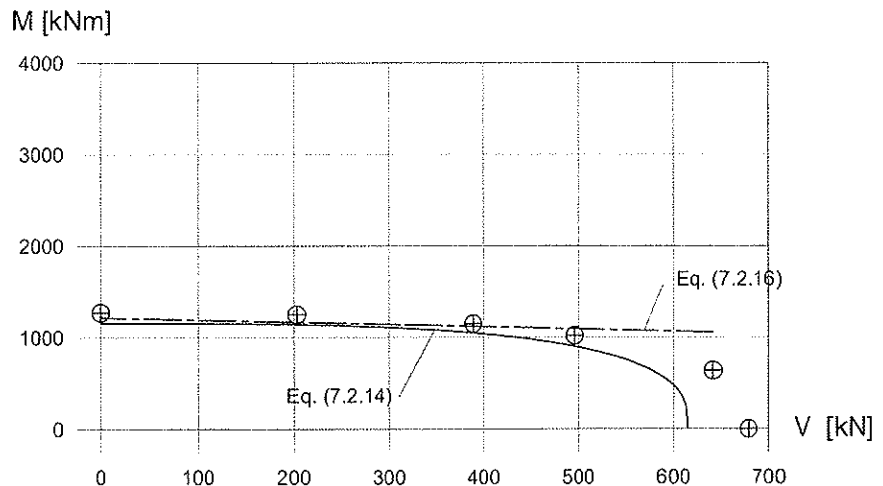


Fig. 7.2.28 Interaction diagram for the girder in Table 7.2.9, i.e. with small flanges and transverse stiffeners

The interaction curve based on Eq. (7.2.14) is included in Fig. 7.2.28 together with the straight line representing Eq. (7.2.16). The curve is determined from

- $V_{c,mod} = 615$ kN
- $M_{buckl,mod} = 1156$ kNm

All results in Fig. 7.2.28 lie above the interaction curve.

Fig. 7.2.29 shows the buckled shape in Q125C50T1M11 at maximum shear combined with 99 % of $M_{buckl,mod}$. The maximum transverse displacement is 20 mm, i.e. $D/25$.

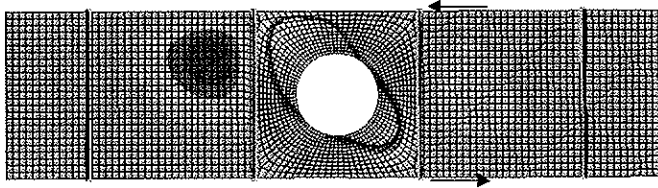


Fig. 7.2.29 Buckles in Model Q125C50T1M11 at maximum shear and $M = 0,99M_{buckl,mod}$

Conclusion

The results of the three girders with moment-shear interaction confirm that

- The lowest value from Eqs. (7.2.14) and (7.2.16) is governing for moment-shear interaction
- The effect of the additional flange force is included in Eq. (7.2.14)
- Only the four values $V_{c,mod}$, $M_{buckl,mod}$, M_{buckl} , and a_c are required to perform a design check of moment-shear interaction for girders with circular web openings.

A further simplification may be achieved if M_{buckl} is assumed equal to $M_{buckl,mod}$. Eqs. (7.2.14) and (7.2.16) are also valid for beams, where $M_{buckl,mod}$ is equal to M_m from Eq. (3.3.2) and M_{buckl} is equal to $f_y W_p$.

7.2.7 Openings in lower part of webs

Three simulations are performed to study the effect of having openings in the lower part of webs. The openings of girders I63C50, I125C50 and I250C50T2 are lowered, such that only 20 mm is left of the web between the opening and the lower flange. The results are presented in Table 7.2.10.

The new girders M63C50, M125C50 and M250C50T2 have circular openings without stiffening. In order to be consistent, the simulations are therefore included in the present section, i.e. Section 7.2. However, the girders do not comprise the basic set of secondary factors, as defined in Section 6.3. In this case the vertical position of openings is altered. Like all the remaining simulations in the present thesis, these girders have an alternative set of secondary factors. The adjustment factors c_2 can be calculated according to Eq. (6.3.3),

and show the reduction in shear capacity for girders with lowered opening relative to girders with the opening at mid-height.

As the c_2 - factors are important parts of the present thesis, the calculation of them is emphasized by the following example:

- Girders I63C50 and M63C50 comprise a girder pair
- I63C50 is the basic girder. Table 7.2.3 shows $\chi_{w,mod,basic} = 0,45$
- M63C50 is the alternative girder. Column 7 in Table 7.2.10 shows $\chi_{w,mod} = 0,38$
- $c_2 = 0,38/0,45 = 0,84$ as presented in Column 8 in Table 7.2.10

Reduction in shear capacity can be observed for all girders of Table 7.2.10, and the largest reduction occurs for $h/t = 125$. The reason appears to be that the buckled web carries a smaller part of the load in compression compared to the basic girder. The width of the buckle has increased compared to the basic girder, as there are no restraining effects in the lower part of the web. The load-carrying capacity of the tension bands is not reduced in the same way, as lost material in the lower part is compensated by increased material in the upper part. This is reflected for the girders with $h/t = 250$. Here, the buckled web carries little load in compression anyway, and the overall reduction in shear capacity is small.

Table 7.2.10 Effect of lowered openings

1	2	3	3	4	6	7	8
Run	Girder	h/t	D/h	a/h	Transverse stiffeners	$\chi_{w,mod}$	c_2
97	M63C50	63	0,50	4	-	0,38	0,84
98	M125C50	125	0,50	4	-	0,23	0,77
99	M250C50T2	250	0,50	2	FL63x8	0,21	0,98

Fig. 7.2.30 shows the buckles of I125C50 and M125C50 at maximum shear. The maximum transverse displacement increases from 38 mm in I125C50 to 61 mm in M125C50.

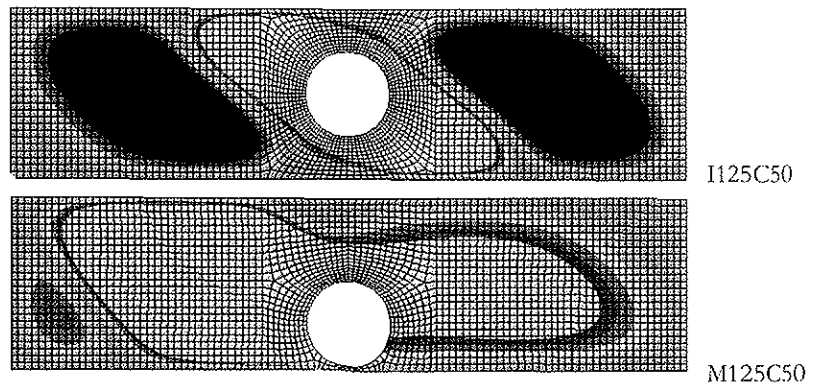


Fig. 7.2.30 Buckles in girders I125C50 and M125C50 at maximum shear

7.3 Single opening with sleeve

7.3.1 Sleeve on one side of web

The effects of local stiffening of openings by means of sleeves have been investigated and the results presented in this and the next section. In the strict sense a sleeve means a ring-shaped stiffener that goes through the opening, such that the stiffener is symmetric with regard to the web plane. Results for such girders are presented in Section 7.3.2. However, to achieve simpler fabrication, it may be preferred to weld ring-shaped stiffeners on one side of web only. Stiffeners are often placed 10 to 20 mm from the edge of opening to allow fillet welds all around.

The girders are based on the preceding girders in Table 7.2.3, with the prefix I replaced by J. For instance, for Girder J125C25T2 all geometry and load application are the same as in Girder I125c25T2, except for the sleeve and the initial imperfections. The size of sleeve is for all girders chosen such that the weight of the sleeve is equal to the weight of the removed plate in the opening. Width/thickness ratios of sleeves are from 6 to 8. The sleeves are “welded” to the edge of the opening in order to simplify models. Initial imperfections are based on eigenmodes from the models with sleeves with maximum amplitudes 7,5 mm and 4,1 mm, as in the girders without sleeves.

Results for 16 simulations of girders with one-side sleeves are presented in Table 7.3.1. Column 7 gives the reduction factor $\chi_{w,mod}$, and Column 8 shows the factor c_2 .

The effect of sleeves is considerable, especially for the larger openings, where up to 55 % increased shear capacity is achieved.

Table 7.3.1 also includes some “fictitious” girders, marked with brackets []. However, these girders have not been run because $\chi_{w,mod}$ would obviously reach the upper limits of 0,75 for openings with $D/h = 0,25$ and 0,50 for openings with $D/h = 0,50$, determined by yield shear stress in the minimum section above and below the openings. Some increased shear capacity due to extra material in the sleeve may be present, but is conservatively disregarded in the present thesis. The girders are included because they have a corresponding girder in Table 7.2.3.

Table 7.3.1 Effect of sleeves on the reduction factor $\chi_{w,mod}$

1	2	3	4	5	6	7	8
Run	Girder	h/t	D/h	a/h	Sleeve	$\chi_{w,mod}$	c_2
61	J63C25	63	0,25	4	FL80x12,5	0,75	1,06
[67]	J63C25T2	63	0,25	2	FL80x12,5	[0,75]	[1,04]
[73]	J63C25T1	63	0,25	1	FL80x12,5	[0,75]	[1,01]
[79]	J63C25T0	63	0,25	0,5	FL80x12,5	[0,77]	[1,00]
62	J125C25	125	0,25	4	FL63x8	0,50	1,09
68	J125C25T2	125	0,25	2	FL63x8	0,56	1,12
74	J125C25T1	125	0,25	1	FL63x8	0,67	1,06
80	J125C25T0	125	0,25	0,5	FL63x8	0,76	1,07
63	J250C25	250	0,25	4	FL40x6,3	0,31	1,07
69	J250C25T2	250	0,25	2	FL40x6,3	0,41	1,17
75	J250C25T1	250	0,25	1	FL40x6,3	0,54	1,17
81	J250C25T0	250	0,25	0,5	FL40x6,3	0,64	1,16
64	J63C50	63	0,50	4	F1125x16	0,56	1,24
[70]	J63C50T2	63	0,50	2	F1125x16	[0,50]	[1,11]
[76]	J63C50T1	63	0,50	1	F1125x16	[0,50]	[1,09]
[82]	J63C50T0	63	0,50	0,5	F1125x16	[0,50]	[1,04]
65	J125C50	125	0,50	4	FL80x12,5	0,44	1,47
71	J125C50T2	125	0,50	2	FL80x12,5	0,48	1,50
[77]	J125C50T1	125	0,50	1	FL80x12,5	[0,50]	[1,39]
[83]	J125C50T0	125	0,50	0,5	FL80x12,5	[0,50]	[1,16]
66	J250C50	250	0,50	4	FL63x8	0,27	1,50
72	J250C50T2	250	0,50	2	FL63x8	0,34	1,55
78	J250C50T1a	250	0,50	1	FL63x8	0,42	1,45
84	J250C50T0	250	0,50	0,5	FL63x8	0,49	1,36

$\chi_{w,mod}$ are plotted against the relative slenderness in Fig. 7.3.1. A curve for the EC3 proposal for girders without openings are also included, but here limited to maximum 0,75 for $D/h = 0,25$ and 0,50 for $D/h = 0,50$. These limits are reached for most of the girders with relative slenderness below 1,6. For most of the other girders with $D/h = 0,25$ the sleeve increases the shear capacity to the value for webs without opening. For the girders with $D/h = 0,50$ more than 75 % of the shear capacity for webs without opening is achieved.

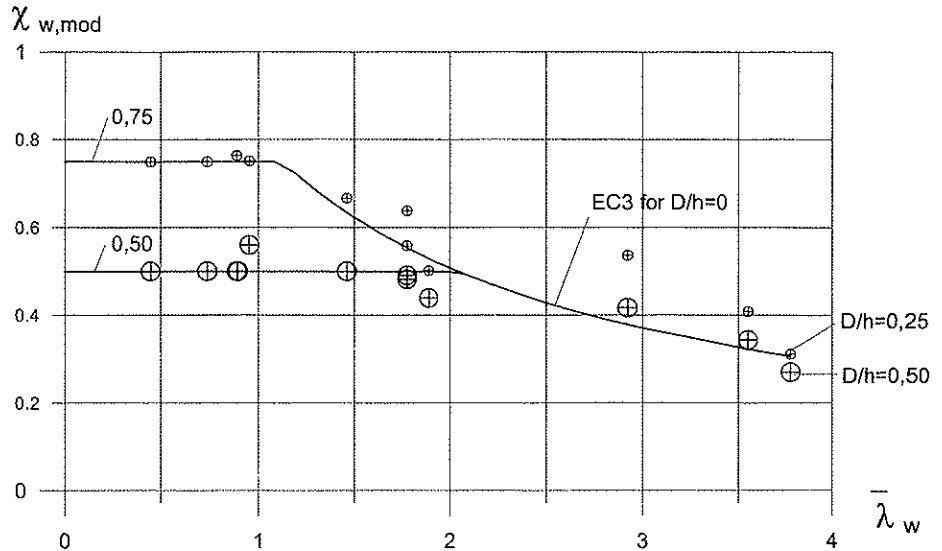


Fig. 7.3.1 $\chi_{w,mod}$ for relative slenderness when $f_y = 420 \text{ N/mm}^2$ and sleeves are used

7.3.2 Centric sleeve

In order to assess the effect of placing the sleeve centric in the opening, i.e. such that the sleeve is symmetric with regard to the web plane, two simulations are run. As seen from Fig. 7.3.1, two girders given in Table 7.3.1 have a potential for improved shear capacity. These are J125C50 and J250C50, which have been modified to J125C50C and J250C50C. The only modification is that the sleeves are centric.

The results are shown in Table 7.3.2. Column 9 shows the effect of centric sleeve relative to the case with eccentric sleeve by means of the factor c_{rel} , i.e. the ratio between $\chi_{w,mod}$ and the corresponding $\chi_{w,mod}$ as given in Table 7.3.1.

The effect of centric sleeves is good, but the relative effect, as compared to sleeves on one side only, is small.

Table 7.3.2 Effect of centric sleeves on $\chi_{w,mod}$

1	2	3	4	5	6	7	8	9
Run	Girder	h/t	D/h	a/h	Sleeve	$\chi_{w,mod}$	c_2	c_{rel}
166	J125C50C	125	0,50	4	FL80x12,5	0,47	1,54	1,06
167	J250C50C	250	0,50	4	FL63x8	0,30	1,61	1,10

7.3.3 Sleeve for openings in lower part of webs

The three girders of Table 7.2.10 have also been studied with sleeves on one side of the web. The results are presented in Table 7.3.3. Column 10 shows the effect of one-side sleeve relative to the case without sleeve as the factor c_{rel} , i.e. the ratio between $\chi_{w,mod}$ and the corresponding $\chi_{w,mod}$ as given in Table 7.2.10.

The effect is good for N63C50, which recovers the shear capacity to the maximum possible, i.e. $\chi_{w,mod} > 0,50$. For N125C50 the reduction factor $\chi_{w,mod} = 0,40$ is 91 % of that of J125C50, which has the opening in the horizontal centerline of the web. For N250C50T2 the effect of sleeve is smaller, as $\chi_{w,mod} = 0,24$ is only 71 % of that of J250C50T2. This means that a sleeve has large effect on the shear capacity of slender webs when the opening is in the horizontal centerline of the web, but less effect when the opening is in the lower part of web.

Table 7.3.3 Effect of sleeves on $\chi_{w,mod}$ for openings in lower part of web

1	2	3	4	5	6	7	8	9	10
Run	Girder	h/t	D/h	a/h	Transverse stiffeners	Sleeve	$\chi_{w,mod}$	c_2	c_{rel}
109	N63C50	63	0,50	4	-	FL125x16	0,54	1,21	1,42
110	N125C50	125	0,50	4	-	FL80x12,5	0,40	1,31	1,74
111	N250C50T2	250	0,50	2	FL63x8	FL63x8	0,24	1,13	1,13

7.4 Single opening with doubler plate

7.4.1 Doubler plate on one side of web

Small doubler plates

In stead of sleeves, web openings may be stiffened by doubler plates. In Section 3.12 rather heavy plates were recommended in order to restore the full shear capacity of a web with opening. In the present section, the idea is to start with "small" doubler plates, i.e. plates of the same weight as the weight of removed plate in the opening. This also means that the weight of the doubler plate is equal to the weight of the sleeve in the corresponding models in Section 7.3.1. It is therefore possible to compare directly the effect of a doubler plate to that of a sleeve.

The girders are based on the corresponding girders in Table 7.3.1, with the prefix J replaced by K and the subscript "b" indicating one small doubler plate. For instance, for Girder K125C25b the geometry and load application are the same as in Girder J125C25, except for the doubler plate and the initial imperfections. The thickness of doubler plates is for all girders the same as the thickness of the web. The doubler plate is "welded" to the web both on the inner and outer edge. The inner edge is located 15 mm from the edge of the opening. Initial imperfections are based on eigenmodes from the models with doubler plates with amplitudes 7,5 mm, as in the girders without doubler plates.

Results for three simulations of girders with one-sided “small” doubler plates are presented in Table 7.4.1. Column 6 gives the doubler plate dimension as \emptyset (outer diameter - inner diameter) x thickness. Column 9 shows the effect of doubler plate compared to the case with sleeve by means of the factor c_{rel} , i.e. the ratio between $\chi_{w,mod}$ and the corresponding $\chi_{w,mod}$ as given in Table 7.3.1.

The effect of a small doubler plate on one side of a web is about the same, as that of a sleeve on one side of a web.

Table 7.4.1 Effect of small doubler plates on $\chi_{w,mod}$

1	2	3	4	5	6	7	8	9
Run	Girder	h/t	D/h	a/h	Doubler plate	$\chi_{w,mod}$	c_2	c_{rel}
91	K63C25b	63	0,25	4	$\emptyset(384 - 280) \times 16$	0,76	1,07	1,01
92	K125C25b	125	0,25	4	$\emptyset(384 - 280) \times 8$	0,50	1,09	1,00
93	K250C25b	250	0,25	4	$\emptyset(384 - 280) \times 4$	0,30	1,03	0,97

Large doubler plates

Results for three runs of girders with one-sided “large” doubler plates are presented in Table 7.4.2. Large plates means that the weight of the doubler plates is about three times the weight of the plate removed from the opening.

The girders are based on the corresponding girders given in Table 7.4.1, with the subscript “a” indicating one large doubler plate. For instance, Girder K125C25a has the same geometry and load application as Girder K125C25b, except for the doubler plate and the initial imperfections. The thickness of doubler plates is for all girders the same as the thickness of the web. The doubler plate is “welded” to the web both at the inner and outer edge. The inner edge of the doubler plate is located 15 mm from the edge of the opening. Initial imperfections are based on eigenmodes from the same models with amplitude 7,5 mm.

Column 6 in Table 7.4.2 gives the doubler plate dimension as \emptyset (outer diameter - inner diameter) x thickness. Column 9 shows the effect of large doubler plate compared to the case with sleeve by means of the factor c_{rel} , i.e. the ratio between $\chi_{w,mod}$ and the corresponding $\chi_{w,mod}$ as given in Table 7.3.1.

The effect of a large doubler plate on one side of web is moderate for the girders with the thinnest webs, as compared to the girders with sleeves that were 1/3 of the weight. Here, the doubler plates cannot increase the shear capacity above that of the web without opening. For the girder with the thickest web, the effect is better, and the capacity is increased above the capacity based on the minimum section above and below the opening.

Table 7.4.2 Effect of large doubler plates on $\chi_{w,mod}$

1	2	3	4	5	6	7	8	9
Run	Girder	h/t	D/h	a/h	Doubler plate	$\chi_{w,mod}$	c_2	c_{rel}
88	K63C25a	63	0,25	4	Ø(530 - 280)x16	0,81	1,14	1,08
89	K125C25a	125	0,25	4	Ø(530 - 280)x8	0,52	1,13	1,04
90	K250C25a	250	0,25	4	Ø(530 - 280)x4	0,32	1,10	1,03

7.4.2 Doubler plates on both sides of web

Small plates

As the main purpose of using two doubler plates is to increase the shear capacity up to that of the web without opening, small doubler plates on both sides of a web is assumed in-efficient. Hence, it is not investigated further.

Large plates

Results for three runs of girders with two-sided "large" doubler plates are presented in Table 7.4.3. The weight of both doubler plates together is about six times the weight of the plate removed from the opening.

The girders are based on the corresponding girders given in Table 7.4.2, the removed subscript indicating two large doubler plates. For instance, for Girder K125C25, the geometry and load application are the same as for Girder K125C25a, except for the doubler plates and the initial imperfections. The thickness of doubler plates is for all girders the same as the thickness of the web. The doubler plates are "welded" to the web both at the inner and outer edge. The inner edge is located 15 mm from the edge of the opening. Initial imperfections are based on eigenmodes from the same models with amplitude 7,5 mm.

Column 6 in Table 7.4.3 gives the doubler plate dimension as 2[plates]Ø(outer diameter - inner diameter) x thickness. Column 9 shows the effect of two doubler plates compared to the case with only one doubler plate by means of the factor c_{rel} , i.e. the ratio between $\chi_{w,mod}$ and the corresponding $\chi_{w,mod}$ as given in Table 7.4.2.

The effect of large doubler plates on both sides of a web, compared to plate on one side only, is small for all girders. Even for K63C25 with the thickest web, the capacity is far less than the full yield shear capacity of the web without opening. Such a result is perhaps a bit disappointing in view of the theories of Chapter 3.12, but is due to global buckling of the web.

Table 7.4.3 Effect of two large doubler plates on $\chi_{w,mod}$

1	2	3	4	5	6	7	8	9
Run	Girder	h/t	D/h	a/h	Doubler plates	$\chi_{w,mod}$	c_2	c_{rel}
85	K63C25	63	0,25	4	2 \emptyset (530 - 280)x16	0,83	1,17	1,02
86	K125C25	125	0,25	4	2 \emptyset (530 - 280)x8	0,54	1,17	1,04
87	K250C25	250	0,25	4	2 \emptyset (530 - 280)x4	0,33	1,14	1,03

The results from Tables 7.4.1 to 7.4.3 are plotted in Fig. 7.4.1. as a function of the relative slenderness. The curve for the EC3 proposal for webs without openings is also included. The figure shows that the shear capacities cannot be increased above those corresponding to global buckling of the web.

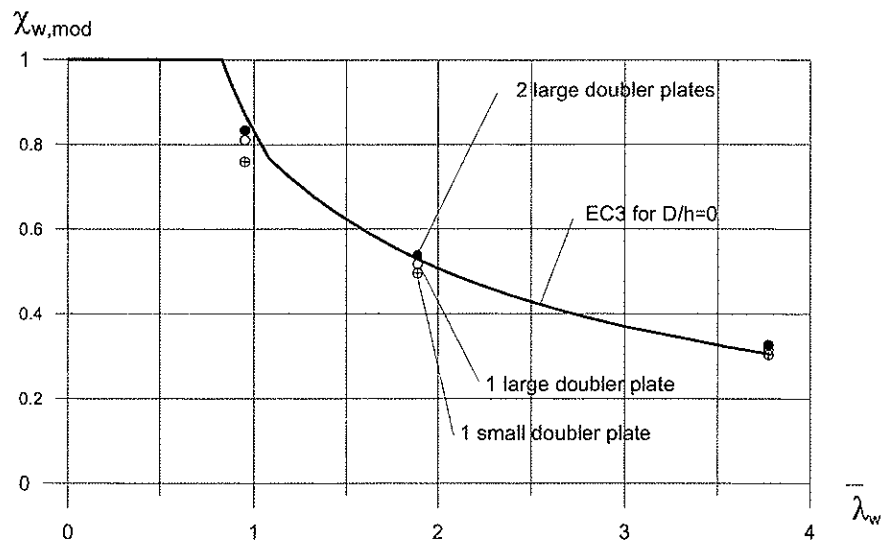


Fig. 7.4.1 $\chi_{w,mod}$ vs relative slenderness when doubler plates are used ($f_y = 420 \text{ N/mm}^2$)

Fig. 7.4.2 shows the buckle shapes of girders K125C25b, K125C25a and K125C25 at maximum shear. The maximum transverse displacements are 34 mm for [the girder with] small plate on one side, 31 mm for large plate on one side and 27 mm for large plates on both sides. The maximum transverse displacement for the corresponding girder without any stiffening, i.e. I125C50, is 41 mm.

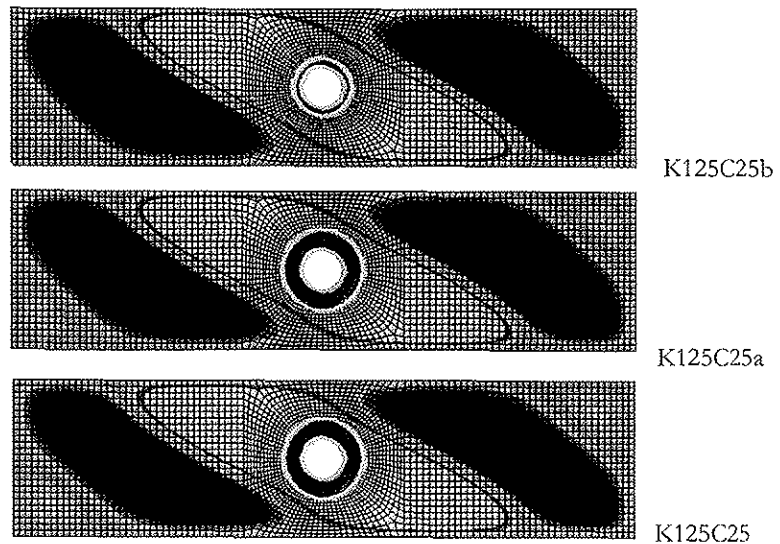


Fig. 7.4.2 Buckle shapes at maximum shear for girders K125C25b, K125C25a and K125C25

7.5 Two openings without stiffening

7.5.1 Two openings horizontally spaced

Two or more adjacent openings spaced along the web are common in practice design of girders, but scarcely described in the literature. The results of nine simulations of girders with two openings of ratio $D/h = 0,50$ are shown in Table 7.5.1.

The girders studied are variations of the girders I63C50, I125C50 and I125C50F2, see Table 7.2.3. Prefixes refer to the horizontal center to center distances c_a between the openings. The distances are $1,04D$, $1,5D$, $2D$ and $3D$ for configuration R, S, T and U respectively. The configurations are shown in Fig. 7.5.2. All openings are placed symmetric about the midpoint of the girders. These locations give zero primary moment in the section halfway between the two openings. Hence, only small primary moments are present in the vertical sections in the center of both openings, which may influence the results compared to the results of the girders with single openings. However, based on the discussions on shear and moment interaction in Section 7.2.7, the influence is considered very small.

Column 6 and 7 in Table 7.5.1 show the ratios c_a/D and S_a/D , where S_a is the clear distance between openings. In the R-girders the clear distances between the openings are 20 mm for reasons of modeling. Initial imperfections are based on the eigenmodes of the models and amplitude 7,5 mm. Column 9 gives the reduction factor $\chi_{w,mod}$ and Column 10 shows the factor c_2 .

Factor c_2 is plotted in Fig. 7.5.1 against the ratios c_a/D and S_a/D . For the thickest web there is no interaction effect of two openings for $S_a/D = 2$. This is a somewhat higher value than recommended by AISC for beams, where according to Eq. (3.3.33) the limit is $S_a/D = 1,5$. For the thinner web, the interaction has not completely disappeared for $S_a/D = 2$, and the reason may be that two openings disturb the buckle patterns far away from the web post between the openings.

Table 7.5.1 Effect of increased horizontal distance between two openings

1	2	3	4	5	6	7	8	9	10
Run	Girder	h/t	D/h	a/h	c_a/D	S_a/D	Transverse stiffener	$\chi_{w,mod}$	c_2
191	R63C50	63	0,50	4	1	0	-	0,30	0,67
193	S63C50	63	0,50	4	1,5	0,5	-	0,38	0,84
198	T63C50b	63	0,50	4	2	1	-	0,41	0,91
199	U63C50	63	0,50	4	3	2	-	0,45	1,00
192	R125C50	125	0,50	4	1	0	-	0,22	0,73
194	S125C50	125	0,50	4	1,5	0,5	-	0,26	0,87
196	T125C50	125	0,50	4	2	1	-	0,26	0,87
200	U125C50	125	0,50	4	3	2	-	0,28	0,93
201	R125C50T2	125	0,50	2	1	0	FL63x8	0,24	0,75

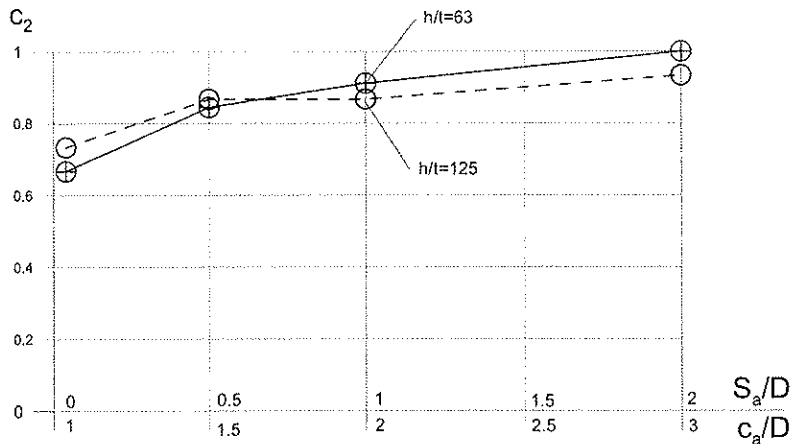


Fig. 7.5.1 Reduction of shear capacity for girders with two openings compared to girders with a single opening. Horizontal spacing, $D/h = 0,50$ and $f_y = 420 \text{ N/mm}^2$

For the girders R125C50, S125C50, T125C50 and U125C50, i.e. the girders with the thinnest webs, the buckle shapes at maximum shear are shown in Fig. 7.5.2. Compared to the reference Girder I125C50 with a single opening, see Fig. 7.2.21, the buckled shapes are somewhat extended, but the maximum amplitudes are about the same.

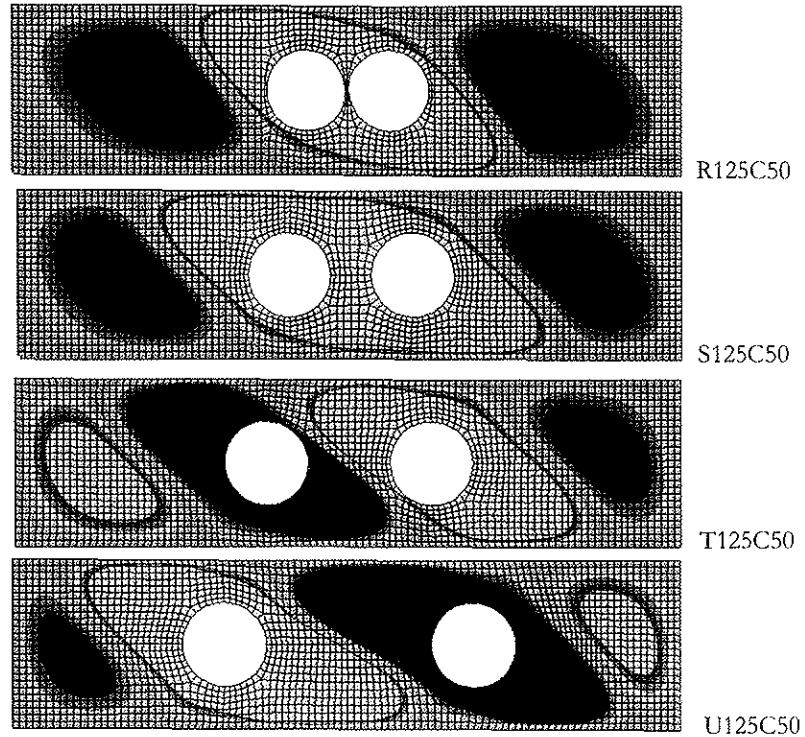


Fig. 7.5.2 Buckles for girders R125C50, S125C50, T125C50 and U125C50 at maximum shear

The response curves for webs with two openings show a slightly “softer” transition at the point of maximum shear, but there is no significant difference, compared to the corresponding curves for single openings.

A frequently asked question in practical design is what happens to the web post, when the width of the post goes to zero in the limit. The R-girders show that there is no local buckling or excessive strain in the narrow web post; the performance corresponds to that of an ordinary large buckle, for instance as in I125C50. However, to see if this really is the case, a one-sided transverse stiffener is added to R125C50, identified as Girder R125C50T2 in Table 7.5.1. The shear capacity of R125C50T2 increased about 12 % compared to that of R125C50. However, most of the increase is due to the reduced aspect ratio for R125C50T2. The factor c_2 for R125C50T2 is based on the reference girder I125C50T2, i.e. a single opening in a web with aspect ratio $a/h = 2$. The influence of the aspect ratio is eliminated by calculating the ratio of the factors c_2 for girders R125C50T2 and R125C50. The ratio is $0,75/0,73 = 1,03$ and hence the effect of buckling of the web post itself is not exceeding 3 %. Also, R125C50T2 is only approximately corresponding to I125C50T2, because each opening is eccentrically located in the part of plate with aspect ratio $a/h = 2$. The 3 % increase may come from the web post or the eccentrically located openings. The buckle shapes in Girder R125C50T2 at maximum shear are shown in Fig. 7.5.3.

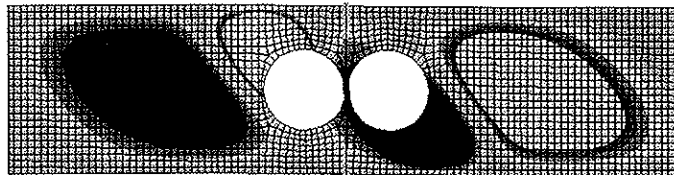


Fig. 7.5.3 Buckle shapes for Girder R125C50T2, i.e. with a transverse stiffener through the web post, at maximum shear

7.5.2 Two openings vertically spaced

Two or more adjacent circular openings in the same vertical section of a web are not very common in practice, but occur from time to time. The author does not know about descriptions in the literature. The results of eight simulations of girders with two openings of ratio $D/h = 0,25$ are shown in Table 7.5.2.

The girders are variations of I63C25 and I125C25, see Table 7.2.3. Prefixes RH, SH, TH and UH refer to vertical center to center distances c_h between the openings, having values of $1,08D$, $1,5D$, $2D$ and $3D$, respectively. The configurations are shown in Fig. 7.5.5.

Column 6 and 7 in Table 7.5.2 show the ratios c_h/D and S_h/D . Here, S_h is the clear distance between openings. In the RH-girders the clear distance is 20 mm for reasons of modeling. Initial imperfections are based on the eigenmodes of the models with amplitude $7,5\text{ mm}$. Column 8 shows $\chi_{w,\text{mod}}$ and Column 9 shows the factor c_2 , based on the reference girders I63C25 and I125C25. Hence, the diameter of the opening in the reference girders is only 50 % of the sum of the opening diameters in the girders with two vertically spaced openings. Column 10 shows alternative comparisons, where the two openings are compared to an elongated circular opening that has the same horizontal dimension and twice the height of each of the two openings. Girders with such openings are simulated in Section 8.2.2. The comparisons are performed by means of the factor c_{rel} , i.e. the ratio between $\chi_{w,\text{mod}}$ and the corresponding $\chi_{w,\text{mod}}$ for the reference girders I63E2550 and I125E2550 as given in Table 8.2.2.

The factor c_2 is plotted in Fig. 7.5.4 against the ratios c_h/D and S_h/D . All values of c_2 are much smaller than 1,0. There is only a minor increase in shear capacity when the openings are more spaced.

The factor c_{rel} shows that a procedure where two vertically spaced openings of the same dimensions are treated as one elongated opening with double height, gives conservative results for $h/t = 125$. For $h/t = 63$ the result is 2 % on the non-conservative side when the openings are located near the flanges. This leads to the conclusion that the proposed design procedure should include the minimum shear area based on both openings, in order to give reliable results.

Table 7.5.2 Effect of increased vertical distance between two openings

1	2	3	4	5	6	7	8	9	10
Run	Girder	h/t	D/h	a/h	c_h/D	S_h/D	$\chi_{w,mod}$	c_2	c_{rel}
202	RH63C25	63	0,25	4	1	0	0,48	0,68	0,99
204	SH63C25	63	0,25	4	1,5	0,5	0,50	0,70	1,02
206	TH63C25	63	0,25	4	2	1	0,50	0,70	1,03
208	UH63C25	63	0,25	4	3	2	0,48	0,68	0,98
203	RH125C25	125	0,25	4	1	0	0,34	0,74	1,02
205	SH125C25	125	0,25	4	1,5	0,5	0,37	0,80	1,11
207	TH125C25	125	0,25	4	2	1	0,39	0,85	1,17
209	UH125C25	125	0,25	4	3	2	0,38	0,83	1,14

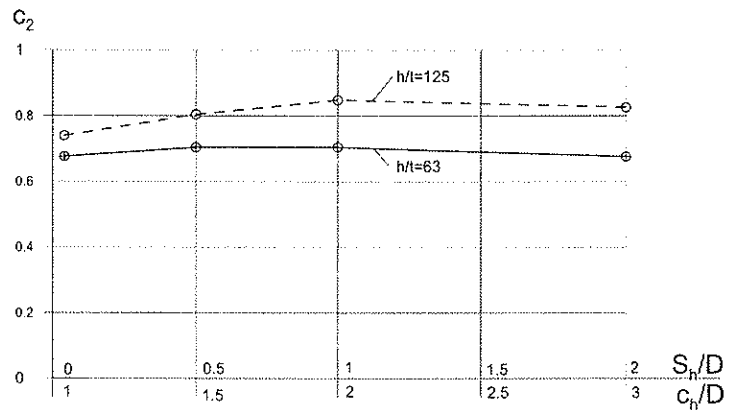


Fig. 7.5.4 Reduced shear capacity for girders with two vertically spaced openings of $D/h = 0,25$ compared to girders with a single opening of $D/h = 0,25$. ($f_y = 420 \text{ N/mm}^2$)

For the girders with the thinnest webs, the buckles at maximum shear are shown in Fig. 7.5.5. Compared to the girder with a single opening, see I125C50 in Fig. 7.2.21, the buckles are somewhat extended, but the maximum amplitudes are about the same.

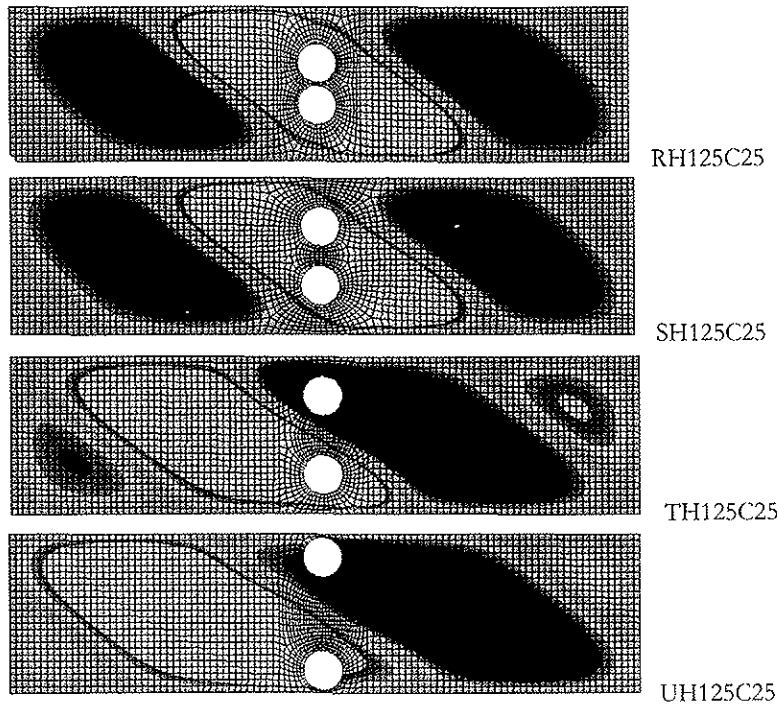


Fig. 7.5.5 Buckles for girders RH125C25, SH125C25, TH125C25 and UH125C25 at maximum shear

The response curves for webs with two openings vertically spaced show a slightly “softer” transition at the point of maximum shear. However, there is no significant difference compared to the corresponding curves for single openings. For increased vertical tip displacement, the reduction in shear capacity for the UH-girders was considerable, as the lower flanges buckled in the web plane. With openings close to the flanges, the small part of web below the opening was not able to prevent a major displacement of the flange.

7.6 Two openings with sleeves

7.6.1 Two openings horizontally spaced

The effect of sleeves is investigated by means of four simulations for girders with two openings of ratio $D/h = 0,50$. The girders are variations of the girders presented in Section 7.5.1. Prefixes V, W, X and Y refer to horizontal center distances c_a between the openings, having the values of $1,04D$, $1,5D$, $2D$ and $3D$, respectively. For instance, for Girder V125C50, geometry and load application are the same as in Girder R125C50, except for the sleeves and the initial imperfections. The sleeves are placed on one side of webs and the dimensions of the sleeves are the same as for the corresponding Girder J125C50 with

one opening only. Two girders are shown in Fig. 7.6.3. Initial imperfections are based on the eigenmodes of the models and amplitude 7,5 mm.

The results of the simulations are shown in Table 7.6.1. Column 11 shows the effect of the horizontal distance relative to the corresponding single opening with sleeve by means of the factor c_{rel} , i.e. the ratio between $\chi_{w,mod}$ and $\chi_{w,mod}$ for Girder J125C50 as given in Table 7.3.1.

The factor c_{rel} is plotted in Fig. 7.6.1 against the ratios c_a/D and S_a/D . As seen, the effect of two openings almost disappears for $S_a/D = 1,5$.

Table 7.6.1 Effect of increased horizontal distance between two openings with sleeves

1	2	3	4	5	6	7	8	9	10	11
Run	Girder	h/t	D/h	a/h	c_a/D	S_a/D	Sleeve	$\chi_{w,mod}$	c_2	c_{rel}
212	V125C50	125	0,50	4	1	0	FL80x12,5	0,39	1,28	0,89
214	W125C50	125	0,50	4	1,5	0,5	FL80x12,5	0,41	1,35	0,93
216	X125C50	125	0,50	4	2	1	FL80x12,5	0,43	1,42	0,98
218	Y125C50	125	0,50	4	3	2	FL80x12,5	0,43	1,43	0,99

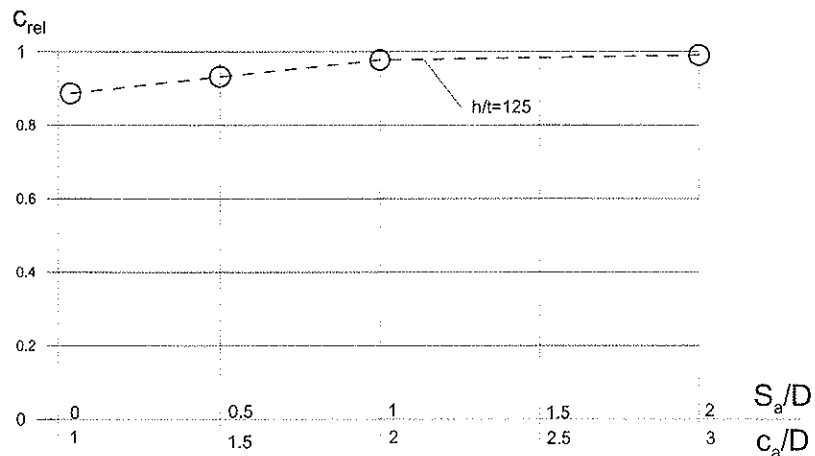


Fig. 7.6.1 Reduction of shear capacity for girders with two openings compared to girders with a single opening. Horizontal spacing, $D/h = 0,50$, sleeves FL 80x12,5 and $f_y = 420 \text{ N/mm}^2$

Buckled shapes at maximum shear for two girders are shown in Fig. 7.6.3. For comparison, the shape of Girder J125C50 with a single opening and sleeve is shown in Fig. 7.6.2. The buckled shape of the girders with two openings are somewhat extended, but the maximum transverse web displacements are about the same for J125C50, V125C50 and W125C50. For X125C50 and Y125C50 the amplitudes have increased, but are still relatively small.

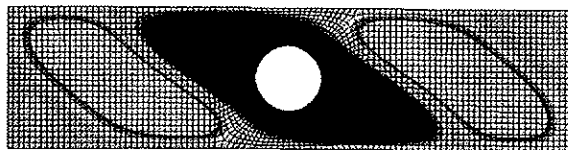


Fig. 7.6.2 Buckles for Girder J125C50, i.e. with a sleeve on one-side of the web

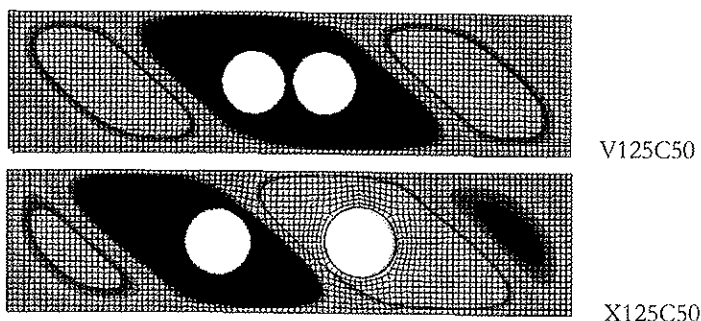


Fig. 7.6.3 Buckles for girders V125C50 and X125C50 at maximum shear

7.6.2 Two openings vertically spaced

The effect of sleeves is investigated by means of four simulations of girders with two openings of ratio $D/h = 0,25$. The girders are variations of the girders presented in Section 7.5.2. Prefixes VH, WH, XH and YH refer to vertical center to center distances c_h between the openings, having values of $1,04D$, $1,5D$, $2D$ and $3D$, respectively. For instance, Girder VH125C25 has the same geometry and load application as Girder V125C25, except for the sleeves and the initial imperfections. The sleeves are placed on one side of webs, and the dimensions are the same as in J125C25 with only one opening. Two girders are shown in Fig. 7.6.5. Initial imperfections are based on the eigenmodes of the models and amplitude of 7,5 mm.

The results are shown in Table 7.6.2. Columns 6 and 7 give the ratios c_h/D and S_h/D , respectively. In the RH-girders the clear distance S_h between the openings is 20 mm for reasons of modeling. Column 8 gives $\chi_{w,mod}$ and Column 9 shows the factor c_2 , based on the reference girder I125C25. Hence, the diameter of the opening in the reference girder is 50 % of the sum of the opening diameters in the girders with two vertically spaced openings. Column 10 shows alternative comparisons, where the two openings are compared to an elongated circular opening with sleeve, that has the same horizontal dimension and twice the height of each of the two openings. A girder with such opening is simulated in Section 8.3.2. The comparisons are performed by means of the factor c_{rel} , i.e. the ratio between $\chi_{w,mod}$ and $\chi_{w,mod}$ for the reference girder J125E2550a as given in Table 8.3.2.

The factor c_2 is plotted in Fig. 7.6.4 against the ratios c_h/D and S_h/D . All values of c_2 are smaller than 1,0. There is only a minor increase in shear capacity when the openings are more spaced.

The factor c_{rel} shows that a procedure where two vertically spaced openings of the same dimensions are treated as one elongated opening with double height, gives good results. This confirms the conclusion from Section 7.5.2 that the proposed design procedure should include the minimum shear area based on both openings.

Table 7.6.2 Effect of increased vertical distance between two openings with sleeves FL63x8

1	2	3	4	5	6	7	8	9	10
Run	Girder	h/t	D/h	a/h	c_h/D	S_h/D	$\chi_{w,mod}$	c_2	c_{rel}
228	VH125C25	125	0,25	4	1	0	0,43	0,86	0,99
229	WH125C25	125	0,25	4	1,5	0,5	0,43	0,86	0,99
230	XH125C25	125	0,25	4	2	1	0,46	0,92	1,05
231	YH125C25	125	0,25	4	3	2	0,46	0,92	1,05

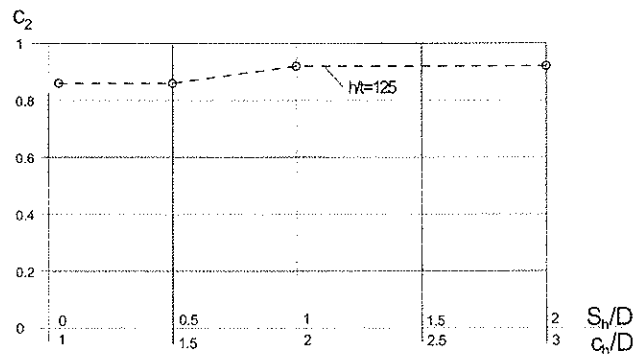


Fig. 7.6.4 Reduction of shear capacity for girders with two openings of $D/h = 0,25$ compared to girders with a single opening of $D/h = 0,25$. Vertical spacing, sleeves FL 63x8 and $f_y = 420 \text{ N/mm}^2$

Buckled shapes at maximum shear for girders VH125C25 and YH125C25 are shown in Fig. 7.6.5. Compared to the girder with a single opening, the buckles are somewhat extended, but the maximum amplitudes are about the same.

The response curves for webs with two vertically spaced openings show a slightly “softer” transition at the point of maximum shear, but there is no major difference compared to the corresponding curves for single openings.

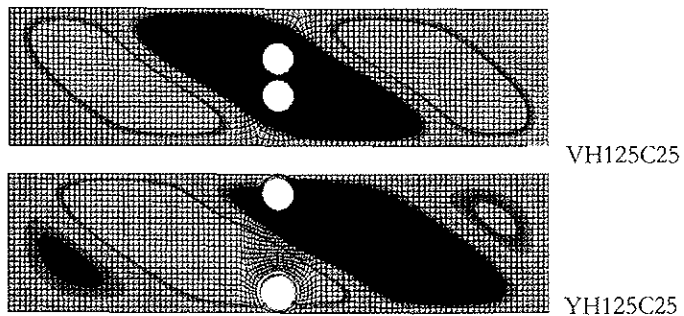


Fig. 7.6.5 Buckled shapes for girders VH125C25 and YH125C25 at maximum shear

7.7 Conclusion

The simulations of girders with circular openings show that

- The response curves for shear force versus tip displacement all have distinct maximum points, followed by a drop in load-carrying capacity. There is no principal difference in the *shape* of the curves for the girders with openings compared to the curves for the similar girders without openings. For all simulations the maximum shear is taken as the shear capacity of the girder in the ultimate limit state.
- The drop in load-carrying capacity continued for increasing tip displacement. No distinct minimum points were found. The shear capacity of the girder in the accidental limit state depends on the value of the tip displacement. This value may vary from case to case, and general criteria cannot be given.
- The shear buckling is of global character. It is possible, for design purpose, to include the effect of buckling for girders with openings by means of the buckling reduction factor given by EC3 for girders without openings, but reduced in order to include the minimum section above and below the opening.
- Transverse displacements of webs in a girder with opening show an almost linear increase up to the point of maximum shear. When the maximum shear is taken as the shear capacity of girders, the size of displacement will not be larger for a girder with opening, than for the similar girder without opening.
- With reference to the proposed design procedure in Chapter 6, the combination of primary moment and shear for girders with openings may be simplified by using the same interaction equation as used in AISC(1990) for beams with openings. It is not necessary to know the actual forces in girder flanges.
- The effect of sleeves on one side of web is considerable, and it is only marginally improved if the position of the sleeve is centric relative to the web plane. Doubler plates have almost the same effect as sleeves, and a weight of sleeve or doubler plate comparable with the weight of the removed plate in the opening is sufficient to ensure the effect.
- An eccentric position of an opening relative to the horizontal centerline of the web reduces the shear capacity, except for very slender webs.
- For girders with two horizontally spaced openings of the same size, there is almost no interaction effect of two openings when the clear distance between the openings exceeds twice the diameter of the opening. However, even a very small clear distance does not result in severe local buckling or plastification, it only reduces the shear capacity to about 2/3 of the capacity of the single opening.
- A major reduction in the shear capacity of all girders with openings arises from the reduced shear area in the opening. For girders with two (or more) vertically spaced openings, this effect must be included by an estimation of the net shear area over the girder height in sections through all openings. The distance between the openings has little effect on the shear capacity, as long as the openings are symmetrically located around the horizontal centerline of girder.

Chapter 8

Simulations of girders with elongated circular openings

8.1 Introduction

This chapter comprises simulations of girders with horizontally and vertically elongated openings. The basic FE-model is the same as the one given in Chapter 7.

8.2 Opening without stiffening

8.2.1 Horizontal long side

Such openings are frequently used for cable trays, where more width than height is required and a full circular opening would reduce the shear capacity too much. Two simulations of girders with one opening $D_a/h = 0,50$ and $D_h/h = 0,25$ have been performed. D_a and D_h are the horizontal and vertical dimensions, respectively. The radius of the ends is $D_h/2$. The girders are termed IxxE5025, where xx is the h/t ratio, E means elongated, "50" refers to the D_a/h ratio and "25" refers to the D_h/h ratio. One girder is shown in Fig. 8.2.1. The opening is placed symmetric about the midpoint of the girders. Initial imperfections are based on the 2. eigenmode with amplitude 7,5 mm.

The results are presented in Table 8.2.1. Column 7 shows $\chi_{w,mod}$ and column 8 gives the factor c_2 , based on the reference girders I63C25 and I125C25. Hence, the diameter of the circular opening in the reference girders is equal to the vertical dimension of the opening in the girders with elongated openings.

The buckled shape at maximum shear for I125E5025 is shown in Fig. 8.2.1. Compared to the girder with circular opening, the buckles are somewhat extended, but the maximum transverse displacements are about the same.

Table 8.2.1 Results for girders with elongated circular openings, horizontal long side

1	2	3	4	5	6	7	8
Run	Girder	h/t	a/h	D_a/h	D_h/h	$\chi_{w,mod}$	c_2
221	I63E5025	63	4	0,50	0,25	0,59	0,83
222	I125E5025	125	4	0,50	0,25	0,40	0,87

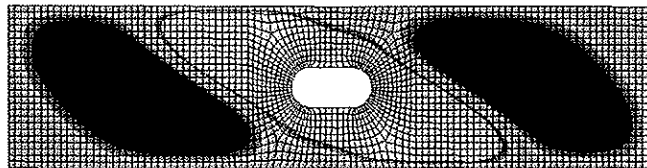


Fig. 8.2.1 Buckles in Girder I125E5025 at maximum shear

8.2.2 Vertical long side

Such openings are frequently used for man-holes, where larger height than width is required and a full circular opening is supposed to reduce the shear capacity too much. Two simulations of girders with one opening $D_a/h = 0,25$ and $D_h/h = 0,50$ have been performed. D_a and D_h are the horizontal and vertical dimensions, respectively. The radius of the end is $D_a/2$. The girders are denoted IxxE2550, where xx is the h/t ratio, E means elongated, "25" refers to the D_a/h ratio and "50" refers to the D_h/h ratio. One girder is shown in Fig. 8.2.2. The opening is placed symmetric around the midpoint of the girders. Initial imperfections are based on the 1. eigenmode with amplitude 7,5 mm.

The results are shown Table 8.2.2. Column 7 gives $\chi_{w,mod}$. The values are about the same as for girders RH63C25 and RH125C25, see Table 7.5.2. Column 8 gives the factor c_2 , based on the reference girders I63C50 and I125C50. The diameter of the circular opening in the reference girders is equal to the vertical dimension of the opening in the girders with elongated openings.

The buckled shape at maximum shear for I125E2550 is shown in Fig. 8.2.2. Compared to the girder with circular opening, the buckles are somewhat extended, but the maximum transverse web displacements are about the same.

Table 8.2.2 Results for girders with elongated circular openings, vertical long side

1	2	3	4	5	6	7	8
Run	Girder	h/t	a/h	D_a/h	D_h/h	$\chi_{w,mod}$	c_2
219	I63E2550	63	4	0,25	0,50	0,49	1,09
220	I125E2550	125	4	0,25	0,50	0,33	1,10

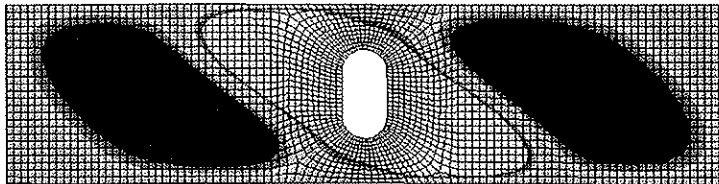


Fig. 8.2.2 Buckles in Girder I125E2550 at maximum shear

8.2.3 Comparison between circular and elongated circular openings

Comparisons between girders with circular and elongated openings may be done in various ways. For a more detailed investigation into the difference between horizontally and vertically elongated openings, Table 8.2.3 shows the relative effect of increasing an opening of $D/h = 0,25$. The shear capacities of the girders I125E2550, I125E5025 and I125C50 are compared to the shear capacity of I125C25. The table shows the values for $\chi_{w,mod}$ from the simulations, and the values relative to I125C25 in brackets ().

Table 8.2.3 Comparison of the effect of elongated openings

	$D_a/h = 0,25$	$D_a/h = 0,50$
	I125C25	I125E5025
$D_h/h = 0,25$	0,46 (1,00)	0,40 (0,87)
	I125E2550a	I125C50
$D_h/h = 0,50$	0,33 (0,72)	0,30 (0,65)

In principle, the location of the governing section of the load-carrying system for horizontally elongated openings is different from those of circular openings. The governing section for the secondary moments is not in a section through the center of the opening. For elongated openings with the long side vertical there is no difference; the governing section is in the vertical section through the opening when buckling is disregarded. Table 8.4.1 shows that the shear capacity for I125E5025 is higher than for I125E2550. Despite the increased secondary moments for horizontally elongated openings, the minimum web section itself is larger. A similar comparison for opening with sleeves gives same conclusion.

The response curves for webs with elongated openings show a slightly more “soft” transition at the point of maximum shear, but except for the value of the maximum shear, there is no significant difference compared to the corresponding curves for circular openings.

8.3 Opening with sleeve

8.3.1 Horizontal long side

The effect of sleeves is investigated by means of two simulations. The girders are variations of the girders in Section 8.2.1. Prefix J refers to sleeves on one side of webs. The weight of the sleeve is approximately the same as the weight of the removed plate in the opening. One girder is shown in Fig. 8.3.1. Initial imperfections are based on the 2. eigenmode with amplitude 7,5 mm.

The results are presented in Table 8.3.1. Column 8 shows $\chi_{w,mod}$ and column 9 gives the factor c_2 , based on the reference girders I63C25 and I125C25. Column 10 shows the increased shear capacity provided by the sleeve compared to the girders with the same elongated openings without sleeve, by means of c_{rel} , i.e. the ratio between $\chi_{w,mod}$ and $\chi_{w,mod}$ for the girders I63E5025 and I125E5025, as given in Table 8.2.1.

The sleeve increases the shear capacity 16 % to 18 %. However, compared to the corresponding girders with *circular* opening $D/h = 0,25$ and sleeve, i.e. J63C25 and J125C25 in Table 7.3.1, the shear capacities of girders J63E5025 and J125E5025 are 9 % and 6 % less, respectively. For the elongated circular opening with the long side horizontal the

sleeve acts as a form of horizontal reinforcement. The requirement to horizontal reinforcement is more demanding than the requirement to circular sleeves.

The buckled shape at maximum shear for J125E5025 is shown in Fig. 8.3.1. Compared to the girder without sleeve, the buckles are somewhat extended, but the maximum transverse displacement is reduced from 40 to 35 mm, i.e. about 13 %.

Table 8.3.1 Results for girders with elongated circular openings and sleeves, horiz. long side

1	2	3	4	5	6	7	8	9	10
Run	Girder	h/t	a/h	D_a/h	D_h/h	Sleeve	$\chi_{w,mod}$	c_2	c_{rel}
225	J63E5025	63	4	0,50	0,25	FL110x12,5	0,68	0,96	1,16
226	J125E5025	125	4	0,50	0,25	FL70x10	0,47	1,02	1,18

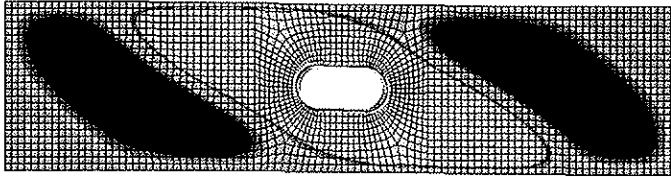


Fig. 8.3.1 Buckles in Girder J125E5025 at maximum shear

8.3.2 Vertical long side

The effect of sleeves is investigated by means of two simulations. The models are variations of the models in Section 8.2.2. Prefix J refers to sleeves on one side of webs. The weight of the sleeve is approximately the same as the weight of the removed plate in the opening. One model is shown in Fig. 8.3.2. Initial imperfections are based on the 1. eigenmode with amplitude 7,5 mm.

The results are presented in Table 8.3.2. Column 8 shows $\chi_{w,mod}$ and Column 9 gives the factor c_2 , based on the reference girders I63C50 and I125C50. Column 10 shows the increased shear capacity provided by the sleeve compared to the girders with the same elongated openings without sleeve, by means of c_{rel} , i.e. the ratio between $\chi_{w,mod}$ and $\chi_{w,mod}$ for the girders I63E2550 and I125E2550, as given in Table 8.2.2.

The sleeve increases the shear capacity from 15 % to 31 %. Compared to the corresponding girders with *circular* opening $D/h = 0,50$ and sleeve, i.e. J63C50 and J125C50 in Table 7.3.1, the shear capacities of girders J63E2550 and J125E2550 are the same. But, as the weight of the sleeves here follows the weight of the opening, the sleeves for the elongated openings are lighter. The conclusion is that girders with vertically elongated circular opening may be designed according to the guidelines for girders with circular openings, provided the diameter is taken as the vertical length of the opening. However, the stiffener dimensions may be chosen according to the weight of the removed plate in the real opening.

The buckled shape at maximum shear for J125E2550 is shown in Fig. 8.3.2. Compared to the girder without sleeve, the widths of the buckles are about the same, but the maximum transverse web displacement is reduced from 39 to 13 mm, i.e. about 67 %.

Table 8.3.2 Results for girders with elongated circular opening and sleeve, vertical long side

1	2	3	4	5	6	7	8	9	10
Run	Model	h/t	a/h	D_a/h	D_h/h	Sleeve	$\chi_{w,mod}$	c_2	c_{rel}
223	J63E2550	63	4	0,25	0,50	FL110x12,5	0,56	1,25	1,15
227	J125E2550a	125	4	0,25	0,50	FL70x10	0,44	1,44	1,31

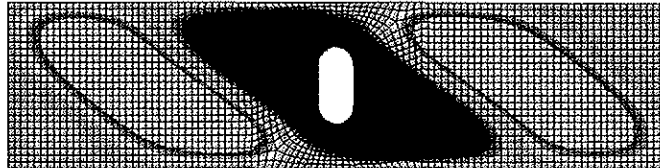


Fig. 8.3.2 Buckles in Girder J125E:2550a at maximum shear

8.4 Conclusion

The simulations of girders with elongated circular openings show that

- There is a principal difference between an opening having the long side horizontal and an opening having the long side vertical. The opening with the horizontal long side is a type of rectangular opening. The opening with the vertical long side behaves as a type of circular opening.
- The shear capacity of girders with an opening with *horizontal* long side and without sleeve, should be determined as for girders with a rectangular opening.
- The shear capacity of girders with an opening with *horizontal* long side and sleeve, should in principle be determined as for girders with a rectangular opening with horizontal reinforcement. The simulations showed that the sleeves were sufficiently anchored to the curved part of opening. However, a rule that the sleeves should have the same weight as the removed plate in the opening, gives a slightly less capacity for elongated openings than for circular openings.
- The shear capacity of girders with an opening with *vertical* long side and without sleeve may be determined as for girders with a circular opening of the same vertical dimension as the elongated opening. The simulations in Section 8.2.2 showed shear capacities about 10 % on the conservative side for this design.
- The shear capacity of girders with an opening with *vertical* long side and sleeve is about the same as for girders with a circular opening with sleeve and of the same vertical dimension as the elongated opening. This is shown by the simulations in Section 8.3.2 for sleeves of the same weight as the removed plate in the opening.

Chapter 9

Simulations of girders with square openings

9.1 Introduction

81 simulations are performed for girders with square openings. The simulations follow the same procedure as used for the simulations of circular openings in Chapter 7, including the basic FE-models. The main purpose is to study the normalized shear capacities, but some features specially connected to square openings are also discussed. In addition, the results for square openings are compared to the similar results for circular openings.

One or two square openings with sides $D_a = D_h = 0,25h$ and $D_a = D_h = 0,50h$ are considered, with and without vertical stiffeners and horizontal reinforcement. Finite elements with dimensions approximately 20 x 20 mm are applied around the openings. Corners have radius $r = 2t = 32$ mm for the thickest plates and $r = 16$ mm for plates with $h/t = 125$ and $h/t = 250$.

9.2 Single opening without stiffening

9.2.1 Comparison with rotated stress field method

Six simulations are performed to study the rotated stress field method and the modified Vierendeel method. In order to compare directly with the diagrams of Höglund (1970), the yield stress $f_y = 260$ N/mm² is used. The girder identities are the same as given in Chapter 7, but now C is replaced by S for square openings. Hence a girder with $h/t = 250$ and opening with sides $0,50h$ is called H250S50.

The simulation results for $\chi_{w,mod}$ are shown in Table 9.2.1 together with the reduction factor from the rotated stress field theory and from the modified Vierendeel method, as given in Höglund (1970). For the openings $D_h/h = 0,25$, values are given for the rotated stress field method only, as the modified Vierendeel method is valid only for larger openings. For square openings $D_h/h = 0,50$, the two methods give identical results. The simulated results are plotted together with the relevant curves from Höglund (1970) in Fig. 9.2.1

The simulated values are generally higher than the values obtained from the rotated stress field method, except for small openings in medium slender plates. The rotated stress field method should be regarded as satisfactory for most openings and plates. The non-conservative value for the small opening in medium slender plates may be related to the use of the critical buckling stress in Eq. (3.6.6) with no correction for elasto-plastic buckling.

Table 9.2.1 Comparison of simulations with values from Höglund (1970)

1	2	3	4	5	6	7	8	9
Run	Girder	h/t	D_h/h	Sim. $\chi_{w,mod,S}$	Rot. stress field $\chi_{w,mod,R}$	Ratio $\chi_{w,mod,S}/\chi_{w,mod,R}$	Modified Vierendeckl $\chi_{w,mod,V}$	Ratio $\chi_{w,mod,S}/\chi_{w,mod,V}$
232	H63S25	63	0,25	0,69	0,67	1,03
233	H125S25	125	0,25	0,51	0,53	0,96
234	H250S25	250	0,25	0,32	0,28	1,14
238	H63S50	63	0,50	0,36	0,33	1,08	0,33	1,08
239	H125S50	125	0,50	0,26	0,23	1,13	0,23	1,13
240	H250S50	250	0,50	0,18	0,16	1,12	0,16	1,12

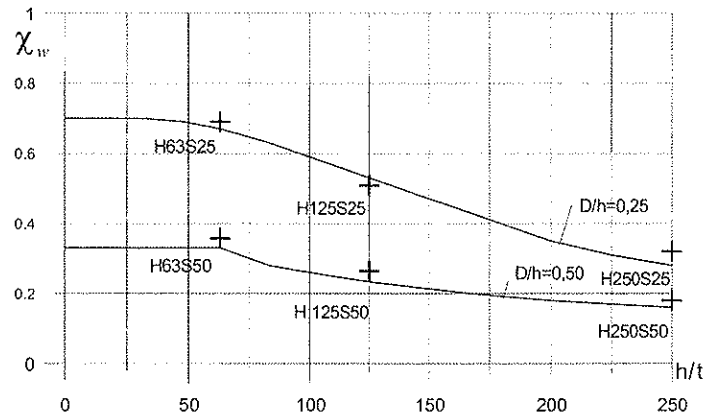


Fig. 9.2.1 Simulated results compared with curves from rotated stress field theory

9.2.2 Transverse displacements and stresses in webs

Plots of transverse web displacement at maximum shear are shown in Figs. 9.2.2 and 9.2.3 for girders H125S25 and H125S50 with medium slender webs. Compared to the circular openings of Figs. 7.2.3 and 7.2.4, the shape and size of buckles are approximately the same. For the small openings, the maximum web displacement is 27 % larger for the square opening than for the circular one. For the larger openings the maximum web displacement for the square opening is 7 % smaller than for the circular opening.

Stress plots at maximum shear for the same girders are shown in Figs. 9.2.4 to 9.2.5. The plots show von Mises stress on the negative surface of elements. Compared to the circular openings of Figs. 7.2.6 and 7.2.7, the stress patterns are approximately the same. However, for the large openings, the diagonal stress pattern for the circular opening is not present for the square opening. Fig. 9.2.6 shows the von Mises stress in the middle surface of H125S50. Unfortunately, ABAQUS is unable to show the stresses in all regions around the opening, but it should be evident that the stresses adjacent to the vertical edges of opening are small.

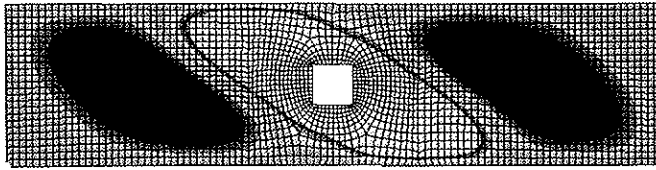


Fig. 9.2.2 Transverse web displacement at maximum shear in Girder H125S25

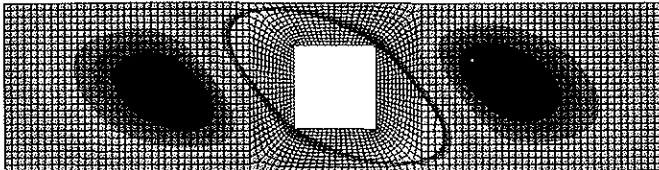


Fig. 9.2.3 Transverse web displacement at maximum shear in Girder H125S50

S, Mises
SNEG, (fraction)
42.607e+02
42.600e+02
42.340e+02
42.000e+02
41.820e+02
41.560e+02
41.300e+02
41.040e+02
47.800e+01
45.200e+01
42.600e+01
40.000e+00

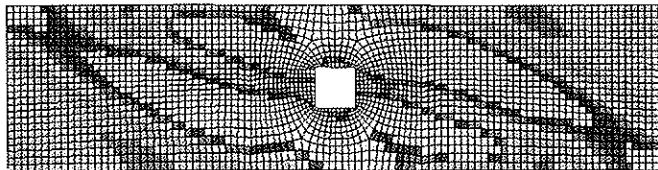


Fig. 9.2.4 Von Mises stress at maximum shear in Girder H125S25

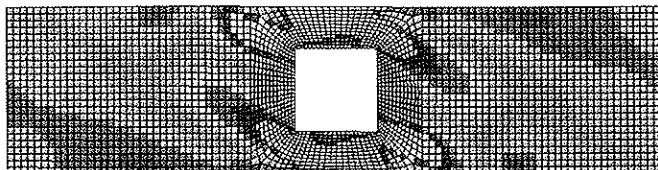


Fig. 9.2.5 Von Mises stresses at maximum shear in Girder H125S50

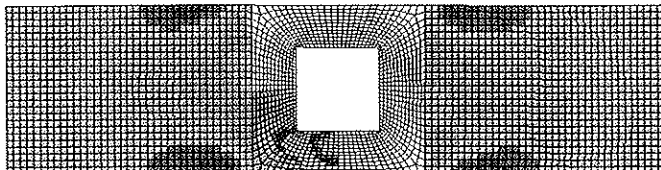


Fig. 9.2.6 Von Mises stress in middle surface at maximum shear in Girder H125S50

9.2.3 Buckling

The response curves for shear versus tip displacement have the same shape as shown in Fig. 7.2.10 for the circular opening, but the “peaks” are generally less pronounced and the negative slopes smaller. The curve for Girder H125S50 is shown in Fig. 9.2.7. There is no evidence of local, column type buckling. However, for square openings, local buckling may be more related to the applied shape of initial imperfections than for circular openings. This issue is discussed in more detail in Section 9.2.7.

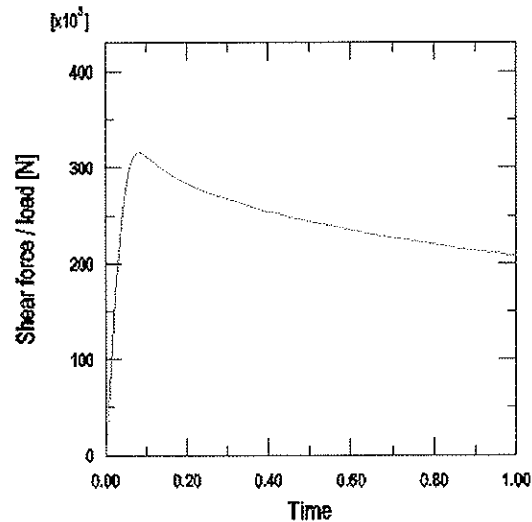


Fig. 9.2.7 Response curve for Girder H125S50

The response curve for transverse displacement of a node on the vertical edge of the opening in Girder H125S50 has the same shape as in Fig. 7.2.11. It is, however, difficult to compare the slopes of the curves directly, because only four edge nodes can be in the same position in the two girders. However, for square openings with $D_h/h = 0,50$, the “stiffness” of the transverse displacement is estimated to about 83 % of the corresponding circular opening. This means that a certain shear force gives about 20 % more transverse web displacement in a web with a square opening compared to a web with a circular opening.

9.2.4 Influence of the yield stress f_y

In order to study the influence of varying the yield stress without changing the other parameters, the simulations of the six girders of Section 9.2.1 are repeated, now with $f_y = 420 \text{ N/mm}^2$. The results for $\chi_{w,mod}$ are included in Table 9.2.2 and in Fig. 9.2.9.

9.2.5 Additional flange forces

Fig. 9.2.8 shows the flange forces of Girder I125S50. The forces are determined, normalized and plotted as explained in Section 7.2.5. For comparison the flange forces ξ_A of Girder I125, without opening, and ξ_B for Girder I125C50, with circular opening, are also included. The dotted line shows $\xi_{A,elastic}$, i.e. the flange forces for a girder without opening based on elastic theory, and disregarding buckling. The additional flange forces are significantly higher for the square opening than for the circular one.

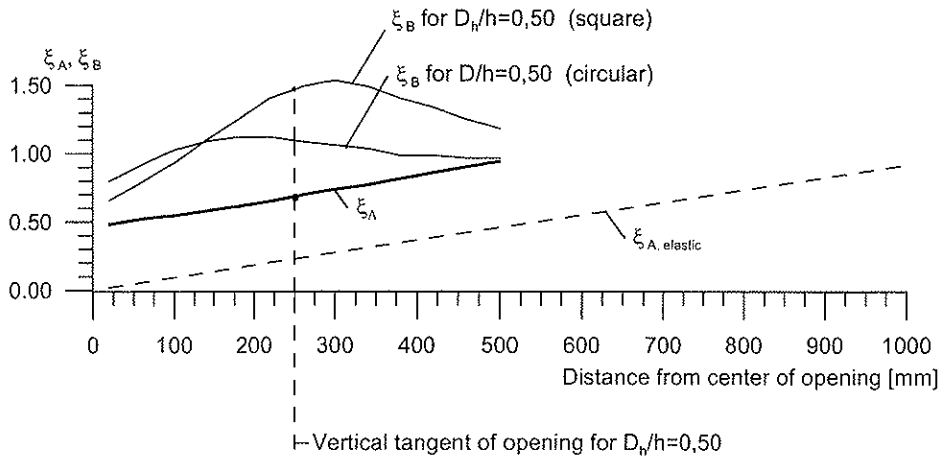


Fig. 9.2.8 Normalized flange forces of girders I125, I125C50 and I125S50 plotted along top flange

9.2.6 Influence of transverse stiffeners

On $\chi_{w,mod}$

The influence of transverse web stiffeners on $\chi_{w,mod}$ in ULS is shown in Table 9.2.2. 12 girders with transverse stiffeners and aspect ratios 2 and 1 are studied. The six girders in Table 9.2.1 and the six girders I63S25, I125S25, I250S25, I63S50, I125S50 and I250S50 are included for comparison. These girders have no transverse stiffeners and the aspect ratio is 4. This gives three h/t ratios, two D_h/h ratios and three a/h ratios and a total of 24 analyses. Material properties and stiffener dimensions are the same as in the girders with circular openings. For some girders with the thinnest webs the transverse stiffeners buckled before the web. These girders are marked with an asterisk in Table 9.2.2. Imperfections were based on the eigenmodes that gave a buckle at the opening. See also Section 9.2.7.

Column 9 of Table 9.2.2 gives the reduction factor for the girders with square openings relative to the one with circular opening, in terms of the ratio c_2 , as given by Eq. (6.3.3). In this comparison the effect of the corners in openings is regarded as a secondary effect, in the same way as the other secondary effects described in Chapter 7 and 8. The reduction in shear capacity is rather consistent for each opening size. The average value of c_2 is 0,93 for the openings with $D_h/h = 0,25$ and 0,77 for the openings with $D_h/h = 0,50$.

Table 9.2.2 $\chi_{w,mod}$ for various h/t , D_h/h , a/h ratios and stiffener sizes

1	2	3	4	5	6	7	8	9
Run	Girder	h/t	D_h/h	a/h	Transverse stiffeners	$\chi_{w,mod}$	$\bar{\lambda}_w$	c_2
232	H63S25	63	0,25	4	-	0,69	0,75	0,92
235	I63S25	63	0,25	4	-	0,66	0,95	0,93
244	I63S25T2	63	0,25	2	FL100x12,5	0,66	0,89	0,92
250	I63S25T1	63	0,25	1	FL100x12,5	0,68	0,74	0,92
233	H125S25	125	0,25	4	-	0,51	1,49	0,93
236	I125S25	125	0,25	4	-	0,44	1,89	0,94
245	I125S25T2	125	0,25	2	FL63x8	0,47	1,78	0,93
251	I125S25T1	125	0,25	1	FL80x10	0,56	1,46	0,89
234	H250S25	250	0,25	4	-	0,32	2,97	0,96
237	I250S25	250	0,25	4	-	0,27	3,78	0,95
246	I250S25T2	250	0,25	2	FL40x5 *	0,32	3,55	0,93
252	I250S25T1	250	0,25	1	FL50x6 *	0,44	2,92	0,93
238	H63S50	63	0,50	4	-	0,36	0,75	0,75
241	I63S50	63	0,50	4	-	0,33	0,95	0,74
247	I63S50T2	63	0,50	2	FL100x12,5	0,33	0,89	0,74
253	I63S50T1	63	0,50	1	FL100x12,5	0,34	0,74	0,75
239	H125S50	125	0,50	4	-	0,26	1,49	0,75
242	I125S50	125	0,50	4	-	0,24	1,89	0,77
248	I125S50T2	125	0,50	2	FL63x8	0,24	1,78	0,76
254	I125S50T1	125	0,50	1	FL80x10	0,34	1,46	0,75
240	H250S50	250	0,50	4	-	0,18	2,97	0,82
243	I250S50	250	0,50	4	-	0,15	3,78	0,83
249	I250S50T2	250	0,50	2	FL40x5	0,17	3,55	0,78
255	I250S50T1	250	0,50	1	FL50x6	0,21	2,92	0,74

The values of $\chi_{w,mod}$ are plotted in Fig. 9.2.9 against relative slenderness, as in Fig. 7.2.20. Fig. 9.2.9 also shows scaled curves based on 70 % and 38 % of the EC3 curve for webs without openings. The ratios are based on $(1-D_h/h)c_2 = 0,75 \cdot 0,93 = 0,70$ and $(1-D_h/h)c_2 = 0,50 \cdot 0,77 = 0,38$; the c_2 - factors are the average values from the simulations.

The results from the simulations with $D_h/h = 0,25$ lie above the 70 % curve, except for the lowest relative slenderness. Similarly, the results from the simulations with $D_h/h = 0,50$ are above the 38 % curve, except for the lowest relative slenderness.

An alternative approach based on a circular opening that enclose the square opening, gives 70 % and 31 % curves, respectively, i.e. the same curve as depicted for the small openings and a conservative curve for the large openings. All simulations of the girders with the large openings lie above a 31 % curve.

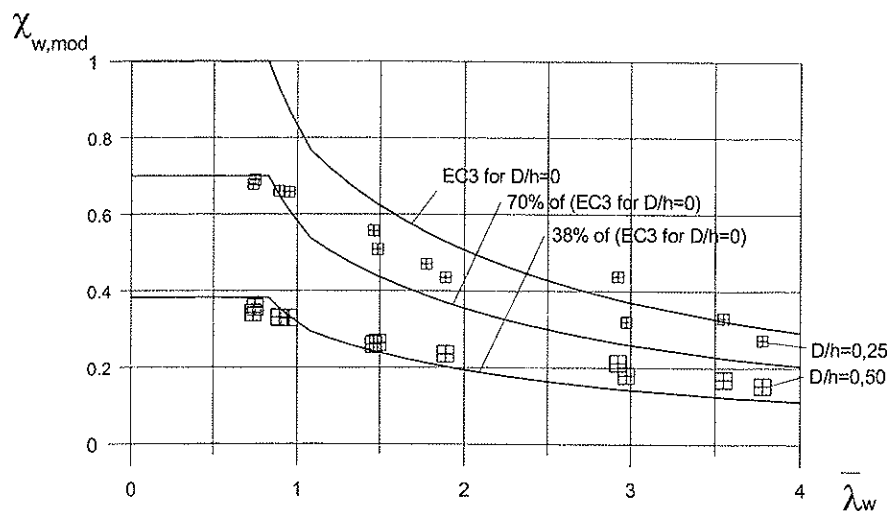


Fig. 9.2.9 $\chi_{w,mod}$ for relative slenderness

Influence of transverse stiffeners on girder stiffness

The vertical tip displacement δ at maximum shear V_{max} for the girders with square openings are about the same as for the corresponding girders with circular openings. Generally, this means that the “girder stiffness”, given by Eq. (7.2.7) and Table 7.2.5, is reduced by the factor c_2 for girders with square openings.

Influence of transverse stiffeners on $\chi_{w,mod}$ in ALS

The reduction factors $\chi_{w,mod}$ for 100 mm tip displacement are smaller than for corresponding girders with circular openings, but the relative reduction is less than for ULS. The response curves are generally of the same shape as in Fig. 7.2.10, but the negative slopes are smaller. Hence, a square opening with sides like the diameter of a circular opening has a clear influence on the ultimate limit capacity, but smaller influence on the ALS shear capacity.

9.2.7 Initial imperfections and eigenmodes

In the literature, buckling of webs with square openings is frequently referred to as local buckling at two corners. The simulations that form the basis for the results listed in Table 9.2.2 show global buckling only, however in some girders the global buckle is divided into two separate regions by the opening. In the simulations the initial imperfections are based on 2. eigenmode, which resembles one global buckle across the compression diagonal. This mode is different from the modes presented in Chapter 5. The present girders have pure

shear in the center of the opening, while the girders in Chapter 5 also have some moment. Perhaps local buckles cannot be expected to occur, unless another eigenmode is used as initial imperfections?

Girders H125S50 and I125S50T1 are reanalyzed using initial imperfections based on higher order eigenmodes in order to assess the sensitivity of the ultimate shear capacity to the mode chosen. For girders in pure shear the eigenvalues occur in pairs, one positive and one negative. As the girder and its finite element model are symmetric, the positive value is associated with a positive shear force and the negative one with a shear force acting in the opposite direction. Hence, only the negative eigenvalues are considered further. Eigenmodes 2, 4 and 6 are shown in Figs. 9.2.10 and 9.2.11 for H125S50 and I125S50T1, respectively. As seen in Table 9.2.3 the second and fourth eigenvalues are farther apart in H125S50 than in I125S50T1. Mode 4 may be interpreted as a local buckling mode in the compression corners, and an additional simulation is carried out for the latter girder using this mode and an amplitude of 7,5 mm as initial imperfection. This simulation is termed I125S50T1a and gives 1 % higher capacity than the simulation based on eigenmode 2. The deformed shape at maximum shear displays a more local pattern. However, too much emphasis should not be placed on this result, as the amplitude chosen may be more important than mode shape. Inspection of Figs. 9.2.8 and 9.2.9 further reveals that eigenmode 6 is associated with local buckling of the vertical edges of the opening for H125S50 and of the horizontal edges for I125S50T1.

An additional girder Q125S50T1e, which is geometrical similar to I125S50 except for reduced flange areas, is also analyzed. The resulting eigenvalues are slightly smaller than those of the latter, but as the web is assumed simply supported at the flanges in the computational model this result is as expected.

Table 9.2.3 Eigenmodes for girders H125S50e, I125S50T1 and Q125S50T1e

1	2	3	4	5	6	7	8
Run	Girder	h/t	D_h/h	a/h	Transverse stiffeners	Mode no.	Eigenvalue
239e	H125S50e	125	0,50	4	-	2	-0,23
						4	-0,28
						6	-0,40
254e	I125S50T1e	125	0,50	1	FL80x10	2	-0,34
						4	-0,37
						6	-0,65
257e	Q125S50T1e has small flanges	125	0,50	1	FL80x10	2	-0,32
						4	-0,35
						6	-0,61

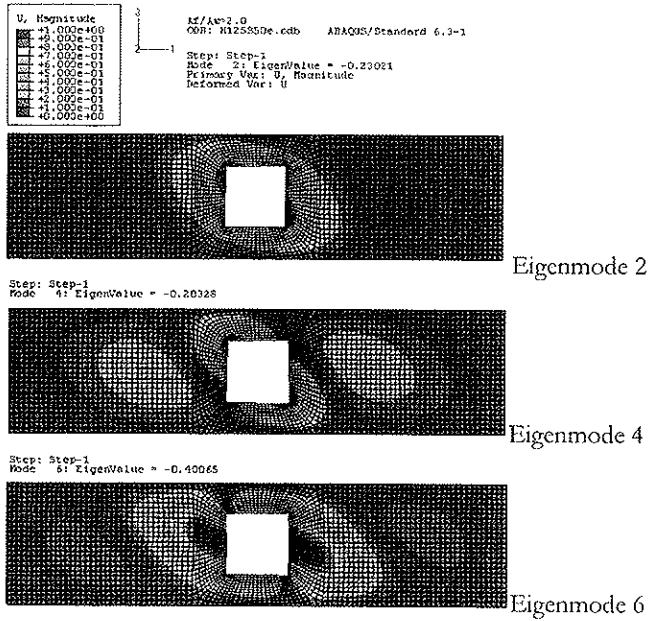


Fig. 9.2.10 Eigenmodes of Girder H125S50

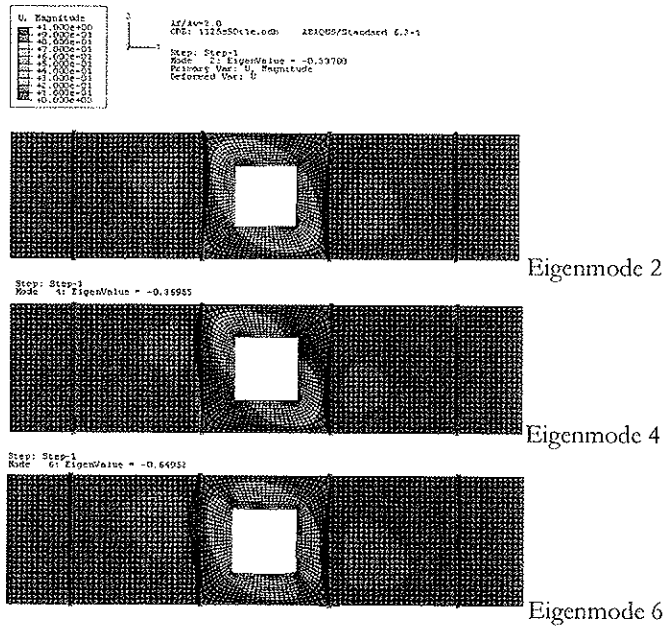


Fig. 9.2.11 Eigenmodes of Girder I125S50T1

9.2.8 Shear and primary moment interaction

The simulations of girders with circular openings showed only a small interaction between shear and primary moment when the flanges were large. For girders with square openings, the additional flange forces caused by secondary moments are relatively larger, as shown in Section 9.2.5. However, it should still be expected that the flange areas must be very small for Eq. (7.2.14) to be invalid. Hence, shear and primary moment interaction for girders with square openings is investigated only for the girder with the smallest flanges in Chapter 7.

The results of six simulations are presented in Table 9.2.4 and plotted in Fig. 9.2.12. The girder considered is similar to I125S50T1, except that the flanges are modeled as rectangular sections FL 200x10. Otherwise the models correspond to those in Table 7.2.9, but with square openings. The flange area is 25 % of the web area, and the flange bending stiffness is also low. The additional flange force at maximum shear is 58 % of the axial force capacity of flange.

Fig. 9.2.12 also shows an interaction curve based on Eq. (7.2.14), for

- $V_{c,mod}$ = 435 kN , which is 35 % of V_c from the EC proposal
- $M_{buckl,mod}$ = 1156 kNm , i.e. same as for the girder with circular opening

All simulated results lie above the curve from Eq. (7.2.14).

Table 9.2.4 Shear and primary moment interaction

1	2	3	4	5
Run	Girder	V_{max} [kN]	M_{max} [kNm]	Remarks
257	Q125S50T1M0	478	0	
258	Q125S50T1M6	448	638	2 steps
259	Q125S50T1M10	331	1020	2 steps
260	Q125S50T1M11	257	1148	2 steps
261	Q125S50T1M12	162	1226	2 steps
262	Q125S50T1M13	-	1247	

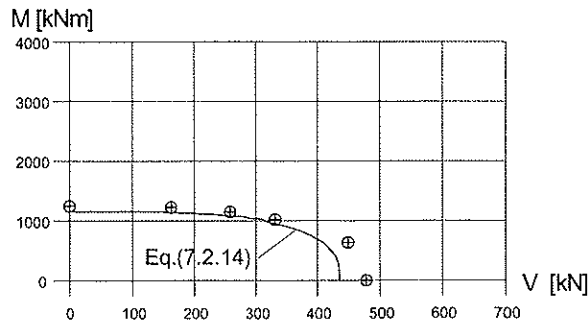


Fig. 9.2.12 Interaction diagram for the results in Table 9.2.4

9.2.9 Openings in lower part of webs

Three girders are studied to determine the effect of having openings in the lower part of webs. The openings of girders I63S50, I125S50 and I250S50T2 are lowered, such that only 40 mm is left of the web between the opening and flange.

Table 9.2.4 shows the result for $\chi_{w,mod}$. Column 8 shows the effect of a lowered square opening relative to that of a girder with circular opening at mid-height, by means of the factor c_2 , as given in Eq. (6.3.3).

Reduced shear capacity occurs for all girders. However, the relative reduction when a square opening is lowered, is less than when a circular opening is lowered.

Table 9.2.4 Effect of lowered openings on $\chi_{w,mod}$

1	2	3	3	4	6	7	8
Run	Girder	h/t	D_h/h	a/h	Transverse stiffeners	$\chi_{w,mod}$	c_2
263	M63S50	63	0,50	4	-	0,31	0,70
264	M125S50	125	0,50	4	-	0,20	0,67
265	M250S50T2	250	0,50	2	FL63x8	0,19	0,86

9.3 Single opening with horizontal reinforcement

9.3.1 Reinforcement on one side of web

Horizontal stiffeners/reinforcement may be considered as an analogy to sleeves for circular openings. For circular openings most of the effect is to alter the shape and the size of the buckle. For square openings the main effect is reinforcement in the corners. Reinforcement on one side only is a preferred solution in practice, due to relative small fabrication cost.

The results of 18 simulations are presented in Table 9.3.1. The labels identifying these girders have the prefix J, otherwise the scheme for describing web slenderness and opening size, shape and location is as before. The size of reinforcement is for all girders chosen such that the weight of the reinforcement is equal to the weight of the removed plate in the opening. As the length of reinforcement is twice the length of the opening, this should have given the same section sizes as the sleeves of Table 7.3.1. However, to fulfill two more requirements for horizontal reinforcement, the section areas are increased about 15%. These requirements are

- Axial capacity of reinforcement at corners is equal to the maximum shear capacity of the anchor length.

- Thickness of reinforcement is equal or greater than the thickness of the web. This ensures that full yield shear capacity can develop in the minimum section above and below the opening.

The weight limit is maintained by snipping off the reinforcement at the ends. For some girders the requirements may be superfluous for one-side-reinforcement, but are retained in order to arrive at consistent solutions, and to allow comparison with horizontal reinforcement on both sides of web in the next section. Width/thickness ratio of reinforcement varies from 4,5 to 9. The reinforcements are “welded” to the web 20 mm from the edge of the opening. Initial imperfections are based on the lowest eigenmodes from each model and amplitude 7,5 mm. For Girder J250S50T1 two eigenmodes had to be used; one with a buckle in the field opposite to the transverse stiffener near the opening and one with a buckle in the unstiffened vertical sides of the opening.

The resulting values of $\chi_{v,mod}$ are given in Table 9.2.1. The table also shows the influence of the horizontal reinforcement, relative to the circular opening without stiffening in the corresponding web and stiffener configuration, in terms of the factor c_2 . Alternatively, the effect of horizontal reinforcements may be compared to the girders with the same square opening without reinforcements by means of the factor c_{rel} , taken as the ratio between $\chi_{v,mod}$ and $\chi_{w,mod}$ as given in Table 9.2.2.

The effect of horizontal reinforcements are considerable, especially for the larger openings, where up to 89 % increased shear capacity is achieved.

In Fig. 9.3.1 $\chi_{w,mod}$ is plotted against the relative slenderness. A curve for the EC3 proposal for webs without openings is also included, together with scaled curves for 75 % and 50 % of the proposal. The relative slenderness of the girders JxxS50T1 is based on the aspect ratio $a/h = 0,25$, in stead of 1, as the horizontal reinforcements span the transverse stiffeners completely.

Most girders achieve the shear capacities given by the scaled curves. For all girders the shear capacity is lower than the yield shear in the minimum section above and below the opening. For the cases with high slenderness, the shear capacities are in general far below the shear capacity of the web without opening.

For ALS the girder J63S50T1 shows an increased shear capacity compared to ULS, the only case in the present investigation to have a such response curve. The ULS shear capacity was taken from the shear force value at 23 mm tip displacement, corresponding to the tip displacement at maximum shear for Girder J63S50T2.

Table 9.3.1 Effect of horizontal reinforcements on one side of web on $\chi_{w,mod}$

1	2	3	4	5	6	7	8	9
Run	Girder	h/t	D_h/h	a/h	Horizontal reinforcement	$\chi_{w,mod}$	c_2	C_{rel}
266	J63S25	63	0,25	4	FL72x16	0,69	0,97	1,04
272	J63S25T2	63	0,25	2	FL72x16	0,70	0,97	1,06
278	J63S25T1	63	0,25	1	FL72x16	0,73	1,00	1,08
267	J125S25	125	0,25	4	FL72x8	0,45	0,94	1,04
273	J125S25T2	125	0,25	2	FL72x8	0,49	0,97	1,05
279	J125S25T1	125	0,25	1	FL72x8	0,64	1,02	1,15
268	J250S25	250	0,25	4	FL46x6,3	0,29	0,95	1,06
274	J250S25T2	250	0,25	2	FL46x6,3	0,36	1,02	1,09
280	J250S25T1	250	0,25	1	FL46x6,3	0,49	1,04	1,11
269	J63S50	63	0,50	4	FL144x16	0,44	1,00	1,35
275	J63S50T2	63	0,50	2	FL144x16	0,45	1,02	1,38
281	J63S50T1	63	0,50	1 (0,25)	FL144x16	0,45	0,99	1,33
270	J125S50	125	0,50	4	FL92x12,5	0,28	0,93	1,20
276	J125S50T2	125	0,50	2	FL92x12,5	0,30	0,94	1,24
282	J125S50T1	125	0,50	1 (0,25)	FL92x12,5	0,44	1,21	1,69
271	J250S50	250	0,50	4	FL72x8	0,19	1,06	1,28
277	J250S50T2	250	0,50	2	FL72x8	0,25	1,13	1,45
283	J250S50T1	250	0,50	1 (0,25)	FL72x8	0,40	1,40	1,89

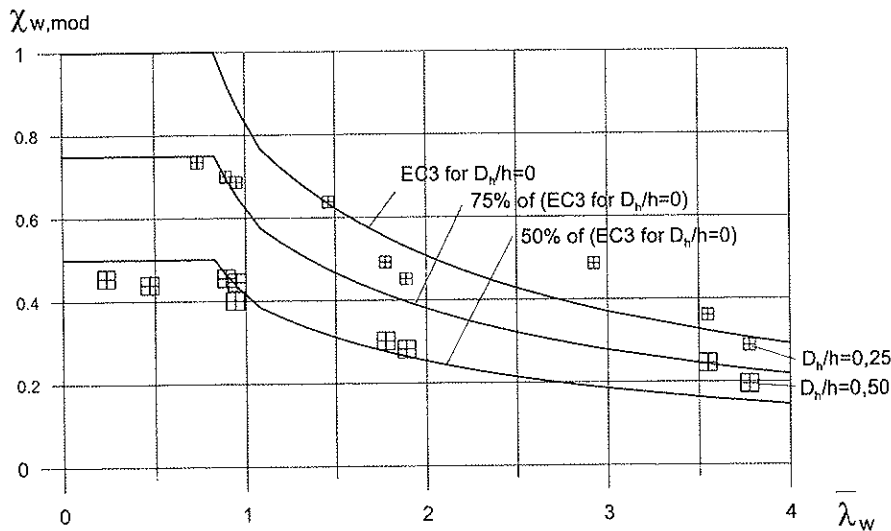


Fig. 9.3.1 $\chi_{w,mod}$ for relative slenderness when $f_y = 420 \text{ N/mm}^2$ and horizontal reinforcements on one side of web are used

9.3.2 Reinforcements on both side of webs

The shear capacity may be increased by using horizontal reinforcements on both sides. To see how much, the girders J125S50 and J250S50 are modified and denoted J125S50C and J250S50C. The modification is that each horizontal reinforcement is split into two halves, placed on each side of the web. Hence, the horizontal reinforcements act centric relative to the web plane.

Table 9.3.2 shows the factors $\chi_{w,mod}$ and c_2 . Column 9 shows the effect of centric reinforcements compared to the case with eccentric reinforcements by means of the factor c_{rel} , i.e. the ratio between $\chi_{w,mod}$ and the corresponding $\chi_{w,mod}$, as given in Table 9.3.1. The benefit of centric reinforcements increases with decreasing relative slenderness. The effect may be estimated to 15 to 13 %. It should be noted that the increased strength is due to some yielding, which explains the more “rounded top” in the response curves before the strength decreases. In ALS nothing is gained from using centric reinforcements compared to reinforcements on one side only.

Table 9.3.2 Effect of centric horizontal reinforcements on $\chi_{w,mod}$

1	2	3	4	5	6	7	8	9
Run	Girder	h/t	D_h/h	a/h	Horizontal reinforcements	$\chi_{w,mod}$	c_2	c_{rel}
284	J125S50C	125	0,50	4	2FL 46x12,5	0,32	1,07	1,15
285	J250S50C	250	0,50	4	2FL 36x8	0,22	1,20	1,13

9.4 Single opening with vertical stiffeners

As shown, the shear capacity of webs with openings is often governed by global buckling. An idea of increasing the capacity by simply suppressing the global buckle is near at hand. It should be sufficient to block the buckle in the position of the opening only. For openings with $D_h/h = 0,50$ this could be done by using the horizontal reinforcements as vertical stiffeners in stead. The stiffener length is sufficient to span the full height between the flanges. The required stiffness of the stiffeners may perhaps also be reduced compared to stiffeners required to stiffen the web for full global shear buckling load.

Two simulations have been made; girders L63S50 and L125S50 are copies of J63S50 and J125S50, but with the horizontal reinforcement used as vertical stiffeners. This actually subdivides the girders into panels with aspect ratio $a/h = 0,5$, a case that was studied in Section 7.2. However, the stiffeners of L63S50 are larger than those of I63T0, and the stiffeners of L125S50 are smaller than those used in I125T0. The 10. eigenmode, that activates local buckling of the horizontal edges of the opening, is included as an additional imperfection, using an amplitude of 4,1 mm.

Table 9.3.1 gives the results in terms of the reduction factor $\chi_{w,mod}$ and the ratios c_2 and c_{rel} . The ratio c_2 refers to the girders I63C50T0 and I125C50T0 and c_{rel} compares the capacity to the cases where the stiffeners are horizontal.

The effect of the new stiffener configuration is negative for L63S50, but positive for L125S50, with 22 % increase.

Table 9.4.1 Effect of vertical stiffeners on $\chi_{w,mod}$

1	2	3	4	5	6	7	8	9
Run	Model	h/t	D/h	a/h	Vertical stiffeners	$\chi_{w,mod}$	c_2	c_{rel}
294	L63S50	63	0,50	0,5	FL144x16	0,38	0,78	0,85
286	L125S50	125	0,50	0,5	FL92x12,5	0,34	0,79	1,22

The deformed shape of L125S50 at maximum shear is shown in Fig. 9.4.1. The global buckle is suppressed, but local buckles occur above and below the opening. The transverse displacements are relatively small.

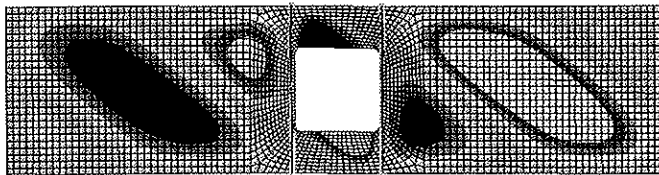


Fig. 9.4.1 Buckles for Girder L125S50

9.5 Single opening with horizontal reinforcement and vertical stiffeners

9.5.1 General

It was shown in Section 9.3 and 9.4 that an improved shear capacity can be achieved, either by horizontal reinforcement or by vertical stiffening. Horizontal reinforcement increases the secondary moment capacity, and vertical stiffening suppresses the global buckling. The best design depends on the relative slenderness of the unstiffened web. In Section 9.3 and 9.4 no girders with openings $D_h/h = 0,50$ reached the full plastic capacity of the remaining web. Another solution may be to use both horizontal reinforcement and vertical stiffeners, which can be done in many ways. In the present investigation the reinforcement/stiffener configurations are grouped according to the required amount of material needed for the reinforcement/stiffening.

The weight of reinforcement/stiffeners is normalized to

$$\mu = \frac{m_s}{m_o} \quad (9.5.1)$$

where m_s is the weight of reinforcement/stiffeners and m_o is the weight of the removed plate material in the opening. Three groups of configurations with $\mu = 1,0, 1,5$ and $2,0$, respectively, are considered. For all configurations an "efficiency index" is calculated on the form

$$H_e = \frac{\chi_{w,mod,B} - \chi_{w,mod,A}}{\mu_B} \quad (9.5.2)$$

where $\chi_{w,mod,B}$ and μ_B refer to the girder that is compared, and $\chi_{w,mod,A}$ is the value achieved for the reference girder, i.e. the girder with similar opening and web, but without any reinforcement and stiffening. Hence, H_e measures the gain in shear capacity relative to the amount of material that has to be used in order to obtain the gain.

9.5.2 Girders with $\mu = 1,0$

Four simulations are made; two with narrow and thick stiffeners and two with higher and thinner stiffeners.

Girders JL125S50a has two vertical stiffeners on one side and two horizontal reinforcements on the opposite side. This is a preferred solution from a fabrication point of view. Girder JL125S50b has the same stiffeners and reinforcement, but on the same side. All stiffeners and reinforcements are FL46x12,5. Hence, the sectional area of the horizontal reinforcements is only half of the area required to take the secondary moments in a Vierendeel analogy. The initial imperfections used are the sum of the 2. eigenmode, with buckles in the adjacent plate panels, and the 19. eigenmode, with buckles in the vertical stiffeners *and* adjacent plate panels. Amplitudes for each eigenmode are 7,5 mm. The eigenmodes are only to a small degree overlapping or cancelling.

Girders JL125S50k and JL125S50l repeat the arrangement from the previous girders, but with FL72x8 as stiffeners/reinforcement. Here, the 20. eigenmode replaces the 19. eigenmode used in the previous analyses.

The results are presented in Table 9.5.1. The girders J125S50 and J125S50C, with horizontal reinforcement only, and L125S50, with vertical stiffeners only, are included for comparison. These girders also have $\mu = 1,0$.

Columns 7 and 8 give $\chi_{w,mod}$ and factor c_2 . The reference girder for c_2 is I125C50. Column 9 shows the effect of stiffeners compared to opening without stiffeners, in terms of c_{rel} , i.e. the ratio between $\chi_{w,mod}$ and $\chi_{w,mod}$ for Girder I125S50 in Table 9.2.2. Column 10 shows the efficiency index, based on the reference girder I125S50.

The four girders with both vertical stiffeners and horizontal reinforcement are clearly better than the girders with either vertical stiffener *or* horizontal reinforcements. The shear capacities of the four girders do not show much variation, but JL125S50a is most efficient. This girder has narrow and thick stiffeners/reinforcements, and the vertical stiffeners are on the opposite side of the horizontal reinforcements.

The buckled shape at maximum shear for JL125S50a is shown in Fig. 9.5.1. Transverse displacement of vertical stiffeners is small up to a load of about 90 % of the maximum shear. When this value is reached, the vertical stiffeners buckle, but the transverse web displacement remains relatively small also at maximum shear.

Von Mises stress at maximum shear is shown in Figs. 9.5.2 and 9.5.3. The positive surfaces are the surfaces facing the viewer. The stress in the upper horizontal reinforcement is shown on the positive surface and in the lower horizontal reinforcement on the lower surface. The left vertical stiffener in Fig. 9.5.2 appears as the right hand stiffener in Fig. 9.5.3. The stress in this stiffener in Fig. 9.5.3 is shown on the positive surface. For the other vertical stiffener the stress is shown on the negative surface.

Table 9.5.1 Effect of reinforcement/stiffeners for $\mu = 1,0$

1	2	3	4	5	6	7	8	9	10
Run	Girder	h/t	D_h/h	a/h	Reinforcement/ stiffeners	$\chi_{w,mod}$	c_2	c_{rel}	H_e
270	J125S50	125	0,50	4	H: 2FL 92x12,5 V: -	0,28	0,93	1,20	0,04
285	J125S50C	125	0,50	4	H: 4FL 46x12,5 V: -	0,32	1,07	1,38	0,08
286	L125S50	125	0,50	0,5	H: - V: 2FL92x12,5	0,34	1,14	1,47	0,10
287	JL125S50a	125	0,50	0,5	H: 2FL46x12,5 V: 2FL46x12,5	0,44	1,46	1,88	0,20
288	JL125S50b	125	0,50	0,5	H: 2FL46x12,5 V: 2FL46x12,5	0,42	1,38	1,79	0,18
296	JL125S50k	125	0,50	0,5	H: 2FL72x8 V: 2FL72x8	0,44	1,45	1,88	0,20
297	JL125S50l	125	0,50	0,5	H: 2FL72x8 V: 2FL72x8	0,43	1,43	1,85	0,19

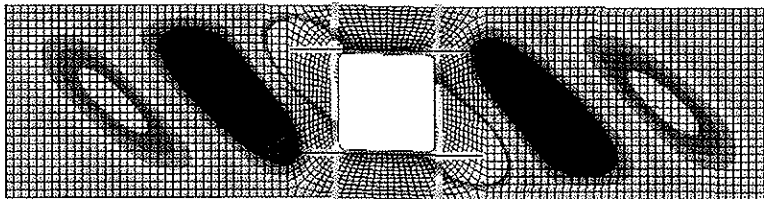


Fig. 9.5.1 Buckles of Girder JL125S50a at maximum shear

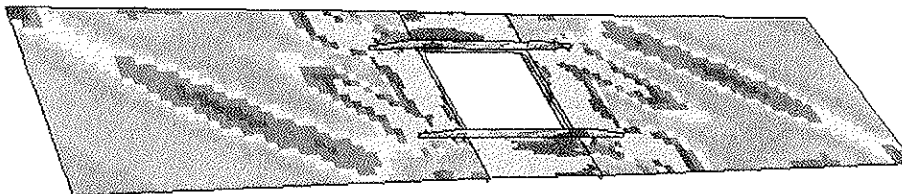
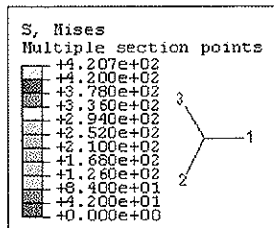


Fig. 9.5.2 Von Mises stress in positive surface of Girder JL125S50a at maximum shear

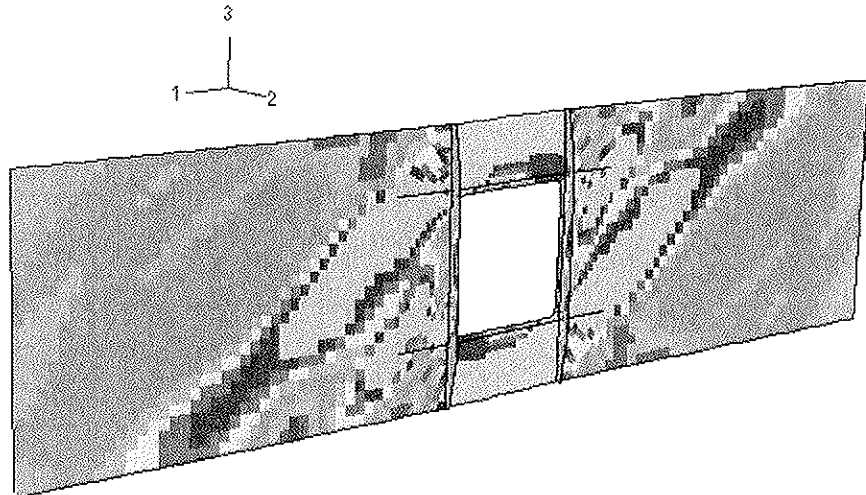


Fig. 9.5.3 Von Mises stress in negative surface of Girder JL125S50a at maximum shear

9.5.3 Girders with $\mu = 1,5$

Five simulations are made; two with narrow and thick stiffeners and three with wide and thinner stiffeners. Initial imperfections are similar to those described in Section 9.5.2.

Girder JL125S50c has two vertical stiffeners on one side and two horizontal reinforcements on the opposite side. Girder JL125S50d has the same vertical stiffeners, but the horizontal reinforcements are split in to halves, one on each side. Vertical stiffeners are FL46x12,5 and horizontal reinforcements are FL92x12,5 or 2FL46x12,5. The section area of the horizontal reinforcements is sufficient to sustain the secondary moments in a Vierendeel analogy.

Girders JL125S50h and JL125S50o have the same stiffener configurations as the previous girders, but with FL72x8 and FL92x12,5 as stiffeners/reinforcements, alternatively 2FL72x8. Girder JL125S50m is similar to JL125S50h, but with all stiffeners/reinforcement on the same side.

The results are presented in Table 9.5.2. The reference girder for c_2 is I125C50. Column 9 shows the effect of increased horizontal reinforcement compared to the best girder presented in Section 9.5.2, given as c_{rel} . This is the ratio between $\chi_{w,mod}$ and $\chi_{w,mod,rel}$ for JL125S50a as given in Table 9.5.1. The efficiency index H_e is again based on the reference girder I125S50.

The five girders are marginally better than the best one of the previous section. The shear capacities show little variation, with JL125S50o as the most efficient. This girder has wide and thin stiffeners and horizontal reinforcements on both sides. With respect to fabrication, Girder JL125S50h is best, and gives almost same shear capacity as JL125S50o.

Table 9.5.2 Effect of stiffeners/reinforcement for $\mu = 1,5$

1	2	3	4	5	6	7	8	9	10
Run	Girder	h/t	D_h/h	a/h	Stiffeners	$\chi_{w,mod}$	c_2	c_{rel}	H_e
289	JL125S50c	125	0,50	0,5	H: 2FL 92x12,5 V: 2FL46x12,5	0,45	1,49	1,02	0,14
290	JL125S50d	125	0,50	0,5	H: 4FL 46x12,5 V: 2FL46x12,5	0,45	1,47	1,01	0,14
295	JL125S50h	125	0,50	0,5	H: 2FL92x12,5 V: 2FL72x8	0,46	1,52	1,04	0,15
298	JL125S50m	125	0,50	0,5	H: 2FL92x12,5 V: 2FL72x8	0,46	1,51	1,03	0,15
299	JL125S50o	125	0,50	0,5	H: 4FL72x8 V: 2FL72x8	0,47	1,55	1,06	0,16

9.5.4 Girders with $\mu = 2,0$

Four girders are considered, one with narrow and thick stiffeners and three with wider and thinner stiffeners. Initial imperfections are similar to those previously used in Section 9.5.2.

Girder JL125S50e has two vertical stiffeners on one side and two horizontal reinforcements on the opposite side. In Girder JL125S50p the vertical stiffeners and the horizontal reinforcements are placed one on each side. Stiffeners are FL92x12,5 or 2FL72x8. In both cases the cross section area of horizontal reinforcement is sufficient to sustain the secondary moments in a Vierendeel analogy. Girder JL125S50p is close to the theoretically ultimate design for centric stiffeners and horizontal reinforcements.

Girders JL125S50f and JL125S50g represent typical stressed skin design. JL125S50f has four vertical stiffeners on one side and two horizontal reinforcements on the opposite side; see Figs. 9.5.4 and 9.5.5. Vertical stiffeners are FL72x8, two of these are placed at the ends of the horizontal reinforcements and two at the opening. Stiffeners and reinforcements have section areas sufficient to develop yield shear in the web above and below the opening, when buckling is disregarded. Girder JL125S50g is similar to JL125S50f, but with all stiffeners and reinforcement on the same side.

The results are presented in Table 9.5.3 in terms of $\chi_{w,mod}$ and c_2 . The reference girder for c_2 is I125C50. Column 9 shows the effect of increased horizontal reinforcement compared to the best girder of Section 9.5.3, in terms of c_{rel} , i.e. the ratio between $\chi_{w,mod}$ and $\chi_{w,mod}$ for JL125S50o as given in Table 9.5.2. The efficiency index is based on the reference girder I125S50.

Only JL125S50p gives higher shear capacity than the best girder of the previous section. This is really the optimum design if the goal is to achieve as high shear capacity as possible, giving 95 % of full plastic capacity. However, the efficiency is more doubtful. With 33 % more material and the stiffeners split in many small parts, the gain in shear capacity is only 3 % compared to JL125S50h.

The results for all four girders may also be compared to Girder S15 of the experiments referred in Chapter 4. Girder S15 was quite heavily stiffened, with $\mu = 6,3$. However, with $\chi_{w,mod} = 0,48$, it had only marginally more shear capacity than the girders in Table 9.5.3.

The extra vertical stiffeners in cases JL125S50f and JL125S50g seem superfluous when compared to JL125S50m. Von Mises stress at maximum shear for JL125S50f is shown in Figs. 9.5.4 and 9.5.5. The legend is the same as in Fig. 9.5.2.

Table 9.5.3 Effect of stiffeners/reinforcement for $\mu = 2,0$

1	2	3	4	5	6	7	8	9	10
Run	Girder	h/t	D_h/h	a/h	Reinforcement/ stiffeners	$\chi_{w,mod}$	c_2	c_{rel}	H_e
291	JL125S50c	125	0,50	0,5	H: 2FL92x12,5 V: 2FL92x12,5	0,47	1,54	0,99	0,12
300	JL125S50p	125	0,50	0,5	H: 4FL72x8 V: 4FL72x8	0,48	1,57	1,01	0,12
292	JL125S50f	125	0,50	0,5	H: 2FL92x12,5 V: 4FL72x8	0,47	1,54	0,99	0,12
293	JL125S50g	125	0,50	0,5	H: 2FL92x12,5 V: 4FL72x8	0,46	1,51	0,98	0,11

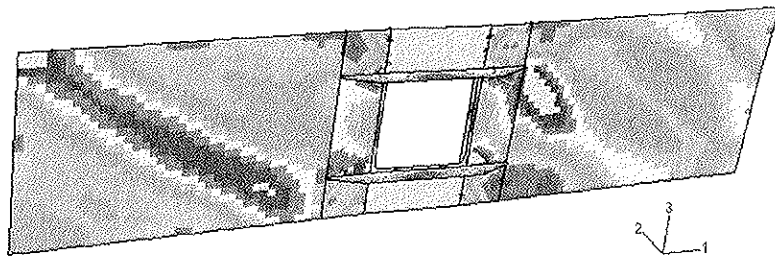


Fig. 9.5.4 Von Mises stress in negative surface of Girder JL125S50f at maximum shear

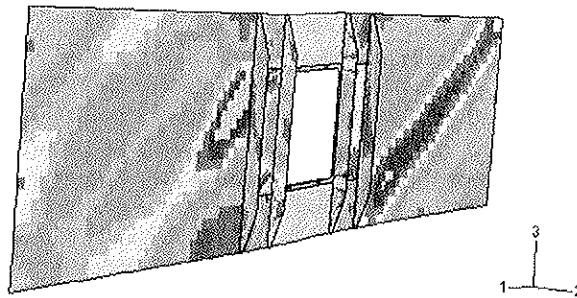


Fig. 9.5.5 Von Mises stress in negative surface of Girder JL125S50f at maximum shear

9.5.5 Comparison of the efficiency index H_e

The values of H_e from Tables 9.5.1, 9.5.2 and 9.5.3 are plotted against μ in Fig. 9.5.6. A value of H_e for Girder S15 is also included. The diagram shows that the efficiency decreases with increasing amount of material, and there is a large variation of the values for $\mu = 1,0$. The best design with respect to way of applying reinforcement and stiffeners is discussed further in Chapter 11.

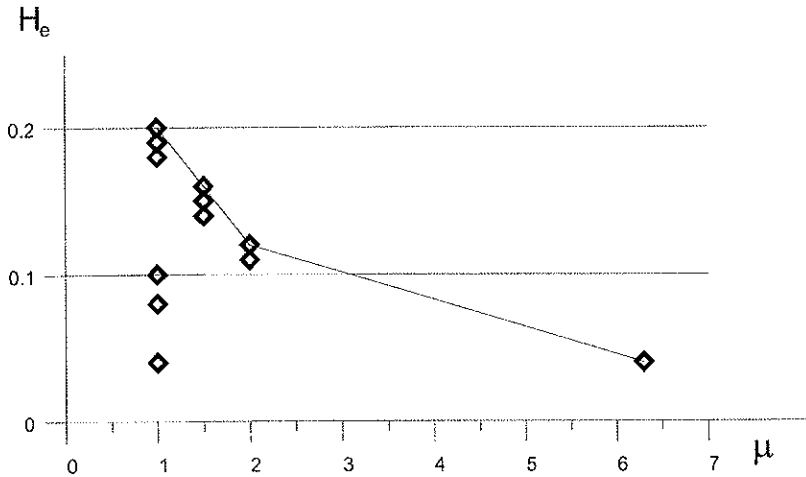


Fig. 9.5.6 Efficiency of reinforcement and stiffeners

9.5.6 Openings in lower part of webs

Girder M125S50 in Section 9.2.9 has been fitted with vertical stiffeners and horizontal reinforcement. NL125S50a has two vertical stiffeners only, and NL125S50b has two vertical stiffeners on one side and one horizontal reinforcement on the opposite side. The section area of the horizontal reinforcement is sufficient to sustain the secondary moments in a Vierendeel analogy. Both girders have $\mu = 1,0$.

The results of the simulations are presented in Table 9.5.4. Column 9 shows the influence of the stiffeners and reinforcement relative to the girder without stiffeners and reinforcement, as c_{rel} , i.e. the ratio between $\chi_{w,mod}$ and $\chi_{w,mod}$ for M125S50 in Table 9.2.4. Column 10 shows the efficiency index, based on the reference girder M125S50.

The effect of stiffeners is good for both girders. The shear capacity of Girder NL125S50a is higher than the result for L125S50 given in Table 9.5.1. The shear capacity of Girder NL125S50b is 96 % of the result for JL125S50a in Table 9.5.1. This confirms the theory of stressed skin, that the position of the opening has little or no influence on the shear capacity.

Table 9.5.4 Effect of stiffeners/reinforcement when $\mu = 1,0$

1	2	3	4	5	6	7	8	9	10
Run	Girder	h/t	D_h/h	a/h	Reinf./stiffeners	$\chi_{w,mod}$	c_2	c_{rel}	H_c
301	NL125S50a	125	0,50	0,5	H: - V: 2FL92x12,5	0,36	1,19	1,79	0,16
302	NL125S50b	125	0,50	0,5	H: 1FL92x12,5 V: 2FL72x8	0,43	1,40	2,10	0,22

9.6 Two openings without stiffening

9.6.1 Two openings horizontally spaced

Girders with two closely spaced square openings along the web are rare in practice, and are scarcely discussed in the literature. Here, four such designs are studied, all with the opening dimension $D_h/h = 0,50$. The girders are modifications of I63S50 and I125S50, with center to center distances between the openings of $c_a = 1,5D_h$ and $c_a = 3D_h$. This gives a clear distance between the openings of $S_a = 0,5D_h$ and $S_a = 2D_h$, respectively. The girders are given identifiers with prefixes S and U; the former referring to the closely spaced openings and the latter to the widely separated openings. The girders are depicted in Fig. 9.6.2.

The results of the simulations are given in Table 9.6.1 in terms of $\chi_{w,mod}$ and the factor c_2 . In addition, the ratio c_{rel} between shear capacities of girders with widely spaced openings to those with one opening, is given in Column 10. The reference girders are I63S50 and I125S50 with $\chi_{w,mod}$ as given in Table 9.2.2.

The ratio c_{rel} is plotted in Fig. 9.6.1 against the ratios S_a/D_h and c_a/D_h . For the thickest web the interaction between two openings has almost disappeared for $S_a/D_h = 2$. For the thinner web, the interaction has not completely disappeared for $S_a/D_h = 2$, and the reason may be that two openings disturb the buckle patterns far away from the web post between the openings.

For the girders with the thinnest webs, the buckles at maximum shear are shown in Fig. 9.6.2. Compared to the girder with a single opening, the buckles are somewhat extended, but amplitudes are about the same.

The response curves for webs with two openings show a slightly more "soft" transition at the point of maximum shear, but except for the value of maximum shear, there is no significant difference compared to the corresponding curves for single openings.

Table 9.6.1 Effect of increased horizontal distance between two openings

1	2	3	4	5	6	7	8	9	10
Run	Girder	h/t	D_h/h	a/h	c_a/D_h	S_a/D_h	$\chi_{w,mod}$	c_2	c_{rel}
309	S63S50a	63	0,50	4	1,5	0,5	0,24	0,53	0,72
305	U63S50	63	0,50	4	3	2	0,33	0,73	0,99
310	S125S50a	125	0,50	4	1,5	0,5	0,16	0,54	0,70
306	U125S50	125	0,50	4	3	2	0,21	0,71	0,91

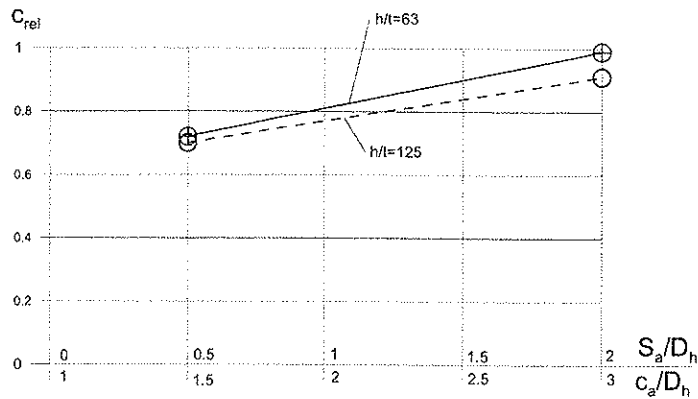


Fig. 9.6.1 Reduction of shear capacity for girders with two openings compared to girders with a single opening. Horizontal spacing, $D_h/h = 0,50$ and $f_y = 420 \text{ N/mm}^2$

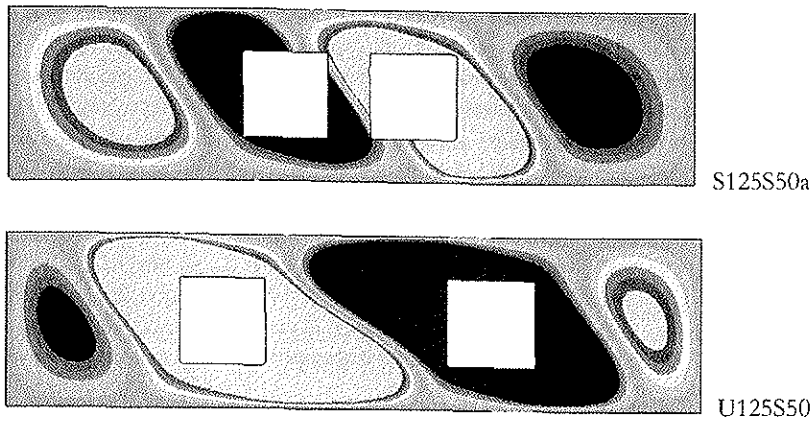


Fig. 9.6.2 Buckles for girders S125S50a and U125S50 at maximum shear

9.6.2 Two openings vertically spaced

Two or more adjacent square openings in the same vertical section of a web are not very common in design of girders, but occur from time to time. The author does not know about descriptions in the literature. Four simulations of girders with two openings with dimensions $D_h/h = 0,25$ are carried out, using girders I63S25 and I125S25 as bases. The vertical center to center distances are $c_h = 1,5D_h$ and $c_h = 3D_h$, giving clear spacing of $S_h = 0,5D_h$ and $S_h = 2D_h$, respectively. The girder identifiers have prefixes SH and UH, referring to clear spacing of 0,5 and 2, respectively. The girders are depicted in Fig. 9.6.4.

The results of the simulations are given in Table 9.6.2 in terms of $\chi_{w,mod}$ and c_2 . Values for the girders I63R2550 and I125R2550 are also included, based on the results in Section 10.2.2 for girders with rectangular openings. Here, the girders are considered as girders

with two openings in the limit where $S_h/D_h = 0$. The factors c_2 are based on the reference girders I63C25 and I125C25. These girders have one circular opening that are only 50 % of the sum of the vertical dimensions of the openings in the girders with two vertically spaced openings.

The values for $\chi_{w,mod}$ in Table 9.6.2 are much lower than the corresponding values for the girders with single opening. The main reason is that the shear area is reduced.

The factor c_2 is plotted in Fig. 9.6.3 against the ratios S_h/D_h , and c_h/D_h . For the thickest web there is a small decrease in the shear capacity when the openings are wider spaced. For the thinnest web there is a small increase in the shear capacity.

For the girders with the thinnest webs, the buckled shapes at maximum shear are shown in Fig. 9.6.4. Compared to the girder with a single opening, the buckles are somewhat extended, but the amplitudes are about the same.

The response curves for webs with two vertically spaced openings show a slightly softer transition at maximum shear. But, except for the value of maximum shear capacities, the curves differ little from to the corresponding curves for single openings.

Table 9.6.2 Effect of increased vertical distance between two openings

1	2	3	4	5	6	7	8	9
Run	Girder	h/t	D_h/h	a/h	c_h/D_h	S_h/D_h	$\chi_{w,mod}$	c_2
315	I63R2550	63	0,25	4	1,0	0	0,43	0,61
307	SH63S25	63	0,25	4	1,5	0,5	0,39	0,55
311	UH63S25	63	0,25	4	3	2	0,38	0,53
316	I63R2550	125	0,25	4	1,0	0	0,30	0,66
308	SH125S25	125	0,25	4	1,5	0,5	0,30	0,65
312	UH125S25	125	0,25	4	3	2	0,31	0,67

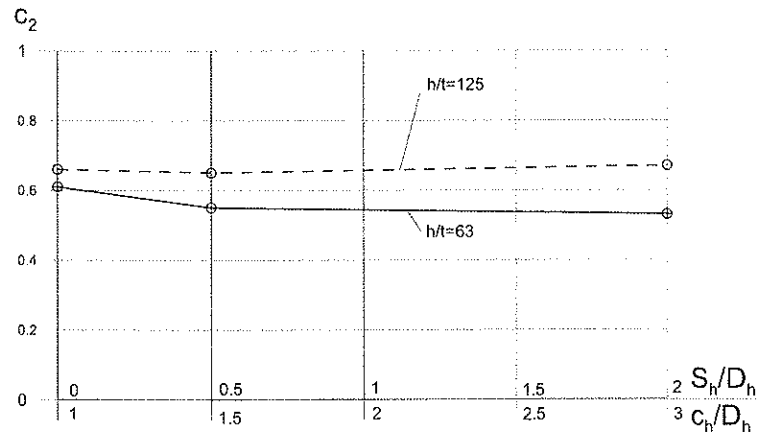


Fig. 9.6.3 Reduction of shear capacity for webs with two openings of $D_h/h = 0,25$ compared to webs with a single opening of $D_h/h = 0,25$. Vertical spacing $f_y = 420 \text{ N/mm}^2$

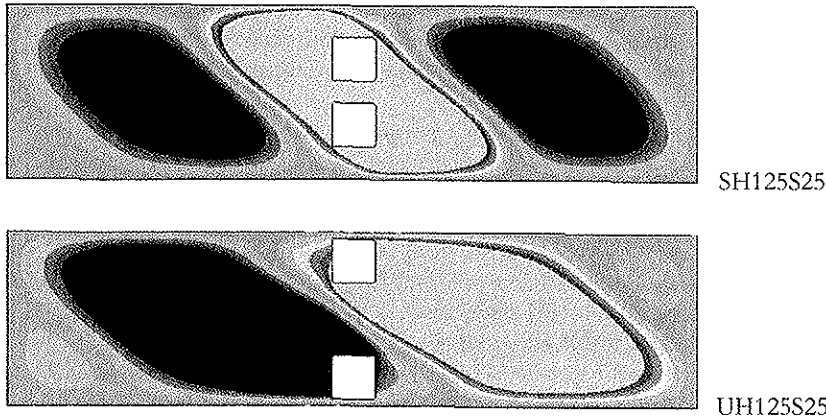


Fig. 9.6.4 Buckles for girders SH125S25 and UH125S25 at maximum shear

9.7 Two openings with stiffeners and reinforcement

9.7.1 Simulations

Girder S125S50a of Table 9.6.1 is modified to include vertical stiffeners and horizontal reinforcement. Girder WL125S50a has four vertical stiffeners only, with $\mu = 0,5$ for each opening. Girder WL125S50b has four vertical stiffeners on one side of web and two horizontal reinforcements on the other side, with $\mu = 1,5$ for each opening.

Results for the two girders are presented in Table 9.7.1. in terms of $\chi_{w,mod}$ and factor c_2 , the latter is based on W125C50 as the reference girder. Column 9 shows the influence of the stiffeners and reinforcement on the shear capacity relative to that of the girder without stiffeners and reinforcement, by means of c_{rel} , i.e. the ratio between $\chi_{w,mod}$ and $\chi_{w,mod}$ for Girder S125S50a. Column 10 shows the efficiency index H_e , based on the reference girder S125S50a.

The effect of stiffeners and reinforcement is good for both girders, with the efficiency of the vertical stiffeners highest. However, the shear capacity of Girder WL125S50a is lower than that of L125S50, as given in Table 9.5.1. The shear capacity of WL125S50b is 90 % of the result for JL125S50a in Table 9.5.1.

Fig. 9.7.1 shows the buckled shape at maximum shear for WL125S50b.

Table 9.7.1 Effect of stiffeners/reinforcements for two openings with spacing $S_a/D_h = 0,5$

1	2	3	4	5	6	7	8	9	10
Run	Girder	h/t	D_h/h	a/h	Reinforcement/ stiffeners	$\chi_{w,mod}$	c_2	c_{rel}	H_e
312	WL125S50a	125	0,50	0,5	H: - V: 4FL92x12,5	0,26	0,65	1,62	0,20
313	WL125S50b	125	0,50	0,5	H: 4FL82x8 V: 4FL72x8	0,40	0,97	2,44	0,16

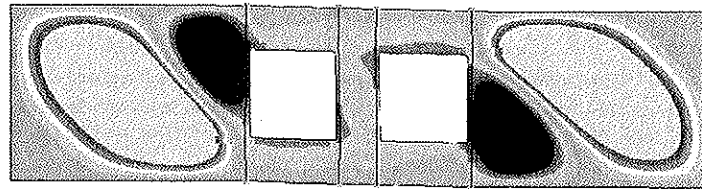


Fig. 9.7.1 Buckles for Girder WL125S50b at maximum shear

9.7.2 Comparison with stressed skin theory

Figs. 9.7.2 to 9.7.4 show the von Mises stress for Girder WL125S50b. The legend is the same for all figures. The stress in the middle surface conforms well to stressed skin theory. A calculation of the shear capacity for the same girder using the method described in Section 3.10 gives $\chi_{w,mod} = 0,39$, i.e. 98 % of the value from the simulations. Here, the stressed skin model comprised the left opening with web, stiffeners and reinforcement. The length of the model was taken as the distance from the vertical centerline between the openings to the left end of reinforcement. The effective web plate width of $30t$ was used for the calculation of reinforcement and stiffener properties. The buckling length of horizontal reinforcement was assumed to be the length of the opening, and the buckling length of vertical stiffeners was taken as the height of girder. However, before a conclusion is made, a closer look at the stressed skin method may be useful:

It is important to realize that the stressed skin theory comprises three main parts

- Calculation model to determine the forces around the opening
- Combination of global and local buckling
- Design of horizontal reinforcement and vertical stiffeners

The calculation model seems to give reliable results if the length of the model is taken as the length of the horizontal reinforcement. In the case of two openings the model may be limited by the vertical centerline between the openings.

For combinations of global and local buckling the simulations unfortunately give no proof of the buckling part of the stressed skin theory, as the chosen web thickness does not give local buckling in the panels between the reinforcement and stiffeners.

For design of horizontal and vertical stiffeners the use of the stressed skin method *for girders with openings* appears more doubtful, for the following reasons

- An effective width of $30t$ may be suitable for structures for instance in living quarter walls, but may be “out of range” for girder webs. Consider a panel above a window opening in a 3200 mm high wall with 6 mm thick plate. Here, an effective width of $30t$ comprises $30 \cdot 6 = 180$ mm in a height of, say 1000 mm, i.e. 18 %. For Girder WL125S50b the effective width of $30t$ comprises $30 \cdot 8 = 240$ mm in a panel height of 250 mm, i.e. 96 %. Obviously there is some inconsistency, both regarding the part of panel that is left to take the shear and the moment arm used in the calculation model for the reinforcement.

- Normally the combination of shear stress in the panel and axial stress in the reinforcement is not checked, even though a part of the panel is included in the sectional area of the reinforcement. Presumably this is not governing for the slender plates of living quarters, because both the shear and axial stresses are far below the yield stress. In girders this may be different as the slenderness is often much lower. In Girder WL125S50b a von Mises combination of stresses reduced the theoretical shear capacity to $\chi_{w,mod} = 0,34$, i.e. 85 % of the result from the simulation.

A possible method to avoid the inconsistency of utilizing the web panel twice, is to assume one part of the panel contributing to the shear capacity and another part included as part of the reinforcement. This approach gave a shear capacity of $\chi_{w,mod} = 0,26$, i.e. 65 % of the result from the simulation. Here, the effective width was chosen to give an effective area of the same size as the reinforcement itself. Hence, the plastic neutral axis of the section was in the transition between web and reinforcement, thus maintaining small moments of eccentricity.

The author has come to the conclusion that the *design part* of the stressed skin method conceptually is the same as finding the maximum capacity for shear and secondary moment as described in Section 3.3.2. The exact solution can only be found by iteration. It is always conservative to let the shear be taken by the web and the secondary moment by reinforcement/flanges. To use $30t$ as the effective width may be non-conservative unless the shear and axial stresses are combined.

Finally, some other conclusions can also be made

- Stress plots from the simulations give evidence of eccentricity moments, and hence such moments should be included.
- Buckling lengths must be prescribed, but in practice the buckling reduction is small for most girders.
- If the objective is a design that utilizes the maximum possible shear capacity at the opening, some modifications to the stressed skin method are necessary:
 - a) The length of the model must be chosen such that $\tau_1 = \tau_2 = \tau_y$, see Fig. 3.10.2 and Eqs. (3.10.5) to (3.10.7). The maximum shear capacity cannot exceed the value given by full yield in shear above and below the opening. The part of web that is between the horizontal reinforcement and the edge of opening is inactive for shear. This may explain why Girder JL125S50p in Table 9.5.3 and Girder S15 in Chapter 4 did not reach $\chi_{w,mod} = 0,50$.
 - b) The effective width of plate can only include the part of plate that is between the reinforcements/stiffeners and the edge of opening, as the rest of the web per definition is fully utilized for shear. The consequence is that relative large reinforcement and stiffeners are required to take the axial forces given by Eqs. (3.10.8) to (3.10.11). This may explain the decrease in efficiency for the horizontal reinforcement depicted in Fig. 9.5.6. For cases with reinforcement/stiffeners on one side only, an additional consequence is that the eccentricity moments increase. In the limit the moment arm is about half the width of the reinforcement, and the required section area is almost doubled compared to stiffeners on both sides.

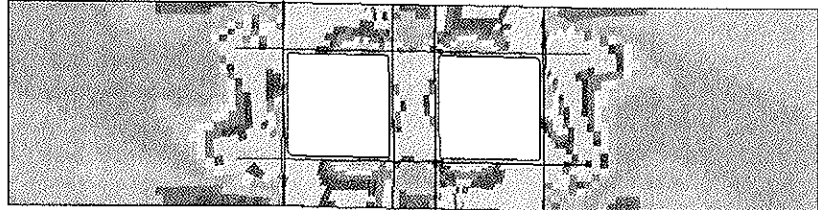
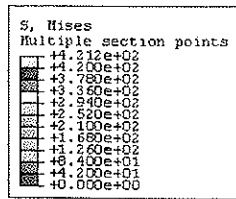


Fig. 9.7.2 Von Mises stress in middle surface for Girder W1.125S50b at maximum shear

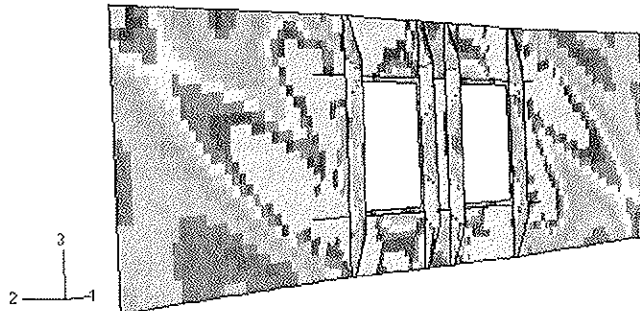


Fig. 9.7.3 Von Mises stress in positive surface for Girder W1.125S50b at maximum shear

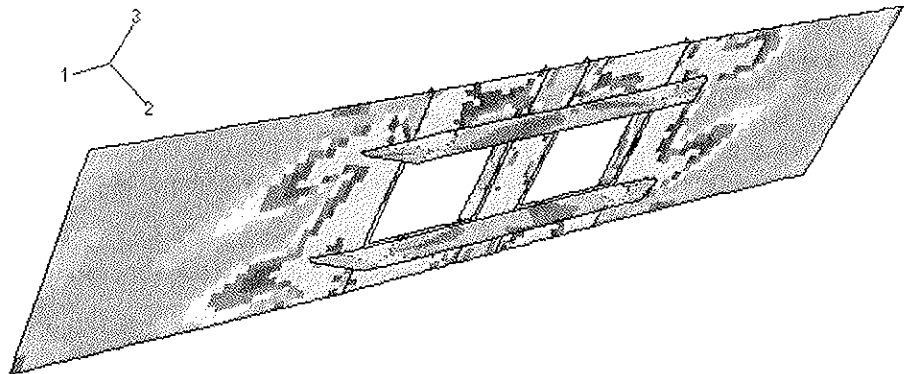


Fig. 9.7.4 Von Mises stress in negative surface for Girder W1.125S50b at maximum shear

9.8 Conclusion

The simulations of girders with square openings show that

- Most response curves for shear force versus tip displacement have marked maximum points, followed by a drop in load-carrying capacity. For all simulations except one, the maximum shear force was taken as the shear capacity of the girder in the ultimate limit state. For the girder without a maximum point, the shear capacity was based on a chosen tip displacement value.
- The drop in load-carrying capacity continued for increasing tip displacement. No distinct minimum points were found. General criteria for determination of the shear capacity in the accidental limit state cannot be given.
- For design purpose the shear capacity of girders with openings should be linked to the similar girders without openings. This ensures a consistent design as the opening size goes to zero in the limit. Tension field effects may be utilized as far as they are allowed in the similar girder without opening. Transverse web displacements and stresses should not exceed those of the girder without opening.
- The shear buckling is of global character. It is possible, for design purpose, to include the effect of buckling for girders with openings by means of the buckling reduction factor given by EC3 for girders without openings, but reduced in order to include the minimum section above and below the opening and the effect of secondary moments.
- The interaction equation used in AISC(1990) for beams with openings may be used also for girders. It is not necessary to know the actual forces in girder flanges.
- The effect of the horizontal reinforcement on one side only of web is significant for all plates, and the efficiency increases for decreasing slenderness. There is a small increase in the shear capacity if the reinforcement is placed on both sides of the web.
- For moderate and slender webs vertical stiffeners may be a more efficient way to increase the shear capacity than horizontal reinforcement.
- An eccentric position of a square opening relative to the horizontal centerline of the web reduces the shear capacity, but the reduction for square openings is smaller than for circular openings.
- The major reduction in shear capacity arises from the reduced shear area in the opening. Compared to the girders with circular openings, a further reduction in shear capacity for girders with square openings is due to secondary moments.
- For girders with two horizontally spaced openings of the same size, there is almost no extra effect of two openings when the clear distance between the openings exceeds twice the diameter of the opening.
- The distance between two vertically spaced openings has little extra effect on the shear capacity, as long as the openings are symmetrically located around the horizontal centerline of girder.
- Stressed skin theory is an efficient mean to determine the shear flow in girders with two openings. However, the stressed skin method should be adjusted if the objective is to utilize the maximum possible shear capacity in girders with two openings.

Chapter 10

Simulations of girders with rectangular openings

10.1 Introduction

This chapter comprises simulations of girders with rectangular openings, where the longest side is either horizontal or vertical. The basic FE-model is the same as the one given in Chapter 9.

10.2 Opening without stiffening

10.2.1 Horizontal long side

Such openings are frequently used for cable trays, if the space for an elongated circular opening is not sufficient. Two simulations of girders with opening dimensions $D_a/h = 0,50$ and $D_h/h = 0,25$ are performed. D_a and D_h are the horizontal and vertical dimensions, respectively. The girders are denoted IxxR5025, where xx is the h/t ratio, R means rectangular, "50" refers to the D_a/h ratio and "25" refers to the D_h/h ratio. One girder is shown in Fig. 10.2.1. The opening is placed symmetric about the midpoint of the girders. Initial imperfections are based on the 2. eigenmode with amplitude 7,5 mm.

The results are presented in Table 10.2.1. Column 7 shows $\chi_{w,mod}$ and Column 8 gives the factor c_2 , based on the reference girders I63C25 and I125C25. Hence, the diameter of the circular opening in the reference girders is equal to the vertical dimension of the opening in the girders with rectangular openings.

Compared to the corresponding girders with *elongated circular* openings, i.e. I63E5025 and I125E5025 in Table 8.2.1, the reductions are 8 % for both girders with rectangular openings.

Table 10.2.1 Results for girders with rectangular openings, horizontal long side

1	2	3	4	5	6	7	8
Run	Girder	h/t	a/h	D_a/h	D_h/h	$\chi_{w,mod}$	c_2
317	I63R5025	63	4	0,50	0,25	0,54	0,76
318	I125R5025	125	4	0,50	0,25	0,37	0,80

The buckled shape at maximum shear for Girder I125R5025 is shown in Fig. 10.2.1. Compared to the girder with a circular opening, the buckles are somewhat extended, but the maximum transverse displacements are about the same.

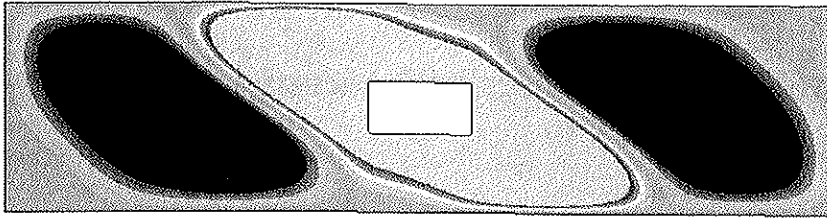


Fig. 10.2.1 Buckles in Girder I125R5025 at maximum shear

10.2.2 Vertical long side

Such openings are very rare in practice, but are included here for reasons of completeness. Two simulations of such girders with opening dimensions $D_a/h = 0,25$ and $D_h/h = 0,50$ are performed. The girders are denoted IxxR2550, where xx is the h/t ratio, R means rectangular, "25" refers to the D_a/h ratio and "50" refers to the D_h/h ratio. One girder is shown in Fig. 10.2.2. The opening is placed symmetric around the midpoint of the girder. Initial imperfections are based on the 1. eigenmode with amplitude 7,5 mm.

The results are shown Table 10.2.2. Column 7 gives $\chi_{w,mod}$ and Column 8 gives the factor c_2 , based on the reference girders I63C50 and I125C50. The diameter of the circular opening in the reference girders is equal to the vertical dimension of the opening in the girders with rectangular openings.

Compared to the corresponding girders with *elongated circular* openings, i.e. I63E2550 and I125E2550 in Table 8.2.2, the reductions are 11 % and 9 % for girders I63R2550 and I125R2550, respectively.

Table 10.2.2 Results for girders with rectangular openings, long side is vertical

1	2	3	4	5	6	7	8
Run	Girder	h/t	a/h	D_a/h	D_h/h	$\chi_{w,mod}$	c_2
315	I63R2550	63	4	0,25	0,50	0,43	0,97
316	I125R2550	125	4	0,25	0,50	0,30	1,00

The buckled shape at maximum shear for Girder I125E2550 is shown in Fig. 10.2.2. Compared to the girder with circular opening, the buckles are somewhat extended, but the maximum amplitudes of the transverse displacements are about the same.

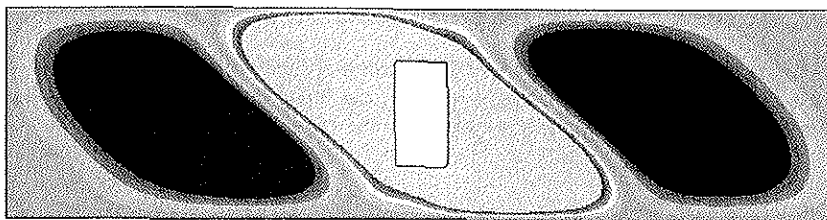


Fig. 10.2.2 Buckles in Girder I125R2550 at maximum shear

10.3 Opening with stiffeners and reinforcement

10.3.1 Horizontal long side

The effect of stiffeners and reinforcement is investigated by means of two simulations. The girders are variations of Girder I125R5025 in Section 10.2.1. Girder L125R5025 has two vertical stiffeners on one side of web, and Girder JL125R5025 has the same vertical stiffeners, and in addition horizontal reinforcement above and below the opening on the other side. The weight ratio of stiffeners and reinforcement is $\mu = 1,0$ for L125R5025 and $\mu = 3,0$ for JL125R5025. The horizontal reinforcement has sufficient sectional area to take the secondary moments caused by full yield shear in the minimum section above and below the opening in a Vierendeel model. Initial imperfections are based on the sum of the 2. and 10. eigenmodes, with amplitudes of 7,5 mm and 4,05 mm, respectively. For JL125R5025, the 18. eigenmode is used instead of the 10. eigenmode. The higher eigenmodes are included to ensure that local buckling is not suppressed in the web parts between the vertical stiffeners above and below the opening.

The results are presented in Table 10.3.1. Column 8 shows $\chi_{w,mod}$ and Column 9 gives the factor c_2 , based on the reference girder I125C25. Column 10 shows the increased shear capacity provided by the stiffeners/reinforcement compared to the girders with the same rectangular openings without stiffeners/reinforcement, in terms of c_{rel} . This is the ratio between $\chi_{w,mod}$ and $\chi_{w,mod}$ for I125R5025 in Table 10.2.

The vertical stiffeners increase the shear capacity by 42 %, and the horizontal reinforcement increase the shear capacity by a further 15 % to a total increase of 57 % compared to I125R5025. Column 11 gives the efficiency index, as defined in Eq. (9.5.2). H_e is based on the reference girder I125R5025. Again, vertical stiffeners appear as an efficient solution.

A girder with an opening will normally not be reinforced to obtain a shear capacity that exceeds the shear capacity of the girder without the opening. In this case Girder I125 has neither opening nor transverse stiffeners, and has $\chi_{w,mod} = 0,53$ as given in Table 7.2.3. Girders L125R5025 and JL125R5025 exceed the shear capacity of Girder I125 by 0,5 % and 11 %, respectively. Hence, the design limit is reached by L125R5025 and the configuration with horizontal reinforcement is superfluous. This interesting conclusion is further elaborated in Chapter 11.

Table 10.3.1 Results for girders with stiffened rectangular openings, horizontal long side

1	2	3	4	5	6	7	8	9	10	11
Run	Girder	h/t	D_a/h	D_b/h	a/h	Stiffeners	$\chi_{w,mod}$	c_2	c_{rel}	H_e
320	L125R5025	125	0,50	0,25	0,5	H: - V: 2FL72x8	0,53	1,14	1,42	0,16
322	JL125R5025	125	0,50	0,25	0,5	H: 2FL92x12,5 V: 2FL72x8	0,58	1,26	1,57	0,07

The buckled shape at maximum shear for L125R5025 is shown in Fig. 10.3.1. Compared to the girder without stiffeners, the buckle in the middle is partly prevented by the stiffeners, and the maximum transverse displacement is reduced from 39 to 21 mm, i.e. by about 46 %. One of the vertical stiffeners appears too weak, as the buckle goes through.

However, according to the discussion above, it has sufficient strength for the girder to achieve the upper limit for required shear capacity.

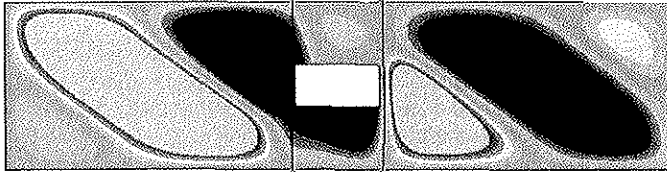


Fig. 10.3.1 Buckles in Girder L125R5025 at maximum shear

10.3.2 Vertical long side

The effect of stiffeners and reinforcement is again investigated by means of two simulations. The girders are variations of Girder I125R2550 in Section 10.2.2. Girder L125R2550 has two vertical stiffeners on one side of web, and Girder JL125R2550 has the same vertical stiffeners, and in addition horizontal reinforcement above and below the opening on the other side. The weight ratio of stiffeners and reinforcement is $\mu = 1,0$ for L125R2550 and $\mu = 1,5$ for JL125R2550. The horizontal reinforcement has sufficient sectional area to take the secondary moments caused by full yield shear in the minimum section above and below the opening in a Vierendeel model. Initial imperfections are based on the sum of the 1. and 17. eigenmodes, with amplitudes of 7,5 mm and 4,05 mm, respectively. The higher eigenmodes are included to ensure that local buckling is not missed in the web parts between the vertical stiffeners above and below the opening.

The results are presented in Table 10.3.2. Column 8 shows $\chi_{w,mod}$ and Column 9 gives the factor c_2 , based on the reference girder I125C50. Column 10 shows the increased shear capacity provided by the stiffeners/reinforcement compared to the girders with the same rectangular openings without stiffeners/reinforcement, by means of c_{rel} . This is the ratio between $\chi_{w,mod}$ and $\chi_{w,mod}$ for Girder I125R2550 in Table 10.2.2. The efficiency index H_e is also based on the reference girder I125R2550. Vertical stiffeners increase the shear capacity by 47 %, and the horizontal reinforcement increases the shear capacity by a further 13 % to a total increase of 60 % compared to I125R2550.

Table 10.3.2 Results for girders with stiffened rectangular openings, vertical long side

1	2	3	4	5	6	7	8	9	10	11
Run	Girder	h/t	D_a/h	D_h/h	a/h	Stiffeners	$\chi_{w,mod}$	c_2	c_{rel}	H_e
319	L125R2550	125	0,25	0,50	0,25	H: - V: 2FL72x8	0,44	1,47	1,47	0,14
321	JL125R2550	125	0,25	0,50	0,25	H: 2FL72x8 V: 2FL72x8	0,49	1,60	1,60	0,13

The buckled shape at maximum shear for Girder L125R2550 is shown in Fig. 10.3.2. Compared to the girder without stiffeners, the buckle in the middle is prevented by the stiffeners, and the maximum transverse displacement is reduced from 40 to 12 mm, i.e. by

about 70 %. It should be noted that the vertical stiffener dimension of girders L125R5025 and L125R2550 is the same. However, the stiffeners in L125R2550 did not buckle, as did one stiffener in L125R5025. This is due to the lower overall stress level in L125R2550. The question of how large the vertical stiffeners need to be, is discussed in Chapter 11.

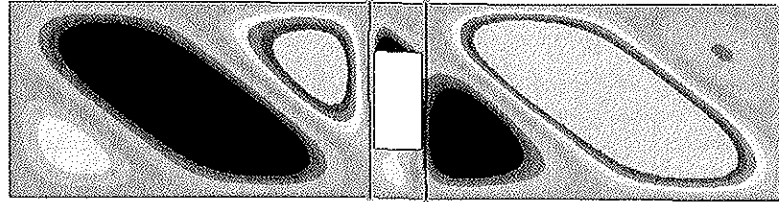


Fig. 10.3.2 Buckles in Girder L125E2550 at maximum shear

10.4 Conclusion

The simulations of girders with rectangular openings show that

- The factors c_2 vary much more than for square openings
- Vertical stiffeners may be a more efficient measure to increase the shear capacity than horizontal reinforcement
- Simple design rules based on the factors c_2 from comparisons with circular openings may be difficult to achieve. This is especially the case if vertical stiffeners are applied near the opening. The need arise for a more comprehensive study of the c_2 - factors and the choice of vertical stiffeners as a mean to increase shear capacities in girders with openings.

Chapter 11

Development of the new design procedure

11.1 Introduction

The simulations showed that the proposed design procedure in Chapter 6 may be simplified: For primary moment and shear acting together, the design can be based on a simple interaction equation. It was confirmed that the main reduction in shear capacity for girders with openings could be given by the factor $(1-D_h/h)$. Reduction due to buckling can be covered by χ_w , i.e. the same reduction factor as for webs without opening, provided that the adjustment factor c_2 has an appropriate value. Hence, the shear capacity of girders with openings may be given by

$$V_{c,mod} = \left(1 - \frac{D_h}{h}\right) \chi_w c_2 \frac{f_y}{\sqrt{3}} ht \quad (11.1.1)$$

However, the accuracy of the FE-models must be addressed, and the best way to determine c_2 should be further elaborated. The effect of vertical stiffeners close to the opening, the design criteria for these stiffeners, the choice between vertical stiffeners and horizontal reinforcement, and the design criteria for girders with sleeves, also need a more detailed discussion. Girders with openings in the lower part of webs and girders with two openings are also discussed. Finally, a cut-off on the shear capacity for girders with stocky webs is proposed, and miscellaneous requirements included. The results of the discussions are summarized as design guidelines in Section 12.2.

11.2 Non-conservative results

As mentioned in Chapter 7 the results from the simulations are generally from 2 to 7 % on the non-conservative side. In order to study this issue in more detail the results of $\chi_{w,mod}$ for the girders in Table 7.2.3 are divided by the factor 1,07 and the reduced results plotted in a diagram in Fig. 11.2.1. Corresponding to Fig. 7.2.20, the curves for $\chi_{w,mod} = 0,75\chi_w$ and $\chi_{w,mod} = 0,50\chi_w$ are also shown. The reduced results are above these curves, except for the stockiest webs. Hence, there is reason to believe that the shear capacity given by Eq. (11.1.1) with $c_2 = 1,0$ is conservative for slender webs. For $\chi_w = 1,0$ the reduced results are clearly below the said curves, and this fact is further discussed in Section 11.11.

The c_2 – values from the simulations presented in Chapters 7 to 10 are based on comparisons of girder pairs. Systematic errors in the single results of shear capacities are assumed to have little influence on the c_2 – values, as the errors will cancel out.

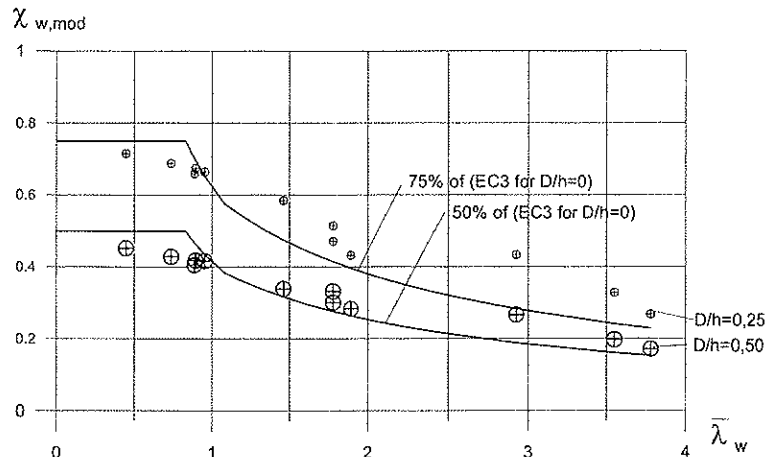


Fig. 11.2.1 Reduced $\chi_{w,mod}$ from the simulations of girders with unstiffened circular openings

11.3 The adjustment factor c_2

This factor covers all effects that are not covered by the other factors. In practice, the main effect is the secondary moment action. It was shown in Chapter 7 that c_2 can be set to 1,0 for *circular* openings without stiffening, located with the center in the horizontal centerline of girders. Such openings are denoted *basic openings*. Due to buckling, the secondary moment is not necessarily zero in the minimum section through the opening, but this relatively small effect is covered by χ_w . For non-circular openings the effect of the secondary moment is larger. The simulations of Section 7.2.8, 7.3 to 7.6 and Chapter 8, 9 and 10 give values of c_2 relative to the basic openings. In Fig. 9.2.9 curves for the shear capacity are given for square openings of $D_h/h = 0,25$ and $D_h/h = 0,50$, indicating c_2 - factors of 0,93 and 0,77, respectively. However, to cover a wider range of opening shapes, the need arises for a general function for c_2 . This function has to give a factor consistent with the design procedure proposed in Chapter 6, i.e. the main reduction in shear capacity shall be included by means of the factor $(1-D_h/h)$, and the buckling covered by χ_w . A possibility is as follows:

Fig. 11.3.1 shows a cantilevered member of length L with a shear force V acting in the left end. This gives the shear force V and the moment VL in the fixed end. The member section is a tee with web height s_f and thickness t .

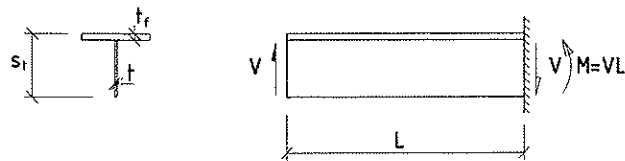


Fig. 11.3.1 Cantilevered tee-member

Assume that the plastic neutral axis of the tee is in the flange, as it normally is. At full plastification in the fixed end of the web, the bending stress and the shear stress are, respectively

$$\sigma = \frac{VL}{\frac{1}{2}s_f^2t} = \frac{2VL}{s_f^2t} \quad \tau = \frac{V}{s_f t} \quad (11.3.1)$$

These stresses must satisfy the von Mises criterion, which gives

$$\sigma_e = \sqrt{\left(\frac{2VL}{s_f^2t}\right)^2 + 3\left(\frac{V}{s_f t}\right)^2} = \frac{V}{s_f t} \sqrt{4\left(\frac{L}{s_f}\right)^2 + 3} \leq f_y \quad (11.3.2)$$

From this

$$V \leq \frac{\sqrt{3}}{\sqrt{4\left(\frac{L}{s_f}\right)^2 + 3}} \frac{f_y}{\sqrt{3}} s_f t = c_2 \frac{f_y}{\sqrt{3}} s_f t \quad (11.3.3)$$

Assuming that the cantilevered member constitutes the top tee of a girder with opening, and that there exists a similar bottom tee with height s_b , Eq. (11.3.3) can be reformulated to

$$V \leq c_2 \frac{f_y}{\sqrt{3}} (s_f + s_b) t = c_2 \frac{f_y}{\sqrt{3}} \left(1 - \frac{D}{h}\right) h t = \left(1 - \frac{D}{h}\right) c_2 \frac{f_y}{\sqrt{3}} h t \quad (11.3.4)$$

where

$$c_2 = \frac{\sqrt{3}}{\sqrt{4\left(\frac{L}{s_f}\right)^2 + 3}} \quad (11.3.5)$$

In principle, Eq. (11.3.3) is similar to the expression in brackets in Eq. (3.3.9), given by AISC(1990). However, Eq. (3.3.9) includes a linearisation of the von Mises stress, which is not needed in the present procedure. Furthermore, L/s_f in Eq. (11.3.5) is *not* the aspect ratio v_f of the top tee, as used in Eq. (3.3.9).

Neither is L the length of the opening, but it is related to the horizontal part of the opening by means of a factor α_L :

$$L = \alpha_L (0,5D_a - r) + 0,5D_a - r \quad (11.3.6)$$

D_a is the length of the opening, r is the corner radius, and α_L expresses the location of the inflexion point for the secondary moments. Hence, $\alpha_L = 0$ when there is no local buckling, while $\alpha_L > 0$ when buckling occurs.

In the design procedure presented in Chapter 6, buckling is per definition not included in c_2 , and hence $\alpha_L = 0$. This gives $L = 0,5D_a - r$, which when inserted in Eq. (11.3.5) gives

$$c_2 = c_{2,basic} = \frac{\sqrt{3}}{\sqrt{4\left(\frac{0,5D_a - r}{s_t}\right)^2 + 3}} \quad (11.3.7)$$

Eq. (11.3.7) is independent of web thickness and is valid for all opening shapes. For circular openings $c_{2,basic} = 1,0$. Fig. 11.3.2 shows a diagram of c_2 as a function of $(0,5D_a - r)/s_t$.

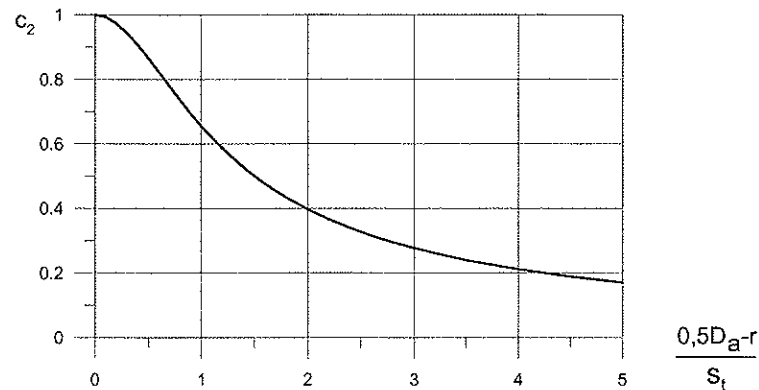


Fig. 11.3.2 The adjustment factor $c_2 = c_{2,basic}$

The values of c_2 from Eq. (11.3.7) are compared to results of the 32 simulations for girders with elongated circular, square and rectangular openings without stiffening, as given in Table 11.3.1. Column 1 refers to the tables where the results from the simulations are given, Column 6 shows c_2 calculated according to (Eq. 11.3.7) and Column 7 the average c_2 from the simulations. It can be seen that the theoretical factors are higher than the factors from the simulations for the smaller openings, and lower for the larger openings.

Column 5 lists the s_t/t ratios of the web above the opening. A wide range is covered, but it appears that this ratio has no influence on the results.

Table 11.3.1 Comparison of c_2 -factors for openings without reinforcement

1	2	3	4	5	6	7
Table	h/t	D_h/h	$(0,5D_a-r)/s_t$	s_t/t	Theoretical c_2	Simulated c_2
8.2.1	63	0,25	0,33	23	0,93	0,83
	125	0,25	0,33	47	0,93	0,87
8.2.2	63	0,50	0,00	16	1,00	1,09
	125	0,50	0,00	31	1,00	1,10
9.2.2	63	0,25	0,25	23	0,96	0,92
	125	0,25	0,29	47	0,95	0,92
	250	0,25	0,29	94	0,95	0,94
	63	0,50	0,87	16	0,70	0,75
	125	0,50	0,94	31	0,68	0,76
	250	0,50	0,94	63	0,68	0,79
	10.2.1	63	0,25	0,58	23	0,83
125	0,25	0,62	47	0,81	0,80	
10.2.2	63	0,50	0,37	16	0,92	0,97
	125	0,50	0,44	31	0,89	1,00

It appears that the corner radius that is included in Eq. (11.3.7) should be reduced, as it gives non-conservative results for the elongated circular openings with horizontal long side. Also for the other openings there is non-conformance, as the openings with $r = 32$ mm radius have smaller c_2 -values from the simulations than the openings with $r = 16$ mm. However, it is too conservative to disregard the radius all together and the consistency between circular, elongated, square and rectangular openings would be broken. Hence, the following value for r is proposed for use in Eq. (11.3.7):

$$r_{red} = r \left(\frac{2r}{D_a} \right)^2 \quad (11.3.8)$$

Here, $r_{red} = r$ for circular openings and elongated circular openings with the long side vertical. For the elongated circular openings with horizontal long side in Table 8.2.1 $r_{red} = 0,25r$, and for the square and rectangular openings r is practically eliminated.

Table 11.3.2 shows the amended c_2 -values when r_{red} is used in Eq.(11.3.7). The values for the larger openings appear to be on the conservative side compared to the simulations. However, it should be noted that the c_2 -values from the simulations show the *ratio* of shear capacity for non-circular openings to those of the corresponding circular openings. Even though global buckling and inaccuracies in the FE-models are supposed to be eliminated by this approach, the result may not include only the effect of the secondary moments. If the shear capacities of the large circular openings are actually less than those given by yield shear in the minimum section, this will be reflected in increased c_2 -values from the simulations. The discussions in Section 11.11 point at reduced shear capacities in the minimum section. In the end, Eq. (11.3.7) can only be proved by applying it to the simulated girders as part of Eq. (11.1.1). This is done in Section 11.13 and Appendix B.

The factor c_2 is also used to include the effects of horizontal reinforcement and sleeves, as described in Section 11.5 and 11.6, respectively.

Table 11.3.2 Comparison of amended c_2 -factors for openings without reinforcement

1	2	3	4	5	6	7
Table	h/t	D_h/h	r_{red} [mm]	$(0,5D_a-r_{red})/s_t$	Amended c_2	Simulated c_2
8.2.1	63	0,25	31	0,58	0,83	0,83
	125	0,25	31	0,58	0,83	0,87
8.2.2	63	0,50	125	0,00	1,00	1,09
	125	0,50	125	0,00	1,00	1,10
9.2.2	63	0,25	2	0,33	0,94	0,92
	125	0,25	0	0,33	0,93	0,92
	250	0,25	0	0,33	0,93	0,94
	63	0,50	1	1,00	0,66	0,75
	125	0,50	0	1,00	0,65	0,76
	250	0,50	0	1,00	0,65	0,79
10.2.1	63	0,25	1	0,67	0,79	0,76
	125	0,25	0	0,67	0,79	0,80
10.2.2	63	0,50	2	0,49	0,87	0,97
	125	0,50	0	0,50	0,87	1,00

11.4 Contribution to shear capacity from vertical stiffeners

Vertical stiffeners close to the opening can be an efficient mean to increase the shear capacity, as shown in Chapters 9 and 10 for girders with square and rectangular openings. This is the case also for circular openings. By comparing the simulations of girders I250C50 and I250C50T0 in Table 7.2.1, it appears that the shear capacity has increased by 100 %.

In the proposed design procedure the effect of the vertical stiffeners is solely connected to an increased χ_w , arising from a smaller aspect ratio. There is neither a change in the factor $(1-D_h/h)$, nor in c_2 . Girders I250C50 and I250C50T0 have χ_w -values of 0,31 and 0,55, respectively. Hence, the proposed design procedure gives an increase of 77 %. The effect is visualized in Fig. 11.6.1, as the vertical distance between the points b) and c).

The effect of the vertical stiffeners is related to the relative slenderness of the web without the stiffeners. For low values of the relative slenderness the possible increase in χ_w is limited, and for a relative slenderness below 0,83 the effect is zero.

The part of the web between the vertical stiffeners is divided in two separate parts when the opening is square, as seen in Fig. 9.4.1 for Girder L125S50. Also the buckle is divided in two parts. Although such a buckle may be regarded as two separate and local buckles, it is still convenient to treat the phenomenon as global buckling. The proposed design procedure gives $\chi_{w,mod} = 0,50 \cdot 0,68 \cdot 0,94 = 0,32$, while the simulation gave $\chi_{w,mod} = 0,34$. It is therefore concluded that the use of χ_w -values based on global buckling of webs without openings is conservative.

11.5 Contribution to shear capacity from horizontal reinforcement

The effect of horizontal reinforcement is also covered by the factor c_2 , which is increased from the value for openings without reinforcement to a value less or equal to 1,0. Although Eq. (11.3.7) might possibly be adjusted to include the increase, it is preferred to let the increase vary linearly with the dimension of the reinforcement. The modified expression for c_2 reads

$$c_2 = c_{2,r} = c_{2,basic} + (1 - c_{2,basic}) \frac{A_r}{A_{r,max}} \beta \leq 1,0 \quad (11.5.1)$$

where $c_{2,basic}$ is given by Eq. (11.3.7). A_r is the sectional area of the reinforcement and the part of web plate that is between the reinforcement and the edge of opening. $A_{r,max}$ is given by Eq. (3.3.26). β includes the effect of reinforcement on one or both sides of the web. Based on the simulations referred in Section 9.3.2, it is chosen to use $\beta = 0,7$ and $\beta = 1,0$ for stiffeners on one or both sides, respectively.

11.6 Contributions to shear capacity from vertical stiffeners and horizontal reinforcement

The combined effect of vertical stiffeners and horizontal reinforcement is covered by the product $\chi_w c_{2,r}$. Here, χ_w is based on global buckling of the web panel between the vertical stiffeners, disregarding the opening and the horizontal reinforcement, and $c_{2,r}$ is given by Eq. (11.5.1).

A buckling reduction factor determined as described above may appear far from the reality in cases where two separate parts are supported along all four sides. However, the simulations of girders referred in Section 9.5 show that this is an adequate procedure. A higher value of χ_w based on the smaller aspect ratios should not be used. Neither is it necessary to use lower values of χ_w based on local buckling of the stiffeners and reinforcement, provided the vertical stiffeners comply with the stiffness requirement described in Section 11.8. For Girder JL125S500 the proposed design procedure gives $\chi_{w,mod} = 0,50 \cdot 1,00 \cdot 0,94 = 0,47$, but limited to $\chi_{w,mod} = 0,46$ by Eq. (11.11.4). The simulation obtained $\chi_{w,mod} = 0,47$.

Design example

The contributions from stiffeners and reinforcement are shown for a design example, using Girder I125 as a case. This girder has a relative slenderness $\bar{\lambda}_w = 1,89$, and a square opening with dimension $D_h/h = 0,50$ is introduced. The reduction factor $\chi_{w,mod}$ may be computed by three procedures

Curve 1 $\chi_{w,mod} = (1 - D_h/h)\chi_w c_2 = 1,00 \cdot \chi_w \cdot 1,00 = \chi_w$
 Curve 2 $\chi_{w,mod} = (1 - D_h/h)\chi_w c_2 = 0,50 \cdot \chi_w \cdot 0,68 = 0,34\chi_w$
 Curve 3 $\chi_{w,mod} = (1 - D_h/h)\chi_w c_2 = 0,50 \cdot \chi_w \cdot 1,00 = 0,50\chi_w \leq 0,46$

The procedures are presented by the three curves in Fig. 11.6.1

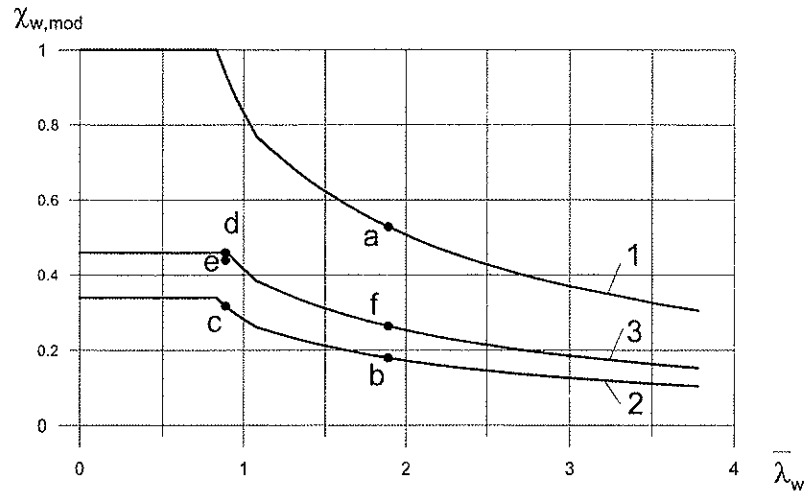


Fig. 11.6.1 Design example for girders with square openings

Curve 1 is valid for girders without openings, while curve 2 is valid for girders with square openings with dimension $D_h/h = 0,50$, corner radius $r/D_a = 0,03$ and without reinforcement. Curve 3 represents girders with the same opening dimensions as Curve 2, but with horizontal reinforcements on both sides of the web. The cross sectional area of the reinforcement is $A_{r,max}$. The limit $\chi_{w,mod} = 0,46$ is given by Eq. (11.11.4).

For a relative slenderness $\bar{\lambda}_w = 1,89$ Curve 1 gives $\chi_{w,mod} = 0,53$ for Girder I125, marked as point a) in the figure. The introduction of the opening turns Girder I125 into I125S50. The relative slenderness is still $\bar{\lambda}_w = 1,89$ and Curve 2 gives $\chi_{w,mod} = 0,18$, marked by the point b).

If the shear capacity of I125S50 is insufficient, the introduction of vertical stiffeners may be the most efficient way of increasing the capacity for such slender webs. Two vertical stiffeners transform the girder into Girder L125S50, and reduce the relative slenderness to $\bar{\lambda}_w = 0,89$. Also here Curve 2 is applicable and gives $\chi_{w,mod} = 0,32$, marked by the point c) in Fig. 11.6.1.

If this capacity is still too small, horizontal reinforcement must be applied. Girder L125S50 is then transformed to Girder JL125S50o. The relative slenderness remains at $\bar{\lambda}_w = 0,89$ and Curve 3 gives $\chi_{w,mod} = 0,46$, represented by the point d). This is the maximum value that can be obtained, and horizontal reinforcement on both sides of web must be used.

As the main fabrication costs is usually connected to preparing and welding, it is hardly a good practice to use reinforcement with cross sectional area smaller than $A_{r,max}$. However, if a smaller shear capacity is sufficient, horizontal reinforcement on one side of web only would give $\chi_{w,mod} = 0,44$, marked e). Alternatively, the vertical stiffeners could be omitted. This increases the relative slenderness to the initial value of $\bar{\lambda}_w = 1,89$. Curve 3 is valid and gives $\chi_{w,mod} = 0,26$, at point f). In the latter case the shear stress in the web panel above the opening is considerably less than the yield shear stress, indicating that the requirement to $A_{r,max}$ in Eq. (11.5.1) could be relaxed in an iterative process. However, this should be avoided, because the proposed design procedure anticipates a shift of the inflexion points for the secondary moments, although not explicitly reflected in the design equations. See Fig. 3.7.3. When a lower shear stress acts over a longer distance, the force in the reinforcement may still be so large that $A_{r,max}$ is required for the given shear capacity to be achieved.

11.7 Contributions to shear capacity from sleeves and doubler plates

The effect of sleeves and doubler plates may be considered analogous to the use of both vertical stiffeners and horizontal reinforcement for square openings. The effect is included in the product $\chi_w c_{2,r}$, but it is difficult to identify the effect of the single factors. However, the simulations showed that sleeves with a weight ratio $\mu = 1,0$ increased the shear capacity up to the capacity of the girder without opening, with an upper limit given by $(1-D/h) \cdot 1,00 \cdot 1,00$, see Fig. 7.3.1. A simple way to handle this case is to include all effects of the sleeves and doubler plates in the factor c_2 .

Apparently the approach makes c_2 a function of the global buckling, which violates the basic premiss that all buckling should be included in the factor χ_w . However, the design guidelines are considerably simplified with this approach. The modified factor reads

$$c_2 = c_{2,s} = c_{2,basic} + \left(\frac{1}{\chi_w} - 1\right) \mu \beta \quad \text{for } \chi_w \geq \left(1 - \frac{D_h}{h}\right) \quad (11.7.1)$$

$$c_2 = c_{2,s} = c_{2,basic} + \frac{\frac{D_h}{h}}{\left(1 - \frac{D_h}{h}\right)} \mu \beta \quad \text{for } \chi_w < \left(1 - \frac{D_h}{h}\right) \quad (11.7.2)$$

$c_{2,basic}$ is given by Eq. (11.3.7). Eqs. (11.7.1) and (11.7.2) are valid for circular and elongated circular openings. For circular openings and elongated circular openings with vertical long side $c_{2,basic} = 1,0$. The factor β includes the effect of sleeves or doubler plates on one or both sides of the web. Based on the simulations in Section 7.3 and 7.4, it is chosen to use $\beta = 0,6$ and $\beta = 0,7$ for sleeves on one side and centric sleeves, respectively. For doubler plates the same factors can be used. The value of μ should not exceed 1,0 in the equations.

Design example

The contribution from sleeves is shown for a design example, again using Girder I125 as a case. This girder has a relative slenderness $\bar{\lambda}_w = 1,89$, and a circular opening with dimension $D/h = 0,50$ is introduced. The reduction factor $\chi_{w,mod}$ may be computed by three procedures

$$\text{Curve 1 } \chi_{w,mod} = (1 - D/h)\chi_w c_2 = 1,00 \cdot \chi_w \cdot 1,00 = \chi_w$$

$$\text{Curve 2 } \chi_{w,mod} = (1 - D/h)\chi_w c_2 = 0,50 \cdot \chi_w \cdot 1,00 = 0,50\chi_w \leq 0,42$$

$$\text{Curve 3 } \chi_{w,mod} = (1 - D/h)\chi_w c_{2,s}$$

Curve 3 has two parts, given by $c_{2,s} = 1,0 + \left(\frac{1}{\chi_w} - 1\right)0,6$, and $c_{2,s} = 1,60$, respectively.

The procedures are presented by the three curves in Fig. 11.7.1

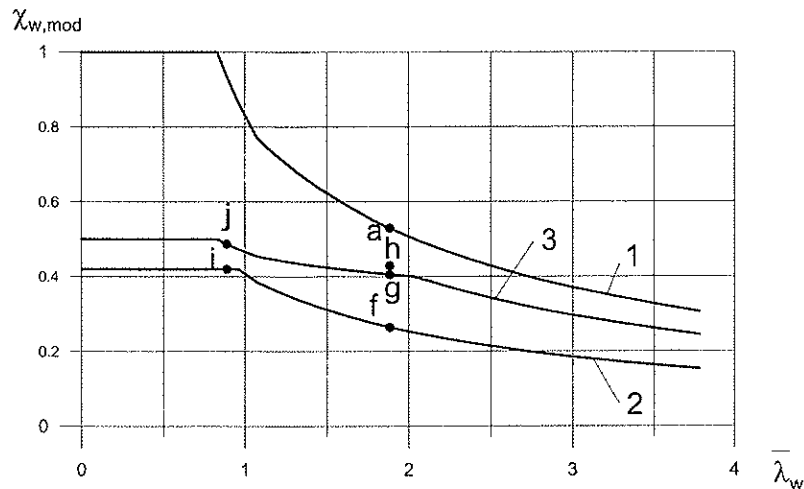


Fig. 11.7.1 Design example for girders with circular openings

Curve 1 is valid for girders without openings, while Curve 2 is valid for girders with circular openings with dimension $D/h = 0,50$ without stiffening. Curve 3 represents girders with the same opening dimensions as Curve 2, but with sleeves on one side of the web, and the weight of the sleeves are equal to the weight of the removed plate material in the opening. The limit $\chi_{w,mod} = 0,42$ is given by Eq. (11.11.2).

For a relative slenderness $\bar{\lambda}_w = 1,89$ Curve 1 gives $\chi_{w,mod} = 0,53$ for Girder I125, marked as point a) in the figure. The introduction of the opening turns Girder I125 into I125C50. The relative slenderness is still $\bar{\lambda}_w = 1,89$ and Curve 2 gives $\chi_{w,mod} = 0,26$, marked by the point f).

If the shear capacity of I125C50 is insufficient, the introduction of a sleeve on one side may be a good solution. The girder is transformed to Girder J125C50. Curve 3 is applicable and gives $\chi_{w,mod} = 0,41$, marked with g).

If this value is still too small, the sleeve may be placed centric in the opening as in Girder J125C50C, which gives $\chi_{w,mod} = 0,43$, and is marked with h).

This is the maximum value that can be obtained, unless vertical stiffeners are applied, as in the design example of Section 11.5. Applying two vertical stiffeners and no sleeve gives $\chi_{w,mod} = 0,42$ by Curve 2, marked by the point i). For vertical stiffeners and sleeve on one side Curve 3 gives $\chi_{w,mod} = 0,49$, marked by the point j). In this case there is no gain in placing the sleeve centric, as this will also give $\chi_{w,mod} = 0,49$.

11.8 Design of vertical stiffeners

Vertical stiffeners may be an efficient mean to increase the shear capacity of girders with openings. Efficiency indexes calculated in Section 9.5, based on the simulations, give evidence of this. The effect is also obvious from Figs. 11.6.1 and 11.7.1. However, the question remains of how the stiffeners are to be designed. The author suggests the following:

1. In the proposed design procedure, buckling is handled by means of the factor χ_w , and based on EC3. Hence, the design requirement for vertical stiffeners given in EC3 should apply, i.e. the stiffeners should be checked for strength and stiffness.
2. According to EC3 the strength of intermediate rigid stiffeners should be checked for an axial force equal to

$$N = V - \chi_w \frac{f_y}{\sqrt{3}} ht \quad , \text{ but } N \geq 0 \quad (11.8.1)$$

where V is the shear force in the web. χ_w is calculated for the web panel between adjacent transverse stiffeners, assuming the stiffener under consideration is removed.

In the case of openings, it is presupposed that the shear capacity of the girder without the opening *and the new transverse stiffeners*, is sufficient. This means

$$V \leq \chi_w \frac{f_y}{\sqrt{3}} ht \quad (11.8.2)$$

Hence, N is always zero and the strength criteria can be omitted.

The stiffness criteria in EC3 is expressed in terms of the minimum second moment of area of the stiffener:

$$I_{st} \geq 1,5 \frac{h^3 t^3}{a^2} \quad \text{for low aspect ratio, i.e. } \frac{a}{h} < \sqrt{2} \approx 1,4 \quad (11.8.3)$$

$$I_{st} \geq 0,75 ht^3 \quad \text{for high aspect ratio, i.e. } \frac{a}{h} \geq \sqrt{2} \approx 1,4 \quad (11.8.4)$$

where I_{st} is calculated for the stiffener and the effective flange of web plate.

For girders with openings the purpose of the stiffeners is to prevent global buckling of the web. In order to determine the stiffener requirement it may be convenient first to consider the buckling problem of the original web, i.e. without opening and the new stiffeners. This can be done by merging the two stiffeners into one fictitious stiffener, placed at the position of the center of opening. This stiffener can be designed according to Eqs. (11.8.3) and (11.8.4), taking a as the half length of the original panel. These two sub-panels clearly have a shear capacity that exceeds that of original panel. As the shear force never exceeds the capacity of the original panel, the stiffness of the fictitious stiffener is conservative.

The stiffness of the real stiffeners may now be taken as 50 % of the value of the fictitious one. Even though the actual shear force acting in the girder with opening is lower than the force acting in the girder without opening, a further reduction in stiffness should be avoided for the following reasons:

- The purpose of the vertical stiffeners is to increase the shear capacity of the girder with opening up to a level comparable with that of the girder without opening.
- The stiffness requirement for stiffeners in girders without openings is not related to the actual shear force in the girder.

11.9 Openings in lower or upper part of webs

Circular openings with the center located at a distance e from the horizontal centerline of web, reduce the shear capacity of the girders, compared to a location on the horizontal centerline. Due to symmetry, locations below or above the horizontal centerline give the same reduction for the same e . The reduction is relatively high for stocky and slender webs, but small for very slender webs. The reduction influences the product $\chi_w c_2$. A simple way to include the effect in the design procedure is to modify the factor c_2 only, although this approach makes c_2 a function of global buckling. The modified factor for circular and elongated circular openings with vertical long side, without sleeves, reads:

$$c_2 = c_{2,off-set,circ} = 1,0 \left(1 - 2 \frac{e D_h}{h^2} \right) \quad \text{for } \chi_w \geq 0,5 \quad (11.9.1)$$

$$c_2 = c_{2,off-set,circ} = 1,0 \left(1 - 8 \frac{e D_h}{h^2} \chi_w^2 \right) \quad \text{for } \chi_w < 0,5 \quad (11.9.2)$$

The values 2 and 8 are based on curve fitting of the simulated results. The factor D_h/h is added to give consistency with the similar equations for rectangular openings.

For openings with sleeves or doubler plates c_2 is given by Eqs. (11.7.1) to (11.7.3), provided $c_{2,basic}$ in these equations are replaced by $c_{2,off-set,circ}$ from Eqs. (11.9.1) and (11.9.2). The factors β should be taken as

$$\beta = 0,6 \left(1 - \frac{e}{2h\chi_w} \right) \quad \text{for sleeves or doubler plates on one side} \quad (11.9.3)$$

$$\beta = 0,7 \left(1 - \frac{e}{2h\chi_w} \right) \quad \text{for sleeves or doubler plates on both sides} \quad (11.9.4)$$

For square and rectangular openings, an off-set location may increase or reduce the shear capacity of girders, compared to the location on the horizontal centerline. According to the theory in Section 11.3 there are two c_2 -factors; one for the top tee and one for the bottom tee. For lowered locations, c_2 for the top tee increases and c_2 for the bottom tee decreases. The increase is always larger than the decrease, resulting in an overall increase. However, for stocky and slender plates, this increase is counteracted by an "extra" reduction due to buckling. The total result may be either an increase or decrease in the shear capacity, depending on the size of the off-set. The extra reduction from buckling means that the factor χ_w must be reduced in these cases. For practical reasons, the reduction is included in c_2 , as done for circular openings. For very slender webs the effect caused by extra buckling diminishes and the off-set location results in an increase in shear capacity compared to the location on the horizontal centerline. The simulations of girders I250S50T2 and M250S50T2 show this effect. The approach is valid for all square and rectangular openings, with and without vertical stiffeners and horizontal reinforcement.

$$c_2 = c_{2,off-set} = \frac{c_{2,t}S_t + c_{2,b}S_b}{h\left(1 - \frac{D_h}{h}\right)} \left(1 - 2\frac{eD_h}{h^2}\right) \quad \text{for } \chi_w \geq 0,5 \quad (11.9.5)$$

$$c_2 = c_{2,off-set} = \frac{c_{2,t}S_t + c_{2,b}S_b}{h\left(1 - \frac{D_h}{h}\right)} \left(1 - 8\frac{eD_h}{h^2}\chi_w^2\right) \quad \text{for } \chi_w < 0,5 \quad (11.9.6)$$

where $c_{2,t}$ and $c_{2,b}$ are the basic c_2 -factors for the top and bottom tee, respectively, calculated according to Eqs (11.3.7).

For openings with reinforcement c_2 is given by Eqs. (11.5.1), provided $c_{2,basic}$ in this equation is replaced by $c_{2,off-set}$ from Eqs. (11.9.5) and (11.9.6). The factors β should be taken as

$$\beta = 0,7\left(1 - \frac{e}{2h\chi_w}\right) \quad \text{for reinforcement on one side} \quad (11.9.7)$$

$$\beta = 1,0\left(1 - \frac{e}{2h\chi_w}\right) \quad \text{for reinforcement on both sides} \quad (11.9.8)$$

11.10 Two openings close together

Cases with two openings horizontally spaced may be handled by a modified c_2 - factor, based on a factor $c_{2,I}$ for the single opening and another factor $c_{2,II}$ for a fictitious opening with twice the length of the single opening. The two factors are calculated from the respective equations for single openings and combined linearly. The approach is valid for all openings without stiffening and for openings with sleeves. The modified factors read

$$c_2 = c_{2,two} = c_{2,I} \quad \text{for } S_a \geq 2D_a \quad (11.10.1)$$

$$c_2 = c_{2,two} = c_{2,I} - (c_{2,I} - c_{2,II})\left(1 - \frac{S_a}{2D_a}\right) \quad \text{for } S_a < 2D_a \quad (11.10.2)$$

Cases with two openings of same size and vertically spaced may be handled by a modified factor c_2 , based on a fictitious opening with height twice the height of the single opening, located with its center on the horizontal centerline of the web. The capacity is taken to be independent of the vertical spacing.

In the suggested design guidelines in Section 12.2 the above procedures are linked together to a generalized procedure for multiple openings. The procedure recognizes weighted influences from the adjacent openings for the opening to be checked. Clusters of openings are common in practice, but usually only one or two openings are large, the others are small. Furthermore, the centers of openings are not necessarily on the horizontal centerline of the girder or in the same horizontal or vertical position. No simulations have been performed for such configurations. However, the generalized procedure covers the simulations that *have* been performed and the author presumes that it is suitable for most occasions and will give conservative results.

11.11 Cut-off on shear capacities

The results of the simulations for girders with circular openings without reinforcement are lower than the values given by Eq. (11.1.1) for stocky webs. In Fig. 11.2.1 the results are reduced with 7 %, which may be conservative. However, also Figs. 7.2.15 and 7.2.20 depict reductions larger than $(1-D/h)$ for $\chi_w = 1,0$. In Section 7.2.6 the extra reductions were explained by the non-linear analyses themselves. In the literature Ueno and Redwood (1977) reported that for openings smaller than $D = 0,30h$ the reduction follows the minimum shear area. For openings with $D > 0,30h$ the reduction is larger than $(1-D/h)$. On the other hand Höglund (1970) states that the diameter must be larger than $D = 0,70h$ for the reduction in shear capacity to be larger than $(1-D/h)$.

The author has come to the conclusion that the reduction is larger than $(1-D/h)$ for circular openings in stocky webs *if the opening has no stiffening*. The reason is that a T-section cannot obtain the same distribution of shear stress as an I-section. The simulation of the large circular opening in Section 3.4 showed this. Here, buckling was excluded *a priori*, but the shear capacity reached only 91 % of the value based on the minimum section. Fig. 3.4.7 indicates areas in the minimum section near the opening edges having shear stress smaller than the yield shear stress. The relative influence of these areas decreases with decreasing opening diameter. Hence, for the small circular opening with $D/h = 0,10$ in Section 3.4 the effect of the non-plastified areas disappeared.

The extra reduction for a T-section appears only in the limit when pure yield shear stress occurs. If buckling takes place or secondary moments are acting, the extra reduction is already included by means of χ_w or c_2 . Hence, it is proposed to still determine the shear capacity by Eq. (11.1.1), but to apply a cut-off on the shear capacity by means of

$$V_{c,mod,cut-off} = \alpha_c \left(1 - \frac{D}{h}\right) \frac{f_y}{\sqrt{3}} ht \quad (11.11.1)$$

α_c is a factor that includes the effect of opening dimension, sleeves, doubler plates and horizontal reinforcement. For openings in general the factor may be taken as

$$\alpha_c = (1 - 0,32 \frac{D}{h}) \quad (11.11.2)$$

This means that the shear capacity for stocky plates with a circular opening $D = 0,50h$ is limited to 84 % of the capacity based on yield shear stress in the minimum section. An opening with $D/h = 0,25$ has $\alpha_c = 0,92$. Further, $\alpha_c = 1,0$ when D goes to zero in the limit, and $\alpha_c = 0$ when D goes to h in the limit. Eq. (11.11.2) reflects that the extra reduction is relatively smaller for small openings than for large openings. The value of 0,32 is chosen in order to give conservative values compared to the simulated results, when the simulated results are divided by 1,07. A smaller value than 0,32 is probably more correct, but this question is left to further studies. The simulations gave no evidence of a more distinct value of inaccuracy than 7 % on the non-conservative side.

The cut-off also applies when $\chi_{w,c_2} \geq \alpha_c$. Hence, conservative shear capacities are also prescribed for the cases of medium slender webs where the simulations gave results below the scaled curves for 75 % and 50 % of EC3 for webs without openings.

For the case of openings with sleeves the T-section is transformed to an I-section, and hence the full minimum section is available for shear. For the case of doubler plates the sectional area in itself is increased. In both cases the limiting factor is replaced by

$$\alpha_{c,s} = \mu \leq 1 \quad (11.11.3)$$

if these values are larger than α_c given by Eq. (11.11.2).

Also for openings with horizontal reinforcement a limit on shear capacity may apply. The part of web plate that is between the reinforcement and the edge of opening is inactive for shear. Hence

$$\alpha_{c,r} = \frac{h - D_{hr}}{h - D_h} \frac{A_r}{A_{r,max}} \quad (11.11.4)$$

where D_{hr} is the vertical distance between the horizontal reinforcements. The value of $\alpha_{c,r}$ may be used if it is larger than α_c given by Eq. (11.11.2).

It is assumed that a sleeve, doubler plate or reinforcement must be of some size before it has a significant effect. Interpolation between the values given by Eqs. (11.11.2) to (11.11.4) is possible, but this solution is left in favor of a simple rule. For a sleeve that is attached to the web not more than 20 mm from the edge, the sectional area of the sleeve itself is assumed to compensate for the lost shear area outside the I-section. For the case of horizontal reinforcement, the part of web that is between the reinforcement and the opening can be included in A_r .

11.12 Miscellaneous

Some requirements are included in the suggested design guidelines of Section 12.2 and the reasons for these are as follows:

The design guidelines contain no provision to avoid local buckling of the web, as the simulations have shown that this is not necessary, see Column 5 in Table 11.3.1. For reinforcement, the stressed skin method requires a width/thickness ratio about equal to or less than eight, and this value was used in the simulations for sleeves, stiffeners and reinforcement. The requirement is easy to fulfil and many simulations showed full plastification over the reinforcement cross-section. The other buckling requirements concern primary moments and are taken from AISC(1990).

The restrictions on opening sizes included in AISC(1990) are disregarded in the suggested design guidelines, as the shear capacities for very large openings will be very small. A small shear capacity is in itself a restriction. In addition, the requirement for a buckling check of the tee is also a restriction for large openings. The requirement for opening radii is also taken from AISC(1990).

The requirement for welds for sleeves, doubler plates and horizontal reinforcement concerns full plastification of parts of these elements, and it is difficult to identify where this plastification will occur. Detailed calculations for welds are not feasible in practice. However, a possible relaxation for the welds between web and flange may be useful, if the design shear force allows it. Increasing the size of these welds may be impractical from a fabrication point of view, and is only to be done if really required.

11.13 Verification of the proposed guidelines

The proposed guidelines are applied to all girders with openings described in Chapters 7 to 10, and the shear capacities are compared to the results from the simulations. Details can be found in Appendix B. 186 girders are considered and the guidelines give conservative values for all except three cases. In one of these cases the simulated girder had weaker transverse stiffeners than recommended by the guidelines. In the two other cases the shear capacity was determined by buckling in the adjacent panel without opening.

As previously concluded, the results of the simulations may be 2 % to 7 % on the non-conservative side. The proposed guidelines are therefore also compared to reduced values from the simulations. Here, the results from the girders with openings $D_h/h = 0,25$ are reduced with 4,5 % and the results from the girders with openings $D_h/h = 0,50$ are reduced by 7 %. The value 4,5 % is taken as the mean of 2 % and 7 %. Details can be found in Appendix B. The guidelines give conservative shear capacities also for these comparisons, except for some girders with $h/t = 63$ and $h/t = 125$.

For many of the corresponding girders without openings, the simulations give results below the EC3 curve. Hence, it should be reasonable to adjust the simulated results for the girders with openings by the same amount, as the girders without openings are adjusted up to the EC3 curve. By doing this, the design guidelines give conservative results for all girders with $h/t = 63$, and most of the girders with $h/t = 125$.

For three girders with $h/t = 125$ a similar adjustment cannot be justified, because the simulations of the corresponding girders without openings give a capacity exactly equal to

the EC3 value. However, the simulated results are only 1 to 2 % below the values given by the guidelines, when the simulated results are reduced by 7 %. Hence, the proposed guidelines should be acceptable also for these girders.

Finally, the comparisons in Appendix B show that for many girders in the high slenderness range the proposed guidelines are rather conservative. This is mainly caused by the use of the EC3 curve in the guidelines and corresponds to a similar conservatism for girders without openings. The author has not tried to use factors that counteract this effect, as the safety level should be comparable for girders with and without openings.

Chapter 12

Conclusions and suggestions

12.1 Conclusions

The three primary objectives of the thesis have been achieved:

- Reliable numerical models as basis for numerical simulations are established, as described in Chapter 5 and Section 7.1.
- The criteria for determination of the shear capacity are established:

For tests and simulations the shear capacity in the ultimate limit state is taken as the maximum value from response curves for shear force versus tip displacement.

For design purpose the shear capacity in ULS for girders with openings is linked to the capacity of the corresponding girders without openings. This ensures a consistent design that maintains the safety level of the girders with openings, and transverse web displacements and stresses in ULS are about the same for girders with and without openings. Tension field effects are included in so far as they are allowed in the design rules for girders without openings.

It is concluded that no criteria can be given for the accidental limit state.

- Existing load-carrying theories have been reviewed and 260 numerical simulations using the non-linear program ABAQUS performed, covering a wide range of web openings and slenderness ratios. It was possible to establish a set of simple formulae for the shear capacities of girders having one or two large openings of circular or rectangular shape, with or without stiffening. The procedure is developed in Section 7.2, 9.2 and in Chapter 11, which also includes two design examples. Guidelines are suggested in Section 12.2, including all formulae required for practical design with a minimum of calculations. The guidelines are linked to international codes and cover both beams and girders. Hence, there is consistence between the suggested formulae and the AISC(1990) guidelines for beams with openings, and, for pure shear, the EC3 rules for girders without openings.

12.2 Design guidelines

The suggested guidelines are based on the discussions in Section 7.2 and 9.2 for combinations of primary moments and shear. For pure shear, the discussions are included in Chapter 11. For easy use of the guidelines in practice, all required equations are repeated here, but with a minimum of explanations. The initial equation numbers are kept, and it should be easy to find the basis for each equation. For design purpose the term “capacity” is replaced by “design resistance”, i.e. partial factors γ_{M_d} are included and “Rd” added to the subscripts in some equations. These equations have an “a” added to the initial equation

number, if applicable. Girders with the web in Class 1 or 2 in bending are denoted beams. The word “horizontal” is used for the direction of the longitudinal axis of girders and beams. The word “vertical” is related to the direction of an axis in the web plane, normal to the longitudinal (horizontal) axis and pointing upwards. Structural elements related to the opening only, are denoted vertical stiffeners and horizontal reinforcement, in order to avoid confusion with transverse and longitudinal stiffeners for other purpose.

1. Moment and shear

For all beams and girders with openings the verification should be based on the interaction equation

$$\left(\frac{M}{M_{buckl,mod,Rd}} \right)^3 + \left(\frac{V}{V_{c,mod,Rd}} \right)^3 \leq 1 \quad (7.2.14a)$$

M and V are the primary moment and shear force, acting in a vertical section through the center of the opening. $M_{buckl,mod,Rd}$ and $V_{c,mod,Rd}$ are the design resistances for moment and shear as given in Pt. 2 and Pt. 3 below. Load factors shall be included in the action effects M and V .

2. Moment

2.1 The design moment of resistance for girders is given by

$$M_{buckl,mod,Rd} = \frac{f_y}{\gamma_{M0}} W_{eff,mod} \quad (12.2.1)$$

The effective areas of the girder cross section are initially determined according to EC3 Part 1-5, neglecting the opening and possible reinforcement. The opening is then introduced, and the parts of the effective areas that fall within the opening are deleted, giving the effective cross section for which the section modulus $W_{eff,mod}$ is calculated. Horizontal reinforcement, if any, shall not be included. The yield stress f_y is assumed equal for web and flanges. The partial factor γ_{M0} is to be assigned the same value as for girders without openings.

2.2 The design moment of resistance for beams is given by

$$M_{buckl,mod,Rd} = M_m = \frac{f_y}{\gamma_{M0}} \left[W_p - D_h t \left(\frac{D_h}{4} + e \right) \right] \quad (3.3.2a)$$

W_p is the plastic section modulus of the girder cross section without opening. D_h is the height of the opening and $e = |e|$ is the eccentricity of the opening relative to the plastic neutral axis.

- 2.3 It is always conservative to calculate $M_{buckl,mod,Rd}$ on the basis of the flanges only.
- 2.4 For large moments, a section aside the opening may be governing, see Section 7.2.7.

3. Shear

- 3.1 The design resistance for shear for all beams and girders with openings of regular shapes, with and without stiffening or reinforcement, are given by

$$V_{c,mod,Rd} = \left(1 - \frac{D_h}{h}\right) \chi_w c_2 \frac{f_y}{\gamma_{M1} \sqrt{3}} ht \quad (11.1.1a)$$

but shall not be taken larger than

$$V_{c,modcut-off,Rd} = \alpha_c \left(1 - \frac{D_h}{h}\right) \frac{f_y}{\gamma_{M1} \sqrt{3}} ht \quad (11.1.1a)$$

h is the clear web height (depth) between flanges, and t is the web thickness. χ_w is the buckling reduction factor, c_2 is an adjustment factor, and α_c is a cut-off factor, given in Pt. 3.2, Pt 3.3 and Pt.3.4, respectively. The partial factor γ_{M1} is to be assigned the same value as for girders without openings.

- 3.2 The buckling reduction factor χ_w

- (1) The factor χ_w is taken according EC 3 Part 1-5 for girders without openings. Table 12.2.1 gives χ_w as a function of the relative slenderness $\bar{\lambda}_w$.

Table 12.2.1 Reduction factor χ_w

	χ_w for rigid end post	χ_w for non-rigid end post
$\bar{\lambda}_w < 0,83$	1,00	1,00
$0,83 \leq \bar{\lambda}_w < 1,08$	$0,83 / \bar{\lambda}_w$	$0,83 / \bar{\lambda}_w$
$\bar{\lambda}_w \geq 1,08$	$1,37 / (0,7 + \bar{\lambda}_w)$	$0,83 / \bar{\lambda}_w$

- (2) The relative slenderness is given as a function of the shear buckling coefficient k_τ

$$\bar{\lambda}_w = \frac{h}{37,4t\varepsilon\sqrt{k_\tau}} \quad (12.2.2)$$

where

$$\varepsilon = \sqrt{\frac{235}{f_y}} \quad (12.2.3)$$

- (3) The shear buckling coefficient is taken as a function of the aspect ratio a/h

$$k_{\tau} = 5,34 + \frac{4}{(a/h)^2} \quad \text{for } a/h \geq 1 \quad (12.2.4)$$

$$k_{\tau} = 4,00 + 5,34(a/h)^2 \quad \text{for } a/h < 1 \quad (12.2.5)$$

where a is the distance between the transverse stiffeners.

- (4) Vertical stiffeners close to the opening may increase the shear capacity of girders with openings. The effect is an increased value of χ_w , that is calculated from Table 12.2.1 and Eqs. (12.2.1) to (12.2.5).
- (5) Vertical stiffeners are usually provided in pair, i.e. one stiffener on each side of the opening. The stiffeners are intended to prevent buckling only, and there are no strength requirements. Stiffener on one side of web is common. Each stiffener must satisfy the stiffness criteria

$$I_{st} \geq 0,375ht^3 \quad \text{for high aspect ratio, i.e. } \frac{a}{h} \geq \sqrt{2} \approx 1,4 \quad (12.2.6)$$

$$I_{st} \geq 0,75 \frac{h^3 t^3}{a^2} \quad \text{for low aspect ratio, i.e. } \frac{a}{h} < \sqrt{2} \approx 1,4 \quad (12.2.7)$$

where a is the distance between the transverse stiffeners, i.e. disregarding the (new) vertical stiffeners. See Section 11.8. I_{st} is the second moment of area of the stiffener and the effective width of web plate, calculated in a horizontal section through the opening. The effective width is taken as $15t$ to each side of the stiffener; the thickness of the stiffener is to be added, and parts of opening, interfering into the effective width, is to be subtracted. Flatbar stiffeners should have a width/thickness ratio less or equal to eight. Other types of stiffeners should comply with Eq. (3.10.12). Only minimum welds are required between web and vertical stiffeners.

3.3 The adjustment factor C_2

- (1) For a single opening without stiffening or reinforcement, where the center of the opening coincides with the horizontal centerline of the web, the adjustment factor is given as

$$C_2 = C_{2,basic} = \frac{\sqrt{3}}{\sqrt{4 \left(\frac{0,5D_a - r_{red}}{s_t} \right)^2 + 3}} \quad \text{from (11.3.7)}$$

D_a is the length of opening in the horizontal direction and s_t is the vertical distance from the top of opening to the upper edge of web. r_{red} is the reduced corner radius given as

$$r_{red} = r \left(\frac{2r}{D_a} \right)^2 \quad (11.3.8)$$

where r is the real corner radius. Eqs. (11.3.7) and (11.3.8) are valid for all openings of regular shapes, i.e. shapes described solely by the three dimensions D_a , D_h and r . Eq. (11.3.7) gives $c_{2,basic} = 1,0$ for circular openings.

- (2) For a single opening with sleeves or doubler plates, where the center of the opening coincides with the horizontal centerline of the web, the adjustment factor is given as

$$c_2 = c_{2,s} = c_{2,basic} + \left(\frac{1}{\chi_w} - 1 \right) \mu \beta \quad \text{for } \chi_w \geq \left(1 - \frac{D_h}{h} \right) \quad (11.7.1)$$

$$c_2 = c_{2,s} = c_{2,basic} + \frac{\frac{D_h}{h}}{1 - \frac{D_h}{h}} \mu \beta \quad \text{for } \chi_w < \left(1 - \frac{D_h}{h} \right) \quad (11.7.2)$$

where $c_{2,basic}$ is given by Eq. (11.3.7). μ is the ratio between the weight of the sleeve(s) or doubler plate(s) and the weight of the removed plate in the opening. The value for μ shall not exceed 1,0 in the equations even if the real value is larger. β includes the effect of sleeve(s) or doubler plate(s) on one or two sides of the web. The following values apply

$$\beta = 0,6 \quad \text{for sleeve or doubler plate on one side} \quad (12.2.8)$$

$$\beta = 0,7 \quad \text{for sleeves or doubler plates on both sides} \quad (12.2.9)$$

Eqs. (11.7.1) and (11.7.2) are valid for openings where $D_a \leq 4r$, but for doubler plates the openings must be circular. Sleeves and doubler plates should be located with the inner surface/diameter not more than 20 mm from the edge of opening. Sleeves should satisfy the criterion $h_{st}/t_{st} \leq 8$, where h_{st} is the height and t_{st} the thickness of the sleeve. For doubler plates the criterion is $h_{st}/t_{st} \leq 30$, but here h_{st} is the difference between the outer and inner diameter of the doubler plate and t_{st} is the thickness of the doubler plate.

- (3) For a single opening with horizontal reinforcement, with the center of the opening located on the horizontal centerline of the web, the adjustment factor is given as

$$c_2 = c_{2,r} = c_{2,basic} + (1 - c_{2,basic}) \frac{A_r}{A_{r,max}} \beta \leq 1,0 \quad (11.5.1)$$

where $c_{2,basic}$ is given by Eq. (11.3.7). A_r is the sectional area of the reinforcement and the part of web plate that is between the reinforcement and the edge of opening. $A_{r,max}$ is the required sectional area of reinforcement based on yield shear strength of the web above the opening. β includes the effect horizontal reinforcement on one or two sides of the web. The following values apply

$$A_{r,max} = \frac{D_c t}{2\sqrt{3}} \quad (3.3.26)$$

$$\beta = 0,7 \quad \text{for reinforcement on one side} \quad (12.2.10)$$

$$\beta = 1,0 \quad \text{for reinforcement on both sides} \quad (12.2.11)$$

Horizontal reinforcement should be located with the near surface not more than 20 mm from the edge of opening, and should satisfy the criterion $h_{st}/t_{st} \leq 8$, where h_{st} is the height and t_{st} is the thickness of the reinforcement. The anchoring length must be minimum

$$l_{min} = \frac{A_r \sqrt{3}}{2t} \quad (3.3.31)$$

- (4) For a single opening without stiffening or reinforcement, where the center of the opening has an eccentricity $e = |e|$ relative to the horizontal centerline of the web, the adjustment factor is given by

$$c_2 = c_{2,off-set} = \frac{c_{2,t}s_t + c_{2,b}s_b}{h\left(1 - \frac{D_h}{h}\right)} \left(1 - 2\frac{eD_h}{h^2}\right) \quad \text{for } \chi_w \geq 0,5 \quad (11.9.5)$$

$$c_2 = c_{2,off-set} = \frac{c_{2,t}s_t + c_{2,b}s_b}{h\left(1 - \frac{D_h}{h}\right)} \left(1 - 8\frac{eD_h}{h^2}\chi_w^2\right) \quad \text{for } \chi_w < 0,5 \quad (11.9.6)$$

$c_{2,t}$ and $c_{2,b}$ are calculated according to Eq. (11.3.7) for the top and bottom tee, respectively. For the calculation of $c_{2,b}$, s_t is replaced by s_b , i.e. the vertical distance from the bottom of opening to the lower edge of web. Eqs. (11.9.5) and (11.9.6) are valid for all openings of regular shapes. For circular openings, and elongated circular openings with vertical long side, Eqs. (11.9.5) and (11.9.6) simplify to

$$c_2 = c_{2,off-set,circ} = \left(1 - 2\frac{eD_h}{h^2}\right) \quad \text{for } \chi_w \geq 0,5 \quad (11.9.1)$$

$$c_2 = c_{2,off-set,circ} = \left(1 - 8\frac{eD_h}{h^2}\chi_w^2\right) \quad \text{for } \chi_w < 0,5 \quad (11.9.2)$$

- (5) For a single opening with sleeve, doubler plates or horizontal reinforcement, where the center of opening has an eccentricity $e = |e|$ relative to the horizontal centerline of the web, the adjustment factor is given by Pt. 3.3 (2) or (3), provided that $c_{2,basic}$ is replaced by $c_{2,off-set}$ from Eqs. (11.9.5) and (11.9.6), alternatively by $c_{2,off-set,circ}$ from Eqs. (11.9.1) and (11.9.2). The factors β are to be taken as

$$\beta = 0,6\left(1 - \frac{e}{2h\chi_w}\right) \quad \text{for sleeves or doubler plates on one side} \quad (11.9.3)$$

$$\beta = 0,7\left(1 - \frac{e}{2h\chi_w}\right) \quad \text{for sleeves or doubler plates on both sides} \quad (11.9.4)$$

$$\beta = 0,7\left(1 - \frac{e}{2h\chi_w}\right) \quad \text{for reinforcement on one side} \quad (11.9.7)$$

$$\beta = 1,0\left(1 - \frac{e}{2h\chi_w}\right) \quad \text{for reinforcement on both sides} \quad (11.9.8)$$

- (6) For two or more openings closely spaced the interaction between the openings must be considered. This may be done by transforming the set of openings to one single fictitious opening with horizontal and vertical dimensions D_{af} and D_{hf} , respectively, and treating this opening as previously described. All openings must be checked, but it is usually easy to determine the governing case. Fig. 12.2.1 shows a girder with a set of openings A, B, C and D. In the following the biggest opening A, with dimensions D_a , D_h and corner radius r , is taken as the starting point.

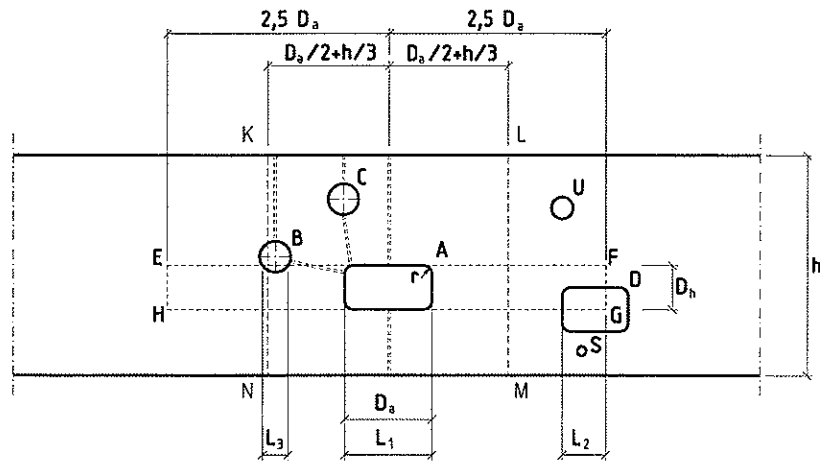


Fig. 12.2.1 Girder web with group of openings

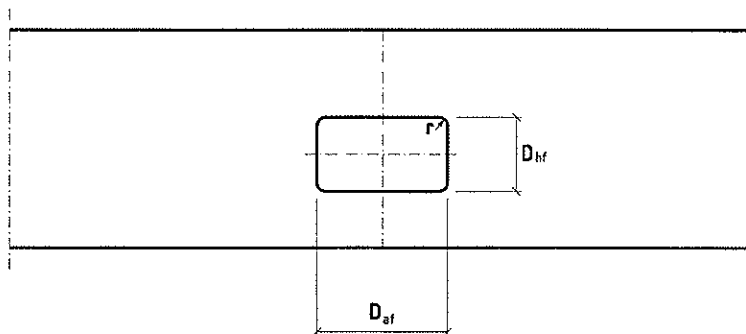


Fig. 12.2.2 The fictitious opening for opening A in Fig.12.2.1

The procedure is as follows:

For the rectangular opening A a rectangle E-F-G-H is defined by "extending" the top and bottom edges of the opening a distance $\pm 2,5D_o$ from the center of the opening, as seen in the figure. The height of the rectangle is equal to the dimension D_h . For circular openings, the rectangle is defined by extending an upper and a lower horizontal tangent in the same manner. The length D_{of} is obtained by adding the contributions L_i from all openings lying within the rectangle, i.e. in this case the openings A, B and D.

$$D_{of} = L_1 + L_2 + L_3 \quad (12.2.13)$$

Openings C, S and U are neglected as they lie outside the rectangle. For openings that only partially lie within the rectangle the figure gives guidelines for the determination of L_i . In case some of the lengths L_i overlap, the contribution should only be included once.

In order to define the vertical dimension D_{hf} of the fictitious opening, a second rectangle K-L-M-N is defined by drawing vertical lines at a distance $\pm (D_o/2 + h/3)$ from the center of the opening A, as shown in the figure. All openings that lie completely or partially within this rectangle contribute to D_{hf} . Drawing lines from the top of the web through the openings to the bottom of the web may identify a number of possible shear failure lines. In Fig. 12.2.1 the doubly dashed lines indicate three such lines. The shortest net length of these shear failure lines is denoted h_n , and the dimension D_{hf} is given by

$$D_{hf} = h - h_n \quad (12.2.14)$$

The resulting fictitious opening is shown in Fig 12.2.2. The adjustment factor for the fictitious opening is given as

$$c_{2,f} = \frac{c_{2,tf}s_{tf} + c_{2,bf}s_{bf}}{h \left(1 - \frac{D_h}{h} \right)} \quad (12.2.15)$$

where $c_{2,tf}$ and $c_{2,bf}$ are calculated according Eq. (11.2.7), using D_{of} and s_{tf} and s_{bf} for the top and bottom tee of the fictitious opening. The values of s_{tf} and s_{bf} are taken as proportional to the similar values for the real opening. r is taken as the corner radius of the real opening.

- (6.1) If the real opening has no stiffening or reinforcement, the adjustment factor is given by

$$c_2 = c_{2,off-set,f} = c_{2,f} \left(1 - 2 \frac{eD_h}{h^2} \right) \quad \text{for } \chi_w \geq 0,5 \quad (12.2.16)$$

$$c_2 = c_{2,off-set,f} = c_{2,f} \left(1 - 8 \frac{eD_h}{h^2} \chi_w^2 \right) \quad \text{for } \chi_w < 0,5 \quad (12.2.17)$$

where $c_{2,f}$ is given by Eqs. (12.2.15) and D_h and e are the values for the real opening. The design resistance for shear is determined by Eq. (11.1.1a), using D_h and $c_{2,off-set,f}$ or by Eq.(11.11.1a), using D_{hf} .

- (6.2) If the real opening has sleeves, doubler plates or horizontal reinforcement, the adjustment factor is given by Pt. 3.3 (2) or (3), provided that $c_{2,basic}$ is replaced by $c_{2,off-set,f}$ from Eqs. (12.2.16) and (12.2.17). μ and $A_{r,max}$ shall be based on the fictitious opening. The factors β shall be taken from Eqs. (11.9.3), (11.9.4), (11.9.7), or (11.9.8) with e based on the real opening. The design resistance for shear is determined by Eq. (11.1.1a), using D_h and $c_{2,s}$ or $c_{2,r}$, or by Eqs. (11.11.1a) using D_{hf} . The cut-off factor α_c shall be based on μ and $A_{r,max}$ for the fictitious opening.

3.4 The cut-off factor α_c

- (1) The factor α_c is for all openings given as

$$\alpha_c = (1 - 0,32 \frac{D_h}{h}) \quad (11.11.2)$$

- (2) For openings with sleeve(s) or doubler plate(s) the factor α_c may be taken as

$$\alpha_{c,s} = \mu \leq 1 \quad (11.11.3)$$

if this value is larger than α_c given by Eq. (11.11.2). μ is defined in Pt. 3.3 (2).

- (3) For openings with horizontal reinforcement the factor α_c may be taken as

$$\alpha_{c,r} = \frac{h - D_{hr}}{h - D_h} \frac{A_r}{A_{r,max}} \quad (11.11.4)$$

if this value is larger than α_c given by Eq. (11.11.2). A_r and $A_{r,max}$ are defined in Pt. 3.3 (3). D_{hr} is the clear vertical distance between the horizontal reinforcements.

3.5 Welds

- (1) In order to obtain the design resistance for shear given by Eq. (11.1.1a) the welds must be designed for the following shear flows:

Web to flanges above and below the opening:

$$q_{\beta} = \chi_w c_2 \frac{f_y}{\sqrt{3}} t \quad (12.2.18)$$

Web to sleeves/doubler plates:

$$q_s = \mu \frac{f_y}{\sqrt{3}} t \leq \frac{f_y}{\sqrt{3}} \quad (12.2.19)$$

Horizontal reinforcement to web above and below the opening

$$q_{r,o} = \frac{A_r}{A_{r,max}} \frac{f_y}{\sqrt{3}} t \quad (12.2.20)$$

Horizontal reinforcement to web along the anchoring length

$$q_{r,a} = \frac{A_r f_y}{l} \quad (12.2.21)$$

where l is the anchoring length. If the anchoring length is at least $0,5D_o$, a single fillet can be used in the opening part of the reinforcement and double fillets in the anchoring parts.

- (2) If the shear capacity is not utilized, the weld between web and flange may be designed for the nominal shear flow based on the shear force V

$$q_{fl,nom} = \frac{V}{h - D_h} \quad (12.2.22)$$

4. Miscellaneous

- (1) Corner radii of the opening should be the greater of $2t$ and 16 mm.
- (2) Concentrated loads above or below the opening are not allowed.
- (3) Lateral buckling of compression flange. The torsional constant of the beam/girder should be multiplied by

$$\left[1 - \left(\frac{D_o}{L_b} \right) \frac{D_o t - 2A_r}{t(h + 2b_f)} \right]^2 \leq 1 \quad (3.3.20)$$

where L_b is the unbraced length of compression flange. $A_r = 0$ when there is no reinforcement and when the reinforcement is on only one side of the web. Beams/girders reinforced on one side of the web should not be used for long laterally unsupported spans. For shorter spans, the lateral bracing closest to the opening should be designed for an additional load equal to 2 % of the force in the compression flange, disregarding secondary moments from shear.

- (4) Vertical buckling of a tee without reinforcement in compression should be investigated as an axially loaded column, but is not required when the aspect ratio of the tee web is less or equal to four.
- (5) Vertical buckling check of the tee in compression with reinforcement is only required for large openings in regions of high primary moment.

12.3 Calculation of shear capacity by means of FE-models

When the design guidelines of Section 12.2 do not give sufficient capacity or cannot be used for other reasons, the shear capacity may be calculated based on non-linear FE-analyses. For instance, the design guidelines are not applicable in cases where concentrated loads are applied above or below the opening. Other cases comprise cluster of openings, where Section 12.2 Pt. 3.3. (6) may give conservative results. Based on experience from the simulations, recommendations for FE-models are given as follows

- (1) The length of the model must be at least three times the height of the girder, and should include all transverse stiffeners within this length. The connections between web and flanges should be modeled as hinges, but stiffeners and reinforcement can be "welded" on.
- (2) The number of elements must be sufficient to allow all governing buckle modes to be included. It is recommended to use as many elements as possible, within the restrictions regarding the solution time. *A priori* limitations of the model based on assumed load-carrying paths and buckling shapes should be avoided. The FE-model will give the answer. For the same reason, efforts to limit the model based on symmetry considerations should also be done with great care. However a study of eigenmodes will often provide insight in the performance of the model. Analyses to determine eigenmodes take considerably shorter time than full nonlinear solutions.
- (3) Automatic meshing techniques should be used to the full extent provided by the program. Regular meshes might be preferred, but some of the present simulations showed small difference in the result for models with regular mesh compared to models with free mesh. It is the element size that counts, and a few trial and error efforts are often sufficient to find a good mesh.
- (4) Imperfections should be applied by means of eigenmodes from the model, and with amplitudes given by EC3. This means that somewhat smaller amplitudes are often sufficient, than used in the present simulations. The imperfection must include the appropriate eigenmode(s), which should be chosen manually. A missing or wrong eigenmode may give non-conservative results. Program facilities for automatic inclusion of eigenmodes are to be used with care, as shear produces negative and positive eigenmodes in pair, and two eigenmodes may counteract each other.
- (5) The non-linear analyses are preferably to be performed in displacement-control. If this is not possible, the analyses may be done as described in Section 7.2 for moment-shear interaction.
- (6) The actual shear capacity is usually easy to find, as the response curve for the applied displacement most often has a distinct maximum value. Over 99 % of the simulations showed a well defined ultimate load. If there is a more "soft" top, the maximum value can be determined based on a chosen value of the applied displacement.
- (7) The models may give non-conservative results, errors up to 7 % might be expected, unless a significant denser element mesh is used, than was used in the simulations. It is suggested that models and analyses are compared or verified against some known results, for instance the simulations in this thesis, in order to avoid mistakes and to adjust for non-conservative results.
- (8) The obtained shear capacity should be reduced with the appropriate partial factor. The result should also be evaluated with regard to transverse web displacements and stresses in the serviceability limit state.

12.4 Suggestions for further study

In the design guidelines a generalized procedure for multiple openings is proposed. No simulations have been performed for such configurations. However, the procedure covers the simulations that have been performed and the author presumes that it is suitable for most occasions and will give conservative results. It is suggested to perform a study in order to confirm this part of the design guidelines.

A cut-off in shear capacities is proposed for all girders with stocky webs and unstiffened circular openings. The reason is the yield shear stress distribution in T-sections, but the size of the cut-off may be too conservative. This question has economical aspects regarding the actual need for sleeves and should be further studied.

References

- ABAQUS 1998. *Abaqus/Standard User's Manual*. Version 5.8. Vol. I-II-III. Hibbitt, Karlsson & Sorensen, Inc. Pawtucket, RI.
- ABAQUS 2002. *Abaqus/Standard User's Manual*. Version 6.3-1. Online edition. Hibbitt, Karlsson & Sorensen, Inc. Pawtucket, RI.
- AISC 1978. *Specification for the Design, Fabrication and Erection of Structural Steel for Buildings*. American Institute of Steel Construction. Chicago
- AISC 1990. David Darwin. *Design of steel and composite beams with web openings*. 2nd. Printing 1992. American Institute of Steel Construction. Chicago.
- BASLER, K. and THÜRLIMANN, B. Aug.1961. *Strength of plate girders in bending*. Paper No. 2913, J. Structural Div., ASCE.
- BASLER, K. Oct. 1961a. *Strength of plate girders in shear*. Paper No. 2967., J. Structural Div. ASCE.
- BASLER, K. Oct. 1961b. *Strength of plate girders under combined bending and shear*. Paper No. 2968, J. Structural Div. ASCE.
- BERGSHOLM, T. 1999. *Platbeærere med store stegutkapp*. Hovedoppgave ved Inst. for konstruksjonsteknikk, NTNU. Trondheim.
- BOWER, J.E. et al. 1971, for ASCE Subcommittee on beams with web openings. *Suggested design guides for beams with web holes*. Paper No. 8536, J. Structural Div. Vol. 97, ST 11. ASCE.
- BOX, G.E.P., HUNTER, W.G. and HUNTER, J.S. 1978. *Statistics for experimenters*. New York. John Wiley & Sons
- BUCKLAND, P.G., BARTLETT, F.M. and WATTS, R.D. 1988. *Practical design of holes in steel webs*. Can. J. Civ. Eng. Vol. 15. No. 3, pages 456-469.
- CEN 1995. *Annex N: Openings in webs. Background note: Opening in stiffened web panels*. British Standards Institution. Secretariat of CEN/TC 250/SC 3. Document CEN/TC 250/SC3/N 478 E. European Committee for Standardization.
- CONSTRADO 1977. *Holes in beam webs. Allowable stress design*. Constructional Steel Research and Development Organisation.
- DARWIN, D. and DONAHEY, R.C. 1988. *LRFD for composite beams with unreinforced web openings*. J. Struct. Eng. ASCE. Vol. 114. No. 3, page 535-552.
- DIN 17100 1980 *Allgemeine Baustabe. Gittenorm*. Deutsches Institut fur Normung. Berlin.

DnV 1993. *Rules for classification of ships. Newbuildings. Hull and equipment. Main Class. Part 3, Chapter 1. C500.* Det norske Veritas Classification. Oslo.

DnV 2004. *Design of offshore steel structures, General (LRFD method).* Offshore Standard DNV-OS-C101. Det norske Veritas. Oslo

DUBAS, P. and GEHRI, E. (ed) 1986. *Behaviour and design of steel structures.* Publication No. 44, ECCS TC 8 – Structural Stability – TWG 8.3 – Plated Structures, Applied Statics and Steel Structures. Swiss Federal Institute of Technology. Zürich.

ENV 1993 Annex N 1998, i.e. ENV 1993-1-1:1992/A2:1998. *Annex N [Informative]. Openings in webs.*

EC3, i.e. EC3 Part 1-5, see below

EC3 Part 1-5. 2003, i.e. *prEN 1993-1-5: 20xx. Eurocode 3: Design of steel structures – Part 1-5: Plated structural elements.* Stage 34 draft. European Committee for Standardization. Brussel

GREENSPAN, M. 1944. *Effect of a small hole on the stresses in a uniformly loaded plate.* Quart. Appl. Math. Vol. 2

HÖGLUND, T. 1970. *Bärförmåga hos tunnväggig I-balk med cirkulärt eller rektangulärt hål i livet.* Inst. for byggnadstatik, KTH. Meddelande nr 87. Stockholm.

HÖGLUND, T. 1971. *Simply supported long thin plate I-girders without web stiffeners subjected to distributed transverse load.* IABSE colloquium. London.

HÖGLUND, T. 1973. *Design of thin plate I girders in shear and bending with special reference to web buckling.* Royal Institute of Technology, Department of Building Statics & Structural Engineering. Stockholm. Meddelande 94.

HÖGLUND, T. 1997. *Shear buckling resistance of steel and aluminium plate girders.* Thin-Walled Structures. Vol. 29. No. 1-4, pages 13-30.

KIKUKAWA, M. 1953. *On plane stress problems in domains of arbitrary profiles.* Proc. 3rd. Jap. Nat. Congr. Appl. Mech.

KUHN, P., PETERSON, J.P. and LEVIN, L.R. May 1952. *A summary of diagonal tension.* Parts I and II. NACA Tech. Notes 2661 and 2662. Washington.

LEE, M.M.K., KAMTEKAR, A.G. and LITTLE, G.H. Jan. 1989. *An experimental study of perforated steel web plates.* The Structural Engineer, Vol. 67, No. 2, pages 27-38.

LEE, M.M.K., Feb. 1990. *A theoretical model for collapse of plate girders with perforated webs.* The Structural Engineer, Vol. 68, No. 4, pages 72-80.

LEE, M.M.K., Jun. 1990. *Numerical study of plate girder webs with holes.* Structural Engineering Group paper 9523. Proc. Instn. Civ. Engineers, , Vol. 79, Part 2, pages 183-206.

- LEVY, S., MCPHERSON, A.E. and SMITH, F.C. 1948. *Reinforcement of a small circular hole in a plane sheet under tension*. J. Appl. Mech. Vol. 15. Pages 160-168
- MAQUOI, R. 1992. *Plate girders containing web openings, Section 9 of Chapter 2.6 Plate Girders*. In: *Constructional Steel Design – An International Guide*, edited by Dowling, Harding and Bjorhovde. Elsevier Applied Science. Page 158 – 162.
- MINSAAS, L. 1983. *Platebærere med store utkapp*. Hovedoppgave ved Inst. for stålkonstruksjoner, NTH. Trondheim.
- NARAYANAN, R. and ROCKEY, K.C. Sep. 1981. *Ultimate load capacity of plate girders with webs containing circular cut-outs*. Proc. Instn. Civ. Engineers, Vol. 71, Part 2, paper 8481, pages 845-862.
- NARAYANAN, R. 1983a. *Ultimate shear capacity of plate girders with openings in webs*. Ch. 2 in: *Plated Steel Structures, Stability and Strength*, pages 39-76. Elsevier Applied Science.
- NARAYANAN, R. and DER AVANESSIAN, N.G.V. 1983b. *Ultimate strength of plate girders having reinforced cut-outs in webs*. In: *Instability and plastic collapse of steel structures*, ed: Morris, L.J. Granada. Pages 360-370.
- NARAYANAN, R. and DER AVANESSIAN, N.G.V. June 1983. *Equilibrium solution for predicting the strength of webs with rectangular holes*. Proc. Instn. Civ. Engineers, Vol. 75, Part 2, paper 8655, pages 265-282.
- NARAYANAN, R. and DER AVANESSIAN, N.G.V. March 1984. *Strength of webs with corner openings*. The Structural Engineer, Vol. 62B, No. 1, pages 6-11.
- NARAYANAN, R. and DER AVANESSIAN, N.G.V. 1984b. *Elastic buckling of perforated plates under shear*. Thin-walled structures 2, pages 51-73.
- NARAYANAN, R. and DER AVANESSIAN, N.G.V. June 1984. *An equilibrium method for assessing the strength of plate girders with reinforced web openings*. Proc. Instn. Civ. Engineers, Vol. 77, Part 2, paper 8722, pages 107-137.
- NARAYANAN, R. and DER AVANESSIAN, N.G.V. April 1985. *Design of slender webs having rectangular holes*. ASCE Journal of Structural Engineering, Vol. 111, No. 4, paper 19673, pages 777-787.
- NARAYANAN, R. and DARWISH, I.Y.S. 1985. *Strength of slender webs having non-central holes*. The Structural Engineer, Vol. 63B, No. 3, pages 57-62.
- NS-ENV 1993-1-1 1993. *Eurocode 3: Design of steel structures. Part 1-1: General rules and rules for buildings*. Oslo. Norges Standardiseringsforbund.
- NORSOK STANDARD M-101 1997. *Structural steel fabrication*. Rev. 3. Oslo. Norsk Teknologisenter.
- PORTER, D.M., ROCKEY, K.C. and EVANS, H.R. 1975. *The collapse behaviour of plate girders loaded in shear*. The Structural Engineer. Vol. 53.

- REDWOOD, R.G. 1973. *Design of beams with web holes*. Canadian Steel Industries Construction Council. Ontario.
- REDWOOD, R.G. 1983. *Design of I-beams with web perforations*. In: Beams and Beam Columns, edited by Narayanan. Applied Science Publishers.
- RODE, H.H. 1916. *Beitrag zur Theorie der Knickerscheinungen*. Eisenbau
- SELBERG, A. 1973. *Brudd i skjærbelastede livplater. Kritisk vurdering av Basler og Rockey's metoder*. Nordiske forskningsdager for stålkonstruksjoner.
- SOLLID, K. 1983. *Bæreevne av platebærere med store utkapp. Foreløpig rapport fra forsøk utført til og med 1982*. Upublisert. Inst. for stålkonstruksjoner, NTH. Trondheim.
- SOLLID, K. 1985. *Bæreevne av platebærere med store utkapp. Foreløpig rapport fra forsøk utført til og med 1985*. Upublisert. Inst. for stålkonstruksjoner, NTH. Trondheim.
- SOLLAND, G. and FRANK, E. 1988. *Rational design of stressed skin offshore modules*. The 5th International Conference on Behaviour of Offshore Structures, BOSS 88. Trondheim.
- TIMOSHENKO, S.P. and GERE, J.M. 1963. *Theory of elastic stability*. Second edition. New York. McGraw-Hill.
- UENOYA, M. and REDWOOD, R.G. 1977. *Elasto-plastic shear buckling of square plates with circular holes*. Comput. Struct. Vol. 8, p. 231-300
- UENOYA, M. and REDWOOD, R.G. 1978. *Buckling of webs with openings*. Comput. Struct. Vol. 9, p. 191-199.
- WAGNER, H. 1929. *Ebene Blechwandträger mit sehr dünnem Stegblech*. Zeitschrift f. Flugtechnik u. Motorluftschiffahrt.
- WEISS, H.J., PRAGER, W. and HODGE, P.G., JR. 1952. *Limit design of a full reinforcement for a circular cutout in a uniform slab*. Journal of Applied Mechanics. Pages 397-401. ASME.

Appendix A

Overview of simulations

Chapter	Name	Runs	Chapter	Name	Runs
3. Stress concentration	D...	8			
5. Sim. of the prior experiments	S..., E...	33			
7. Sim. of girders with circular openings		122	9. Sim. of girders with square openings		81
Introduction		2			
Introduction	I...	3			
Rotated stress field method	H...	6	Rotated stress field method	H...	6
Yield stress	L...	6	Yield stress	L...	6
Transverse stiffeners	L...T2	9	Transverse stiffeners	L...T2	6
Transverse stiffeners	L...T1	9	Transverse stiffeners	L...T1	7
Transverse stiffeners	L...T0	9			
Shear and prim. mom. interaction	P...M...	6			
Shear and prim. mom. interaction	Q...M...	6			
Shear and prim. mom. interaction	Q...T1M...	6	Shear and prim. mom. interact	Q...T1M...	6
Opening in lower part of web	M...	3	Opening in lower part of web	M...	3
Sleeves	J...	6	Horizontal reinf. one-side	J...	6
Sleeves + transv. stiffeners	J...T2	4	Hor. reinf. one-side + transv. stiff	J...T2	6
Sleeves + transv. stiffeners	J...T1	3	Hor. reinf. one-side + transv. stiff	J...T1	6
Sleeves + transv. stiffeners	J...T0	3			
Centric sleeves	J...C	2	Hor. reinf. two-side	J...C	2
			Vertical stiffeners	L...	2
			Hor. reinf. + vert. stiff. two-side	JL...	13
Sleeves in lower part of web	N...	2	Opening in lower part of web with hor. reinf. + vert. stiffeners	NL...	2
Sleeves in lower part of web	N...T2	1			
Doubler plates	K...	9			
Two openings horizontally spaced	R...	2	Two openings horizontally spaced	S...	2
Two openings horizontally spaced	S...	2			
Two openings horizontally spaced	T...	2	Two openings horizontally spaced	U...	2
Two openings horizontally spaced	U...	2			
Two openings vertically spaced	RH...	2	Two openings vertically spaced	SH...	2
Two openings vertically spaced	SH...	2			
Two openings vertically spaced	TH...	2	Two openings vertically spaced	UH...	2
Two openings vertically spaced	UH...	2			
Two sleeves horizontally spaced	V...	1	Two openings hor. spaced with hor. reinf + vert. stiffeners	WL...	2
Two sleeves horizontally spaced	W...	1			
Two sleeves horizontally spaced	X...	1			
Two sleeves horizontally spaced	Y...	1			
Two sleeves vertically spaced	VH...	1			
Two sleeves vertically spaced	WH...	1			
Two sleeves vertically spaced	XH...	1			
Two sleeves vertically spaced	YH...	1			
8. Sim. of girders with elongated openings		8	10. Sim. of girders with rectangular openings		8
Openings without stiffening	I...	4	Openings without stiffening	I...	4
Openings with stiffening	J...	4	Openings with stiffening	JL...	4

Appendix B

Design guidelines applied to the simulated girders

The guidelines proposed in Chapter 12 are applied to 186 girders with openings described in Chapters 7 to 10. The resulting shear capacities are compared to the results from the simulations by means of the following tables:

- Table B1. Shear capacities for 71 girders with single circular openings. The table also includes 15 corresponding girders without openings.
- Table B2. Shear capacities for 80 girders with single non-circular openings. The girders with elongated circular, square and rectangular openings are included here.
- Table B3. Shear capacities for 35 girders with multiple openings. The girders have two circular or two square openings.

In addition Table B4 includes shear capacities based on the alternative method of Section 11. 10 for girders with two openings close together. The girders are the same as in Table B3.

Tables B1 to B3 have a column 34 marked "Guideline $\chi_{w,mod,G}$ ", where the values are calculated from the equations given in Chapter 12. This is also the case for Table B4, but here the values are based on equations in Chapter 11.

$$\chi_{w,mod,G} = \frac{V_{c,mod,Rd}}{\frac{f_y}{\gamma_{M1}\sqrt{3}}} = \left(1 - \frac{D_h}{h}\right) \chi_w c_2 \leq \alpha_c \left(1 - \frac{D_h}{h}\right) \quad (B.1)$$

All tables have columns marked "Simulated $\chi_{w,mod}$ " and "Simulated, reduced $\chi_{w,mod,red}$ ". The former columns give the values as are, i.e. the values are the same as in the tables of Chapters 7 to 10. In the latter columns the simulated values are divided by 1,02 for the girders without openings, by 1,045 for the girders with openings $D/h = D_h/h = 0,25$, and by 1,07 for the girders with openings $D/h = D_h/h = 0,50$. For the girders with two vertically spaced openings $D/h = D_h/h = 0,25$, the reduced simulated values are based on division by 1,07.

The basic comparison is

$$\chi_{w,mod} \geq \chi_{w,mod,G} \quad (B.2)$$

It can be seen that this criterion is fulfilled for all girders with openings except three, which are marked with Note 1). One of these cases, Girder JL125S50d, has weaker transverse stiffeners than recommended by the guidelines. In the two other cases, girders L125R5025 and JL125R5025, the shear capacity is determined by buckling in the adjacent panel without opening. Several girders without openings do not fulfill the criterion (B.2) and these are marked with Note 2) in Table B1.

Alternatively, the comparison may be done by means of the factor C_{rel} , which is determined as

$$c_{rel} = \frac{\chi_{w,mod,red}}{\chi_{w,mod,G}} \geq 1 \quad (\text{B.3})$$

Some girders with $h/t = 63$ and $h/t = 125$ do not fulfill this criterion. These are marked with Note 3) in the tables. However, the simulations of the corresponding girders without openings gave results below the EC3 curve. Hence, it should be reasonable to adjust the reduced simulated results for the girders with openings by the same amount as the corresponding girders without openings are adjusted up to the EC3 curve. This is done by means of

$$c_{rel}' = \frac{\chi_{w,mod,red}}{\chi_{w,mod,G}} \cdot \frac{\chi_w}{\chi_{w,sim}} \quad (\text{B.4})$$

where χ_w is the buckling reduction factor from EC3 and $\chi_{w,sim}$ is the value from the simulation of the girder without opening. Values of $\chi_{w,sim}$ can be found in Column 35 in Table B1. For instance for Girder I63S25T1,

$$c_{rel}' = \frac{0,65 \cdot 1,00}{0,69 \cdot 0,93} = 1,01 \quad (\text{B.5})$$

where the value 0,93 is taken from the corresponding girder I63T1 without opening. For Girder L125R5025 the corresponding girder is taken as I125T0. The design guidelines should be accepted because $c_{rel}' \geq 1$ for all girders marked with Note 3).

For three girders with $h/t = 125$ a similar adjustment cannot be justified, because the simulations of the corresponding girders without openings gave a result exactly on the EC3 curve. The girders are marked with Note 4) in the tables. However, the guidelines give shear capacities that are only 1 to 2 % above the simulated results, when these are reduced by 7 %.

DEPARTMENT OF STRUCTURAL ENGINEERING
NORWEGIAN UNIVERSITY OF SCIENCE AND TECHNOLOGY

N-7491 TRONDHEIM, NORWAY
Telephone: +47 73 59 47 00 Telefax: +47 73 59 47 01

"Reliability Analysis of Structural Systems using Nonlinear Finite Element Methods",
C. A. Holm, 1990:23, ISBN 82-7119-178-0.

"Uniform Stratified Flow Interaction with a Submerged Horizontal Cylinder",
Ø. Arntsen, 1990:32, ISBN 82-7119-188-8.

"Large Displacement Analysis of Flexible and Rigid Systems Considering Displacement-Dependent Loads and Nonlinear Constraints", K. M. Mathisen, 1990:33, ISBN 82-7119-189-6.

"Solid Mechanics and Material Models including Large Deformations",
E. Levold, 1990:56, ISBN 82-7119-214-0, ISSN 0802-3271.

"Inelastic Deformation Capacity of Flexurally-Loaded Aluminium Alloy Structures",
T. Welo, 1990:62, ISBN 82-7119-220-5, ISSN 0802-3271.

"Visualization of Results from Mechanical Engineering Analysis",
K. Aarnes, 1990:63, ISBN 82-7119-221-3, ISSN 0802-3271.

"Object-Oriented Product Modeling for Structural Design",
S. I. Dale, 1991:6, ISBN 82-7119-258-2, ISSN 0802-3271.

"Parallel Techniques for Solving Finite Element Problems on Transputer Networks",
T. H. Hansen, 1991:19, ISBN 82-7119-273-6, ISSN 0802-3271.

"Statistical Description and Estimation of Ocean Drift Ice Environments",
R. Korsnes, 1991:24, ISBN 82-7119-278-7, ISSN 0802-3271.

"Properties of concrete related to fatigue damage: with emphasis on high strength concrete",
G. Petkovic, 1991:35, ISBN 82-7119-290-6, ISSN 0802-3271.

"Turbidity Current Modelling",
B. Brørs, 1991:38, ISBN 82-7119-293-0, ISSN 0802-3271.

"Zero-Slump Concrete: Rheology, Degree of Compaction and Strength. Effects of Fillers as Part
Cement-Replacement",
C. Sørensen, 1992:8, ISBN 82-7119-357-0, ISSN 0802-3271.

"Nonlinear Analysis of Reinforced Concrete Structures Exposed to Transient Loading",
K. V. Høiseth, 1992:15, ISBN 82-7119-364-3, ISSN 0802-3271.

"Finite Element Formulations and Solution Algorithms for Buckling and Collapse Analysis of Thin
Shells", R. O. Bjærum, 1992:30, ISBN 82-7119-380-5, ISSN 0802-3271.

"Response Statistics of Nonlinear Dynamic Systems",
J. M. Johnsen, 1992:42, ISBN 82-7119-393-7, ISSN 0802-3271.

"Digital Models in Engineering. A Study on why and how engineers build and operate digital models for decision support", J. Høyte, 1992:75, ISBN 82-7119-429-1, ISSN 0802-3271.

"Sparse Solution of Finite Element Equations",
A. C. Damhaug, 1992:76, ISBN 82-7119-430-5, ISSN 0802-3271.

"Some Aspects of Floating Ice Related to Sea Surface Operations in the Barents Sea",
S. Løset, 1992:95, ISBN 82-7119-452-6, ISSN 0802-3271.

"Modelling of Cyclic Plasticity with Application to Steel and Aluminium Structures",
O. S. Hopperstad, 1993:7, ISBN 82-7119-461-5, ISSN 0802-3271.

"The Free Formulation: Linear Theory and Extensions with Applications to Tetrahedral Elements with Rotational Freedoms", G. Skeie, 1993:17, ISBN 82-7119-472-0, ISSN 0802-3271.

"Høyfast betongs motstand mot piggdekkslitasje. Analyse av resultater fra prøving i Veisliter'n",
T. Tveter, 1993:62, ISBN 82-7119-522-0, ISSN 0802-3271.

"A Nonlinear Finite Element Based on Free Formulation Theory for Analysis of Sandwich Structures", O. Aamlid, 1993:72, ISBN 82-7119-534-4, ISSN 0802-3271.

"The Effect of Curing Temperature and Silica Fume on Chloride Migration and Pore Structure of High Strength Concrete", C. J. Hauck, 1993:90, ISBN 82-7119-553-0, ISSN 0802-3271.

"Failure of Concrete under Compressive Strain Gradients",
G. Markeset, 1993:110, ISBN 82-7119-575-1, ISSN 0802-3271.

"An experimental study of internal tidal amphidromes in Vestfjorden",
J. H. Nilsen, 1994:39, ISBN 82-7119-640-5, ISSN 0802-3271.

"Structural analysis of oil wells with emphasis on conductor design",
H. Larsen, 1994:46, ISBN 82-7119-648-0, ISSN 0802-3271.

"Adaptive methods for non-linear finite element analysis of shell structures",
K. M. Okstad, 1994:66, ISBN 82-7119-670-7, ISSN 0802-3271.

"On constitutive modelling in nonlinear analysis of concrete structures",
O. Fyrileiv, 1994:115, ISBN 82-7119-725-8, ISSN 0802-3271.

"Fluctuating wind load and response of a line-like engineering structure with emphasis on motion-induced wind forces",
J. Bogunovic Jakobsen, 1995:62, ISBN 82-7119-809-2, ISSN 0802-3271.

"An experimental study of beam-columns subjected to combined torsion, bending and axial actions", A. Aalberg, 1995:66, ISBN 82-7119-813-0, ISSN 0802-3271.

"Scaling and cracking in unsealed freeze/thaw testing of Portland cement and silica fume concretes", S. Jacobsen, 1995:101, ISBN 82-7119-851-3, ISSN 0802-3271.

"Damping of water waves by submerged vegetation. A case study of laminaria hyperborea",
A. M. Dubi, 1995:108, ISBN 82-7119-859-9, ISSN 0802-3271.

"The dynamics of a slope current in the Barents Sea",
Sheng Li, 1995:109, ISBN 82-7119-860-2, ISSN 0802-3271.

- "Modellering av delmaterialenes betydning for betongens konsistens",
Ernst Mørtsell, 1996:12, ISBN 82-7119-894-7, ISSN 0802-3271.
- "Bending of thin-walled aluminium extrusions",
Birgit Søvik Opheim, 1996:60, ISBN 82-7119-947-1, ISSN 0802-3271.
- "Material modelling of aluminium for crashworthiness analysis",
Torodd Berstad, 1996:89, ISBN 82-7119-980-3, ISSN 0802-3271.
- "Estimation of structural parameters from response measurements on submerged floating tunnels",
Rolf Magne Larssen, 1996:119, ISBN 82-471-0014-2, ISSN 0802-3271.
- "Numerical modelling of plain and reinforced concrete by damage mechanics",
Mario A. Polanco-Loria, 1997:20, ISBN 82-471-0049-5, ISSN 0802-3271.
- "Nonlinear random vibrations - numerical analysis by path integration methods",
Vibeke Moe, 1997:26, ISBN 82-471-0056-8, ISSN 0802-3271.
- "Numerical prediction of vortex-induced vibration by the finite element method",
Joar Martin Dalheim, 1997:63, ISBN 82-471-0096-7, ISSN 0802-3271.
- "Time domain calculations of buffeting response for wind sensitive structures",
Ketil Aas-Jakobsen, 1997:148, ISBN 82-471-0189-0, ISSN 0802-3271.
- "A numerical study of flow about fixed and flexibly mounted circular cylinders",
Trond Stokka Meling, 1998:48, ISBN 82-471-0244-7, ISSN 0802-3271.
- "Estimation of chloride penetration into concrete bridges in coastal areas",
Per Egil Steen, 1998:89, ISBN 82-471-0290-0, ISSN 0802-3271.
- "Stress-resultant material models for reinforced concrete plates and shells",
Jan Arve Øverli, 1998:95, ISBN 82-471-0297-8, ISSN 0802-3271.
- "Chloride binding in concrete. Effect of surrounding environment and concrete composition",
Claus Kenneth Larsen, 1998:101, ISBN 82-471-0337-0, ISSN 0802-3271.
- "Rotational capacity of aluminium alloy beams",
Lars A. Moen, 1999:1, ISBN 82-471-0365-6, ISSN 0802-3271.
- "Stretch Bending of Aluminium Extrusions",
Arild H. Clausen, 1999:29, ISBN 82-471-0396-6, ISSN 0802-3271.
- "Aluminium and Steel Beams under Concentrated Loading",
Tore Tryland, 1999:30, ISBN 82-471-0397-4, ISSN 0802-3271.
- "Engineering Models of Elastoplasticity and Fracture for Aluminium Alloys",
Odd-Geir Lademo, 1999:39, ISBN 82-471-0406-7, ISSN 0802-3271.
- "Kapasitet og duktilitet av dybelforbindelser i trekonstruksjoner",
Jan Siem, 1999:46, ISBN 82-471-0414-8, ISSN 0802-3271.
- "Etablering av distribuert ingeniørarbeid; Teknologiske og organisatoriske erfaringer fra en norsk ingeniørbedrift", Lars Line, 1999:52, ISBN 82-471-0420-2, ISSN 0802-3271.
- "Estimation of Earthquake-Induced Response",

- Simon Ólafsson, 1999:73, ISBN 82-471-0443-1, ISSN 0802-3271.
- "Coastal Concrete Bridges: Moisture State, Chloride Permeability and Aging Effects"
Ragnhild Holen Relling, 1999:74, ISBN 82-471-0445-8, ISSN 0802-3271.
- "Capacity Assessment of Titanium Pipes Subjected to Bending and External Pressure",
Arve Bjørset, 1999:100, ISBN 82-471-0473-3, ISSN 0802-3271.
- "Validation of Numerical Collapse Behaviour of Thin-Walled Corrugated Panels",
Håvar Ilstad, 1999:101, ISBN 82-471-0474-1, ISSN 0802-3271.
- "Strength and Ductility of Welded Structures in Aluminium Alloys",
Miroslaw Matusiak, 1999:113, ISBN 82-471-0487-3, ISSN 0802-3271.
- "Thermal Dilation and Autogenous Deformation as Driving Forces to Self-Induced Stresses in High Performance Concrete",
Øyvind Bjøntegaard, 1999:121, ISBN 82-7984-002-8, ISSN 0802-3271.
- "Some Aspects of Ski Base Sliding Friction and Ski Base Structure",
Dag Anders Moldestad, 1999:137, ISBN 82-7984-019-2, ISSN 0802-3271.
- "Electrode reactions and corrosion resistance for steel in mortar and concrete",
Roy Antonsen, 2000:10, ISBN 82-7984-030-3, ISSN 0802-3271.
- "Hydro-Physical Conditions in Kelp Forests and the Effect on Wave Damping and Dune Erosion. A case study on Laminaria Hyperborea",
Stig Magnar Løvås, 2000:28, ISBN 82-7984-050-8, ISSN 0802-3271.
- "Random Vibration and the Path Integral Method",
Christian Skaug, 2000:39, ISBN 82-7984-061-3, ISSN 0802-3271.
- "Buckling and geometrical nonlinear beam-type analyses of timber structures",
Trond Even Eggen, 2000:56, ISBN 82-7984-081-8, ISSN 0802-3271.
- "Structural Crashworthiness of Aluminium Foam-Based Components",
Arve Grønsund Hanssen, 2000:76, ISBN 82-7984-102-4, ISSN 0809-103X.
- "Measurements and simulations of the consolidation in first-year sea ice ridges, and some aspects of mechanical behaviour",
Knut V. Høyland, 2000:94, ISBN 82-7984-121-0, ISSN 0809-103X.
- "Kinematics in Regular and Irregular Waves based on a Lagrangian Formulation",
Svein Helge Gjøesund, 2000-86, ISBN 82-7984-112-1, ISSN 0809-103X.
- "Self-Induced Cracking Problems in Hardening Concrete Structures",
Daniela Bosnjak, 2000-121, ISBN 82-7984-151-2, ISSN 0809-103X.
- "Ballistic Penetration and Perforation of Steel Plates",
Tore Børvik, 2000:124, ISBN 82-7984-154-7, ISSN 0809-103X.
- "Freeze-Thaw resistance of Concrete. Effect of: Curing Conditions, Moisture Exchange and Materials",
Terje Finnerup Rønning, 2001:14, ISBN 82-7984-165-2, ISSN 0809-103X
- Structural behaviour of post tensioned concrete structures. Flat slab. Slabs on ground",
Steinar Trygstad, 2001:52, ISBN 82-471-5314-9, ISSN 0809-103X.

- "Slipforming of Vertical Concrete Structures. Friction between concrete and slipform panel", Kjell Tore Fosså, 2001:61, ISBN 82-471-5325-4, ISSN 0809-103X.
- "Some numerical methods for the simulation of laminar and turbulent incompressible flows", Jens Holmen, 2002:6, ISBN 82-471-5396-3, ISSN 0809-103X.
- "Improved Fatigue Performance of Threaded Drillstring Connections by Cold Rolling", Steinar Kristoffersen, 2002:11, ISBN: 82-421-5402-1, ISSN 0809-103X.
- "Deformations in Concrete Cantilever Bridges: Observations and Theoretical Modelling", Peter F. Takács, 2002:23, ISBN 82-471-5415-3, ISSN 0809-103X.
- "Stiffened aluminium plates subjected to impact loading", Hilde Giæver Hildrum, 2002:69, ISBN 82-471-5467-6, ISSN 0809-103X.
- "Full- and model scale study of wind effects on a medium-rise building in a built up area", Jónas Thór Snæbjörnsson, 2002:95, ISBN82-471-5495-1, ISSN 0809-103X.
- "Evaluation of Concepts for Loading of Hydrocarbons in Ice-infested water", Amor Jensen, 2002:114, ISBN 82-417-5506-0, ISSN 0809-103X.
- "Numerical and Physical Modelling of Oil Spreading in Broken Ice", Janne K. Økland Gjosteen, 2002:130, ISBN 82-471-5523-0, ISSN 0809-103X.
- "Diagnosis and protection of corroding steel in concrete", Franz Pruckner, 2002:140, ISBN 82-471-5555-4, ISSN 0809-103X.
- "Tensile and Compressive Creep of Young Concrete: Testing and Modelling", Dawood Atrushi, 2003:17, ISBN 82-471-5565-6, ISSN 0809-103X.
- "Rheology of Particle Suspensions. Fresh Concrete, Mortar and Cement Paste with Various Types of Lignosulfonates", Jon Elvar Wallevik, 2003:18, ISBN 82-471-5566-4, ISSN 0809-103X.
- "Oblique Loading of Aluminium Crash Components", Aase Reyes, 2003:15, ISBN 82-471-5562-1, ISSN 0809-103X.
- "Utilization of Ethiopian Natural Pozzolans", Surafel Ketema Desta, 2003:26, ISSN 82-471-5574-5, ISSN:0809-103X.
- "Behaviour and strength prediction of reinforced concrete structures with discontinuity regions", Helge Brå, 2004:11, ISBN 82-471-6222-9, ISSN 1503-8181.
- "High-strength steel plates subjected to projectile impact. An experimental and numerical study", Sumita Dey, 2004:38, ISBN 82-471-6281-4 (elektr. Utg.), ISBN 82-471-6282-2 (trykt utg.), ISSN 1503-8181.
- "Alkali-reactive and inert fillers in concrete. Rheology of fresh mixtures and expansive reactions." Bård M. Pedersen, 2004:92, ISBN 82-471-6401-9 (trykt utg.), ISBN 82-471-6400-0 (elektr. utg.), ISSN 1503-8181.
- "Behaviour of aluminium extrusions subjected to axial loading". Østen Jensen, 2005:7, ISBN 82-471-6872-3 (elektr. utg.), ISBN 82-471-6873-1 (trykt utg.), ISSN 1503-8181.

